Sensory processing in the mouse circadian system

A thesis submitted to The University of Manchester for the degree of

Doctor of Philosophy

in the Faculty of Life Sciences

2016

Lauren Walmsley

Table of Contents

Total word count = 73,161

List of Figures

Chapter 1

Chapter 2

Chapter 3

Chapter 4

Chapter 5

Chapter 6

List of Tables

Chapter 3

Chapter 4

List of Abbreviations

$[Ca^{2+}]$ - Calcium concentration

$[Ca^{2+}]i$ - Intracellular calcium concentration

5-HT - Serotonin

AC - Adenylate cyclase

AH - Anterior Hypothalamus

AHP - Afterhyperpolarisation

AII - Angiotensisn II

AMPA - α-amino-3-hydroxy-5-methyl-4-isoxazolepropionic acid

AVP - Arginine vasopressin

CaMKII - Ca^{2+}-calmodulin-dependent kinase II

CCGs – Clock-controlled genes

ChR2 - Channelrhodopsin

$Cnga3^{-/-}$ - Coneless mouse strain

Contra- Contralateral

Cry/CRY - Cryptochrome gene/protein

CT - Circadian time

DD - Constant darkness

dLGN - Dorsal lateral geniculate nucleus

DM - Dorsomedial

DRN - Dorsal raphé nucleus

ENK - Enkephalin

FDR - Fast delayed rectifier

GABA - γ-aminobutyric acid

GAD - Glutamate decarboxylase

GFP - Green fluorescent protein

GHT - Geniculohypothalamic tract

GLU - Glutamate

GPCR - GTP-binding protein-coupled receptor

GRP - Gastrin releasing peptide

HCN - Hyperpolarisation-activated cyclic nucleotide-gated channel

IGL - Intergeniculate leaflet

IH - Hyperpolarisation-activated conductance

IP_3 - inositol 1,4,5 tri-phosphate

IPL - Inner plexiform layer

ipRGCs – Intrinsically photosensitive retinal ganglion cells

Ipsi - Ipsilateral

L-cones - Long wavelength cones

LD – Light/dark cycle

LED - Light emitting diode

LGN – Lateral geniculate nucleus

LH - Lateral Hypothalamus

LWS - Long wavelength sensitive

M-cones - Medium wavelength cones

MEA - Multielectrode array

MRN - Median raphé nucleus

MWS - Medium wavelength sensitive

ND - Neutral density

NIF - Non-image forming vision

NKCC - $Na^+/K^+/2Cl^-$ cotransporter

NMDA - N-methyl-D-aspartate

NO - Nitric oxide

NOS - Nitric oxide synthase

NPY - Neuropeptide Y

OPN - Olivary pretectal nucleus

Opn1mw^{R} - Redcone mouse strain

PAC - PACAP receptor

PACAP - Pituitary adenylyl cyclase activating peptide

p-CREB -Phosphorylated CREB

PDE - phosphodiesterase

Per/PER - Period gene/protein

PKA - Protein kinase A

PKG - Protein kinase G

PLC - Phospholipase C

PLR - Pupil light reflex

PRC - Phase response curve

pSON - Peri-supraoptic nucleus

rd/rd - Retinal degradation mutation

rd/rd cl - Rodless coneless mutation

rdta- Rodless coneless mutation

rdta/cl - Rodless coneless mutation (more extensive than rdta)

RF - Receptive field

RGCs - Retinal ganglion cells

Rh - Rhodopsin

Rh* - Metarhodopsin

RHT - Retinohypothalamic tract

RMP - Resting membrane potential

RPE - Retinal pigment epithelium

RyR - Ryanodine receptors

SC - Superior colliculus

SCN - Suprachiasmatic nucleus

S-cones - Short-wavelength sensitive cones

TTX - Tetrodotoxin

UVS - UV sensitive

VIP- Vasoactive intestinal polypeptide

VL - Ventrolateral

vLGN - Ventral lateral geniculate nucleus

VPAC - VIP receptor

vSPZ - Ventral subparaventricular zone

WT - wildtype

λmax - Specific maximum spectral sensitivity of an opsin

Abstract

In order to anticipate the predictable changes in the environment associated with the earth's rotation, most organisms possess intrinsic biological clocks. To be useful, such clocks require a reliable signal of 'time' from the external world. In mammals, light provides the principle source of such information; conveyed to the suprachiasmatic nucleus circadian pacemaker (SCN) either directly from the retina or indirectly via other visual structures such as the thalamic intergeniculate leaflet (IGL). Nonetheless, while the basic pathways supplying sensory information to the clock are well understood, the sensory signals they convey or how these are processed within the circadian system are not.

One established view is that circadian entrainment relies on measuring the total amount of environmental illumination. In line with that view, the dense bilateral retinal input to the SCN allows for the possibility that individual neurons could average signals from across the whole visual scene. Here I test this possibility by examining responses to monocular and binocular visual stimuli in the SCN of anaesthetised mice. In fact, these experiments reveal that SCN cells provide information about (at most) irradiance within just one visual hemisphere. As a result, overall light-evoked activity across the SCN is substantially greater when light is distributed evenly across the visual scene when the same amount of light is non-uniformly distributed. Surprisingly then, acute electrophysiological responses of the SCN population do not reflect the total amount of environmental illumination.

Another untested suggestion has been that the circadian system might use changes in the spectral composition of light to estimate time of day. Hence, during 'twilight', there is a relative enrichment of shortwavelength light, which is detectable as a change in colour to the dichromatic visual system of most mammals. Here I used a 'silent substitution' approach to selectively manipulate mouse cone photoreception, revealing a subset of SCN neurons that exhibit spectrally-opponent (blue-yellow) visual responses and are capable of reliably tracking sun position across the day-night transition. I then confirm the importance of this colour discrimination mechanism for circadian entrainment by demonstrating a reliable change in mouse body temperature rhythms when exposed to simulated natural photoperiods with and without simultaneous changes in colour.

This identification of chromatic influences on circadian entrainment then raises important new questions such as which SCN cell types process colour signals and do these properties originate in the retina or arise via input from other visual regions? Advances in mouse genetics now offer powerful ways to address these questions. Our original method for studying colour discrimination required transgenic mice with red-shifted cone sensitivity – presenting a barrier to applying this approach alongside other genetic tools. To circumvent this issue I validated a modified approach for manipulating wildtype cone photoreception. Using this approach alongside optogenetic cell-identification I then demonstrate that the thalamic inputs to the SCN are unlikely to provide a major source of chromatic information.

To further probe IGL-contributions to SCN visual responses, I next used electrical microstimulation to show that the thalamus provides inhibitory input to both colour and brightness sensitive SCN cells. Using local pharmacological inhibition I then show that thalamic inputs supress specific features of the SCN light response originating with the contralateral retina, including colour discrimination. These data thus provide new insight into the ways that arousal signals reaching the visual thalamus could modulate sensory processing in the SCN. Together then, the work described in this thesis provides important new insight into sensory control of the circadian system and the underlying neural mechanisms.

Declaration

No portion of the work referred to in the thesis has been submitted in support of an application for another degree or qualification of this or any other university or other institute of learning

Copyright Statement

i. The author of this thesis (including any appendices and/or schedules to this thesis) owns certain copyright or related rights in it (the "Copyright") and s/he has given The University of Manchester certain rights to use such Copyright, including for administrative purposes.

ii. Copies of this thesis, either in full or in extracts and whether in hard or electronic copy, may be made only in accordance with the Copyright, Designs and Patents Act 1988 (as amended) and regulations issued under it or, where appropriate, in accordance with licensing agreements which the University has from time to time. This page must form part of any such copies made.

iii. The ownership of certain Copyright, patents, designs, trade marks and other intellectual property (the "Intellectual Property") and any reproductions of copyright works in the thesis, for example graphs and tables ("Reproductions"), which may be described in this thesis, may not be owned by the author and may be owned by third parties. Such Intellectual Property and Reproductions cannot and must not be made available for use without the prior written permission of the owner(s) of the relevant Intellectual Property and/or Reproductions.

iv. Further information on the conditions under which disclosure, publication and commercialisation of this thesis, the Copyright and any Intellectual Property and/or Reproductions described in it may take place is available in the University IP Policy (see http://documents.manchester.ac.uk/DocuInfo.aspx?DocID=487), in any relevant Thesis restriction declarations deposited in the University Library, The University Library's regulations (see http://www.manchester.ac.uk/library/aboutus/regulations) and in The University's policy on Presentation of Theses .

Contributions to Thesis

Chapters 2-5: Dr Timothy M. Brown (University of Manchester, Faculty of Life Sciences) wrote the LabView programs for control of the light stimuli during electrophysiological experiments and MATLAB programs for dissociating SCN neuronal responses to brightness and contrast.

Chapter 3: A subset of the single cells(~33%) contributing to data presented in in Figures 3.6-3.8 were provided by Dr Timothy M. Brown for inclusion in the dataset. Dr Frank Martial designed the light source for use in behavioural experiments. Dr David A. Bechtold provided the ibuttons for implantation to measure internal body temperature. Dr David A. Bechtold and Dr Alexander West implanted the ibuttons.

Acknowledgements

This PhD thesis would not have been possible without the help of many individuals.

Foremost, I would like to express my sincere gratitude to my PhD supervisor Tim Brown, who has helped me at every stage throughout my PhD. I appreciate the time and energy Tim has put into my work; without his help I certainly would not be where I am now.

I must also thank my advisor Rob Lucas for his support and guidance throughout my PhD and all members of the Brown/Lucas lab, past and present, who have all been such an invaluable source of knowledge and advice throughout my PhD.

Finally, I would like to say thank you to my family and friends, who have always been interested in and enthusiastic about what I've been doing. A special thank you goes to Graham whose support and encouragement, particularly towards the end of my PhD, is greatly appreciated.

At this point I would also to acknowledge the Biotechnology and Biological Sciences Research Council, who provided funding for this PhD.

Chapter 1: General Introduction

All living organisms possess endogenous time-keeping mechanisms known as circadian clocks ("circa"= about "dies"= day). The presence of a circadian clock increases an organism's chance of survival by allowing it to anticipate oncoming changes within the natural environment. Under natural conditions, the clock is synchronised (entrained) to a 24 hour period by exogenous environmental signals known as *zeitgebers* (Roenneberg and Merrow, 2005, Hastings, 1991), allowing organisms to optimise behaviour and physiology to the appropriate time of day (Kalsbeek et al., 2006). Under constant conditions, where these external signals are absent, circadian clocks exhibit a 'free-running' period of approximately 24 hours (24.1 hours in man). Accordingly, they slowly lose synchronicity with the external environment (Aschoff, 1965, Golombek and Rosenstein, 2010).

In order to entrain to local time, circadian clocks thus require sensory input pathways to report daily environmental variations. For the vast majority of species, light provides the most reliable indicator of time of day, with ambient illumination (irradiance) varying up to nine decades between day and night (Lucas et al., 2012). Accordingly, light is widely recognised to be the most important cue for circadian entrainment. In mammals, this influence of light is primarily mediated by direct retinal input to a central master clock located in the suprachiasmatic nuclei (SCN) of the hypothalamus, which in turn coordinates rhythmic activity across the brain and body (Moore, 1983, Moore, 1995, Moore and Eichler, 1972, Stephan and Zucker, 1972).

Since our biological day and night is determined by the entrainment of the SCN to environmental cues, sudden alterations in environmental exposure can change the phase of the clock to a point where biological time no longer matches with that of the environment. For example, most of us have experienced 'jet-lag' at one time or another, which results because the SCN clock requires several days to re-synchronise to the altered timing of day and night when crossing multiple time zones (Aschoff, 1965). While jet-lag is generally viewed as an inconvenience, long-term circadian desynchrony can have adverse effects on health. Shift-workers are exposed to conflicting circadian timing cues (social vs environmental) which can lead to psychological and physiological difficulties and loss of

productivity in the workplace (Rosekind et al., 2010). More seriously, there are also links between long term shift work and metabolic disorder (Tucker et al., 2012), increased risks of stroke (Brown et al., 2009) and an increased risk of cancers (Schernhammer et al., 2001, Schernhammer et al., 2003, Schernhammer et al., 2011).

1.1 Light parameters of the photic environment

As discussed above, light is considered to be the most important entraining signal for the mammalian circadian clock. As is the case for more conventional aspects of vision, in mammals, the eyes are the origin of light input to the circadian clock. Indeed, if the eyes are removed there is no pathway for light to reach the SCN and entrainment of the clock is abolished (Freedman et al., 1999). To better understand how light influences the circadian system, then, it is first useful to consider what parameters of the photic environment may be specifically important for the clock and then how the retina extracts such signals from the environment.

1.1.1 Timing

The sensitivity of the circadian system to light varies throughout the circadian day. A simple way of assessing the effects of light on the circadian system is to examine the activity level of an organism: locomotor function is under circadian control, with nocturnal organisms (e.g. mice) displaying a higher level of activity during the night and diurnal organisms being more active during light hours. The wheel-running activity of an organism can be used to quantify the effect of a light stimulus upon the phase of the circadian rhythm by counting the number of revolutions of the wheel in relation to the time of the circadian day (CT).

Free-running rodents housed in constant dark (DD) exhibit no phase shifts in locomotor activity when exposed to a photic stimulus in the subjective day (CT 0-12) (Pittendrigh and Daan, 1976). If stimulated early in the subjective night (CT 12-18; Figure 1.1, A), there is a phase delay in the timing of the circadian rhythm (Van Den Pol et al., 1998) and upon

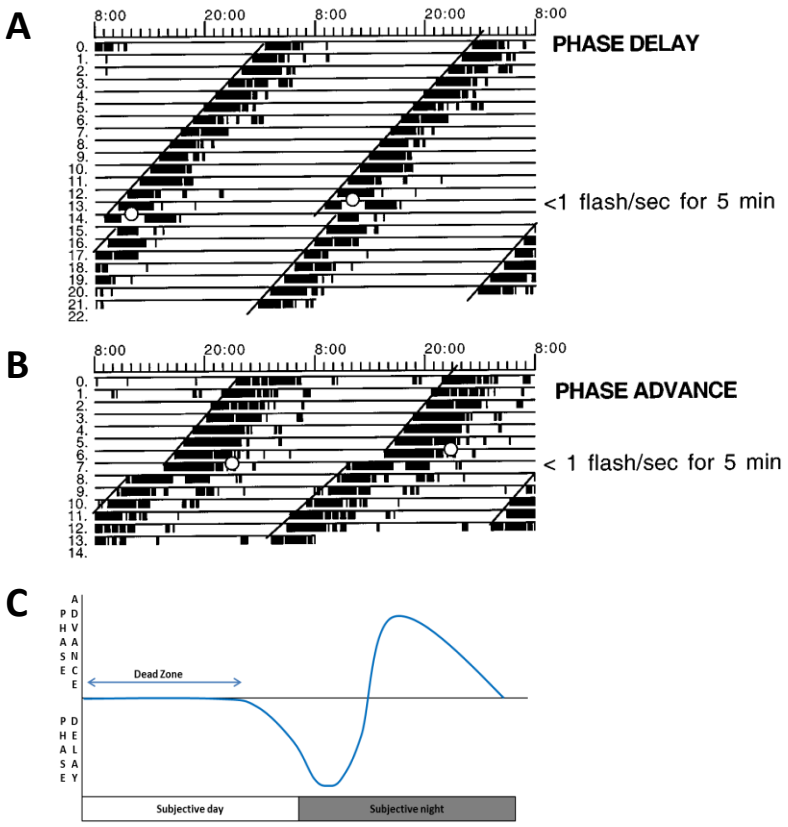

Figure 1.1: The circadian response to light depends of time of day (Van Den Pol et al., 1998).

(A&B) Actograms displaying the effect of light flashes on mouse locomotor activity at different points in circadian time (CT). (A) 2ms light flashes at 5 second intervals for 5 minutes at CT 12 results in a phase delay. (B) 2ms light flashes at 5 second intervals for 5 minutes at CT 18-14 results in a phase advance. (C) The phase response curve. Light presented at different times of the circadian day can either advance or delay the phase of the circadian clock. Light presented during the 'dead zone' (the subjective day)(Pittendrigh and Daan, 1976) does not invoke a phase shift in either direction. A light stimulus in the early subjective night produces a delay in phase and during late night, a photic stimulus results in a phase advance. The shape of this curve is conserved across a wide range of organisms (Kennaway, 2004).

stimulation late in the night (CT 18-24 Figure 1.1, B), a phase advance is observed (Van Den Pol et al., 1998).

Plotting change in circadian phase vs. the timing of the light stimulus thus produces a characteristic phase response curve (PRC) (Pittendrigh and Daan, 1976, Johnson, 1999, Kennaway, 2004). A typical PRC (Figure 1.1, C) features a 'dead zone' where there is no shift in phase in response to photic stimulus (Pittendrigh and Daan, 1976, Kennaway, 2004) due to the insensitivity of the circadian clock to photic stimulus during the subjective day. While the relative amplitude of advance and delay portions of the PRC varies between organisms, the general shape of the curve is qualitatively similar across a wide range of both diurnal and nocturnal species (Kennaway, 2004). This basic mechanism then, whereby light exerts opposing effects upon circadian phase depending on time of day, is a major determinant of how organisms synchronise their internal clocks with the solar cycle.

1.1.2 Irradiance

Although the mechanism discussed above plays a key role in appropriately adjusting clock timing in response to light detected around dawn and dusk, such a mechanism would be of no use without a way of also distinguishing photic signals that are indicative of time of day from those that are not. The large daily variation in the irradiance (brightness) of light has been widely considered to provide the most important cue of this nature. Indeed, studies of the sensory properties of the photoentrainment pathway in nocturnal rodents (Takahashi et al., 1984, Nelson and Takahashi, 1991, Nelson and Takahashi, 1999, Lall et al., 2010) revealed two key properties consistent with this role: 1) Circadian rhythms in locomotor activity are relatively unaffected by dim light (equivalent to starlight), protecting the clock from aberrant resetting during night-time activity; 2) The circadian system appears to act as a 'photon-counter', producing a graded response that effectively integrates the total amount of ambient illumination experienced over extended epochs (at least 1h). Thus, light pulses of different durations containing equivalent numbers of photons illicit an essentially identical response.

Consistent with this photon-counting property of the circadian system at the whole animal level, early electrophysiological investigations of the rodent clock clearly revealed the presence of large numbers of SCN cells that encode irradiance (Meijer et al., 1986). Although such light responsive SCN cells can be light-activated or light-suppressed (Meijer et al., 1986, Groos and Mason, 1978), the mean discharge rate of both types is indicative of the level of ambient illumination presented to the eye. Moreover, subsequent work (discussed in more detail below) confirms that the integrated spike rate of such irradiance coding cells is indeed highly predictive of the magnitude of circadian phase shifts (Brown et al., 2011). As such, it is clear that information about overall levels of illumination is indeed one of the principle sources of information about external time available to the circadian system.

1.1.3 Contrast

In addition to the slow changes in irradiance over the solar day, as an organism moves and surveys its environment, the quantity of light entering the eye can change very rapidly in comparison to the slow changes in background illumination encoding the day/night cycle. Detection of such visual 'contrast' is the foundation of spatial vision, whereas, traditionally, such signals have been viewed as irrelevant for the circadian system, effectively averaged out by the long integration time of the circadian light response mentioned above.

In recent years, however, interest in the idea that visual contrast might also influence the clock has gained some ground with demonstrations that under at least some circumstances (e.g. brief light flashes), the normal photon-counting properties of the clock breakdown (Vidal and Morin, 2007, Lall et al., 2010, Najjar and Zeitzer, 2016). Consistent with this view, closer examination of the electrophysiological response of irradiance coding SCN neurons reveals a biphasic profile, with a large transient increase in firing which reduces to a smaller, sustained response (Brown et al., 2011). Thus, rapid fluctuations in light levels are in fact predicted to evoke an overall greater degree of activation within the SCN relative to a temporally uniform light stimulus. Moreover, it has also emerged that at least some light-responsive neurons in the SCN do not encode irradiance at all and in fact only respond to rapid light:dark transitions (Brown et al., 2011).

At present it is unclear whether these 'transient' cells contribute to the circadian entrainment mechanism or are instead involved in other light-dependent changes in physiology. Nonetheless, together, there is clear evidence to believe that under the right circumstances, visual contrast can influence the magnitude of circadian responses and/or related physiological/behavioural changes.

1.1.4 Wavelength/colour

In addition to fluctuations in intensity, organisms will experience wide variations in the spectral composition of incident light across the day: either due to differences in the reflectance of objects in the environment or due to daily variations in light quality due to filtering in the upper atmosphere. Indeed, during 'twilight', there is an increase in the relative availability of short wavelength light, due to the increased amount of ozone that indirect sunlight must pass through to reach the Earth's surface (Hulbert, 1953).

Since these daily changes in the spectral composition of daylight should be relatively unaffected by weather patterns, and occur during the most important portion of the day for entrainment, the idea that organisms might use these to regulate their biological clock has been around for some time (Roenneberg and Foster, 1997). There have been a number of reports suggesting that various species ranging from the single-celled dinoflagellate *Gonyaulax polyedra* (Roenneberg, 1996) to birds (Pohl, 1999) and fish (Pauers et al., 2012) use daily changes in the spectral composition of light as a circadian timing cue. By contrast, the possibility that such signals might regulate the mammalian clock has not been investigated in detail.

In this regard, it is important to note that there are two possible ways that variations in the spectral composition of light could influence circadian responses. Firstly, since the biological photoreceptors used to detect light are not equally sensitive to all wavelengths, apparent 'brightness' will vary depending on what mixture of wavelengths the light contains (see Takahashi et al., 1984). Although such a possibility could have a major impact on responses to artificial light, the broad spectrum of wavelengths contained in natural

daylight suggest this is unlikely to have a major impact under a natural setting. Secondly, specific mechanisms for discriminating changes in colour from changes in brightness (involving multiple photoreceptors) could have much more of an influence. Effectively studying the possibility that colour provides an important source of information to the circadian system first then requires knowledge of the properties of the biological photoreceptors providing input to the clock.

1.2 Photic input to the circadian system

As discussed above, the eye is the origin of visual input to the mammalian circadian clock and light detection by the eye originates with photoreceptor cells. These absorb light and transmit chemical signals that are processed by a network of cell types within the retina before reaching the retinal ganglion cells (RGCs) that relay these signals to the brain via the optic nerve (Purves et al., 2001). In total then, conventional vision involves 5 types of cell; photoreceptors, bipolar cells, horizontal cells, ganglion cells and amacrine cells (Figure 1.2). These basic features are common to all mammalian retinas. However, insofar as the principal model organism used for circadian studies is now mice, where possible the discussion below focuses most specifically on details of the mouse retina.

1.2.1 The outer retina: rods and cones

Photoreceptors are divided into two classes: rods and cones. Rod and cone photoreceptors have a simple structure consisting of outer and inner segments, a cell body and an axon that synapses onto bipolar and horizontal cells. The outer segment of rods and cones is densely packed with discs containing the light responsive proteins (opsins) (Carter-Dawson and LaVail, 1979). The outer segments of rods and cones differ in shape. In cones, the outer segment is conical in shape and the discs remain attached to the photoreceptor outer membrane. The outer segment of rods is cylindrical and the photoreceptor discs exist separately from each other. These photosensitive discs are found close to the retinal epithelium and therefore in order for photons to be absorbed, they must first pass through the non-light sensitive elements of the retina before reaching the photopigment located in rods and cone cells (Purves et al., 2001).

The distribution of rods and cones varies between species (Ahnelt and Kolb, 2000). The retina of mice (and other nocturnal rodents) is rod dominated (Carter-Dawson and LaVail, 1979, Jeon et al., 1998), making the murine retina adapted for vision at low light (scotopic) levels. The photoreceptors in mice are evenly distributed across the retina, rendering them adapted to efficiently sample the entire visual scene (Huberman and Niell, 2011). Primates on the other hand are adapted to allow high acuity vision (i.e. discriminating fine detail) with 99% of their cones residing in the 'fovea', a specially adapted structure that occupies only 1% of the retinal area (Perry and Cowey, 1985).

1.2.1.1 Rod & Cone opsins

Opsins are part of the GTP-binding protein-coupled receptor (GPCR) superfamily of proteins (Fredriksson et al., 2003). GPCRs are membrane-bound proteins with seven transmembrane domains that form a photosensitive compound when bound to a retinal-based chromophore. As discussed above, like any other biological photoreceptor, opsins are not equally sensitive to all wavelengths of light and instead exhibit a characteristic absorption profile with a distinct wavelength of maximum spectral sensitivity (λmax). Rhodopsin is the only photopigment present in the light-sensitive discs of rod cells and has a λmax of around 500nm. In contrast, cone-opsins vary between organisms in both the number of opsins present and their spectral sensitivity.

Humans and most old-world primates possess three cone opsins within the retina: a short- (blue, λmax=426nm), medium- (green, λmax=530nm) and long wavelength-sensitive (red, λmax=552nm) pigment. Most other mammals, however, possess only possess two types of cone opsin: a short wavelength-sensitive opsin (SWS/UVS) and a medium (MWS) or long wavelength-sensitive (LWS) opsin (in mice: UVS, λmax=360nm; MWS; λmax=511nm respectively) (Calderone and Jacobs, 1995, Szél et al., 1992, Lall et al., 2010). The retinal locations of cones expressing these opsins in the mouse has been well described in literature (Szél et al., 1992, Röhlich et al., 1994, Applebury et al., 2000, Glosmann and Ahnelt, 1998, Haverkamp et al., 2005). Unusually, the majority of mouse cone cells co-express both M- and S-opsins (Applebury et al., 2000, Nikonov et al., 2006), with both of

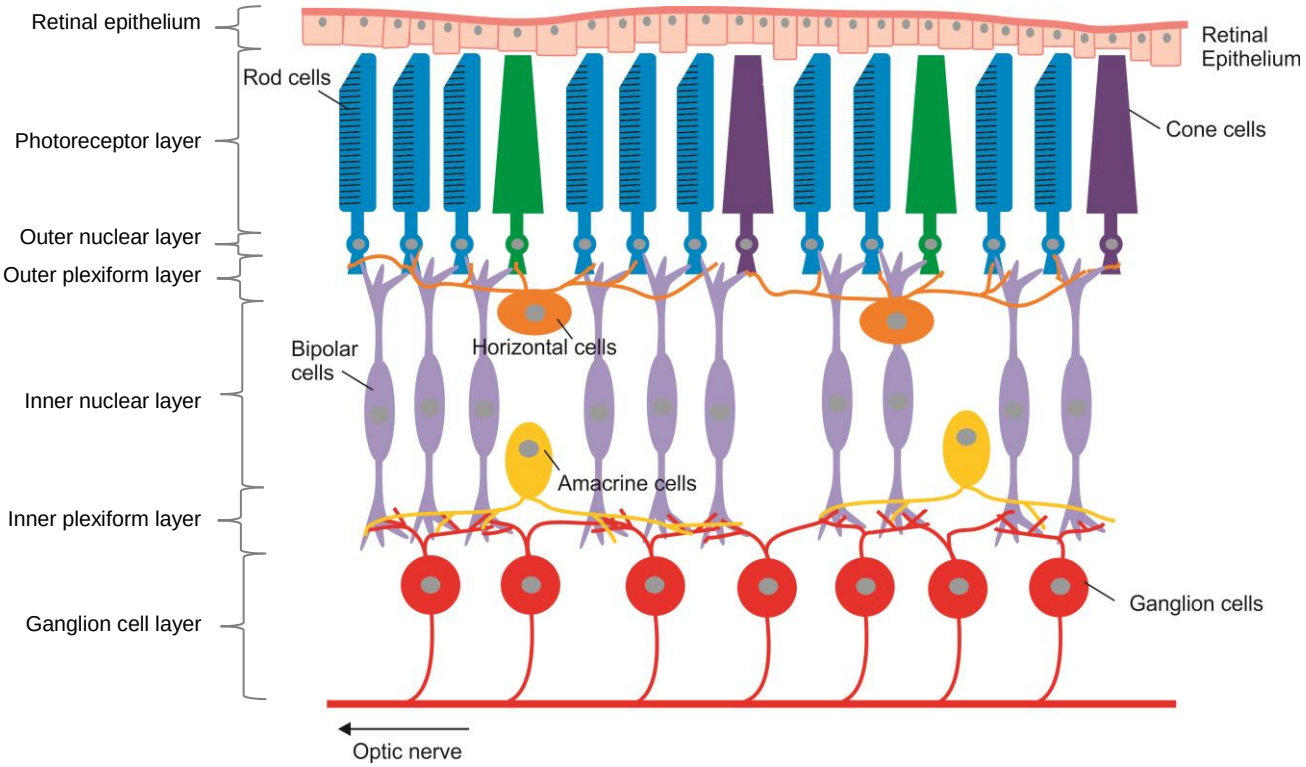

Figure 1.2: The structure of the retina

A cross-section of the retina demonstrating the layout of the retinal circuitry involved in conventional and non-image forming vision. The most direct pathway for light to reach the brain involves three cells: a photoreceptor, a bipolar cell and a ganglion cell. Horizontal and amacrine cells are responsible for lateral transmission of signals within the retina. In order for light to reach the photoreceptor outer segments where photons are absorbed, it must pass first through the ganglion and bipolar cell layers. 'Inner' refers to being close to the centre of the eye and 'outer' is away from the centre, towards the eye periphery.

the co-expressed opsins capable of driving transduction in the same cone (Nikonov, 2005). In particular, almost all cones express M-opsin, but in a decreasing gradient from dorsal to ventral regions of the retina (Applebury et al., 2000). S-opsin expression remains constant across the retina except in the far dorsal region where S-opsin expression is suppressed, leaving cones exclusively expressing M-opsin (Applebury et al., 2000). Interspersed with these opsin co-expressing cones, a subset of cones (~3-5% of the total population) exclusively express S-opsin and are present in equal numbers across the dorsal-ventral axis of the retina (Haverkamp et al., 2005).

1.2.1.2 Phototransduction

The role of the photoreceptors is to convert photic information into electrical signals that can be communicated to the brain. This process is known as phototransduction.

1.2.1.2.1 Activation of the transduction cascade

Unlike other neurons, rods and cones do not fire actions potentials. Instead, they signal using small, graded changes in membrane potential, becoming hyperpolarised in response to a light stimulus (Bortoff, 1964, Werblin and Dowling, 1969). In the dark, the resting membrane potential of a photoreceptor is maintained at ~40mV by a variety of mechanisms which act to regulate the concentrations of Na^+, Ca^{2+} and K^+ ions on either side of the plasma membrane (Cervetto et al., 1989):

- Na^+/ $Ca^{2+}K^+$ pumps that exchange extracellular Na^+ for intracellular Ca^{2+} and K^+ (Schnetkamp, 2004).
- cGMP gated channels that transport Na^+ and Ca^{2+} into the cell (Molday and Molday, 1998).
- Na^+/ K^+ pumps that actively transport Na^+ out of the cell and K^+ in (Ames et al., 1992).
- Ungated K^+ 'leak' channels generating a continuous outwards flow of K^+ ions

In the dark, photoreceptors are relatively depolarised (much more so than neurons) and have a relatively high concentration of intracellular calcium (Barnes and Kelly, 2002), triggering the tonic release of the neurotransmitter glutamate onto downstream cells (Schmitz and Witkovsky, 1997).

The first stage in transduction is the absorption of a photon by the photopigment in the photoreceptor discs (in rods this is rhodopsin –Rh; Figure 1.3). As discussed above, opsins are GPCRs. In darkness, the rhodopsin is inactive, bound to the chromophore *11-cis* retinal that regulates its function. Upon absorption of a photon, the *11-cis* retinal is photoisomerised to the *all-trans* state, resulting in a conformational change in the opsin that results in its activation (Farahbakhsh et al., 1993, Farrens et al., 1996). It is this active form of the opsin (metarhodopsin-Rh*; Figure 1.3) that triggers the transduction cascade by allowing binding of the G-protein transducin (Okada et al., 2001).

Upon binding to metarhodopsin, transducin exchanges GTP for GDP to form a GTP-transducin complex (Kühn et al., 1981). This activates the enzyme cGMP phosphodiesterase (PDE) which hydrolyses cGMP to 5'-GMP (Fesenko et al., 1985, Haynes and Yau, 1985, Baylor, 1996), closing cGMP-gated ion channels reducing intracellular Ca^{2+} levels. Continuous K^{+} leakage hyperpolarises the cell and closes voltage gated Ca^{2+} channels that further lowers intracellular Ca^{2+} (Barnes and Kelly, 2002). Reduction in calcium levels inhibits the release of glutamate, signalling to downstream retinal neurons.

1.2.1.2.2 Amplification of the transduction cascade

An important feature of the phototransduction cascade is that it undergoes extensive signal amplification at various points during the cascade. The activation of a single rhodopsin molecule can interact with around 800 transducin molecules (Vuong et al., 1984). Although a single transducin only activates a single PDE molecule, each of these hydrolyses up to six cGMP molecules, resulting in the closure of hundreds of ion channels (Burns and Baylor, 2001). This amplification increases the sensitivity of photoreceptor, enabling them to respond to small changes in irradiance. Indeed, the most sensitive

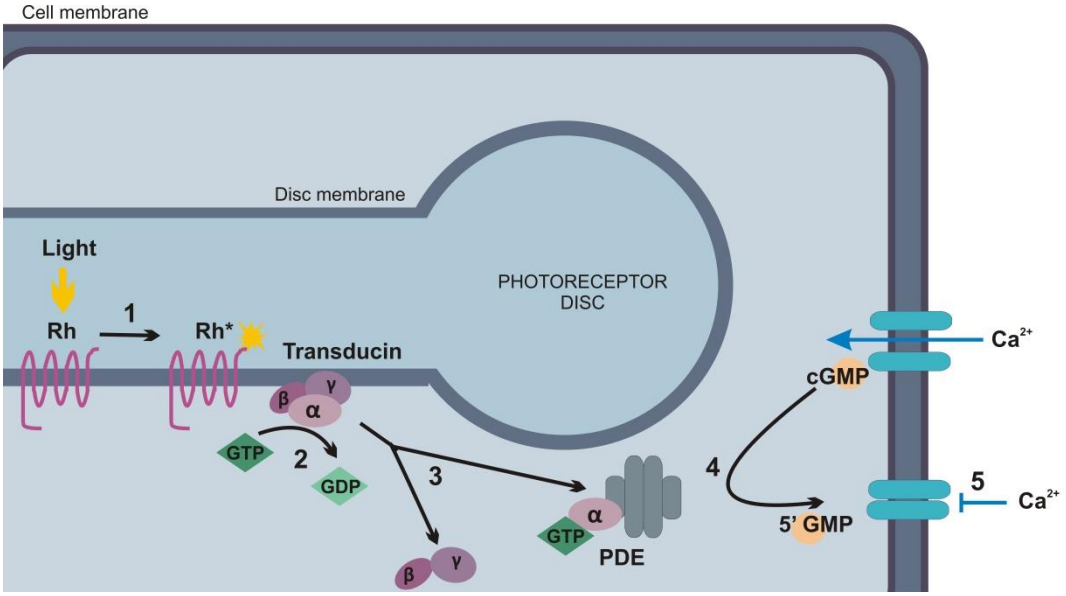

Figure 1.3: The phototransduction cascade.

1. The absorption of photon isomerises *11-cis* retinal into *all-trans* retinal. This causes a conformational change in rhodopsin (Rh), forming metarhodopsin (Rh*). **2.** This activates transducin, which exchanges GDP for GTP. **3.** The activated transducin activates cGMP-phosphodiesterase (PDE). **4.** PDE hydrolyses cGMP to 5'GMP, reducing intracellular cGMP levels. **5.** This closes cGMP-gated cation channels in the photoreceptor membrane, preventing influx of cations (Adapted from Purves et al 2001).

mammalian photoreceptors (rods) are capable of signalling the absorption of a single photon (Sharpe and Stockman, 1999).

1.2.1.2.3 Deactivation of the transduction cascade

Metharhodopsin itself is phosphorylated by rhodopsin kinase, reducing the action of the transduction cascade (Xu et al., 1997). However, complete inactivation of the cascade requires both phosphorylation of metarhodopsin and binding of the protein arrestin (Bownds et al., 1972, Pulvermüller et al., 1993, Bennett and Sitaramayya, 1988, Kühn, 1978), which prevents transducin binding. The time course of phosphorylation and arrestin binding determines the lifetime of metarhosopsin and therefore the light response (Pepperberg et al., 1992, Rieke and Baylor, 1998).

In order for another photon to be reabsorbed, the photopigment must be regenerated and *all-trans* -retinal converted back into *11-cis*-retinal. *All-trans*-retinal is converted to *all-trans*-retinal by *all-trans*-retinol dehydrogenase (Haeseleer et al., 1998). This leaves the photoreceptor discs and is transported to the retinal pigment epithelium (RPE), where it is re-isomerised back into *11-cis*-retinal (Palczewski and Saari, 1997). 11-cis-retinal is transported back into the discs where it recombines with the dephosphorylated opsin (Crouch et al., 1996).

1.2.1.2.4 Light adaptation

Large variations in brightness occur throughout the solar cycle. In order to function, cells within the retina must therefore adapt to allow vision across all of these conditions. At low light levels, photoreceptors are at their most sensitive. As light levels increase, the sensitivity of photoreceptors decreases, preventing saturation and increases the range of light levels at which photoreceptors can function - the process of light adaptation. Both rods and cones exhibit these changes in sensitivity under constant light, to preserve their ability to respond to visual contrast (Nakatani et al., 1991, Kraft et al., 1993, Schneeweis

and Schnapf, 1999). Intracellular Ca^{2+} has been implicated as a major factor in multiple mechanisms that mediate light adaptation.

One mechanism of light adaptation involves the Ca^{2+}-dependent regulation of guanylate cyclase (Lolley and Racz, 1982, Koch and Stryer, 1988). Guanylate cyclase is a membrane-bound enzyme that synthesises cGMP. As previously discussed, light decreases intracellular Ca^{2+} concentrations in the photoreceptor and induces the hydrolysis of cGMP. Simultaneously, this decrease in concentration also increases the activity of guanylate cyclase (Lolley and Racz, 1982, Koch and Stryer, 1988), counteracting this degradation. This raises cGMP levels and cGMP channels re-open. Whilst this is occurring, decreased Ca^{2+} increases the affinity of the cGMP channels to cGMP binding. The action of cGMP-gated channels is also modulated by the Ca^{2+}-binding protein calmodulin (Hsu and Molday, 1993). The light-associated decrease in Ca^{2+} also increases the probability of opening the cGMP channels (Chen et al., 1994, Grunwald et al., 1998, Grunwald and Yau, 2000). These mechanisms act to reduce the sensitivity of cGMP-gated channels to additional phototransduction events.

A second adaptation pathway involves the modulation of rhodopsin kinase activity. At high calcium levels, rhodopsin kinase is inhibited by a protein known as recoverin (Kawamura, 1993, Kawamura et al., 1993), preventing metarhodopsin phosphorylation. Light and the associated decrease in intracellular [Ca^{2+}], removes the inhibitory influence of recoverin and consequently shortens the lifetime of metarhodopsin (Chen et al., 2010).

The relative contribution of each of these mechanisms to light adaptation has been studied (Koutalos and Yau, 1996, Nikonov et al., 2000). At dim-moderate conditions, all adaptation can be attributed to the regulation of guanylate cyclase, with metarhodopsin phosphorylation contributing in bright conditions (Koutalos and Yau, 1996). A second study attributed all light adaptation to the turnover of cGMP and the regulation of guanylate cyclase (Nikonov et al., 2000). Therefore guanylate cyclase is responsible for the majority of light adaptation with the other mechanisms providing a minor, supporting role.

1.2.1.3 Colour discrimination

It is the expression of multiple cone opsins that form the basis of colour vision. As discussed above, humans are trichromatic, and possess cones that express one of three opsins (short, medium and longwave) with overlapping spectral sensitivity. Importantly, these individual cone opsins are themselves unable to distinguish differences in the amount vs. differences in spectral content of light. Instead, it is only by comparing the relative activation of each cone opsin that the retina is able to extract information about colour.

The ability to discriminate colour thus arises as an emergent property of the retinal networks processing cone signals (discussed in more detail below). Surprisingly, the full details of these processing steps are still controversial (e.g. see Marshak and Mills, 2014 for review). It nonetheless remains clear that a key step is the emergence of antagonistic responses to stimulation of the various cone types in the retinal ganglion cells (RGCs), providing a neural substrate for an early theoretical model of colour vision: the opponent process theory (Ewald Herring, 1920). This theory suggested that colour vision resides with neural pathways sensitive to one of three opposing colour pairs: black-white, blue-yellow and red-green. Activation of one member of the opsin pair inhibits the action of the other and so no two members of one pair can be seen at one time (See Hurvich and Jameson, 1957 for review).

Hence, we now know that our own ability to distinguish red-green colours involves comparisons between activation of the medium and long-wavelength sensitive cones that are conveyed to the brain by so-called midget ganglion cells (Dacey, 1999). Similarly, the blue-yellow sensitive ganglion cells allow us to differentiate short vs. longer wavelength light (the yellow side of this axis being comprised by an additive mixture of signals from medium and long-wavelength sensitive cone opsins). This is how we are able to see yellow, even though we do not possess a specific yellow cone. Finally, the ‘achromatic’ black-white colour axis essentially encodes the brightness (or perhaps more accurately the lightness) of the stimulus and provides the fine detail of an image. This achromatic channel primarily involves the addition of the signals from medium+long-wavelength sensitive cones (Goldstein, 2013).

As discussed above, however, most mammals differ from this scheme, being only dichromatic (see Peichl, 2005 for review). In particular, the ability to discriminate red-green colour appears to be a relatively recent emergence in mammalian evolution. Thus the dominant form of colour discrimination among mammals is the ability to distinguish short vs. long wavelength light (analogous to our own blue-yellow colour channel).

In the specific case of mice, despite containing the two opsin types necessary for this form of colour discrimination, one might imagine that the extensive cone opsin co-expression in the mouse retina (Applebury et al., 2000, Nikonov et al., 2006) presents a substantial impediment to the colour opponent mechanism. In fact, however, the retinal circuitry required to support colour discrimination is certainly present in mice (reviewed in Marshak and Mills, 2014), and RGCs (and other retinal cells) displaying colour opponent responses have indeed been identified in this species (Ekesten and Gouras, 2005, Chang et al., 2013).

1.2.2 Signal processing within the retinal network

After photon absorption within the photoreceptor and resulting phototransduction cascade, the subsequent reduction in glutamate release modulates the activity of downstream cells. An overview of the key processing steps within the retina is detailed below:

1.2.2.1 Bipolar cells

Bipolar cells form an essential intermediary in the export of photoreceptor signals from the retina. In mice, rods signal to a single class of bipolar cells, whereas cones signal to at least nine different types of bipolar cells (Ghosh et al., 2004). Cone bipolar cells can be further subdivided into two categories: ON-cells that depolarise in response to light and OFF-cells that hyperpolarise in response to light (Kolb et al., 1981).

It is the presence of different classes of glutamate receptors that determine whether a bipolar cell is ON or OFF. ON-bipolar cells express the metabotropic glutamate receptor mGluR6 (Nomura et al., 1994, Masu et al., 1995, Vardi et al., 2000) and thus respond to reduced levels of glutamate by opening cation channels (Slaughter and Awatramani, 2002) resulting in cell depolarisation (Sharma et al., 2005). OFF-bipolar cells express AMPA-type ionotropic glutamate receptors (Brandstätter et al., 1997, Qin and Pourcho, 1999, Hack et al., 2001, Haverkamp and Wässle, 2000, Haverkamp et al., 2001) and respond to reduced levels of glutamate by closing cation channels, leading to cell hyperpolarisation. These distinct properties thus provide an important step in the extraction of feature related information from the photoreceptors. For example, ON/OFF bipolar cells that selectively sample from specific cone types form one of the key retinal mechanisms supporting the emergence of colour opponency in RGCs (Marshak and Mills, 2014).

By contrast with cones, rods only have one bipolar cell: the rod ON-bipolar cell. In order to convey photic information over dim-moderate light levels, rods signal via two distinct retinal circuits. Under scotopic conditions, signals pass through the bipolar pathway. The rod ON-bipolar cells then signal to RGCs via amacrine AII cells (Sharpe and Stockman, 1999). At mesopic light intensities, however, rods bypass the rod ON-bipolar cells and instead convey signals directly to cones through gap junctions, allowing rods to transmitting signals to RGCs via the cone bipolar cells (Sharpe and Stockman, 1999, Altimus et al., 2010, Belenky et al., 2003, Bloomfield and Dacheux, 2001).

1.2.3 Retinal ganglion cells

There are 10-15 types of RGCs present in the retina, characterised by their unique morphology and/or feature selectivity (Masland, 2001). Importantly, however, retinal input to the SCN arises almost exclusively from a rare subset of these cells (<5% of all RGCs) that are intrinsically photoreceptive (Berson et al., 2002, Hattar et al., 2002). Such 'ipRGCs' can be distinguished from conventional RGCs by the presence of the photopigment melanopsin (Gooley et al., 2010, Hattar et al., 2002); a light-activated GPCR (Provencio et al., 1998, Newman et al., 2003) that maximally absorbs photons (λmax) at 480nm (Panda et al., 2005). These melanopsin-expressing ganglion cells project to a variety of brain areas in

addition to the SCN, most notably the intergeniculate leaflet (IGL) and the olivary pretectal nucleus (OPN), the structure responsible for driving the pupillary light reflex (Baver et al., 2008, Hattar et al., 2002, Hattar et al., 2006, Ecker et al., 2010). A characteristic feature of the central nuclei most heavily targeted by ipRGCs is a specific role in physiological responses that are dependent on an accurate assessment of levels of environmental illumination (full range of targets summarised in figure 1.4).

1.2.3.1 Melanopsin

Unlike rods and cones, ipRGCs lack specialised structures for photon absorption. Instead, melanopsin protein is expressed throughout the ipRGCs cell body and processes forming a photoreceptive next across the retina (Provencio et al., 2002). Also unlike rods and cones, photon absorption by melanopsin leads to cell depolarisation, allowing ipRGCs to fire action potentials and signal light detection to the brain (mechanisms of melanopsin phototransduction are discussed below). Arguably the most characteristic feature of the melanopsin photoresponse however is its incredibly slow kinetics. Hence, when simulated with light, synaptically isolated ipRGCs respond with latencies of up to 1 minute and can continue to fire for several minutes after the light stimulus has ended (Berson et al., 2002).

By contrast, the melanopsin photoresponse shows an impressive efficiency, capable of signalling the absorption of a single photon of light with a large and sustained response, greater than that of rods (Do et al., 2009). This is achieved by maintaining the membrane potential close to the threshold for spike firing so that a small change in current can result in the firing of action potentials (Do et al., 2009). This remarkable phototransduction efficiency is counterbalanced, however, by the very low photon capture probability for an ipRGC (10^6 fold-less than that of rods), explaining the widely reported low sensitivity of melanopsin-dependent signalling (Do et al., 2009). Together, then, these properties seem to specialise melanopsin for encoding information about a very specific feature of the light environment: the relatively slow changes in ambient light intensity encountered around the daytime-twilight transition.

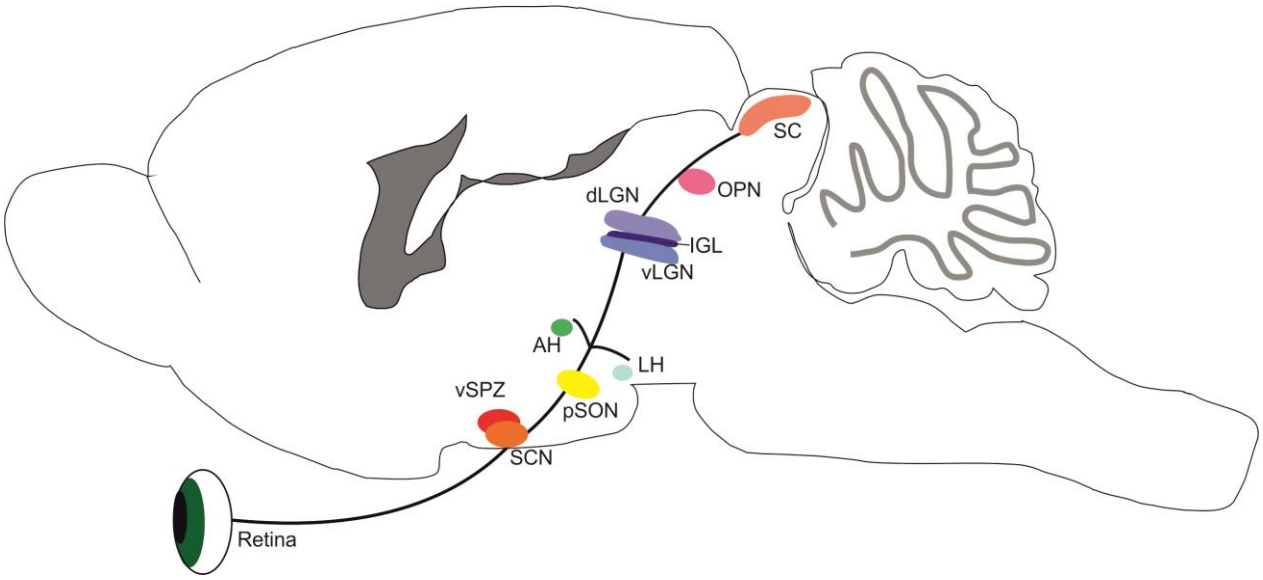

Brain Region		Function
SCN	Suprachiasmatic nucleus	Circadian entrainment
vSPZ	Ventral subparaventricular zone	Circadian regulation of sleep and body temperatures
pSON	Peri-supraoptic nucleus	Neuroendocrine organ
AH	Anterior Hypothalamus	Circadian regulation of sleep and body temperatures
LH	Lateral Hypothalamus	Energy homeostasis and arousal
vLGN	Ventral lateral geniculate nucleus	Visuomotor functions, brightness discrimination, the pupillary light reflex
IGL	Intergeniculate leaflet	Integration of photic and non-photic entrainment cues
dLGN	Dorsal lateral geniculate nucleus	Image forming vision
OPN	Olivary prectctal nucleus	The pupillary light reflex - controlling pupil size
SC	Superior colliculus	Visuomotor functions – controls eye and head movements

Figure 1.4: The targets of ipRGC projections.

Top: A summary schematic of the brain regions innervated by ipRGCs. Adapted from Berson (2003). Bottom: A list of these areas with their abbreviations and functions (Hattar et al., 2006)

It is also important to note here that the mouse melanopsin gene is alternatively spliced forming two distinct isoforms, a short (OPN4S) and a long (OPN4L) isoform (Pires et al., 2009, Hughes et al., 2012). These two isoforms both form fully functional photopigments in the retina but it is so far unclear whether how these differ in terms of functional properties. What is clear is that these two isoforms appear to differentially contribute to distinct aspects of non-image forming (NIF) responses: the short isoform appears to play a greater role in pupillary responses whilst the long isoform plays a greater role in direct effects of light on behavioural activity. It will thus be important in the future to determine whether these differing roles represent a difference in the fundamental nature of the resulting light response and/or differences in the relative expression of these two isoforms in subsets of ipRGCS with different anatomical targets.

1.2.3.1.1 Melanopsin Phototransduction

Based on sequence homology, melanopsin differs from the mammalian rod and cone opsins in that it bears much greater similarity to the rhabdomeric invertebrate opsins. As discussed above, a key feature of vertebrate phototransduction is the release of *all-trans*-retinal upon photon absorption, with recovery of photosensitivity requiring the regeneration of *11- cis*-retinal in cells of the retinal pigment epithelium (RPE). By contrast, the rhabdomeric opsins of invertebrates are bistable. Hence, the activated meta-state of invertebrate phototransduction is stable and these proteins possess a photoisomerase activity that is used to regenerate *11-cis*-retinal and terminate signalling (Hillman et al., 1983). Thus, while vertebrate transduction only uses photons to drive the activation of photopigments, invertebrate transduction exploits photons to drive both activation and regeneration pathways (Kiselev and Subramaniam, 1994).

The mechanisms behind melanopsin phototransduction remain elusive. However, in line with its homology to the invertebrate photopigments, melanopsin has been reported to utilise transduction mechanisms typical of invertebrate rhabdomeric photopigments (Isoldi et al., 2005) which use light to regenerate *11-cis*-retinal in an arrestin-independent manner (Pepe and Cugnoli, 1992, Kiselev and Subramaniam, 1994). For example, expression of melanopsin (Melyan et al., 2005, Panda et al., 2005) in *in vitro* cell cultures conveys light

responsiveness to cells in the presence of *11-cis*- and *all-trans*-retinal. Additionally, after a saturating light pulse, the retinal composition of the photoproduct still contains *11-cis*-retinal in significant amounts, indicating that melanopsin can convert between *11-cis*- and *all-trans* retinal to generate a photosteady state mixture (Matsuyama et al., 2012). Moreover, melanopsin-dependent light responses *in vitro* are reportedly restored after bleaching by stimulation using long wavelength light unsuitable for direct photoactivation (Mure et al., 2007, Mure et al., 2009), further suggesting that melanopsin may be bistable. Importantly, however, subsequent work in rodless coneless (rd/rd cl) mice found no evidence that pre-treating with long wavelength light has any significant effect upon melanopsin sensitivity to photic stimuli (Brown et al., 2013), indicating that the findings above may not reflect melanopsin bistability. Indeed, more recent work suggests that melanopsin is in fact 'tristable', existing in an equilibrium of three isoforms with similar spectral sensitivity (Matsuyama et al., 2012, Emanuel and Do, 2015): two inactive states (λmax: 453 and 471nm) and an active signalling 'meta' state (λmax: 476nm).

It would therefore appear that mammals possess both bistable/tristable (melanopsin) and bleachable opsins (rods and cones) and that there is functional division between opsins most associated with image and non-image forming vision. While the functional impact of melanopsin bistability/tristability remains to be determined, we know that a key property of melanopsin responses is that they do not light adapt to the same extent as those of rods and cones. Indeed, melanopsin-expressing ipRGCs are able to continuously fire action potentials in constant light for at least 10 hours – in line with their proposed role in signalling environmental irradiance to the clock (Wong, 2012).

1.2.3.2 ipRGC subtypes

In line with the wide range of anatomical targets of ipRGCs (and presumable similarly wide range of functional roles), 5 subsets of ipRGCs (termed M1-M5) have been identified (Ecker et al., 2010) that can be distinguished by the levels of melanopsin expression, membrane potential, cell morphology, and the stratification of dendrites with the inner plexiform layer (IPL) of the retina. The most well categorised subsets of ipRGCs are M1-M3 cells.

M1 cells have dendrites monostratified in the OFF sublamina of the IPL and were the first to be identified (Hattar et al., 2002, Provencio et al., 2002, Berson et al., 2002). M1 cells possess the highest levels of melanopsin (Schmidt and Kofuji, 2009) and are the principal subset that project to the SCN (Baver et al., 2008). The intrinsic light response of M1 cells is faster, larger and occurs at a lower threshold than of at the ipRGC subtypes, making them most directly light sensitive (Zhao et al., 2014, Ecker et al., 2010, Schmidt and Kofuji, 2011).

In contrast, M2 cells have dendrites monostratified in the ON sublamina (Berson et al., 2002). Morphologically, these cells have larger soma sizes and larger, more highly branched dendritic arbors than M1 cells (Schmidt and Kofuji, 2009, Berson et al., 2010, Ecker et al., 2010). Most importantly, at a functional level, M2 cells are ten times less sensitive to light than M1 cells (Schmidt and Kofuji, 2009), presumably owing to their lower levels of melanopsin expression.

Both M1 and M2 cells form mosaic networks than span the entire retina (Berson et al., 2010), albeit with significantly higher densities in the dorsal retina (Hughes et al., 2013). This 'photoreceptive net' presumably helps to maximise photon capture by melanopsin across the visual field, a feature that is of obvious utility for the key targets of such cells - the SCN and OPN (Baver et al., 2008). There are, however, key differences in the relative M1/M2 innervation of these regions: whereas M1 cells provide 80% of the input to the SCN, the OPN seems to receive approximately equal innervation from both types (perhaps reflecting the fact the latter requires more information about rapid changes in light intensity that can only be provided by outer retinal photoreceptors).

M3 cells have highly branched dendritic arbors and are similar to M2 cells in terms of their morphology and the low sensitivity of their intrinsic light response (Schmidt and Kofuji, 2011, Zhao et al., 2014). M3 cells are, however, distinguishable from M2 cells in terms of their stratification in the IPL: they are bistratified, possessing dendrites that terminate in both ON and OFF sublaminae (Viney et al., 2007, Schmidt and Kofuji, 2009, Berson et al., 2010). M3 cells are found less commonly within the retina than M1 and M2 cells. The further two subtypes of ipRGCS (M4 and M5), are not distinguishable using conventional

immunostaining – suggesting they express very low levels of melanopsin protein and exhibit correspondingly weak intrinsic light responses (Ecker et al., 2010).

The retinal circuitry supplying M1-3 ipRGC subtypes was investigated in mice that lack melanopsin expression ($Opn4^{-/-}$). Upon photic stimulation, the responses of M2 and M3 ipRGCs are similar to those of wildtype animals, suggesting that conventional photoreceptors (rods and cones) are the primary drivers of responses within these subsets of ipRGCs (Schmidt and Kofuji, 2010, Schmidt and Kofuji, 2011). The same is presumably true of the M4 and M5 subtypes, given their low levels of melanopsin expression. By contrast, M1 cell responses to the same stimuli are severely attenuated, illustrating that the melanopsin- driven intrinsic light responses of these cells plays an especially important role in their downstream signalling (Schmidt and Kofuji, 2010, Schmidt and Kofuji, 2011). Nonetheless, since all subtypes receive some rod/cone input, any brain region targeted by M1 ipRGCs can potentially also receive outer retinal signals.

Although it is clear from the above that the properties of melanopsin photoreception specialise ipRGCs towards encoding irradiance related information, the presence of ipRGC projections to brain regions such as the lateral geniculate nucleus (LGN) and superior colliculus (SC) imply they also play some role in more conventional aspects of vision (Hattar et al., 2006, Ecker et al., 2010). Consistent with this view, all ipRGC subtypes respond robustly to moving light stimuli, with each subtype having a preferential speed (Zhao et al., 2014). Additionally, M2-M5 cells are able to detect differences in spatially structured stimuli, demonstrating that ipRGCs are capable of contributing to pattern vision (Zhao et al., 2014). Indeed, recent work implicates melanopsin in conscious perception of brightness (Brown et al., 2012) and studies of rodless/coneless mice indicate that melanopsin can indeed supports a crude spatial representation of the visual scene in the visual thalamus (Procyk et al., 2015).

1.2.3.3 Horizontal cells

Horizontal cells are found within the outer plexiform layer (OPL; Figure 1.2) and play a key role in lateral information transfer within the retina. In the mouse, there is only one type of horizontal cell (Peichl and González-Soriano, 1994). Horizontal cells have elongated axons that project laterally to photoreceptor terminals, covering widespread areas of the retina (Raven et al., 2005, Reese et al., 2005). Horizontal cells are also connected to one another by gap junctions resulting in much larger receptive fields than the area of their dendritic field (McMahon et al., 1989).

Like OFF-bipolar cells, horizontal cells express AMPA-type ionotropic receptors and so hyperpolarise in response to a light evoked reduction in glutamate release from photoreceptors. In turn, horizontal cells provide negative feedback to photoreceptors, increasing their intake of Ca^{2+} (Verweij et al., 1996, Thoreson et al., 2008). Importantly then this arrangement ensures that cone photoreceptors become depolarised by light detected by the surrounding cones – establishing a 'centre-surround' arrangement that optimises the detection of object boundaries.

1.2.3.4 Amacrine cells

Amacrine cells are located in the inner plexiform layer (IPL; Figure 1.2) and found postsynaptic to bipolar cells and presynaptic to retinal ganglion cells (RGCs). They are responsible for modulating bipolar cell input to RGCs. They are one of the most diverse cell types within the retina, with over 30 subtypes of amacrine cells within the mammalian retina (MacNeil and Masland, 1998, Badea and Nathans, 2004). Amacrine cells are grouped into narrow-field (30-150µm), small-field (150-300 µm), medium-field (300-500 µm) and wide-field (>500 µm) based on the size of their dendritic fields (Kolb et al., 1981, Kolb, 1982). The vast majority of amacrine cells are inhibitory, expressing the neurotransmitters GABA or glycine (Crooks and Kolb, 1992).

Glycinergic amacrine cells tend to be of the small-field variety (Vaney, 1990, Menger et al., 1998, Pourcho and Goebel, 1985) and have a defined role in transmitting retinal signals: they carry ON inhibition to the OFF cells and carry OFF inhibition to the ON cells (Roska et al., 2006, Chávez and Diamond, 2008, Molnar et al., 2009). This mechanism has been best characterised in the AII amacrine cell (Manookin et al., 2008). Wide-field amacrine cells are GABAergic (Pourcho and Goebel, 1983) and play a role in modulating the receptive fields of RGCs (Cook and McReynolds, 1998). Although amacrine cells express either glycine or GABA, these neurotransmitters are co-expressed with a wide variety of other neurotransmitters such as glutamate (Johnson et al., 2004), dopamine (Dacey, 1990, Kolb et al., 1990), serotonin (Vaney, 1986), acetylcholine (O'Malley et al., 1992) and substance P (Kolb et al., 1995). Amacrine cells are therefore a heterogeneous population, with a wide variety of modulatory functions within the retina.

1.2.4 Photoreceptor contributions to photoentrainment

Experiments that initially began to further our understanding of photoreceptor pathways driving circadian entrainment involved mice that are homozygous for the mutation *retinal degradation (rd/rd)* These mice have a deficiency in cGMP-PDE (Schmidt and Lolley, 1973, Lolley et al., 1977), resulting in a build-up of cGMP that initiates photoreceptor cell death (Farber and Lolley, 1974). These mice undergo a postnatal rapid degradation of rods followed by a subsequent degradation of cones. Although they lack conventional vision, *rd/rd* mice possess normal circadian phase locomotor responses that are indistinguishable to those of control mice with healthy retinas (*rd/+ and +/+*) (Foster et al., 1991, Foster et al., 1993, Provencio et al., 1994). Following on from these experiments, a transgenic mouse was generated (*rdta*), that lacks rods due to ablation by diphtheria toxin and possess cones that lack photoreceptive outer segments (Lupi et al., 1999). These mice possess a circadian phenotype different to *rd/rd* and wild type mice. They possess a 2.5 times greater phase shift in response to light stimuli and have a shortening of the circadian period in locomotor activity. These two studies together provided evidence that rods, and perhaps also cones are not required in circadian response to light as rhythms remain responsive to light after their removal.

In line with these data, using diphtheria toxin to ablate cones alone did not affect phase shifts in mouse locomotor activity (Freedman et al., 1999), again suggesting that a non-cone photoreceptor had an effect upon photoentrainment. Moreover, mice with more extensive rod and cone lesions (*rdta/cl*) also displayed an unattenuated phase shift when subjected to a light pulse. Additionally, these mice displayed a normal suppression of pineal melatonin in response to light (Lucas et al., 1999), confirming that a non-rod, non-cone photoreceptor was indeed involved in mediating circadian responses to light.

As outlined above, it subsequently became apparent that SCN-projecting RGCs were intrinsically photoreceptive (Berson et al., 2002), due to expression of the opsin-based photopigment, melanopsin (Provencio et al., 2000, Hattar et al., 2002). Although this discovery provided a clear explanation for the earlier results of Foster and others, it soon became apparent that mice lacking melanopsin also entrain well to light/dark cycles over a wide range of irradiances (Panda et al., 2005, Ruby et al., 2002, Altimus et al., 2010, Morin and Studholme, 2011). Thus while not required, rods and cones are apparently sufficient for photoentrainment. Importantly, however, photoentrainment is lost following genetically directed lesions of ipRGCs, indicating that these cell types represent the principal route for both melanopsin and rod/cone signals to reach the SCN (Guler et al., 2008, Göz et al., 2008, Hatori et al., 2008).

Indeed, while ipRGCs are unique in that they possess an intrinsic mechanism to detect light, like other RGCs they also receive input from rods and cones (Dacey et al., 2005, Belenky et al., 2003, Østergaard et al., 2007, Wong et al., 2007, Schmidt and Kofuji, 2010, Weng et al., 2013). Accordingly, mice lacking all three photoreceptors lose photoentrainment, ruling out the possibility that a fourth as of yet unidentified photoreceptor class is involved (Hattar et al., 2003, Panda et al., 2003). Presumably, then, each of these three sources of photoreceptive input each provides their own unique contribution to the integrated circadian response to light.

1.2.4.1 Rods

Rods are the most sensitive of all of the photoreceptors (Lucas et al., 2012), possessing adaptations for absorption and transmission of single photons (Sharpe and Stockman, 1999) and so are involved in photoentrainment at low (scotopic) light intensities, too dim for the activation of melanopsin and cone photoreceptors (Altimus et al., 2010, Sampath et al., 2005, Lall et al., 2010). Under bright, indoor lighting (500 lux), rod-only mice that lack functional cones and melanopsin entrain well to LD cycles, verifying that rods alone can be used by the SCN to distinguish between dark and light across a wide range of light intensities (Altimus et al., 2010).

Although behavioural studies have shown that rods play a role in photoentrainment, electrophysiological experiments conducted within the SCN have yielded little evidence of direct rod-driven responses. Hence, rods appear to play only a minor role modulating SCN neuronal firing activity in anaesthetised mice (Brown et al., 2011). This apparent discrepancy may reflect the fact that the mice used for this work were not long-term dark adapted as is the case for most behavioural studies. Broadly in line with this view, Aggelopoulos and Meissl (2000) do report SCN responses under very low light levels following extensive (10h) dark adaptation. Nethertheless, even in that study, the observed responses appear of relatively modest magnitude, suggesting that even small changes in SCN cellular activity may be sufficient to drive behavioural phase shifts providing they are maintained for sufficient periods of time.

1.2.4.2 Cones

As discussed above, only 3% of photoreceptors in the murine retina are cones. Despite this, cone driven responses are widely apparent in retinorecipient regions in the mouse (Allen et al., 2011, Brown et al., 2011, Allen et al., 2014). Cones are characteristically much less sensitive than rods and have not been considered to play a major role in entrainment since ‘cone-only’ mice fail to entrain to LD cycles (Mrosovsky and Hattar, 2005) and entrainment to LD cycles persists after substantial cone degeneration (Freedman et al., 1999). Despite this, cones certainly do transmit signals to ipRGCs (Belenky et al., 2003, Østergaard et al.,

2007) and electrophysiological studies have documented cone-driven responses within ipRGCs (Dacey et al., 2005) and the SCN (Aggelopoulos and Meissl, 2000, Brown et al., 2011), indicating that cones must play some role in the light input pathway to the SCN.

Indeed, the large contrast-dependent increases in SCN firing discussed above can be attributed to cones. These responses last <500ms under dark adapted conditions (Drouyer et al., 2007, Brown et al., 2011) but, following continued light stimulation, are strongly reduced due to photoreceptor light adaptation (Perlman and Normann, 1998, Wong et al., 2005, Drouyer et al., 2007). This taken alongside behavioural data (discussed in more detail below) suggests that light adaptation places a strict limit on how much of a role cone influence can have on circadian entrainment (Dkhissi-Benyahya et al., 2007, Dollet et al., 2010, Altimus et al., 2010, Lall et al., 2010).

To date, most of the available literature concerns the role of M-cone opsin in circadian resetting. Hence, mice lacking M-opsin expression show deficient phase shifting behaviour to brief (5 min) but not more extended (15 min) long wavelength light pulses (Dkhissi-Benyahya et al., 2007, Dollet et al., 2010). Moreover, in mice with long wavelength shifted M-opsin expression, stimuli capable of activating M/L-cones but not melanopsin result in a strong increase in the firing rate of SCN neurons at the onset of light but generate little sustained response (Brown et al., 2011). Consistent with these findings, 15 minute light pulses that selectively activate cones do not evoke behavioural shifts in these mice, whereas fifteen 1 minute light impulses (of equivalent photon flux) evoke very large behavioural responses (Lall et al., 2010). By contrast, cone-deficient mice display a wild-type phase shifting pattern with a 15 minute light pulse but show deficient phase-shifting ability to 1 minute light pulses (Lall et al., 2010). Together then these data indicate that M-cone input to the SCN selectively contributes to responses immediately following a change in light intensity (Lucas et al., 2012, Brown et al., 2011). As a consequence, while the clock is not overly sensitive to visual contrast *per se*, the photoreceptor contributions (and hence spectral sensitivity) of circadian resetting responses will differ based of the temporal profile of the light stimulus.

In contrast to the above, UV light elicits sustained, irradiance dependent responses in SCN neurons that are similar to those seen when the SCN is stimulated by white light, even in the absence of melanopsin (van Oosterhout et al., 2012). Based on the irradiance range over which these responses are observed, it appears that such responses may be mediated by S-cone opsin. Consistent with this idea, previous work in another target of ipRGCs, the olivary pretectal nuclei (OPN), suggested that S-opsin driven responses are indeed much more sustained than those driven by M-opsin (Allen et al., 2011). Together then, these data suggest that cones exclusively expressing S-opsin might play a qualitatively different role in entraining the SCN clock relative to the more numerous opsin co-expressing cones.

Insofar as for cone signals to influence the clock they must presumably pass through M1 ipRGCs (Chen et al., 2011), one might then expect M1 ipRGCs to exhibit a similar disproportionate sensitivity to S-opsin derived signals. This possibility has been evaluated by assessing the spectral tuning of the ipRGC light response (Hughes et al., 2013). Hence, previous studies have also shown that the changeable S:M opsin ratio in the murine retina (discussed above) results in an anatomical variation in the spectral tuning of light responses recorded from both bipolar (Breuninger et al., 2011) and ganglion cells (Wang et al., 2011). If ipRGCs primarily sample primordial S-cones (which do not follow the more typical opsin expression gradient) such anatomical variation in spectral tuning should be absent. In fact, however, patterns of white or UV light-evoked *c-fos* expression in M1 ipRGCs show a clear dorsal:ventral gradient consistent with the involvement of opsin co-expressing cones (Hughes et al., 2013). In sum, while these data do not rule out an involvement of primordial S-cones in circadian responses, it seems unlikely that this population of photoreceptors provide the main source of input to ipRGCs innervating the SCN.

Finally, melanopsin containing ipRGCs that receive colour opponent S-off, (L+M)-on cone input have been found in the macaque retina, following retrograde tracing from the LGN and OPN (Dacey et al., 2005). Considering that, in rodents, both the OPN and SCN receive input from an overlapping population of ipRGCs (Baver et al., 2008), it is certainly possible then that this colour opponent input could be transmitted to the SCN, providing information about changes in the spectral composition of light. However, in the mouse, although both M- and S-cones contribute to responses in ipRGCs, existing data suggests that both classes drive ON responses (Weng et al., 2013). Together then, while the possibility that colour might directly influence SCN/circadian responses remains

uninvestigated, available data suggest such signals are unlikely to be transmitted by mouse ipRGCs.

1.2.4.3 Melanopsin

Melanopsin is the least sensitive of all the photoreceptors (see above). Taken alongside the slow response kinetics of melanopsin phototransduction, this makes melanopsin an ideal candidate for extracting slow changes in irradiance associated with the day/night cycle. Somewhat surprisingly then, while rod/cone degenerate animals reveal intact photoentrainment at high irradiances (Mrosovsky, 2003, Morin and Studholme, 2011), studies of melanopsin knockout (*Opn4*$^{-/-}$) mice have provided little direct evidence that melanopsin is necessary for photoentrainment in the presence of rods/cones. Indeed, as discussed above, *Opn4*$^{-/-}$ mice entrain well to LD cycles over a range of irradiances (Ruby et al., 2002, Panda et al., 2005, Morin and Blanchard, 2001, Altimus et al., 2010).

In contrast with the above, electrophysiological data clearly show that melanopsin plays a major role in SCN light responses under photopic conditions. Hence, while rod/cone-selective stimuli drive only transient light responses in the mouse SCN, stimuli that also activate melanopsin evoke a much more sustained excitations (Brown et al., 2011). Presumably then, contributions of melanopsin to entrainment in the lab are largely masked in animals with an intact outer retina by the fact that entrainment to simple square wave light dark cycles simply requires the ability to distinguish light from dark (a signal that is available from rods). Indeed, it seems likely that a full appreciation of the contributions of melanopsin to entrainment may only be apparent under more natural conditions where light intensity varies gradually around dawn and dusk. Here, combining signals from rods/cones and melanopsin should enable the circadian system to more accurately assess the timing of the day night transition, relative to animals lacking one or more of these photoreceptors (Lucas et al., 2012).

1.3 The SCN neuronal network

1.3.1 The suprachiasmatic nuclei

As discussed above, in mammals, the central master clock is located in the suprachiasmatic nuclei (SCN) of the hypothalamus (Moore, 1983, Moore, 1995, Moore and Eichler, 1972, Stephan and Zucker, 1972). The SCN are a paired structure of approximately 20,000 densely packed neurons (Abrahamson and Moore, 2001), located in the anterior of the hypothalamus, dorsal to the optic chiasm (Moore et al., 2002) on either side of the 3rd ventricle in the brain (Hofman et al., 1996).

The critical evidence establishing the SCN as the master clock came from electrophysiological studies where the SCN was isolated from the rest of the brain in a small hypothalamic "island": daily rhythms in electrophysiological activity were lost elsewhere in the brain but remained in the "island" (Inouye and Kawamura, 1979). Consistent with this view, subsequent lesion studies revealed that ablation of 75% of the SCN completely abolishes circadian rhythm in body temperature and locomotion (Moore, 1982, Pickard and Turek, 1983). Moreover, after ablation of the SCN, a circadian rhythm could be restored when neural tissue containing SCN from a donor was implanted. Critically, experiments using grafts from animals with accelerated circadian periods revealed that the restored rhythms retained the period of the donor animal, indicating that such rhythms were wholly generated by the SCN itself (Ralph et al., 1990).

The SCN have traditionally been divided into two distinct subregions on the basis of gene expression and inputs from the retina/other brain regions: a ventrolateral or core division and a dorsomedial/shell region (Abrahamson and Moore, 2001, Cassone et al., 1988) (Moore et al., 2002). These alternative terminologies relate to subtle anatomical differences between the hamster (core/shell) and rat (ventrolateral/dorsomedial) (Morin, 2007). Although neither of these nomenclature precisely map onto the arrangement in mice, the same basic set of cell groups appear to be well conserved, making these divisions a useful starting point for understanding the general organisation of the SCN network. For simplicity here I use the core/shell terminology throughout.

Below I first discuss the basic evidence indicating that individual SCN cells are themselves autonomous clocks, then how neurochemically distinct subgroups of cells SCN cells communicate and are organised within the intact SCN before discussing current knowledge as to how sensory signals from the retina and other visual nuclei influence the SCN network.

1.3.2 Single cell oscillators

Individual SCN neurons in culture exhibit circadian rhythms in spontaneous firing (Welsh et al., 1995, Liu et al., 1997, Honma et al., 1998, Herzog et al., 1998). These dissociated cells display a wide range in the period and phase of their rhythms, with some cells oscillating in anti-phase. This range of phases is maintained after pharmacological blockade of action potentials using TTX (Welsh et al., 1995), suggesting that SCN neurons are autonomous circadian pacemakers that do not require input from other SCN neurons.

Although individual SCN cells are autonomous in generating a rhythm, in the intact SCN, these neurons usually synchronise to one another (Inouye and Kawamura, 1979, Meijer et al., 1998). The prevailing model of SCN cellular organisation is that SCN neurons form a single population oscillating at a similar circadian phase. This generated by averaging the intrinsic circadian period across the SCN population, to produces a single coherent output signal (Liu et al., 1997, Herzog et al., 1998).

More recent evidence indicates that without intercellular communication, synchrony between rhythmic SCN neurons is lost. Although autonomous rhythms do remain after TTX application (Welsh et al., 1995), in the intact SCN, neuronal populations desynchronise and cellular gene expression rhythms dampen in many cells (Yamaguchi et al., 2003). Therefore the SCN is more likely to be a heterogeneous population of neurons, some possessing an intrinsic autonomous pacemaker and others that require cellular communication to remain rhythmic. The mechanisms of cell synchronisation are unclear but synaptic transmission, gap junction signalling and the release neurotransmitters such as GABA and vasoactive intestinal polypeptide (VIP) have been implicated in this process.

1.3.2.1 The molecular clock

The autonomous oscillations within SCN cells are generated by an auto-regulatory negative feedback loop which facilitates rhythmic gene expression. Figure 1.5 illustrates the components of this feedback loop that generates rhythm within the SCN.

The core components of the mammalian circadian clock are PER, CRY, BMAL1, and CLOCK. In the central circadian loop, the positive elements are CLOCK and BMAL 1. These proteins heterodimerize and bind to E-box regions of target genes such as *Period* (*Per1, Per2 and Per3*) and *Cryptochrome* (*Cry1* and *Cry2*) to initiate their expression (Gekakis et al., 1998). PER:CRY heterodimers are phosphorylated (Lee et al., 2001, Vanselow and Kramer, 2007) and translocate into the nucleus where they suppress their own transcription through an interaction with BMAL1:CLOCK (Kume et al., 1999), functioning as the negative element of the clock (Sato et al., 2006). PER is progressively phosphorylated and is degraded in the proteasome (Akashi et al., 2002, Etchegaray et al., 2009). PER:CRY heterodimers are degraded during the night , which allows BMAL1:CLOCK transcription to begin again and the cycle continues (Relógio et al., 2011).

The BMAL1:CLOCK complex also activates transcription of retinoic acid-related orphan nuclear receptors *Rev-erb (α and β)* and *Ror (α, β and γ)* (Ko and Takahashi, 2006). REV-ERBs and RORs bind to retinoic acid-related orphan receptor response elements (ROREs) that are found in the *Bmal1* promoter. REV-ERBs repress the transcription of BMAL1 and RORs activate its transcription (Preitner et al., 2002). The transcription of *Bmal1* is regulated by competitive binding of RORs and REV-ERBs at the RORE site (Guillaumond et al., 2005). This second feedback loop thus acts to add stability to the core clock mechanism.

Cells within the SCN core region respond to photic stimuli during the night to increase expression of the clock protein PER (Hamada et al., 2004). Subsequently PER expression moves outwards into the shell region (Yan and Okamura, 2002), which displays circadian oscillation of PER protein. This pattern of gene expression activity is presumably also

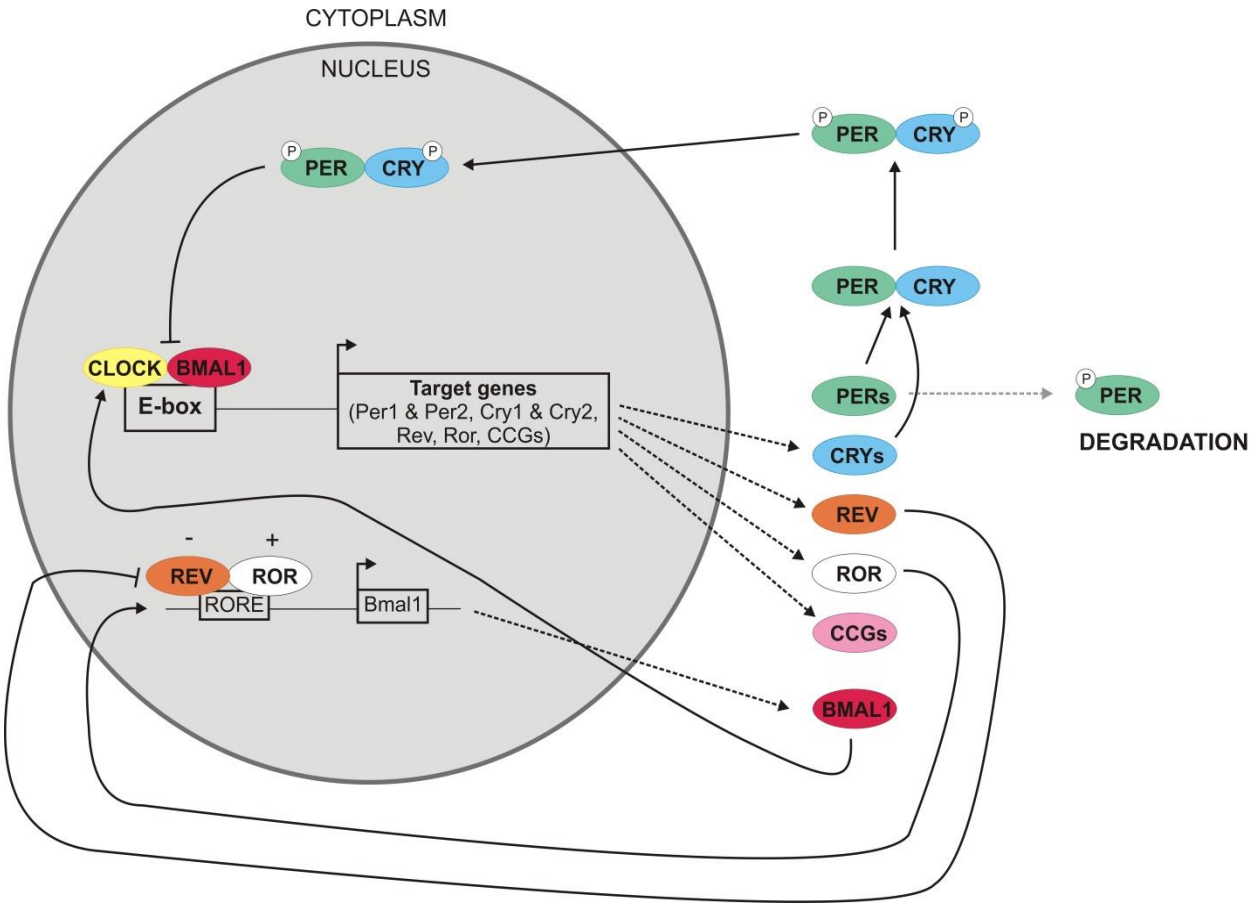

Figure 1.5: The transcriptional feedback loop in the mammalian circadian oscillator.

Within the SCN, the mammalian circadian clock consists of a negative feedback loop. A heterodimer of BMAL1 and CLOCK binds to the E-box in the promoter regions of *Cry* and *Per* and initiate their transcription. CRY and PER heterodimerize and are phosphorylated in order to translocate into the nucleus to halt their own transcription by inhibiting BMAL1/CLOCK activation of gene transcription. PER is progressively phosphorylated and is targeted to the proteasome for degradation. BMAL1:CLOCK activates the transcription of *Ror* and *Rev* genes. ROR and REV regulate the expression of *Bmal1* via interaction with a RORE. *ROR* activates the transcription of *Bmal1* and REV inhibits transcription. Clock genes (ccgs) are activated by the binding of CLOCK:BMAL1 to E-box regions of their promoters and so are expressed in rhythm with the clock (Golombek and Rosenstein, 2010, Ko and Takahashi, 2006).

reflected in SCN neuronal activity, since the *Per1* promoter activity reportedly correlates with the spiking frequency of SCN neurons (Quintero et al., 2003), although see (Belle et al., 2009).

1.3.2.2 Ionic controls of SCN firing

SCN neurons fire action potentials spontaneously, with a firing rate between ~5-21 spikes/second (Thomson et al., 1984, Groos and Hendriks, 1979). Neurons within the nocturnal rodent SCN exhibit a diurnal pattern of firing both *in vivo* (Inouye and Kawamura, 1979, Inouye and Kawamura, 1982) and *in vitro* (Green and Gillette, 1982, Shibata et al., 1982, Groos and Hendriks, 1982), with a higher rate of spontaneous activity during the day than during the night. During the day, SCN neurons are active and relatively insensitive to excitatory stimulation, whereas, during the night, neurons are inactive and are most responsive to excitatory stimuli (Meijer et al., 1998). *In vitro* studies have been instrumental in understanding how ionic mechanisms maintain the spontaneous firing rate within the SCN and determine the responses to stimuli.

Circadian oscillations in membrane potential have been proposed to underlie the circadian rhythm in neuronal firing rate. These oscillations are autonomous and so do not rely on the SCN network (Belle et al., 2009). During the day, SCN neurons are much more depolarised (~11mV) than during the night, where the resting membrane potential (~-55mV) lies close to the threshold for generating action potentials (Kuhlman and McMahon, 2004). SCN cells also exhibit an increase in input resistance during the day vs. subjective night (Kuhlman and McMahon, 2004). To maintain this spontaneous activity, intrinsic mechanisms must act to depolarise the neuron membrane to threshold, fire an action potential and then return the membrane to resting state so another spike can be fired. This is achieved in the SCN by the interaction of multiple ion currents, which are discussed below.

1.3.2.3 Calcium

Calcium plays an important role in generating spontaneous firing in the SCN. Both L-type and T-type calcium (Ca^{2+}) channels are expressed in SCN neurons and function to maintain the excitatory component of resting membrane potential (RMP) oscillations (Pennartz et al., 1997, Jackson et al., 2004, Kononenko et al., 2004). L-type currents are larger in daytime than night and provide the primary pacemaker current (Pennartz et al., 2002). Indeed, replacing Ca^{2+} with Ba^{2+} disrupts the regular firing of SCN neurons (Thomson, 1984), emphasising the importance of Ca^{2+} in regulating spontaneous firing. Action potentials are associated with the influx of calcium and larger daytime currents mean that there are higher levels of Ca^{2+} present in SCN neurons during the day, potentially facilitating a higher rate of firing. Moreover, L-type Ca^{2+}mediated subthreshold oscillations in membrane potential have been characterised in the daytime but not in the night (Pennartz et al., 2002). Diurnal variation in Ca^{2+} current means that it is a good candidate to link the molecular clock to changes in firing rate. By contrast, T-type channels are not involved in the generation spontaneous firing, and are instead thought to play important roles in the SCN neuronal response to glutamate (Kim et al., 2005).

1.3.2.4 Sodium

Persistent Na^+ channels are expressed by almost all SCN neurons (Kononenko et al., 2004). In vitro studies have shown that in dissociated SCN neurons, spontaneous depolarisation of the cell membrane can be attributed to Na^+ when the membrane potential is between -60 and -40mV (Jackson et al., 2004). When blocked with riluzole, spontaneous activity is abolished in some SCN neurons (Kononenko et al., 2004) indicating that these channels play a role in maintaining RMP oscillations. However, riluzole resistant neurons still exhibited low amplitude RMP oscillations when Na^+ current was blocked with TTX, demonstrating that although these channels contribute to oscillations in RMP, the persistent Na^+ current is not required for spontaneous firing (Kononenko et al., 2004).

A second Na^+ channel involved in spontaneous firing is the hyperpolarisation-activated cyclic nucleotide-gated (HCN) channels that are also responsible for the excitation of SCN

neurons. When HCN channels open, Na^+ enters the cell and K^+ leaves, resulting in a slow excitation of the membrane (Biel et al., 2009). Acute blockage of this depolarising current has no effect on circadian pacemaking (de Jeu and Pennartz, 1997, Pennartz et al., 1997), but sustained pharmacological blockade of HCN channels reduces the frequency of action potentials during the day (Atkinson et al., 2011). Since SCN neurons typically fire more during the day, these results indicate that HCN channels may play a role in depolarisation of the membrane at high firing rates.

1.3.2.5 Potassium

Both Ca^{2+} dependent and Ca^{2+} independent K^+ channels are involved in regulating the interspike interval of spontaneous action potential firing (Thomson and West, 1990). There are two Ca^{2+} independent K^+ currents involved in spontaneous firing in the SCN, the rapid activating and slowly inactivating fast delayed rectifier (FDR) current and the transient A-type current (Bouskila and Dudek, 1995).

The FDR was the first demonstrated example of circadian regulation of an intrinsic voltage-gated current in the mammalian SCN. The magnitude of the FDR current exhibits a circadian rhythm that persists in constant darkness, with current peaking during the day when SCN firing is higher (Itri et al., 2005). Pharmacological blockade of this current prevents daily firing rate rhythms (Itri et al., 2005) and the removal of these channels doubles the width of the action potential (Kudo et al., 2011). The FDR is therefore an important part of the ionic generation and modulation of electrical rhythms in SCN neurons.

The A-type current has also been implicated as a likely candidate to modulate spontaneous firing in the SCN, by regulating the neuronal excitability and timing of action potentials (Bouskila and Dudek, 1995, Alvado and Allen, 2008, Itri et al., 2010). The magnitude of the type-A current exhibits a diurnal rhythm that persists during constant darkness and peaks during the day (Itri et al., 2010), demonstrating a second voltage-gated current under circadian control.

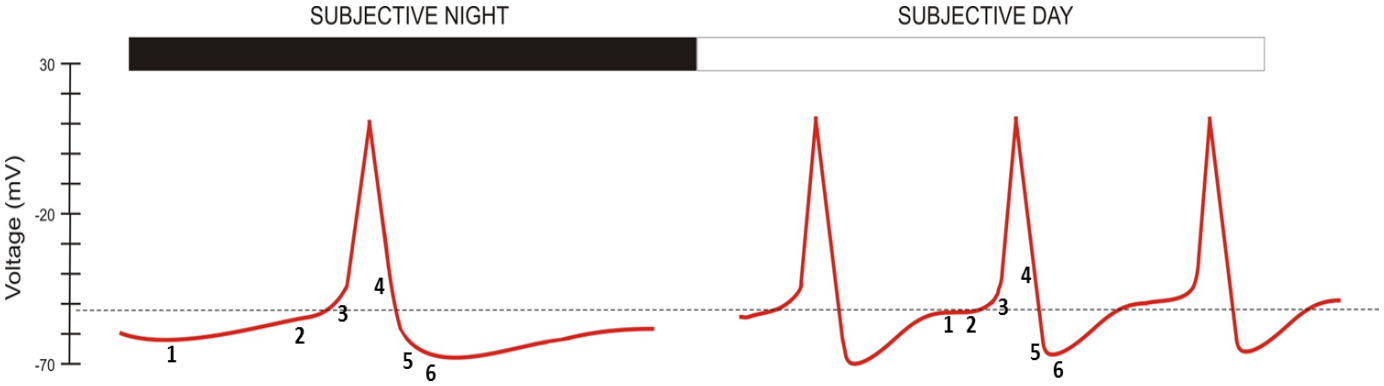

Figure 1.6: Ionic mechanisms controlling SCN spontaneous action potential firing during the day and night. Adapted from Brown and Piggins (2007).

During the night (left): The resting membrane is more hyperpolarised than during the day due to the action of K^+ leak channels and BK K^+ channels, rendering them less likely to fire action potentials (1). Spontaneous SCN firing is dependent on the action of persistent Na^+ channels which open at around at -60mV to begin to depolarise the membrane (2). The depolarisation of the membrane opens L-type Ca^{2+} channels to further depolarise the membrane (3). The duration of the action potential is controlled by Ca^{2+}-dependent K^+ currents (FDR and A-type) which begin to repolarise the membrane (4). Ca^{2+} independent channels further repolarise the membrane (5). Following the action potential, the SCN experiences a brief period of afterhyperpolarisation - TTX-sensitive, voltage-dependent Na^+ channels (a persistent NA^+ channel) and the HCN begin to depolarise membrane, bringing it to threshold so another action potential can occur (6).

During the day (right): The resting membrane is more depolarised during the day due to the suppression of K^+ leak channel and BK K^+ channel activity. SCN neurons are therefore more likely to fire a spontaneous action potential during the day (1). Spontaneous SCN firing is dependent on the action of persistent Na^+ to further depolarise the membrane (2). During the day, currents through L-type Ca^{2+} channels are enhanced, eliciting faster depolarisation (3). Additionally both FDR and A- type K^+ currents are greater during the day triggering faster repolarisation of the membrane (4). The contribution of BK K^+ channels to K^+ currents is reduced during the day reducing the duration of hyperpolarisation after the action potential (5). TTX-sensitive, voltage-dependent Na^+ channels (a persistent NA^+ channel) and the HCN begin to depolarise membrane, bringing it to threshold so another action potential can occur (6).

Ca^{2+}-dependent big potassium channels (BK channels) have a large conductance for K^+ and are rhythmically expressed within the SCN (Panda et al., 2002, Meredith et al., 2006, Pitts et al., 2006) and are a major contributor to the repolarisation of the membrane following an action potential (Cloues and Sather, 2003). As discussed above, SCN neurons exhibit diurnal rhythms in RMP and are much more depolarised during the day. BK channel expression peaks in the middle of the night and so the contribution of the BK to outward K^+ currents is much greater during the night (Pitts et al., 2006), contributing to hyperpolarisation of SCN neurons and the suppression of spontaneous firing (Kent and Meredith, 2008).

After each action potential, a SCN neuron enters a period of afterhyperpolarisation, caused in part by the hyperpolarising BK channel conductance (Cloues and Sather, 2003). Therefore almost all SCN neurons exhibit a prominent hyperpolarisation-activated conductance, termed I_H (Akasu et al., 1993), that causes a robust depolarisation of neurons in response to hyperpolarisation (Jackson et al., 2004), enabling the neurons to return to RMP.

The RMP is maintained by a class of two-pore-domain K^+ 'leak' channels (K2P, TASK and TREK channels) that are active across the whole voltage range of a neuron (Mathie, 2007, Bayliss and Barrett, 2008). K2P channels are encoded by the KNCK gene family. The transcripts *Kcnk1* and *Kcnk2* are expressed within the SCN (Kononenko et al., 2008, Colwell, 2011), with *Kcnk1* being rhythmically expressed (Panda et al., 2002). Their patterns of expression would implicate them in contributing to the nightly hyperpolarisation of SCN neurons (Panda et al., 2002, Colwell, 2011).

One other channel that contributes to maintenance of the RMP in SCN neurons is the Na^+/K^+ ATPase pump, which hydrolyses ATP to transport $3Na^+$ out of the cell per $2K^+$ in, resulting in hyperpolarisation of the cell membrane. A diurnal rhythm has been identified in the activity of this pump in the SCN, with greater activity occurring during the day (Wang and Huang, 2004, Wang and Huang, 2006).

The ionic mechanisms underlying SCN spontaneous action potential firing during the day and night are summarised in figure 1.6.

1.3.3 Functional divisions of the SCN network

As discussed, the SCN have traditionally been divided into two distinct subregions: core and shell. These are can be identified by the expression of certain neuropeptides. The SCN core is characterised by the presence of vasoactive intestinal polypeptide (VIP) and gastrin releasing peptide (GRP) neurons (Card and Moore, 1984, Moore and Silver, 1998, Antle and Silver, 2005, van den Pol and Tsujimoto, 1985) and is traditionally considered as the input region of the SCN, receiving the densest retinal, serotonin (5-HT) and IGL innervation. The core also contains calbindin cells that are considered to play a critical role in cell to cell synchronisation across the whole nuclei (Yamaguchi et al., 2003, Antle and Silver, 2005).

In the SCN shell, neurons are smaller with less cytoplasm (Van den Pol, 1980). This area is characterised by the presence of arginine vasopressin (AVP), angiotensisn II (AII) and calretinin neurons (Golombek and Rosenstein, 2010). The shell receives input from the hypothalamus, the ventrolateral SCN and the limbic system and has traditionally been considered as portion of the SCN responsible for sending rhythmic output to other brain regions (Hamada et al., 2004, Yan and Okamura, 2002).

1.3.3.1 Cell types within the SCN

Although multiple neurotransmitters are present within the SCN, GABA is the only one that is produced or received by almost all SCN neurons (Okamura et al., 1989, Moore and Speh, 1993, Liu and Reppert, 2000). There is ample evidence to suggest that GABA plays an important role in circadian time-keeping as GABA agonists can shift the circadian clock (Ralph and Menaker, 1989) and GABA antagonists can block phase-shifts induced by light and drug application (Smith et al., 1990). These GABA-induced phase shifts are mediated by the $GABA_A$ receptor (Liu and Reppert, 2000). However, despite its abundance, and a clear role in circadian photoentrainment, the role of GABA within the SCN remains complex.

GABA is generally known as an inhibitory neurotransmitter in the CNS, and although exclusively inhibitory responses have been found in the SCN (Liu and Reppert, 2000, Gribkoff et al., 1999, Gribkoff et al., 2003), there is conflicting evidence that suggests that GABA can have both inhibitory and excitatory effects on SCN firing (Wagner et al., 1997, De Jeu and Pennartz, 2002, Choi et al., 2008).

These GABA driven excitatory responses were first reported to occur only during the day (Wagner et al., 1997). Later, De Jeu and Pennartz (2002) demonstrated in the rat that although the number of excitations was small during the daytime (>90% of SCN neurons were inhibited by GABA), during the night levels of GABA-induced excitations and inhibitions were approximately equal. Choi et al (2008) also reported that although GABA primarily inhibited SCN neurons at all times of the day in the mouse, the proportion of excited neurons was much greater during the night.

The response of an SCN neuron to GABA acting at the $GABA_A$ receptor is primarily determined by the intracellular chloride concentration (Alamilla et al., 2014, Choi et al., 2008). Indeed, the $Na^+/K^+/2Cl^-$ (NKCC) cotransporter is essential for excitatory responses to GABA as inhibitors of this ion channel block excitatory responses in the SCN (Choi et al., 2008). NKCC1 is expressed in the SCN and transports Cl^- into the neuron. In the rat, the expression of this channel is upregulated during the night in the dorsal SCN so that it is two-fold higher than in the daytime (Choi et al., 2008). This would raise intracellular Cl^- and elicit more excitatory responses from the SCN (Alamilla et al., 2014) during the night, supporting the findings above.

GABA has also been shown to synchronise the rhythms of SCN neurons in culture (Liu and Reppert, 2000, Albus et al., 2005), although intrinsic synchrony in higher density cultures can persist during chronic blockade of GABAergic signalling within the SCN. However, other studies report contrasting evidence and demonstrate that GABA acts to oppose synchrony within the SCN (Aton et al., 2006, Freeman et al., 2013).

Taken together, these findings implicate a complex role for GABA in the synchronisation and responses of SCN neurons. Moreover, GABAergic SCN cells are known to co-express a variety of neuropeptides (including the three major populations outlined below: VIP, GRP and AVP). It is so far unclear what triggers co-release or how these various neurochemical signals interact to control circadian timing. Further study using the latest generation of tools for targeted cell stimulation and recording will be required to address these unresolved issues.

1.3.3.1.1 Vasoactive intestinal polypeptide (VIP)

VIP is densely expressed retinorecipient regions of the SCN reaching from the ventrolateral SCN, medially until it reaches the third ventricle (Ibata et al., 1989, Morin et al., 2006). Extracellular recordings carried out in SCN slices showed that VIP suppresses 75% of SCN neurons in the subjective night (Reed et al., 2002) and that VIP induces phase shifts in SCN firing activity similar to those seen upon RHT stimulation (Reed et al., 2001). VIP microinjections into the SCN also elicits phase shifts in locomotor rhythms in a circadian time-dependent manner (Piggins et al., 1995). Taken together, these data suggest that VIP is involved in the photic resetting of the circadian clock.

Although the VIP receptor ($VPAC_2$) is expressed in many brain regions, expression is particularly dense within the SCN (An et al., 2012). Therefore it is unsurprising that VIP and its receptor ($VPAC_2$) play an important in the synchronisation of SCN cells (Aton et al., 2005, Hughes et al., 2008, Brown et al., 2005, Brown et al., 2007). Mice lacking $VPAC_2$ exhibit a continuum of behavioural locomotor rhythms, ranging from completely arrhythmic to weakly rhythmic (Brown et al., 2005, Hughes and Piggins, 2008). *In vitro* electrophysiological experiments show that individual SCN neurons also display this continuum of rhythms (Brown et al., 2005), with Individual $VIP^{-/-}$ or $VPAC_2^{-/-}$ SCN neurons tending to exhibit lower amplitude rhythms and impaired intercellular synchrony relative to wildtype cells (Colwell et al., 2003, Cutler et al., 2003, Brown et al., 2005, Brown et al., 2007, Maywood et al., 2006, Hughes et al., 2008). Electrophysiological data also shows that $VPAC_2^{-/-}$ neurons exhibit a lower peak firing than WT neurons (Cutler et al., 2003, Brown et

al., 2005), although daily mean firing rate is unchanged (Aton et al., 2005, Brown et al., 2005).

The general impairments in SCN function seen in individuals lacking the VIP signalling therefore reflect an ability of SCN neurons to effectively gate their activity so that peak firing occurs only at specific points in the circadian cycle. There is a close association between light-induced changes in behaviour and the induction of clock- gene expression in the SCN (Yan and Silver, 2002). This change in gating could therefore affect the expression of clock genes essential for maintaining circadian rhythmicity. Indeed, VIP deficient mice do show altered patterns in light-induced gene expression in both the subjective day and night (Dragich et al., 2010). Additionally, $VPAC_2^{-/-}$ mice exposed to light in the day show a significant increase in SCN Fos induction (Hughes et al., 2004) indicating that VIP and its receptor are required for appropriate gating of light input into the circadian clock.

1.3.3.1.2 Gastrin-releasing Peptide (GRP)

GRP is produced in cells within the ventrolateral SCN and can be found co-localised with VIP in the same neurons (Albers et al., 1991). It is therefore unsurprising that GRP and VIP signals appear partially interchangeable, with *in vitro* application of exogenous GRP acting to promote rhythmicity in the SCN of mice lacking the VIP receptor (Brown et al., 2005, Maywood et al., 2006).

GRP binds to the BB_2 receptor located in the dorsal and medial regions of the mouse SCN (Aida et al., 2002, Karatsoreos et al., 2006), inducing an increase in neuronal activity (Tang and Pan, 1993) in approximately 50% of SCN cells (Piggins and Rusak, 1993). While disruption of GRP signalling in wildtype mice has few effects on SCN neuronal firing rhythms (Brown et al., 2005), microinjection of GRP into the hamster SCN triggers a phase shift in locomotor activity similar to that of light (Piggins et al., 1995), suggesting that GRP plays a role in photic entrainment.

The specific mechanisms underlying the phase shifting action of GRP are unknown, however, antagonists of NMDA receptors blocks such shifts, suggesting that part of this mechanism may involve glutamate release within the SCN (Kallingal and Mintz, 2006). Moreover, in line with its phase shifting actions, *in vivo* microinjection of GRP into the SCN during the late subjective night induces *Per1* expression throughout the SCN, including AVP-expressing neurons (Gamble et al., 2007) and calbindin cells (Antle et al., 2005). Blockage of action potentials using TTX reduces Per1 induction within AVP neurons but not, apparently, in other cells (Gamble et al., 2007), suggesting that GRP phase shifts may involve both spike dependent and independent signalling pathways.

Taken together, these data suggest that GRP acts alongside VIP to communicate temporal information across the SCN network.

1.3.3.1.3 Arginine vasopressin (AVP)

Neurons expressing arginine vasopressin (AVP) are located within the dorsomedial or 'shell' division of the SCN (Abrahamson and Moore, 2001, Morin et al., 2006). In the mouse, only a subset of these receive innervation from the retina (Lokshin et al., 2015). There are 1.8 times the number of AVP-positive SCN neurons in the day than are present in the night and the cells are 1.4 times as large (Hofman and Swaab, 1994). In particular, the volume and number of AVP cells peaks in the early morning and are lowest in the middle of the night (Hofman and Swaab, 1994). Consequently AVP release is under circadian control, occurring at higher levels during the subjective day than during the subjective night *in vivo* (Schwartz et al., 1983, Schwartz and Reppert, 1985) and *in vitro* (Earnest and Sladek, 1986). In line with this data, *In vitro* studies in hamster SCN slices have demonstrated that the rhythm of AVP release precedes that of SCN neuronal firing (Gillette and Reppert, 1987).

AVP has an excitatory effect on SCN neurons (Liou and Albers, 1989), with the majority of cells (75%) responding during the night and a smaller proportion responding in the day (25%). Responses of SCN neurons to exogenous AVP are mediated by V_1-type receptors, however, blockage of V_1 receptors has no effect on the output of SCN neurons at any time

during the day/night cycle (Liou and Albers, 1989, Mihai et al., 1994) appears then that rhythmic AVP release/signalling is not essential for the rhythms in spontaneous firing seen in the cells of the SCN. Surprisingly, however, it does appears that mice lacking V_1-type receptors exhibit larger light-evoked phase shifts than wildtype mice, suggesting that feedback from AVP neurons may act to stabilise the SCN network against external perturbation (Yamaguchi et al., 2013).

Moreover, AVP cells themselves contain an inherent oscillator and recent data indicates that these inherent molecular rhythms are important determinants of mouse behavioural rhythmicity. Hence, the removal of the Bmal1 clock protein in AVP neurons lengthens the free-running period and active time of behavioural rhythms, a phenotype which is absent in AVP deficient mice (Mieda et al., 2015), indicating that output from AVP cells provides a major drive to circadian output rhythms. Consistent with this view, mice lacking the AVP receptor V1a have attenuated circadian rhythms (Li et al., 2009), indicating that oscillations in AVP could be involved in generating high amplitude rhythms in the SCN .

The surgical separation of 'core' and 'shell' desynchronises cells in the AVP-rich shell region (Yamaguchi et al., 2003), emphasising that AVP neurons require input from VIP/GRP neurons to maintain coordinated rhythmicity. Synchronised circadian output therefore involves all three of these neurotransmitters (VIP, GRP and AVP) and communication between the ventrolateral 'core' (VIP/GRP) and dorsomedial 'shell' (AVP) divisions, with VIP providing the primary synchronisation cue within the SCN (Maywood et al., 2011).

1.3.4 Sensory input to the SCN

Although the SCN network is capable of generating its own circadian rhythm, it must be correctly aligned with the environment in order to ensure that physiological processes are occurring at the appropriate time of day. As discussed above, light detected by the retina is the principal entrainment signal used by the SCN. However, this photic information must be delivered from the retina to the SCN. Hence, the SCN is at the centre of an interconnected network of brain regions that all contribute in modulating the phase of the circadian clock.

The contributions of these brain regions are discussed below and are summarised in Figure 1.8.

1.3.4.1 The Retinohypothalamic tract

The retinohypothalamic tract (RHT), a projection of the optic nerve, is the main input pathway to SCN from the retina: if transected, circadian photoentrainment is lost (Johnson et al., 1988a). In the mouse, the RHT is bilaterally symmetrical and unlike in the rat and hamster (Muscat et al., 2003, Johnson et al., 1988b), there is no observed SCN region where input from either eye predominates. Input from each eye is therefore equal across each of the SCN (Morin et al., 2006). Moreover, based on work indicating that the RHT projects across the whole of the mouse SCN (Morin et al., 2006), original suggestions that innervation is restricted to the SCN 'core' in this species (Dai et al., 1998) have now been rejected (Hattar et al., 2006). In fact however, a recent study does show some evidence of anatomical specificity to the mouse RHT (Lokshin et al., 2015). Thus, the area of the mouse SCN receiving the densest innervation from the RHT is the 'core' region (VIP+/GRP+), the shell containing AVP+ve neurons receives moderate RHT innervation and the outermost shell and rostral AVP-ve containing regions of the SCN have few detectable RHT terminals.

1.3.4.1.1 Glutamate

Glutamate is present in the terminals of the RHT (de Vries et al., 1993, Castel et al., 1993) and stimulation of the optic nerve triggers glutamate release in SCN slices (Liou et al., 1986), demonstrating that glutamate transmits photic signals from the eye. SCN neurons express multiple receptors to detect glutamate: ionotropic N-methyl-D-aspartate (NMDA), α-amino-3-hydroxy-5-methylisoxazole-4-propionate (AMPA) and kainite-type receptors, as well as metabotropic (GPCR) glutamate receptors (Meeker et al., 1994, Ebling, 1996). In vitro application of ionotropic glutamate receptor (NMDA) agonists elicit excitatory responses in SCN neurons (Bos and Mirmiran, 1993, Schmahl and Böhmer, 1997) and light (*in vivo*) or stimulation of the RHT (*in vitro*) produces excitatory responses in SCN neurons that can be significantly reduced by ionotropic glutamate receptor agonists (Cahill and

Menaker, 1989, Kim and Dudek, 1991, Cui and Dyball, 1996), demonstrating that glutamate primarily signals to SCN neurons through AMPA/NMDA receptors.

Light induced phase shifts in locomotor activity seen in photoentrainment studies (Van Den Pol et al., 1998) can be mimicked by *in vitro* application of either glutamate or NMDA (Ding et al., 1994, Shibata et al., 1994, Shirakawa and Moore, 1994). Conversely, these behavioural shifts can be blocked by NMDA antagonists (Colwell et al., 1990, Colwell et al., 1991, Vindlacheruvu et al., 1992, Rea et al., 1993), indicating that glutamate is indeed the principal neurotransmitter mediating photoentrainment and NMDA receptors are responsible for phase shifting behaviour to photic stimuli.

As indicated in Figure 1.1, phase shifting responses to light are gated by the circadian clock, with a photic stimulus having no effect on circadian locomotor rhythms during the day and driving phase delays or advances during the subjective night. Similarly, at the cellular level, NMDA receptor-driven Ca^{2+} influx in SCN neurons is markedly increased during the night, suggesting a possible source of the phase-dependent sensitivity of SCN neurons to light/glutamate-induced shifting (Cui and Dyball, 1996, Colwell, 2001, Pennartz et al., 2001).

Indeed, this increase in the concentration of intracellular Ca^{2+} is essential for light-induced phase shifting. The mechanisms by which Ca^{2+} levels are raised differ between the early and late subjective night, however. In the early subjective night (where light induces phase delays), T-type voltage gated Ca^{2+} channels assist in raising intracellular Ca^{2+} (Kim et al., 2005). Calcium levels are then further raised through the action of ryanodine receptors (RyR). RyRs are present in neurons and regulate the release of Ca^{2+} from intracellular stores (McPherson et al., 1991). As such pharmacological activation of RyRs induces glutamate-like delays, but only during the early subjective night. Similarly, RyR inhibitors block glutamate-induced phase delays but not phase advances (Ding et al., 1998, Kim et al., 2005). By contrast, in the late subjective night, it is L-type voltage gated Ca^{2+} channels that assist in raising intracellular Ca^{2+}. These differences in intracellular Ca^{2+} may allow the modulation of different signalling pathways to generate appropriate phase delays and advances.

Increases in intracellular Ca^{2+} associated with NMDA receptor activation (and/or downstream spiking responses) also lead to the activation of Ca^{2+}-calmodulin-dependent kinase II (CaMKII), which in turn activates neuronal nitric oxides synthase (NOS) (Agostino et al., 2004). NOS facilitates the production of neuronal nitric oxide (NO) from L-arginine (Bredt and Snyder, 1992, Bredt et al., 1990, Garthwaite, 1991, Vincent and Hope, 1992) and, consequently, the activation of guanylyl cyclase that increases the level of cGMP (Ding et al., 1994, Bredt et al., 1990). The NO-cGMP pathway activates protein kinase G (PKG) which phosphorylates CREB. Phosphorylated CREB (p-CREB) then activates transcription of light responsive genes such as *c-fos* and *Per1/Per2*. Importantly, Inhibition of cGMP-dependent PKG blocks glutamate induced phase advances, but not delays, indicating that the NO-cGMP pathway mediates phase shifting only during the late subjective night (Ding et al., 1994, Weber et al., 1995, Mathur et al., 1996). Activated CaMKII also mediates CREB phosphorylation directly (Golombek and Ralph, 1995) and indirectly via the phosphorylation of regulated kinase 1/2 ERK (Nomura et al., 2006) to activate transcription of light responsive genes such as *c-fos* and *Per1/Per2*.

Phase delays in the early subjective night instead involve the action of the cAMP and PKA. Light/glutamate raises cAMP levels but cAMP/PKA agonists do not mimic the action of light, indicating that another signal is needed alongside raised cAMP levels (Tischkau et al., 2000). Activation of this pathway enhances glutamate-stimulated phase shifts in early night but blocks photic shifting in the late night (Tischkau et al., 2000). The cAMP/PKA system alters the state of signalling pathways based on time of activation and therefore contributes to the gating of photic shifting by enhancing the effects of glutamate in the early night and opposing glutamate actions in the late night. PKA itself also phosphorylates CREB to activate the transcription of light responsive genes (Motzkus et al., 2007).

Even though the signalling pathways involved in glutamatergic photic resetting begin differently (due to either different sources or concentrations of Ca^{2+}), they have common features such as, the generation of nitric oxide by NOS and subsequent phosphorylation of ERK. Both pathways ultimately alter the expression of the clock genes *Per1/Per2*, modulating circadian phase. However, although glutamate is a major player in the

regulation of circadian phase by light, other neurotransmitters also contribute to this mechanism as discussed below.

1.3.4.1.2 Pituitary adenylyl cyclase activating peptide

Pituitary adenylyl cyclase activating peptide (PACAP) is a second neurotransmitter found in RHT terminals (Hannibal et al., 1997), co-localised with glutamate (Hannibal et al., 2000). PACAP can act on three receptors that are expressed within the SCN: the PAC_1 receptor which is specific for PACAP and, because PACAP is similar in structure to VIP, also $VPAC_1$ and $VPAC_2$ receptors (Harmar et al., 1998). Multiple studies have demonstrated the role of PACAP in photic entrainment via its interaction with the PAC_1 receptor (Chen et al., 1999, Harrington et al., 1999, Nielsen et al., 2001, Kawaguchi et al., 2003, Colwell et al., 2004, Hannibal et al., 2001).

Mice lacking either PACAP or the PAC_1 receptor have altered responses to photic stimulation at night (Hannibal et al., 2001, Kawaguchi et al., 2003, Colwell et al., 2004, Hannibal et al., 2008). Although studies have indicated much variety in the phase shifting responses of mice lacking PACAP signalling (Hannibal et al., 2001, Kawaguchi et al., 2003, Colwell et al., 2004, Hannibal et al., 2008), experiments investigating rhythmic gene-expression (Hannibal et al., 2001) and behavioural studies (Hannibal et al., 2008) have indicated that PACAP is less important in regulating phase advances than phase delays.

The PACAP-mediated signalling pathways involved in the regulation of light responsive genes are not well characterised. All three of the PACAP/VIP receptors belong to the GPCR family (Vaudry et al., 2000). Upon binding at the PAC_1 receptor, multiple transduction pathways are activated. Two divergent GPCR signalling pathways have been the most extensively studied: the Gαs, cAMP/Protein Kinase A (PKA) signalling pathway and the Gαq, inositol 1,4,5 tri-phosphate (IP_3)/phospholipase C (PLC) pathway

In vitro application of PACAP in high concentrations phase advance SCN rhythms in firing rate during the day in both the rat (Hannibal et al., 1997) and hamster (Harrington et al., 1999). However, although these experiments use high PACAP concentrations, PACAP has more light-like effects at micromolar concentrations (Harrington et al., 1999). The phase advancing action of PACAP involves the cAMP/PKA-mediated pathway (Hannibal et al., 1997). Adenylate cyclase (AC) is associated with PAC_1 at the cell membrane, and becomes activated upon neuropeptide binding. AC raises the levels of intracellular cAMP which in turn activates PKA, leading to CREB phosphorylation and regulation of gene expression.

The second GPCR pathway activated by PACAP is the IP_3/PLC pathway which triggers Ca^{2+} release from internal stores (Tanaka et al., 1997, Tanaka et al., 1996, Hamada et al., 1999a) to increase intracellular Ca^{2+}. There are two isoforms of the IP_3 receptors present in the SCN, type I and type III, which are expressed in a circadian fashion and peak during the early and late subjective night respectively (Hamada et al., 1999b) to photic-type phase-resetting. Moreover, PACAP is also known to potentiate L-type Ca^{2+}channel conductance, further increasing levels of intracellular calcium during the late evening (Dziema and Obrietan, 2002, Tanaka et al., 1996).

Application of PACAP in primary cell cultures has contrasting modulatory effects on glutamate signalling (Kopp et al., 2001). Although PACAP has no direct influence on the activation of NMDA receptors directly it amplifies glutamatergic signalling via the activation of AMPA/kainate receptors, which gate NMDA receptor ion channels. Activation of AMPA/kainate receptors activates the NMDA-receptors to increase Ca^{2+} influx. PACAP also seems to reduce calcium increases elicited by glutamate acting on metabotropic (mGLuR) receptors

As depicted in figure 1.7, PACAP thus acts cooperatively with glutamate to regulate changes in circadian phase, impinging on many of the same signal transduction pathways that influence the clock. This mechanism of interconnecting signalling pathways has been identified via the application of neuroactive peptides and elucidated from observations of cellular responses. However, the extent to which the processes described above are a general feature of the photic resetting pathway in individual cells (or whether particular

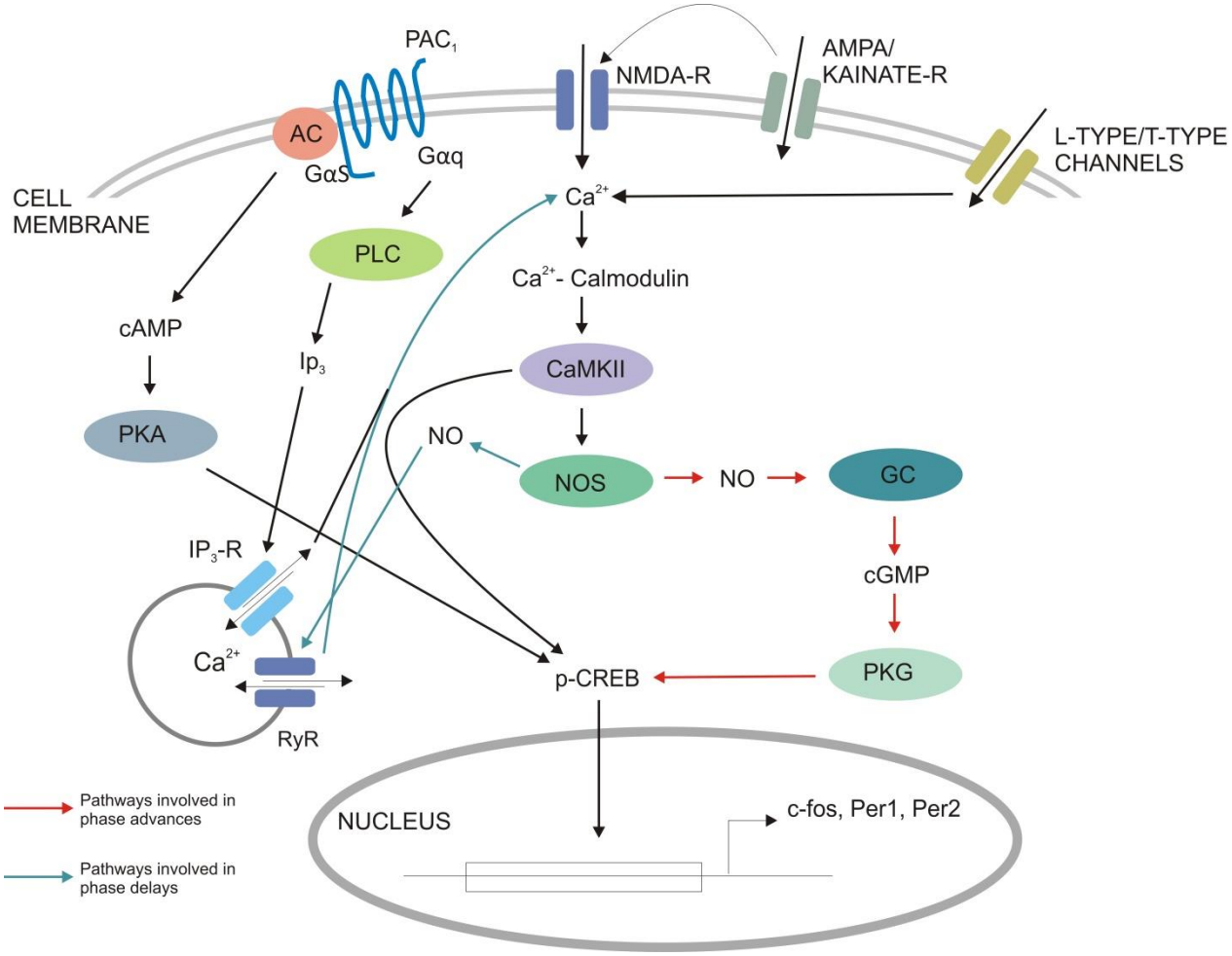

Figure 1.7: General transduction mechanisms of glutamate and PACAP signalling in the SCN.

Glutamate activates NMDA receptors to trigger an influx of Ca^{2+}. This increase intracellular calcium is augmented by the action of voltage-gated L- type Ca2+ channels and release of Ca^{2+} from stores via ryanodine receptors (RyR). Increased intracellular Ca^{2+} leads to the activation of diverse transduction cascades. Calmodulin kinase II (CaMKII) directly phosphorylates CREB and contributes to the cGMP/PKG pathways also leading to CREB phosphorylation. PACAP contributes to raising intracellular Ca^{2+} levels via the activation on IP_3 and also to the phosphorylation of CREB via the cAMP/PKA. Phosphorylated CREB (p-CREB) activates the transcription of *Per1/Per2* genes by binding to a CRE element in their promoter regions.

Downstream from CaMKII/NOS there is a second stage of gating that is poorly understood. There is evidence to suggest specific pathways are activated for causing phase advances and delays. In the early night (where we see phase delays) ryanodine receptors (RyR) are responsible for calcium mobilisation. Pathways involved in phase delays are represented by blue arrows. In the late night (where we see phase advances: represented by red arrows) the NO-cGMP pathway activates protein kinase G (PKG). Pathways involved in phase advances are represented by red arrows.

Adapted from Hannibal (2006); Brown and Piggins (2007); Golombek and Rosenstein (2010).

aspects of the pathway are more or less important for specific cells types) remains to be determined. For example, not all SCN cells receive retinal input and so these must presumably rely on the release of GABA and/or neuropeptides for other SCN cells for photic resetting. As indicated above, VIP and GRP have both been implicated in such a role.

Therefore PACAP/glutamatergic signalling from the RHT, and consequent increase in intracellular calcium, triggers VIP/GRP release in retinorecipient neurons. VIP and GRP (presumably among other signalling molecules) then transmit this photic signal to non-retinorecipient SCN neurons. In line with this view, in VIP-deficient mice, there is a 30% reduction in RHT-induced increases in intracellular Ca^{2+} within the dorsal SCN region targeted by such cells (Vosko et al., 2015).

1.3.4.2 The Intergeniculate Leaflet

In addition to direct retinal input to the SCN via the RHT, the SCN also receives sensory information from the Intergeniculate leaflet (IGL), via the geniculohypothalamic tract (GHT) (Moore and Card, 1994). The GHT originates in neurons throughout the IGL (Card and Moore, 1989), providing a primarily ipsilateral projection that terminates in the same area of the SCN as the RHT (Harrington et al., 1985, Card and Moore, 1989). Despite this anatomical proximity, it is still largely unclear whether GHT input directly influences retinorecipient SCN neurons. Moreover, as discussed below, IGL cells exhibit a range of sensory properties, and it is so far unclear which of these functionally defined cell types contribute to the GHT.

Consistent with anatomical data indicating dense ipRGC projections to the IGL (Hattar et al., 2006), electrophysiological studies have shown that at least 50% of IGL neurons exhibit sustained ON responses to retinal illumination (Harrington and Rusak, 1989, Howarth et al., 2014). Thus, similar to SCN neurons, many IGL cells encode irradiance (Harrington, 1997). Of note, however, IGL cells show much more pronounced responses to low light levels (Brown et al, 2011; Howarth et al 2014). IGL neurons are also known to exhibit various kinds of binocular interaction, including the presence of cells that selectively respond to

interocular differences in irradiance (Harrington and Rusak, 1989, Howarth et al., 2014), and previous work suggests that a subset of IGL neurons in birds are colour sensitive (Maturana and Varela, 1982). The IGL could therefore transmit a wide variety of signals to the SCN, including essential irradiance information used for determining time of day.

In line with the idea that the IGL is involved in regulating the sensory properties of the circadian system, behavioural studies have shown that lesions to the IGL affect circadian locomotor rhythms, inhibiting the period-lengthening effects of constant light (Harrington and Rusak, 1986). IGL-lesioned hamsters also exhibit smaller phase advances and larger phase delays to photic stimulation (Pickard et al., 1987), and lengthened free-running periods in constant darkness (DD) (Pickard, 1994). Taken together, this data indicates that IGL neurons have some involvement in the circadian light response and assist in adjusting circadian phase; however, IGL- lesioned animals do still entrain to LD cycles, suggesting that the IGL is not essential for photic entrainment.

Although photic information from the retina is the primary entrainment signal, other non-photic cues such as feeding cycles (Edmonds, 1977, Abe et al., 2007), temperature (Refinetti, 2010, Refinetti, 2015), behavioural activity (such as wheel running) (Dudley et al., 1998) and arousal or sleep-deprivation (Grossman et al., 2000) can interact with and often antagonise the effects of light in a phase dependent manner. Although this thesis focusses on photic input to the circadian system, it must be noted that the IGL is one possible route for this information to reach the SCN as it receives serotonergic innervation from the dorsal raphé nucleus (DRN), a brain area associated with transmitting arousal-related information (Meyer-Bernstein and Morin, 1996, Vrang et al., 2003). The GHT therefore modifies the signal from the retina and the DRN to transmit an integrated signal to the SCN for entrainment (Lewandowski and Usarek, 2002). The contributions of the raphé nuclei to the circadian network are discussed below.

1.3.4.2.1 IGL neuronal subtypes

The IGL can be divided into two distinct subsets of neurons that can be distinguished by their expression of neuropeptides and areas of innervation. All IGL neurons express the neurotransmitter GABA, however, neurons projecting to the SCN are co-localised with neuropeptide Y (NPY) and neurons projecting to the contralateral IGL co-localise with the neurotransmitter Enkephalin (ENK) (Moore and Speh, 1993, Blasiak and Lewandowski, 2013).

NPY is co-expressed alongside GABA in the neurons of the GHT (Moore and Speh, 1993). NPY neurons form a dense plexus in the SCN core (Harrington et al., 1985) overlapping with retinal efferents, implicating NPY in having a role in modulating photic-input to the clock. Consistent with this view, microinjection of NPY into the SCN during the subjective day *in vivo* (before activity onset in hamsters) elicits phase advances in locomotor activity, that persist under both constant light and constant darkness (Huhman and Albers, 1994). *In vitro* studies of NPYs phase shifting actions in the SCN produce very similar results (Shibata and Moore, 1993, Gribkoff et al., 1998, Soscia and Harrington, 2005, Belle et al., 2014). Moreover, electrical stimulation of the GHT also produces a similar pattern of phase resetting (Rusak et al., 1989), implying that the pharmacological actions of NPY highlighted above most likely reflect a genuine physiological action of NPY cells in the IGL.

The identical action of NPY in both LL and DD (Huhman and Albers, 1994) is consistent with the idea that NPY can both oppose light-induced phase shifting and communicate non-photic information to the SCN. Such a role is also supported by the pattern of efferent projections to the IGL including, photic input from the retina (Hattar et al., 2006) and arousal-related input from the raphé nuclei (Meyer-Bernstein and Morin, 1996, Vrang et al., 2003). Indeed, injections of NPY have been shown to elicit phase shifts in the SCN that mimic those generated by non-photic stimuli during the subjective day, but not during the subjective night (Biello et al., 1997). These NPY-induced phase shifts can be attenuated *in vivo* by subsequent light exposure (Biello and Mrosovsky, 1996) and can be blocked *in vitro* by the application of glutamate (Biello et al., 1997). Conversely, glutamate, a neurotransmitter involved in transmitting photic signals to the SCN (discussed above),

elicits phase shifts during the subjective night but not during the subjective day, that can subsequently be blocked by application of NPY (Biello et al., 1997). Therefore clear evidence exists of antagonistic signals from the retina and the IGL, acting at the level of the SCN. Additionally, NPY also modulates other SCN signalling pathways associated with photic transmission, attenuating *in vitro* phase-shifts induced by NMDA during the projected night (Yannielli and Harrington, 2001, Soscia and Harrington, 2004) and blocking PACAP receptor activation (Harrington and Hoque, 1997) during the projected day. This obvious interaction between photic and NPY input to the SCN, demonstrates a clear role for the IGL in modulating the SCN responses to light.

In line with its ability to shift the phase of the circadian clock, NPY also has been demonstrated to alter the firing rate of SCN neurons in a phase-dependent manner. SCN neurons are more sensitive to NPY during the subjective day (Liou and Albers, 1991, Mason et al., 1987). Although one study has reported excitatory actions of NPY (Mason et al., 1987), most studies report the NPY exerts primarily suppressive effects on SCN neuronal firing (Albers et al., 1990, Liou and Albers, 1991, Cutler et al., 1998, Gribkoff et al., 1998, Belle et al., 2014).

Given that NPY cells are located within the visual thalamus, and has been implicated in modulating photoentrainment, it is surprising that there does not appear to be direct retinal input to cells expressing NPY in the IGL (Thankachan and Rusak, 2005, Morin, 2013), although conflicting evidence exists to dispute this (Takatsuji et al., 1991). Functional studies, paint a similarly conflicting picture: hence, NPY- expressing neurons do not exhibit any signs of light-induced c-Fos expression (Juhl et al., 2007) while IGL neurons antidromically activated from the SCN have been reported to show a variety of responses to retinal illumination including ON excitations, antagonistic responses to binocular stimulation or light-supressed firing (Harrington and Rusak, 1989, Blasiak and Lewandowski, 2013). It is worth noting however that these studies of antidromically activated cells did not sample from large numbers of cells or perform very extensive sensory characterisation. At present then, we must therefore be cautious in attributing transmission of photic information to the SCN to solely NPY neurons.

A second population of cells within the IGL express the neurotransmitter ENK alongside GABA. These cells form reciprocal projections to the contralateral IGL (Card and Moore, 1989, Mikkelsen, 1992, Moore and Card, 1994) and are a distinct population from those that innervate the SCN (Pickard et al., 1987, Moore and Speh, 1993, Blasiak and Lewandowski, 2013). Unlike NPY cells, these ENK-cells do exhibit light-induced *c-fos* (Juhl et al., 2007) and display sustained excitatory responses to light (Blasiak and Lewandowski, 2013). The action of these contralateral-projecting cells is, apparently, to supress firing of the opposing IGL (Zhang and Rusak, 1989) and may thus underlie the ability of some IGL cells to detect difference in inter-ocular irradiance (Howarth et al., 2014). Accordingly, although such cells do not directly give rise to the GHT, these commissural projections could potentially still play some role in shaping sensory signals provided to the SCN.

1.3.4.3 The Olivary Pretectal Nucleus

The OPN is most commonly known for its involvement in the mediation of the pupillary light reflex (PLR). It receives direct innervation from the retina and the neuronal firing rate of OPN cells is directly related to light intensity (Campbell and Lieberman, 1982, Allen et al., 2011). Hence, in the dark, the firing rate of OPN cells is very low and upon illumination the neurons increase their firing rate to a 'tonic ON' state which remains steady for the entirety of a given stimulus (Trejo and Cicerone, 1984). If the brightness of the light stimulus is increased, the tonic firing rate of OPN neurons increases, driving a proportional change in pupil size (Clarke and Ikeda, 1985). Insofar as this change in pupil size naturally reduces the amount of retinal illumination available to drive any kind of visual response, these luminance coding cells in the OPN must indirectly modulate sensitivity of the circadian system.

As indicated above, the OPN is a major target of ipRGCs (Hattar et al., 2006) and is innervated by both M1 and M2 ipRGCs (Baver et al., 2008). OPN neurons therefore receive substantial input from both melanopsin and outer retinal photoreceptors. Rodless/coneless mice retain the sustained components of the OPN light response, demonstrating that melanopsin plays a major role in the irradiance encoding ability of the OPN and consequently controls the level of tonic pupil constriction (Lucas et al., 2001, Allen et al.,

2011). In contrast, cone signals are generally considered to provide the primary source of information about rapid changes in light intensity, responsible for early phases of the pupil response (Lucas et al., 2003, Lall et al., 2010, Allen et al., 2011). There is also data suggesting that, in primates cones provide a yellow-ON/blue-OFF input to the OPN (Dacey et al., 2005, Spitschan et al., 2014). In contrast, data from mice suggest that strongly S-opsin biased cones in fact drive relatively sustained pupil constriction (Allen et al., 2011), suggesting that if chromatic information is used to regulate the mouse pupil this most likely come in the form of a blue-ON signal.

Interestingly, the OPN possesses anatomical connections to the SCN (Moga and Moore, 1997) and the IGL (Moore et al., 2000). Accordingly, lesions of the pretectum reportedly attenuate light-evoked phase shifts (Marchant and Morin, 1999). Although the nature or properties of the OPN cells innervating these regions are currently unknown, it appears then the OPN provides another route via which photic signals may influence photoentrainment (aside from the indirect influence of regulating pupil constriction).

1.3.4.4 The Raphé nuclei

The SCN is innervated by serotonin (5-HT) neurons that project from the raphé nuclei and terminate in the VIP+ region of the SCN (Meyer-Bernstein and Morin, 1996, Moga and Moore, 1997, van Esseveldt et al., 2000). The origin of serotonergic input varies by species. In the hamster, the SCN receives 5-HT input directly via the median raphé nucleus (MRN) and indirectly via the IGL from neurons that originate in the dorsal raphé nucleus (DRN) (Meyer-Bernstein and Morin, 1996, Leander et al., 1998). Whereas, in the rat, 5-HT innervation of the SCN arises from both the MRN and DRN although, similar to in the hamster, the MRN provides the majority of serotonergic input to the SCN (Moga and Moore, 1997).

Electrical stimulation of either the MRN or DRN elicits 5-HT release in the SCN (Glass et al., 2000). However, only 50 % of the MRN neurons projecting the SCN and 40% of those projecting from the DRM to the IGL contain 5-HT (Leander et al., 1998, Hay-Schmidt et al.,

2003), indicating that another as of yet unidentified neurotransmitter transmits information from the raphé nuclei. The pathways of serotonergic innervation in the mouse have not yet been investigated.

There is evidence to suggest that 5-HT is involved in circadian entrainment to non-photic stimuli. Exposure to a non-photic stimulus such as novel access to a running wheel (Dudley et al., 1998) sleep deprivation (Grossman et al., 2000) or dark pulses (Mendoza et al., 2008) during the day elicits a large release of 5-HT at the SCN and advances rhythms in wheel-running behaviour. Electrical stimulation of the MRN/DRN also induces these phase advances and 5-HT release (Meyer-Bernstein and Morin, 1999, Glass et al., 2000, Glass et al., 2003, Yamakawa and Antle, 2010). Application of 5-HT receptor agonists *in vivo* (Challet et al., 1998, Ehlen et al., 2001) and *in vitro* (Sprouse et al., 2004, Prosser et al., 1990, Prosser et al., 1993, Medanic and Gillette, 1992) elicit phase advances in neuronal firing when they occur during mid-subjective day.

Conversely, neurotoxic lesions to the MRN that deplete 5-HT input to the SCN affects locomotor function in the hamster (Meyer-Bernstein and Morin, 1996, Meyer-Bernstein et al., 1997) and rat (Smale et al., 1990), by advancing the onset of wheel-runing and delaying its offest, resulting in a lengthened period of locomotor activity (Smale et al., 1990) but does not block behavioural phase shifting (Bobrzynska et al., 1996). Also, the blockade of 5-HT receptors does not block phase shifts induced by a novel running wheel (Antle et al., 1998), and produces signifcant increases in 5-HT release at the SCN (Antle et al., 2000) throwing some doubt on the role that serotonin plays in non-photic phase shifting.

Single-unit recordings have demonstrated that SCN neurons are most sensitive to 5-HT during the night (Mason, 1986) and that it has an inhibitory effect upon SCN neuronal firing, both *in vivo* (Nishino and Koizumi, 1977, Miller and Fuller, 1990, Ying and Rusak, 1994)and *in vitro* (Huang and Pan, 1993). 5-HT receptor agonists inhibit light-induced changes in SCN firing *in vivo* in the hamster (Ying and Rusak, 1994, Ying and Rusak, 1997).

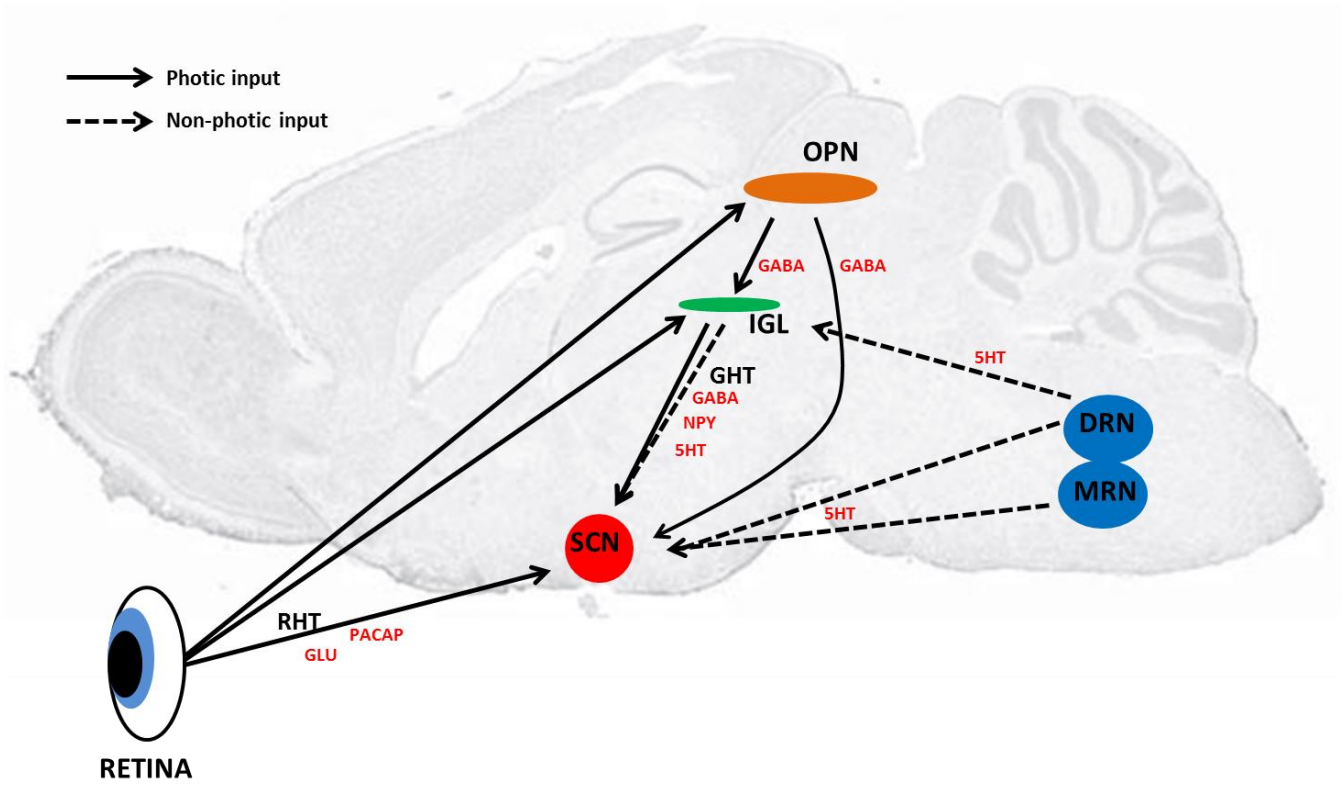

Figure 1.8: Main afferent pathways to the SCN.

The SCN receives direct innervation from the retina via the RHT. The neurotransmitters glutamate (GLU) and PACAP are released onto the SCN from RHT terminals to transmit photic information. A second indirect pathway for photic information to reach the SCN occurs via the GHT, arising from NPY and GABA projections originating in the IGL. Information from non-photic sources is transmitted by serotonin (5-HT) and originates in the raphé nuclei. The dorsal raphé nucleus (DRN) signals to the IGL where non-photic signals are combined with signals from the retina and transmitted to the SCN. Direct 5-HT input to the SCN originates in the median raphé nucleus (MRN). Solid arrows represent photic input, dashed arrows represent non-photic input and the neurotransmitters involved in each of the pathways are shown in red.

Adapted from Dibner et al (2010).

5-HT also attenuates the SCN response to optic nerve stimulation in the hamster (Rea et al., 1994), rat (Jiang et al., 2000, Smith et al., 2001) and the mouse (Pickard et al., 1999), suggesting that 5-HT acts to modulate the RHT-driven excitatory glutamatergic responses in SCN neurons.

Although the MRN/DRN is primarily associated with non-photic input to the SCN, a recent study has also shown that the DRN gets retinal input, at least in some species e.g. the rat (Li et al., 2015), thereby forming another potential pathway for photic input to enter the circadian system.

1.4 Objectives

As outlined above, there is an abundance of information as to the basic anatomical organisation, cellular mechanisms and photoreceptive origins of circadian photoentrainment. There are, however, still key details that we don't know about how visual signals are integrated in the circadian system. For example: how are visual signals integrated within the SCN network, to what extent does colour play and especially significant role in circadian responses and how do direct and indirect sources of photic input interact to coordinate visual processing with the SCN?

This thesis is presented in the 'alternative format', with chapters presented in the format of published papers. The overall aim of this thesis is to examine how visual inputs from the retina are processed within the SCN and connected regions to generate the sensory properties of the circadian system as a whole. As the SCN is the principle output centre of the circadian system, the first two studies start by investigating previously unknown components of the sensory input to the circadian clock: Chapter 2 is published in the Journal of Physiology and chapter 3 in PLoS Biology.

In Chapter 2, I investigate existing theories that synchronisation of the circadian system to the solar cycle relies on a quantitative assessment of total ambient illumination. The SCN

receives light information via dense bilateral input from the two eyes, forming an ideal mechanism to allow individual SCN neurons to measure the average light intensity from across the full visual field. As of yet no-one has investigated whether this integration of photic signals occurred within individual SCN neurons or via network interaction with other cells/brain structures associated with the circadian light response. I address this question using extracellular electrophysiological recordings and visual stimuli to determine how eye-specific inputs are combined within the SCN.

In chapter 3, I aim to determine whether mice could use the highly reliable changes in the colour of daylight that occur around dawn and dusk to help determine time of day. I first, use electrophysiological experiments in human cone knock-in mice alongside visual stimuli that selectively modulate cone photoreception to determine whether SCN neurons are capable of reliably detecting changes in colour and if they could use such information to estimate sun position. I then employ behavioural paradigms and simulated natural or artificial twilight to ascertain whether mice use colour as a circadian timing cue.

In chapter 4, I set out to build on the work described in the previous chapter, by modifying our cone-selective 'silent substitution' approach for use in mice with wildtype (M-opsin expressing) cones. I first validate this approach using *in vivo* extracellular recordings in the lateral geniculate nucleus (LGN) of coneless and WT animals to confirm that such stimuli do not produce rod or melanopsin-based responses. I we next use the modified silent substitution approach alongside optogenetic-based cell identification to characterise the properties of GABAergic neurons in the IGL/vLGN regions to assess the possibility that cells forming the GHT might convey chromatic information to the SCN.

Finally, in chapter 5, I set out to more comprehensively assess the contributions of GHT signals to SCN neuronal light responses. I first use electrical stimulation of the LGN to identify the nature of SCN responses to GHT input and whether this varies based on sensory coding properties. I next use pharmacological inhibition of the visual thalamus to determine the extent to which SCN responses to irradiance and colour are shaped by GHT input.

Chapter 2: Eye-specific visual processing in the mouse suprachiasmatic nuclei

(Published in the Journal of Physiology)

2.1 Abstract

Internal circadian clocks are important regulators of mammalian biology, acting to coordinate physiology and behaviour in line with daily changes in the environment. At present, synchronisation of the circadian system to the solar cycle is believed to rely on a quantitative assessment of total ambient illumination, provided by a bilateral projection from the retina to the suprachiasmatic nuclei (SCN). It is currently unclear, however, whether this photic integration occurs at the level of individual cells or within the SCN network. Here we use extracellular multielectrode recordings from the SCN of anaesthetised mice to show that most SCN neurons receive visual input from just one eye. While we find that binocular inputs to a subset of cells are important for rapid responses to changes in illumination, we find no evidence indicating that individual SCN cells are capable of reporting the average light intensity across the whole visual field. As a result of these local irradiance coding properties, our data establish that photic integration is primarily mediated at the level of the SCN network and suggest that accurate assessments of global light levels would be impaired by non-uniform illumination of either eye.

2.2 Introduction

The ability to anticipate recurring changes in the environment is crucial to the survival of all organisms. One especially pervasive mechanism by which this is achieved is via internal circadian clocks which can be synchronised to daily variations in the environment, most notably the solar cycle (Roenneberg and Foster, 1997). In mammals this process thus relies on direct retinal projections to the hypothalamic suprachiasmatic nuclei (SCN), site of the master circadian pacemaker (Golombek and Rosenstein, 2010, Lucas et al., 2012).

It has long been recognised that the quality of visual information that would be useful to the SCN is quite distinct from that which is important for more conventional visual pathways. Thus, retinal pathways supplying the thalamocortical visual system are organised to allow for a relatively stable representation of form and motion across the ~9 decimal orders of light intensity that separate the darkest night and the brightest day (Rieke and Rudd, 2009). In contrast, detailed information about spatiotemporal patterns of illumination is presumably unimportant to the circadian system, which instead requires an accurate readout of global light intensity to infer time-of-day.

Consistent with this view, numerous behavioural studies have demonstrated that the response of the circadian system to light can be accurately predicted based on the total number of photons that the animal is exposed to (Nelson and Takahashi, 1991, Nelson and Takahashi, 1999, Dkhissi-Benyahya et al., 2000, Lall et al., 2010, Lucas et al., 2012). Thus, for example, short bright light pulses evoke a similar adjustment in clock phase as longer dimmer stimuli. Although there are known specific situations where this relationship breaks down (Vidal and Morin, 2007, Lall et al., 2010), the accepted model of clock resetting is one whereby the retinorecipient SCN act as a photon counter and controls circadian responses accordingly.

The intuitive separation between the desired properties of conventional and circadian visual processing is also supported by extensive anatomical data. Hence, retinal projections to conventional visual targets in the thalamus/tectum arise primarily via the contralateral

hemisphere, with ipsilateral projections coming exclusively from regions of the retina corresponding to the zone of binocular overlap (Morin and Studholme, 2014, Coleman et al., 2009, Sterratt et al., 2013). In contrast, the SCN receives dense bilateral retinal innervation (Morin and Studholme, 2014). Moreover, it is now clear that this retinal input to the SCN derives primarily from a subclass of intrinsically photosensitive retinal ganglion cell (ipRGC), termed M1 (Hattar et al., 2006). These cells appear specialised to encode irradiance and, unusually, project bilaterally to the brain (Hattar et al., 2006, Brown et al., 2010, Brown et al., 2011) - even where their retinal location places their field of view far outside the region of binocular overlap (Muscat et al., 2003).

This anatomical arrangement seems ideally placed to allow individual SCN neurons to measure the average light intensity from across the full visual field although, to date, this hypothesis remains untested. Existing data suggest that removing signals from one eye produces larger than expected deficits in circadian phase shifting and/or SCN Fos induction (Tang et al., 2002, Muscat and Morin, 2005). However, none of the many studies investigating visual response properties within the SCN (Meijer et al., 1986, Brown et al., 2011, Meijer et al., 1992, Drouyer et al., 2007, Mure et al., 2007, Aggelopoulos and Meissl, 2000, Nakamura et al., 2004, van Diepen et al., 2013, Sakai, 2014) have extensively characterised binocular processing at the level of individual neurons. Here we set out to address this issue, via multielectrode recordings from mouse SCN neurons using visual stimuli designed to determine the nature and extent of ipsi-/contralateral visual signals, both across the population and in individual cells.

2.3 Methods

2.3.1 Animals

All animal use was in accordance with the Animals, Scientific Procedures, Act of 1986 (UK). Experiments were performed on adult male (50-80 days) $Opn4^{+/tau\text{-}lacZ}$ reporter mice and wildtype ($Opn4^{+/+}$) littermates (n=19 & n=14 respectively). Consistent with previous reports (Hattar et al., 2003, Lucas et al., 2003, Howarth et al., 2014), there were no observable abnormalities in the visual responses of reporter animals, hence the two datasets were

combined for the analysis presented in this study. Prior to experiments, animals were housed under a strict 12-hour dark/light cycle environment at a temperature of 22°C with food and water ad libitum.

2.3.2 *In Vivo* Neurophysiology

In preparation for stereotaxic surgery, mice were removed from their housing environment ~2-3h before lights off and anaesthetised with urethane (1.55g/kg i.p in 0.9% sterile saline). Mice were then placed into a stereotaxic frame (SR-15M; Narishage International) to hold the skull fixed in place for surgery. The surface of the skull was exposed using a scalpel incision and a hole was drilled using stereotaxic co-ordinates (0.98mm lateral to and 0.3mm posterior to Bregma) obtained from the stereotaxic mouse atlas (Paxinos and Franklin, 2001). The contralateral pupil was dilated with 1% atropine (Sigma Aldrich) and mineral oil (Sigma-Aldrich) added to prevent drying of the cornea.

Recording probes (Buszaki 32L; Neuronexus, MI, USA) consisting of 4 shanks (spaced 200µm), each with 8 closely spaced recordings sites in diamond formation (intersite distance 20-34µm) were coated with fluorescent dye (CM-DiI; Invitrogen, Paisley, UK) and then inserted into the brain parallel to the midline, 1mm lateral and 0.3mm caudal to bregma (centre of probe) at an angle of 9° relative to the dorsal-ventral axis. Electrodes were then lowered to the level of the SCN using a fluid filled micromanipulator (MO-10, Narishige International Ltd., London, UK).

After allowing 30min for neural activity to stabilise following probe insertion, wideband neural signals were acquired using a Recorder64 system (Plexon, TX, USA), amplified (x3000) and digitized at 40kHz. Action potentials were discriminated from these signals offline as 'virtual'-tetrode waveforms using custom MATLAB (The Mathworks Inc., MA, USA) scripts and sorted manually using commercial principle components based software (Offline sorter, Plexon, TX, USA) as described previously (Howarth et al., 2014). All surgical procedures were completed before the end of the home cage light phase, such that

electrophysiological recordings spanned the late projected day-mid projected night, an epoch when the SCN light response is most sensitive (Brown et al., 2011).

2.3.3 Visual Stimuli

Light measurements were performed using a calibrated spectroradiometer (Bentham instruments, Reading, UK).

Full field visual stimuli were generated via two LEDs (λmax 410nm; half-width: ±7nm; Thorlabs, NJ, USA) independently controlled via LabVIEW (National Instruments, TX, USA) and neutral density filter wheels (Thorlabs). Light was supplied to the subject via 7mm diameter flexible fibre optic light guides (Edmund Optics; York, UK), positioned 5mm from each eye and enclosed within internally reflective plastic cones that fit snugly over each eye to prevent off-target effects due to scattered light. Responses to these stimuli were then assessed as follows:

To determine the relative magnitude and sensitivity of eye specific responses in SCN neurons, mice were maintained in darkness and 5s light steps were applied in an interleaved fashion to contra- and/or ipsilateral eyes for a total of 10 repeats at logarithmically increasing intensities spanning 9.8-15.8 log photons/cm^2/s (interstimulus interval 20-50s depending on intensity). Because all mouse photoreceptors display similar sensitivity to the wavelengths contained in our stimuli (Brown et al., 2013, Brown et al., 2012), after correction for pre-receptoral filtering (Govardovskii et al., 2000, Jacobs and Williams, 2007), effective photon fluxes for each mouse opsin were between 0.5 (M- and S-cone opsins) and 0.3 log units (melanopsin) dimmer than this value. Intensities reported in the manuscript reflect effective irradiance for rod opsin, which is intermediate between these extremes (9.4-15.4 log photons/cm^2/s).

To determine components of the SCN response that were dependent on stimulus brightness vs. stimulus contrast, a second protocol was also employed. Here we stepped light intensity independently at each eye every 5s in a pseudorandom sequence spanning effective irradiances between 10.4-15.4 log photons/cm^2/s (total number of steps =840).

The sequence was generated such that, at any one time, the difference in intensity between the two eyes was no more than 2 decimal units and the instantaneous step in light intensity at each eye was one of five possible values (±2, 1 or 0 log units). To determine contrast-dependent components we then averaged cellular responses (0-500ms post change in light intensity) as a function of step magnitude at either eye. Since we found that contrast response relationships varied very little as a function of absolute irradiance data reported in the manuscript were averaged across all irradiances tested. For clarity, we only present data for steps providing contrast at one eye or equal contrast at both eyes.

To assess SCN response components that tracked stimulus brightness, we reanalysed the above to extract steady state firing (1s epochs occurring at least 4s after step in light intensity) as a function of absolute irradiance at either eye (independently or in combination).

2.3.4 Histology

At the end of each experiment, mice were perfused transcardially with 0.1M phosphate buffered saline followed by 4% paraformaldehyde. The brain was removed and post-fixed in 4% paraformaldehyde for 30min and subsequently cryoprotected in 30% sucrose. The following day, brains were sectioned at 100µm on a freezing sledge microtome and either mounted directly onto slides (wildtype mice) using Vectasheild (Vectorlaboratories Ltd., Peterbourogh, UK) or first processed for X-gal staining ($Opn4^{+/tau\text{-}lacZ}$) as described below.

X-gal staining was performed as previously described (Hattar et al., 2006). Brain sections were washed twice for 10 minutes each in buffer B (0.1M PBS at pH 7.4, 2mM $MgCl_2$, 0.01% Na-desoxycholate and 0.02% IGEPAL). Sections were then incubated for 4 hours in staining solution [buffer B with potassium ferricyanide (5mM), potassium ferrocyanide (5mM) and X-gal (Bioline Reagents Ltd, UK; 1mg/ml)] at 37°C in darkness. Following staining, sections were washed twice for 5 minutes in 0.1M PBS and mounted to slides using Vectashield as above.

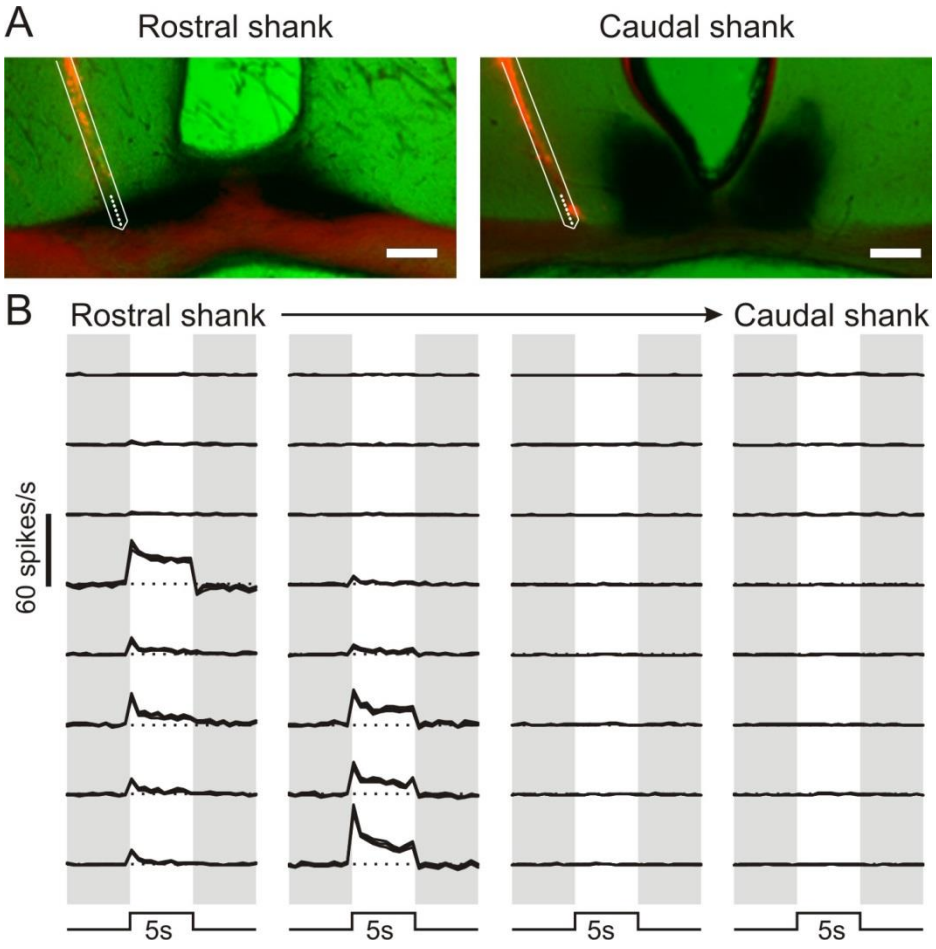

Figure 2.1: Light evoked activity in the retinorecipient SCN region.

(A) X-gal stained histological images showing multielectrode placement in the SCN region of an Opn4$^{+/tau\text{-}lacZ}$ reporter mouse. DiI-labelled probe tracks are in red, light microscopy for X-gal staining is pseudocoloured green (with melanopsin ganglion cell projections evident as darkly stained areas). Overlaid schematic (in white) shows projected locations of the 8 recording sites on each shank. Only the most rostral and caudal shanks for the 4-shank electrode are shown. Scale bars=100µm. (B) Multiunit activity detected across the 4x8 channel electrode placement shown in A, in response to 5s light pulses presented to both eyes (405nm; 15.4 log photons/cm2/s). Traces represent the mean±SEM change in firing (from 10 trials) over baseline (represented by dotted lines). Note that visual responses are absent from electrode cites located outside of the retinorecipient SCN region such as upper sites on the rostral shank and all sites on the caudal shank.

After mounting DiI-labelled probe placements were visualised under a fluorescent microscope (Olympus BX51) with appropriate filter sets and, where appropriate, X-gal staining was visualised by standard light microscopy (Figure 2.1, A). Resulting images were then compared with appropriate stereotaxic atlas figures (Paxinos, 2001), using the optic chiasm, SCN and 3rd ventricle as landmarks, to confirm appropriate probe placement. Consistent with previous anatomical and neurophysiological studies (Morin and Studholme, 2014, Hattar et al., 2006, Brown et al., 2011, Nakamura et al., 2004), visually evoked activity was exclusively observed at electrode sites located within the SCN or its immediate borders (Figure 2.1, B).

2.3.5 Data analysis

In most cases, single cell responses are presented as the mean±SEM change in firing across all trials (at least 10 per stimulus) relative to baseline (average firing rate 3 or 5s before step in light intensity for light- and dark-adapted responses respectively). Measures of monocular preference were calculated as $(Response_{CONTRA}-Response_{IPSI})/(Response_{CONTRA}+Response_{IPSI})$, such that contralateral biased responses tended towards 1 and ipsilateral biased responses towards -1. Where a cell did not show a significant response to stimulation of one of the two eyes (paired t-test between firing during first 500ms of light step and baseline, $p>0.05$), that response component was assigned a value of zero. The eye that evoked the largest response when analysed in this way was designated the 'dominant' eye. Binocular facilitation was analysed in a similar way: $(Response_{BOTH}-Response_{DOMINANT})/(Response_{BOTH}+Response_{DOMINANT})$. We classified as binocular any cell exhibiting significant responses to stimulation of both eyes individually or where the response to binocular stimulation was significantly different to that evoked by stimulating the dominant eye alone (unpaired t-test based on response to 10 trials of each stimulus).

Where average population data is presented, in most cases responses were baseline subtracted (as above) and normalised on a within cell basis according to the largest response within a specific protocol. The exception to this rule was our analysis of

brightness coding, where the absolute firing rates of each cell were normalised to range between zero and one before averaging across the population.

Statistical analyses were performed using GraphPad Prism v.6 (Graphpad Software Inc., CA, USA). Data were, in most cases, fit by 4-parameter sigmoid curves with the minimum constrained to zero as appropriate. Comparisons of sensitivity under various conditions were assessed by F-test for differences in EC_{50}, hill slope and/or maxima. Influences of eye-specific brightness/contrast on responses of various cell types were analysed by 2-way repeated measures ANOVA with dominant and non-dominant eye stimuli as factors.

2.4 Results

2.4.1 Binocular influences on SCN population activity

We first set out to determine how binocular signals were integrated to influence population firing activity within the SCN. To this end we performed multielectrode (32 channel) extracellular recordings of multiunit activity from the SCN and surrounding hypothalamus (n=33 mice) and monitored responses to full field stimuli (410nm LED; 5s from darkness), applied at varying intensity to one or both eyes. Since all mouse photoreceptor classes are equally sensitive in this part of the spectrum (see Methods), any heterogeneity in the photoreceptor populations driving specific responses (Brown et al., 2011, van Oosterhout et al., 2012) should not influence sensitivity as assessed under these conditions.

Surprisingly, given the reported dense bilateral retinal innervation of the mouse SCN (Hattar et al., 2006, Brown et al., 2010, Morin and Studholme, 2014), we found that responses driven by the contralateral retina were reliably larger than those resulting from stimulation of the ipsilateral eye (Figure 2.2, A, B; n=252 electrodes exhibiting visually evoked activity). Thus although the sensitivity of ipsi/contralateral responses were similar (F-test for difference in EC_{50} and/or Hill slope; p=0.64) the maximum amplitude of these were ~2-fold greater following stimulation of the contralateral eye (F-test for difference in

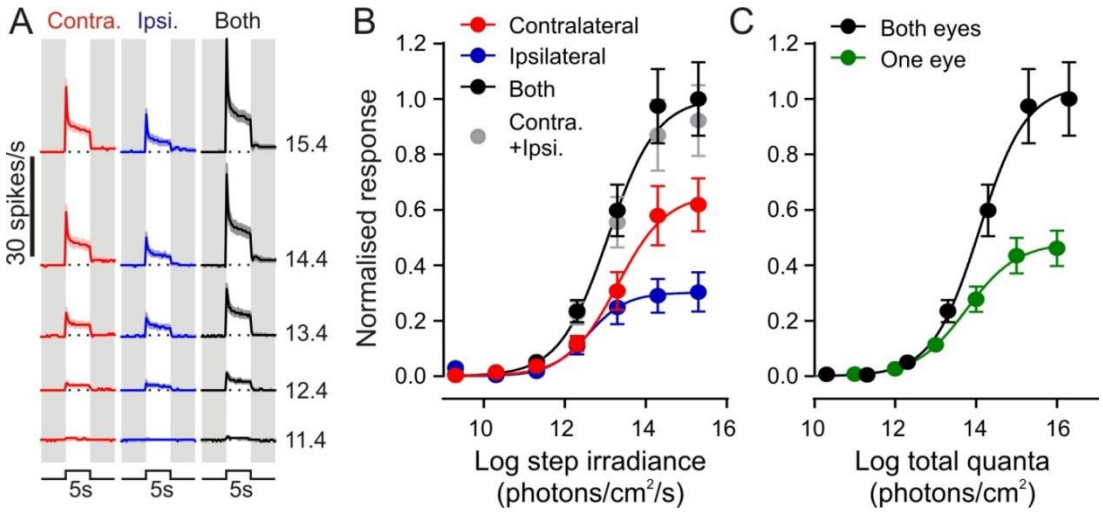

Figure 2.2 SCN population firing activity does not faithfully report global irradiance.

(**A**) Mean±SEM multiunit firing response profile across the retinorecipient SCN-region (n=252 electrodes from 33 mice) in response to 5s light steps (410nm LED, effective intensities 11.4-15.4 log photons/cm^2/s, from darkness) targeting the contralateral and/or ipsilateral eye. Data were normalised by subtracting pre-stimulus (5s before light on) firing rates (represented by dotted lines). (**B**) Normalised multiunit firing response (change in spike rate averaged across 5s light on, mean±SEM) as a function of step irradiance. Responses to stimulating both eyes together were statistically indistinguishable from a linear sum of the measured response evoked by stimulation of contralateral and ipsilateral eyes alone (grey symbols, F-test, p=0.69). (**C**) Normalised multiunit firing response (conventions as in **B**), plotted as a function of total number of photons delivered. The predicated average across left and right SCN (green symbols; average of ipsilateral and contralateral responses from **B**) is significantly lower than the response to stimulating both eyes even when corrected for total number of photons (F-test, p<0.0001).

saturation point, p=0.003). Interestingly, responses evoked by stimulating both eyes together were especially large. In line with the above, this significant difference in maximal response (F-test vs. contralateral only; p<0.001) was not associated with any appreciable difference the sensitivity of binocular vs. monocular responses (p=0.77).

Importantly, we found that SCN population activity driven by stimulation of both eyes was statistically indistinguishable from a simple linear sum of the observed responses to stimulating either eye alone (Figure 2.2, B; F-test, p=0.69). This surprising result indicates that SCN population activity does not accurately follow the total number of photons detected across both retinae. If this were the case then, correcting for the 2-fold difference in total light intensity, the average response across the paired SCN to monocular stimuli should be identical to that of an equivalent irradiance stimulus applied to both eyes. In fact, we found that the monocular responses were markedly smaller than expected given the binocular photon-response relationship (Figure 2.2, C; F-test, p<0.001). Indeed, to evoke a 50% maximal change in SCN population activity, monocular stimuli would need to be ~100 fold brighter than would be sufficient for light detected at both eyes.

2.4.2 Binocular integration in individual SCN neurons

Our data above reveal that population activity within the SCN does not (at least in all cases) exhibit the strict photon counting properties one might predict based on previous behavioural experiments (Nelson and Takahashi, 1991, Nelson and Takahashi, 1999, Lall et al., 2010, Lucas et al., 2012, Dkhissi-Benyahya et al., 2000). Given this unexpected result, we next aimed to determine how these tissue level visual response properties arise through the sensory characteristics of individual SCN neurons.

From our multiunit recordings we were able to isolate the activity of 61 individual cells within or bordering the SCN, of which 51 were light sensitive. Across this population, we observed heterogeneity in eye specific responses to light steps from darkness (Figure 2.3, A-E). This included many cells that responded solely to stimulation of either the contralateral (Figure 2.3 A, E; n=15) or ipsilateral eye (Figure 2.3 B, E; n=19) and other cells

that exhibited clear responses to stimulation of either eye and/or substantially larger responses to binocular vs. monocular stimulation (Figure 2.3, C-E; n=17).

Thus, we found that the majority (~67%) of visually responsive SCN neurons did not integrate binocular signals and, instead, faithfully reported monocular irradiance (Figure 2.3, F). In all cases, responses of these cells to stimulation of the dominant eye vs. both eyes were statistically identical (Figure 2.3, E; *t*-tests based on responses to 10 trials, $p>0.05$).

In contrast, for the smaller proportion of SCN cells that did have access to visual signals from either eye, responses were in most cases biased towards one retina, with the binocular influence most evident as an enhanced response to stimulation of both eyes (Figure 2.3 E, G). Surprisingly, here we found that average binocular responses were in fact significantly larger than even a linear sum of the two monocular inputs (F-test for difference in saturation point, $p=0.007$; not shown). This synergistic effect appeared to diminish over time, however (Figure 2.3 C, D), such that towards the end of the light steps (last 1s) responses were not significantly different from the linear prediction (F-test, $p=0.69$).

Together, these SCN cellular properties explain the unexpectedly small SCN multiunit responses to monocular vs. binocular stimuli (Figure 2.2) – most SCN neurons are strongly biased towards one eye such that at any given intensity many more cells will be activated by stimulating both eyes. Surprisingly, however, the observed multiunit bias towards contralateral driven visual responses (Figure 2.2, B) did not translate into an increased number of contralateral biased SCN neurons. In fact, we observed statistically equivalent proportions of ipsi-/contralateral biased SCN neurons (n=27 and 24 respectively, Fishers exact test, $p=0.77$). These data imply that, across the population, contralateral inputs tend to drive larger responses in individual SCN neurons than do ipsilateral inputs (although among the sample of cells we collected this difference did not attain significance: 3.8±0.7 vs. 2.7±0.7 spikes/s respectively at 15.4 log photons/cm^2/s; paired *t*-test, $p=0.28$).

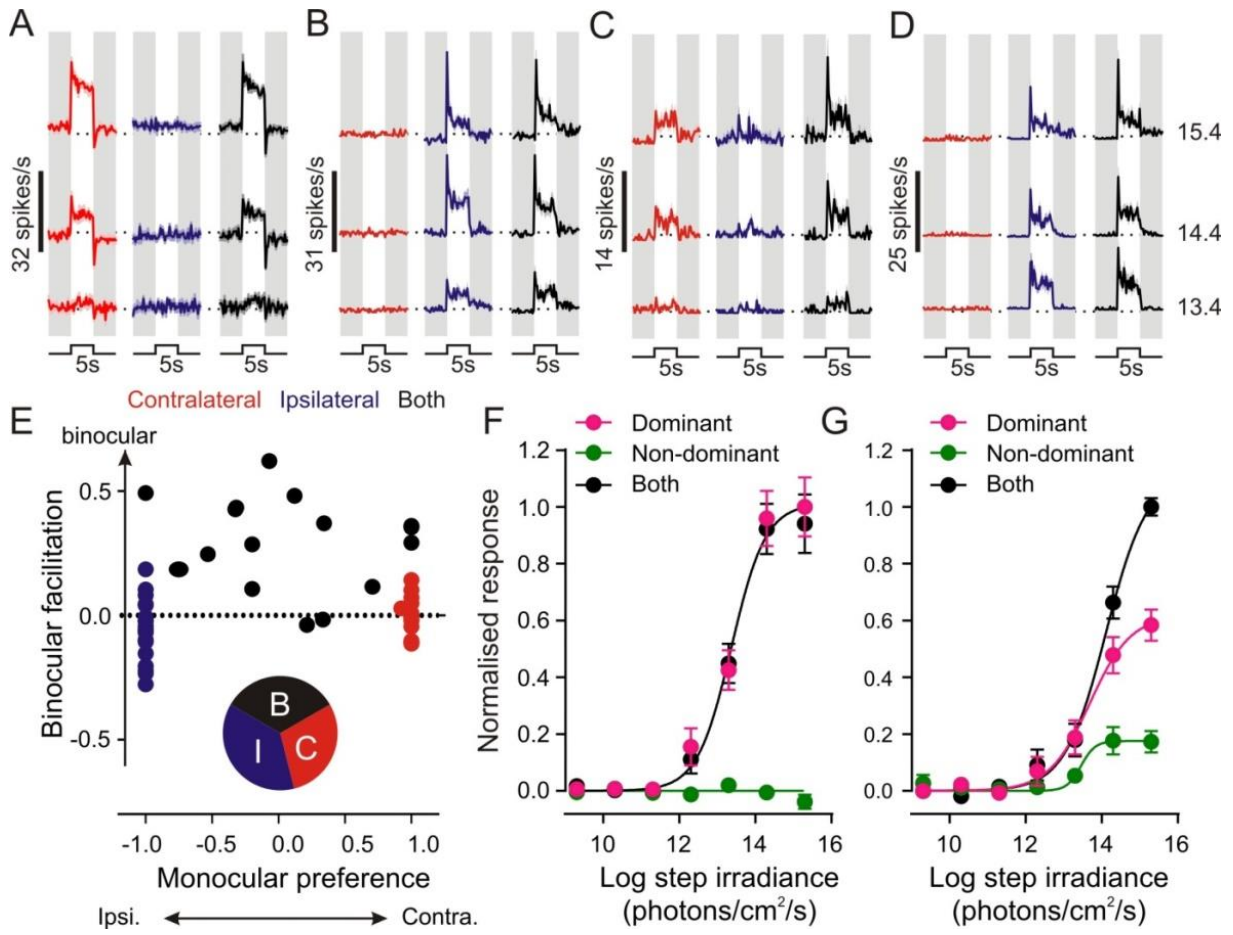

Figure 2.3: Eye-specific response properties of SCN neurons.

(A-D) Example firing response profiles (mean±SEM of 10 trials) for 4 SCN single units in response to 5s light steps (410nm LED, effective intensities 13.4-15.4 log photons/cm^2/s, from darkness) targeting the contralateral and/or ipsilateral eye. Many cells only showed clear responses to stimulation of either contralateral (A) or ipsilateral (B) eye, while a subset showed binocular responses or varying strength (C, D). (E) Population data for 51 visually response SCN neurons showing monocular preference (0=equally matched binocular response) vs. binocular facilitation (positive values=larger response to stimulation of both eyes vs. one eye; see methods for details). Inset pie chart shows proportion of cells exhibiting purely ipsilateral, contralateral or binocular responses. (F) Normalised acute response of monocular cells (change in spike rate across first 500ms of light on, mean±SEM, n=34) as a function of step irradiance. Responses to stimulation of the dominant eye or both eyes together were statistically indistinguishable (F test; p=0.91). (G) Normalised acute response of binocular cells (conventions as in F, n=17). Binocular responses were significantly greater than those driven by the dominant eye alone (F test; p=0.004).

In sum, our data above suggest that while a subset of SCN neurons receives inputs from both eyes, none of these cells alone can effectively integrate photons from across the visual scene to report the total amount of light in the environment. It is worth noting, however, that such light steps applied from darkness represent rather unnatural visual stimuli. Moreover, these do not allow one to distinguish response components that are dependent on the absolute irradiance of the signal vs the relative change in irradiance (brightness vs. contrast). To better understand, then, how SCN neurons track spatio-temporal variations in light intensity under more natural conditions we next assessed responses to smaller modulations in light intensity, using a protocol that allowed us to dissociate response components dependent on stimulus brightness vs. contrast.

2.4.3 Response properties of SCN binocular cells

Since our data indicated that binocular influences were especially pronounced for the initial components of SCN neuronal responses under dark adapted conditions, we first examined how binocular cells responded to acute changes in light intensity in the range up to ±2 log units, applied under light adapted conditions (11.4 to 14.4 log photons/cm^2/s).

Interestingly, we found that when changes in light intensity occurred simultaneously across both eyes, binocular cells exhibited very sharp and robust increases or decreases in firing (Figure 2.4, A) that were near-linear with respect to the log change in irradiance (Figure 2.4, B). In contrast, responses were smaller and much more sluggish when light steps occurred solely at the dominant eye and were virtually undetectable when applied to the non-dominant eye (Figure 2.4, A, B). Together, these data indicate that binocular integration functions in this population of cells to facilitate rapid responses to global changes in light levels.

We next determined the extent to which eye-specific signals influenced the ability of binocular cells to track brightness (Figure 2.5, A), by quantifying steady state firing (4-5s after a change in light intensity) as a function of absolute irradiance. Given the data described above, one might expect the steady state firing of binocular cells to be strongly

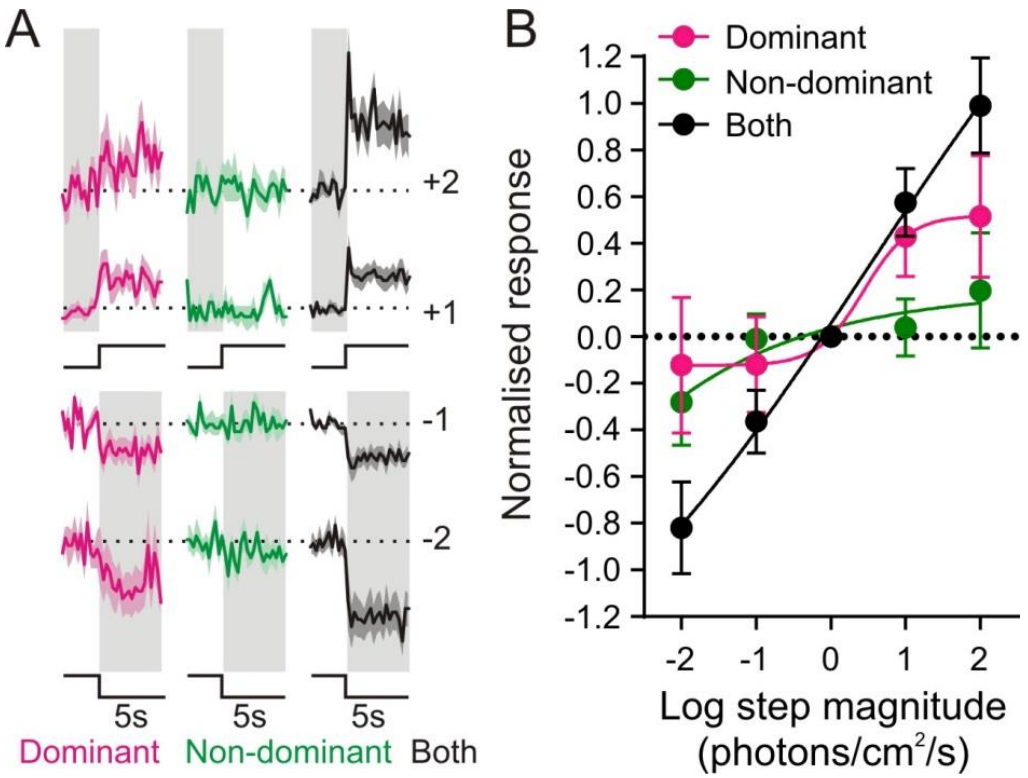

Figure 2.4: Binocular integration is required for robust contrast responses in a subset of SCN neurons.

(A) Mean±SEM normalised response of binocular cells (n=17) to irradiance steps (-2 to +2 log units; 405nm LED) applied to one or both eyes under light adapted conditions (11.4 to 14.4 log photons/cm^2/s). (B) Quantification of data in A showing change in firing over first 500ms of light step. Contrast responses were significantly larger upon stimulation of both eyes vs. the dominant eye only (F test, p=0.02).

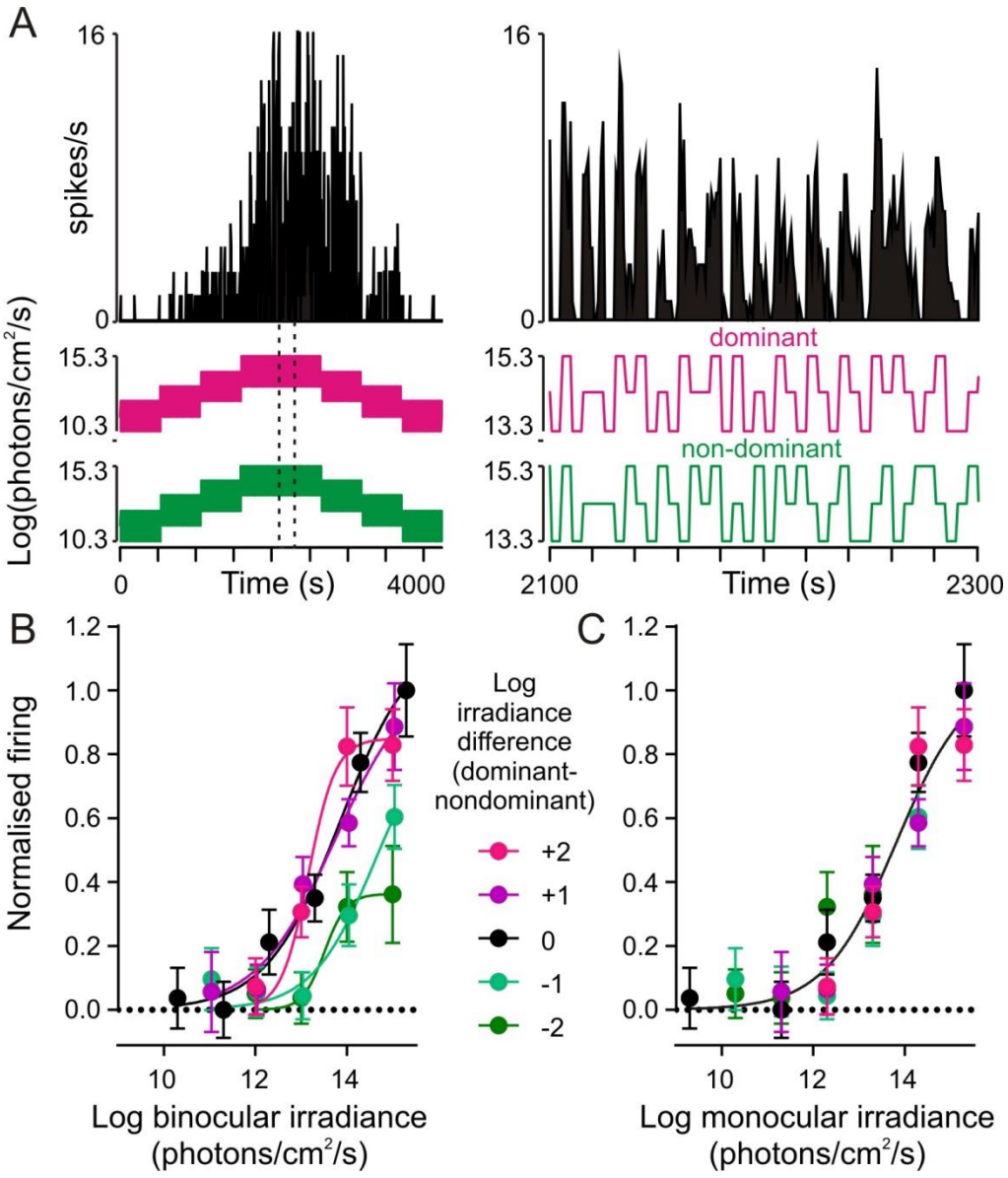

Figure 2.5: SCN binocular cells encode monocular irradiance.

(A) Firing activity of a binocular SCN neuron presented with a pseudorandom irradiance sequence (see methods). Right panels show a portion of the responses at higher temporal resolution (indicated by the dotted region bottom left). (B) Normalised steady state firing activity of binocular cells (spikes occurring 4-5s after a step in irradiance; mean±SEM, n=17) plotted as a function of the average irradiance across the two eyes and split according to the interocular difference in irradiance. When expressed in this manner, irradiance response relationships could not be described by a single sigmoid curve (F-test, $p<0.001$). (C) Data from B plotted according to irradiance at the dominant eye. Under these conditions, all data could be described by a single curve (F test, $p=0.62$).

influenced by the overall irradiance across either eye. In fact, however, we found very little influence of binocular integration on the steady state firing of such cells. Thus, rather than following the mean irradiance across both eyes (Figure 2.5, B; F-test, $p<0.001$) binocular cell firing activity was, instead, entirely accounted for by the irradiance at the dominant eye, regardless of the interocular difference in brightness (Figure 2.5, C; F-test, $p=0.62$). Intriguingly, then, despite clear binocular influences on responses to rapid changes in light levels, basal firing of binocular cells was entirely driven by just one of the two eyes.

2.4.4 Response properties of SCN monocular cells

To better understand how the properties of binocular cells, outlined above, distinguished them from other visually responsive (monocular) SCN neurons, we also examined brightness and contrast components of the monocular cell responses.

Surprisingly, we found that whereas binocular cells reliably exhibited 'ON' responses to visual contrast (i.e. a positive relationship between the step in light intensity and change in firing), only a subset of monocular cells exhibited this property (Figure 2.6, A; n=24/34). Other cells exhibited decreases in firing in response to increased light intensity (OFF, n=5) or displayed transient increases in firing in response to both light increments and decrements (ON/OFF, n=5).

Unlike binocular cells (Figure 2.6, B), all these monocular populations exhibited robust, near-log linear, changes in firing as a function of step magnitude at the dominant eye alone (Figure 2.6, B). Moreover, none of these monocular populations displayed any clear influence of non-dominant eye contrast, (2-way repeated measures ANOVA, non-dominant eye and interaction terms all $p>0.05$)

We have previously reported 'transient' cells in the mouse SCN (Brown et al., 2011), whose visual response properties appear consistent with those of the ON/OFF cells described above. By contrast, the presence of monocular cells exhibiting OFF responses under these

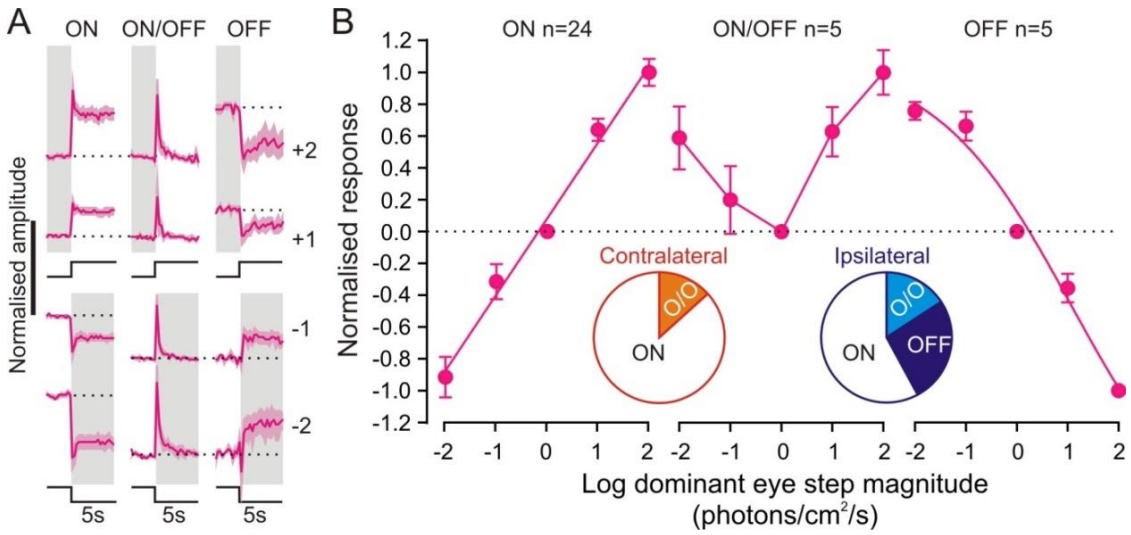

Figure 2.6: Monocular SCN neurons exhibit varying responses to visual contrast.

(A) Mean±SEM normalised response of monocular cell subpopulations to irradiance steps (-2 to +2 log units; 410nm LED) applied to the dominant eye under light adapted conditions (11.4 to 14.4 log photons/cm^2/s). For most cells changes in firing rate were positively related to step magnitude (ON, n=24), while other cells showed the inverse relationship (OFF, n=5) or increased firing in response to both increase and decreases in irradiance (ON/OFF, n=5). (B) Quantification of data in A showing change in firing over first 500ms of light step for the three populations. Inset pie charts indicate the proportion of each cell type driven by either eye (n=15 and 19 total for contralateral and ipsilateral respectively). Note, OFF cells were all driven the ipsilateral eye.

conditions was surprising – not least because all of these cells exhibited excitatory responses to light steps applied from darkness (not shown). Interestingly, these OFF responses also appeared to exclusively originate with the ipsilateral eye (Figure 2.6, B). Based on our sample size there is a low probability that we could have failed to detect an equivalent population of contralateral-driven OFF cells (Fishers exact text, p=0.053). In sum then it appears that ipsilateral retinal influences on the SCN may be more diverse than the primarily ON responses originating with the contralateral eye (Figure 2.6, B).

In line with their responses to visual contrast described above, we found that, whereas the steady state firing of ON cells reliably increased as a function of monocular brightness, that of OFF cells decreased (Figure 2.7 A, B). Importantly, we were also able to identify both ON and OFF cells within the same recording (Figure 2.7, A), indicating that this unusual OFF behaviour could not simply reflect some state or circadian phase-dependent switch in general SCN responsiveness.

By contrast with the other SCN cell types, the steady state activity of ON/OFF cells did not vary as a function of irradiance (Figure 2.8, repeated measures ANOVA, p=0.36), indicating that this population specifically responds only to rapid changes in light intensity.

2.5 Discussion

Here we show that, despite the dense bilateral input that the SCN receive from the retina (Hattar et al., 2006, Brown et al., 2010, Morin and Studholme, 2014, Miura et al., 1997), few individual SCN neurons have access to visual signals from both eyes. Moreover, even where cells do receive input from both eyes, binocular influences are limited to just the initial components of any response to changing irradiance. As a result, no single SCN neuron is capable of providing direct information about global levels of irradiance across the full visual field.

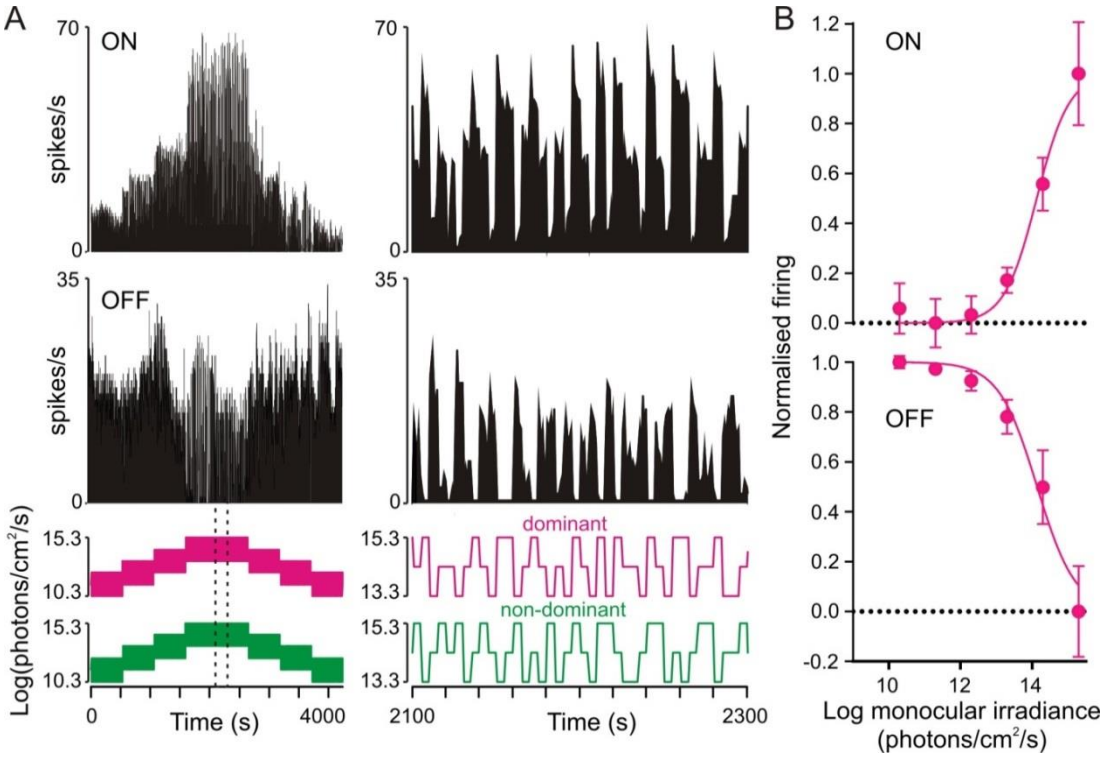

Figure 2.7: Brightness and darkness coding in SCN monocular cells.

(A) Firing activity of simultaneously recorded ON (top) and OFF (bottom) SCN neurons presented with a pseudorandom irradiance sequence (see methods). Right panels show a portion of the responses at higher temporal resolution (indicated by the dotted region bottom left). (B) Normalised steady state firing activity of monocular ON and OFF cells (spikes occurring 4-5s after a step in irradiance; mean±SEM, n=24 & 5 respectively) plotted as a function of irradiance at the dominant eye.

These results are surprising for two reasons. Firstly because we have previously observed extensive binocular integration in the mouse visual thalamus, a region where eye-specific inputs were, until recently, believed to remain entirely segregated (Howarth et al., 2014). Indeed, using similar approaches to those employed here, we observed many single cells in the visual thalamus whose basal firing did encode mean binocular irradiance. More importantly, however, our present results are unexpected because the existing model posits that circadian photoentrainment is reliant on a quantitative assessment of the total amount of light in the environment (Nelson and Takahashi, 1991, Nelson and Takahashi, 1999, Lall et al., 2010, Lucas et al., 2012, Dkhissi-Benyahya et al., 2000). Assuming this model correct, any such assessment of global irradiance could occur neither at the level of individual cells, nor by simply taking the average light-evoked activity across the population of such cells.

In fact, since the degree of visually evoked SCN activity is well correlated with the magnitude of circadian phase shifts (Meijer et al., 1992, Brown et al., 2011), our present data suggest that the current model of circadian photic integration is not entirely accurate. Based on the light-evoked firing we observe in the SCN, we would predict that light falling on one, rather than both, eyes would result in a 50% reduction in phase shift magnitude, rather than a 50% reduction in apparent light intensity (0.3 log units). As far as we are aware, only one study has explicitly tested this possibility, by performing a reversible monocular occlusion before applying phase shifting light stimuli (Muscat and Morin, 2005). Unfortunately, inter-individual variability in phase shift magnitude make a robust assessment of the above difficult although, for long/bright stimuli, monocular phase shifts certainly appear better explained by a 50% reduction in amplitude rather than in total photon flux.

Accordingly, we propose that retinorecipient SCN neurons do accurately measure photon flux, but only within a portion of the visual field. Based on an established view of SCN organisation, suggesting the presence of weak oscillators that are readily reset by light and robust oscillators which integrate circadian inputs from the former (Albus et al., 2005, Brown and Piggins, 2009, Rohling et al., 2011), we propose a model whereby the retinorecipient cells are reset according to ‘local’ light intensity (Figure 2.9). It is then the

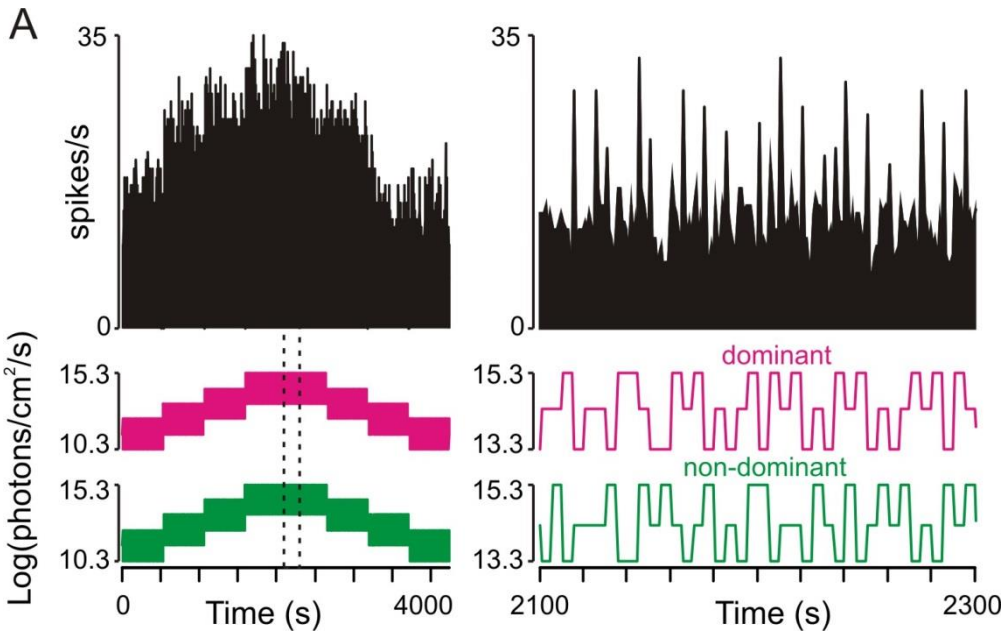

Figure 2.8: SCN ON/OFF cells do not track irradiance.

(A) Firing activity of an ON/OFF SCN neuron presented with a pseudorandom irradiance sequence (see methods). Right panels show a portion of the responses at higher temporal resolution (indicated by the dotted region bottom left). Note that steady state firing does not vary as a function of irradiance.

average phase information supplied by these retinorecipient oscillators that dictates the integrated circadian response. Such a mechanism would account for the behavioural response to monocular visual stimuli and the associated 50% reduction in the number of Fos-positive SCN neurons previously observed (Muscat and Morin, 2005).

We should also note that another study, employing unilateral optic nerve transection, found a much larger (~90%) reduction in light-induced Fos across the hamster SCN (Tang et al., 2002). The reason for this discrepancy is unclear but, again, this observation appears hard to incorporate into a model whereby the SCN response is proportional to the total level of ambient illumination.

Aside from the above, there have been very few investigations of cellular level integration of binocular signals in the SCN. Thus, most previous investigations of neurophysiological effects of light in the SCN have used exclusively monocular (Meijer et al., 1986, Brown et al., 2011, Nakamura et al., 2004) or binocular stimuli (Meijer et al., 1992, Drouyer et al., 2007, Mure et al., 2007, Aggelopoulos and Meissl, 2000, van Diepen et al., 2013). A few studies have investigated the occularity of rat, degus and diurnal ground squirrel SCN cells (Meijer et al., 1989, Jiao et al., 1999), but in each case the number of cells (n=3) and irradiance range tested was too low to draw any solid inferences on binocular processing in the clock of these species.

At present, there is also little information about the specific location(s) or number of retinal ganglion cells (RGCs) from which each retinorecipient SCN cell receives input. Whereas RGC projections to more conventional visual centres adopt a specific organisation to facilitate image forming vision (Sterratt et al., 2013), it feels unlikely that something similar should also be true for the SCN. Indeed, the SCN is known to deviate from this scheme by virtue of the fact it receives input from the nasal and superior regions of the ipsilateral retina (Morin et al., 2003). Moreover, while eye-specific inputs to the hamster SCN appear partially anatomically segregated (Muscat et al., 2003) this doesn't seem to hold true the mouse (Brown et al., 2010, Morin and Studholme, 2014). If instead, then, retinal input to SCN neurons is essentially random, our data suggest that the number of RGC inputs to any one cell must be small. In fact, the near equal numbers of contralateral, ipsilateral and

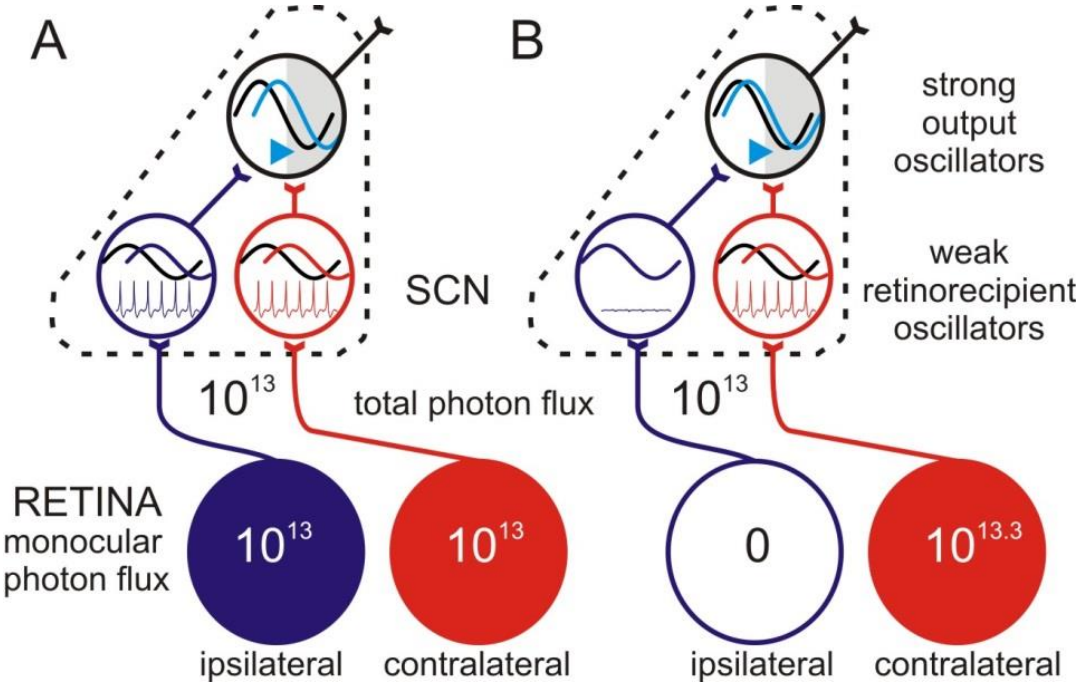

Figure 2.9: Model of binocular integration in the SCN.

Retinorecipient clock cells, with easily perturbed oscillators are reset according to 'local' irradiance (at most brightness across one visual hemisphere). Strong output oscillators integrate circadian signals from the retinorecipient cells and adjust their phase according to the average of this input. As a consequence, illumination of both eyes drives a substantially larger adjustment in clock output (A) than a 2-fold increase in irradiance applied to just one (B).

binocularly responsive SCN neurons we observe suggests that, on average, each of these cells samples from 2 RGCs.

If correct, our suggestion above would imply that most SCN neurons could only measure light intensity within very restricted patches of the visual field (<30° given the known dendritic field sizes of the melanopsin RGCs that provide most of the input; (Berson et al., 2010). Accordingly, individual SCN cells could detect quite different daily patterns of illumination (e.g. if they monitored light intensity exclusively from the lower rather than upper visual field). We tentatively suggest that such a mechanism could contribute to the pronounced, photoperiod-dependent, phase differences in the electrical activity exhibited by SCN neurons (Brown and Piggins, 2009, VanderLeest et al., 2007).

It is also interesting to speculate as to the functional significance of the binocular input to a subset of SCN cells. It is clear from our data that this input makes little contribution to irradiance coding and instead acts to promote rapid and robust responses to sudden changes in light intensity. It is currently unclear why such a property would be useful to the clock, however, existing data indicate that high frequency retinal input and subsequent SCN cell firing are important for triggering internal calcium mobilisation (Irwin and Allen, 2007). It may then be the case that the initial transient response of SCN cells (which often overshoot the steady state level attained for a given irradiance) are especially significant for initiating the intracellular signalling cascade required for phase shifting.

As a final note here, since our SCN recordings were performed in anaesthetised mice, it is important to consider the possibility that responses recorded under our experimental conditions do not fully recapitulate those observed in freely behaving animals. On the basis of the available data, we think it unlikely that the anaesthetic we employ here would result in any qualitative change in the visual responses of SCN neurons. Hence, multiunit recordings in freely moving mice (van Diepen et al., 2013, van Oosterhout et al., 2012) reveal visual responses with essentially identical sensitivity and temporal profile to those we report here and have observed previously (Brown et al., 2011).

Aside from the above, our data also add to existing literature indicating a surprising amount of diversity in the visual responses of hypothalamic neurons (Brown et al., 2011, Drouyer et al., 2007, Aggelopoulos and Meissl, 2000). In line with earlier anatomical data (Sollars et al., 2003, Guler et al., 2008), we previously reported that a subset of cells within or bordering the SCN lacked functional melanopsin input and sustained responses to light (Brown et al., 2011). Another study, performed in awake (head-fixed) mice also reports a small subset of SCN cells with apparently similar properties (Sakai, 2014). Here we confirm that these non-irradiance coding SCN cells in fact specifically encode rapid light increments or decrements. None of these cells exhibited binocular responses, suggesting that this population primarily (if not exclusively) signals visual contrast within a restricted portion of the visual field, as described above for irradiance coding SCN cells. Given these properties, we think it unlikely that such cells play a major role in circadian entrainment, although it is possible that they contribute to more direct SCN-dependent modulations in physiology such as effects on corticosterone secretion (Kiessling et al., 2014).

We also identify an especially unusual population of cells that exhibit OFF responses to visual contrast and whose steady state firing activity is thus inversely related to irradiance. While light-suppressed SCN cells have been reported previously (Meijer et al., 1986, Brown et al., 2011, Meijer et al., 1992, Drouyer et al., 2007, Aggelopoulos and Meissl, 2000), the population of mouse neurons we report here are distinct in that under dark-adapted conditions they display robust excitatory responses. Moreover the inhibitory responses of these OFF cells under light- adaptation are much more rapid than those of the very rare light-suppressed SCN cells we previously reported in the mouse (Brown et al., 2011).

As far as we are aware, then, the ON to OFF switching behaviour we describe above has never previously been reported. Although possible that these observations reflect a circadian phase-dependent effect (light-adapted recordings always followed dark-adapted in our experiments) we think this is unlikely to reflect a global change across the SCN. Hence we routinely observed the more conventional ON responses among simultaneously recorded neurons. It is noteworthy here that all of the OFF cells we recorded were exclusively driven by the ipsilateral retina, suggesting that there may be some differential processing of eye specific signals within the SCN. For example, the switch from excitatory to

inhibitory responses might reflect a changing balance between direct and indirect ipsilateral visual input following light adaption. Such indirect visual input could arise locally, via the opposing SCN or indeed via other brain regions such as the intergeniculate leaflet (Tang et al., 2002, Howarth et al., 2014, Blasiak and Lewandowski, 2013). At present, we can only speculate as to the functional significance of the 'darkness-coding' behaviour that these OFF cells exhibit. Presumably the presence of such cells increase the variety of output signals that the SCN is able to transmit, allowing for differential regulation of various aspects of physiology (Kalsbeek et al., 2006).

In summary, our data provide new insight into the mechanisms through which the circadian clock processes visual signals. Most notably, we show that the ability of individual SCN neurons to detect irradiance is restricted to only a portion of the full visual field. The implication of this arrangement is that asymmetries in the amount of illumination between left and right eyes could lead the circadian system to substantially underestimate the total amount of ambient illumination. Our data thus predict that, in the absence of any compensatory reorganisation, loss of one eye should result in an unexpectedly large deficit in photic integration within the SCN.

2.6 References

AGGELOPOULOS, N. C. & MEISSL, H. 2000. Responses of neurones of the rat suprachiasmatic nucleus to retinal illumination under photopic and scotopic conditions. *J Physiol,* 523 Pt 1**,** 211-22.

ALBUS, H., VANSTEENSEL, M. J., MICHEL, S., BLOCK, G. D. & MEIJER, J. H. 2005. A GABAergic mechanism is necessary for coupling dissociable ventral and dorsal regional oscillators within the circadian clock. *Curr Biol,* 15**,** 886-93.

BERSON, D. M., CASTRUCCI, A. M. & PROVENCIO, I. 2010. Morphology and mosaics of melanopsin-expressing retinal ganglion cell types in mice. *J Comp Neurol,* 518**,** 2405-22.

BLASIAK, T. & LEWANDOWSKI, M. H. 2013. Differential firing pattern and response to lighting conditions of rat intergeniculate leaflet neurons projecting to suprachiasmatic nucleus or contralateral intergeniculate leaflet. *Neuroscience,* 228**,** 315-24.

BROWN, T. M., ALLEN, A. E., AL-ENEZI, J., WYNNE, J., SCHLANGEN, L., HOMMES, V. & LUCAS, R. J. 2013. The melanopic sensitivity function accounts for melanopsin-driven responses in mice under diverse lighting conditions. *PLoS One,* 8**,** e53583.

BROWN, T. M., GIAS, C., HATORI, M., KEDING, S. R., SEMO, M., COFFEY, P. J., GIGG, J., PIGGINS, H. D., PANDA, S. & LUCAS, R. J. 2010. Melanopsin contributions to irradiance coding in the thalamo-cortical visual system. *PLoS Biol,* 8**,** e1000558.

BROWN, T. M. & PIGGINS, H. D. 2009. Spatiotemporal heterogeneity in the electrical activity of suprachiasmatic nuclei neurons and their response to photoperiod. *J Biol Rhythms,* 24**,** 44-54.

BROWN, T. M., TSUJIMURA, S., ALLEN, A. E., WYNNE, J., BEDFORD, R., VICKERY, G., VUGLER, A. & LUCAS, R. J. 2012. Melanopsin-based brightness discrimination in mice and humans. *Curr Biol,* 22**,** 1134-41.

BROWN, T. M., WYNNE, J., PIGGINS, H. D. & LUCAS, R. J. 2011. Multiple hypothalamic cell populations encoding distinct visual information. *J Physiol,* 589**,** 1173-94.

COLEMAN, J. E., LAW, K. & BEAR, M. F. 2009. Anatomical origins of ocular dominance in mouse primary visual cortex. *Neuroscience,* 161**,** 561-71.

DKHISSI-BENYAHYA, O., SICARD, B. & COOPER, H. M. 2000. Effects of irradiance and stimulus duration on early gene expression (Fos) in the suprachiasmatic nucleus: temporal summation and reciprocity. *J Neurosci,* 20**,** 7790-7.

DROUYER, E., RIEUX, C., HUT, R. A. & COOPER, H. M. 2007. Responses of suprachiasmatic nucleus neurons to light and dark adaptation: relative contributions of melanopsin and rod-cone inputs. *J Neurosci,* 27**,** 9623-31.

GOLOMBEK, D. A. & ROSENSTEIN, R. E. 2010. Physiology of circadian entrainment. *Physiol Rev,* 90**,** 1063-102.

GOVARDOVSKII, V. I., FYHRQUIST, N., REUTER, T., KUZMIN, D. G. & DONNER, K. 2000. In search of the visual pigment template. *Vis Neurosci,* 17**,** 509-28.

GULER, A. D., ECKER, J. L., LALL, G. S., HAQ, S., ALTIMUS, C. M., LIAO, H. W., BARNARD, A. R., CAHILL, H., BADEA, T. C., ZHAO, H., HANKINS, M. W., BERSON, D. M., LUCAS, R. J., YAU, K. W. & HATTAR, S. 2008. Melanopsin cells are the principal conduits for rod-cone input to non-image-forming vision. *Nature,* 453**,** 102-5.

HATTAR, S., KUMAR, M., PARK, A., TONG, P., TUNG, J., YAU, K. W. & BERSON, D. M. 2006. Central projections of melanopsin-expressing retinal ganglion cells in the mouse. *J Comp Neurol,* 497**,** 326-49.

HATTAR, S., LUCAS, R. J., MROSOVSKY, N., THOMPSON, S., DOUGLAS, R. H., HANKINS, M. W., LEM, J., BIEL, M., HOFMANN, F., FOSTER, R. G. & YAU, K. W. 2003. Melanopsin and rod-cone photoreceptive systems account for all major accessory visual functions in mice. *Nature,* 424**,** 76-81.

HOWARTH, M., WALMSLEY, L. & BROWN, T. M. 2014. Binocular integration in the mouse lateral geniculate nuclei. *Curr Biol,* 24**,** 1241-7.

IRWIN, R. P. & ALLEN, C. N. 2007. Calcium response to retinohypothalamic tract synaptic transmission in suprachiasmatic nucleus neurons. *J Neurosci,* 27**,** 11748-57.

JACOBS, G. H. & WILLIAMS, G. A. 2007. Contributions of the mouse UV photopigment to the ERG and to vision. *Doc Ophthalmol,* 115**,** 137-44.

JIAO, Y. Y., LEE, T. M. & RUSAK, B. 1999. Photic responses of suprachiasmatic area neurons in diurnal degus (Octodon degus) and nocturnal rats (Rattus norvegicus). *Brain Res,* 817**,** 93-103.

KALSBEEK, A., PERREAU-LENZ, S. & BUIJS, R. M. 2006. A network of (autonomic) clock outputs. *Chronobiol Int,* 23**,** 521-35.

KIESSLING, S., SOLLARS, P. J. & PICKARD, G. E. 2014. Light stimulates the mouse adrenal through a retinohypothalamic pathway independent of an effect on the clock in the suprachiasmatic nucleus. *PLoS One,* 9**,** e92959.

LALL, G. S., REVELL, V. L., MOMIJI, H., AL ENEZI, J., ALTIMUS, C. M., GULER, A. D., AGUILAR, C., CAMERON, M. A., ALLENDER, S., HANKINS, M. W. & LUCAS, R. J. 2010. Distinct

contributions of rod, cone, and melanopsin photoreceptors to encoding irradiance. *Neuron,* 66**,** 417-28.
LUCAS, R. J., HATTAR, S., TAKAO, M., BERSON, D. M., FOSTER, R. G. & YAU, K. W. 2003. Diminished pupillary light reflex at high irradiances in melanopsin-knockout mice. *Science,* 299**,** 245-7.
LUCAS, R. J., LALL, G. S., ALLEN, A. E. & BROWN, T. M. 2012. How rod, cone, and melanopsin photoreceptors come together to enlighten the mammalian circadian clock. *Prog Brain Res,* 199**,** 1-18.
MEIJER, J. H., GROOS, G. A. & RUSAK, B. 1986. Luminance coding in a circadian pacemaker: the suprachiasmatic nucleus of the rat and the hamster. *Brain Res,* 382**,** 109-18.
MEIJER, J. H., RUSAK, B. & GANSHIRT, G. 1992. The relation between light-induced discharge in the suprachiasmatic nucleus and phase shifts of hamster circadian rhythms. *Brain Res,* 598**,** 257-63.
MEIJER, J. H., RUSAK, B. & HARRINGTON, M. E. 1989. Photically responsive neurons in the hypothalamus of a diurnal ground squirrel. *Brain Res,* 501**,** 315-23.
MIURA, M., DONG, K., AHMED, F. A., OKAMURA, H. & YAMADORI, T. 1997. The termination of optic nerve fibers in the albino mouse. *Kobe J Med Sci,* 43**,** 99-108.
MORIN, L. P., BLANCHARD, J. H. & PROVENCIO, I. 2003. Retinal ganglion cell projections to the hamster suprachiasmatic nucleus, intergeniculate leaflet, and visual midbrain: bifurcation and melanopsin immunoreactivity. *J Comp Neurol,* 465**,** 401-16.
MORIN, L. P. & STUDHOLME, K. M. 2014. Retinofugal projections in the mouse. *J Comp Neurol,* 522**,** 3733-53.
MURE, L. S., RIEUX, C., HATTAR, S. & COOPER, H. M. 2007. Melanopsin-dependent nonvisual responses: evidence for photopigment bistability in vivo. *J Biol Rhythms,* 22**,** 411-24.
MUSCAT, L., HUBERMAN, A. D., JORDAN, C. L. & MORIN, L. P. 2003. Crossed and uncrossed retinal projections to the hamster circadian system. *J Comp Neurol,* 466**,** 513-24.
MUSCAT, L. & MORIN, L. P. 2005. Binocular contributions to the responsiveness and integrative capacity of the circadian rhythm system to light. *J Biol Rhythms,* 20**,** 513-25.
NAKAMURA, T. J., FUJIMURA, K., EBIHARA, S. & SHINOHARA, K. 2004. Light response of the neuronal firing activity in the suprachiasmatic nucleus of mice. *Neurosci Lett,* 371**,** 244-8.
NELSON, D. E. & TAKAHASHI, J. S. 1991. Sensitivity and integration in a visual pathway for circadian entrainment in the hamster (Mesocricetus auratus). *J Physiol,* 439**,** 115-45.
NELSON, D. E. & TAKAHASHI, J. S. 1999. Integration and saturation within the circadian photic entrainment pathway of hamsters. *Am J Physiol,* 277**,** R1351-61.
PAXINOS, G. & FRANKLIN, K. 2001. *The Mouse Brain in Stereotaxic Coordinates,* San Diego, Academic Press.
PAXINOS, G. F., K.B.J. 2001. *The mouse brain in stereotaxic coordinates: Second Edition,* San Diego, Academic Press.
RIEKE, F. & RUDD, M. E. 2009. The challenges natural images pose for visual adaptation. *Neuron,* 64**,** 605-16.
ROENNEBERG, T. & FOSTER, R. G. 1997. Twilight times: light and the circadian system. *Photochem Photobiol,* 66**,** 549-61.
ROHLING, J. H., VANDERLEEST, H. T., MICHEL, S., VANSTEENSEL, M. J. & MEIJER, J. H. 2011. Phase resetting of the mammalian circadian clock relies on a rapid shift of a small population of pacemaker neurons. *PLoS One,* 6**,** e25437.
SAKAI, K. 2014. Single unit activity of the suprachiasmatic nucleus and surrounding neurons during the wake-sleep cycle in mice. *Neuroscience,* 260**,** 249-64.

SOLLARS, P. J., SMERASKI, C. A., KAUFMAN, J. D., OGILVIE, M. D., PROVENCIO, I. & PICKARD, G. E. 2003. Melanopsin and non-melanopsin expressing retinal ganglion cells innervate the hypothalamic suprachiasmatic nucleus. *Vis Neurosci,* 20**,** 601-10.

STERRATT, D. C., LYNGHOLM, D., WILLSHAW, D. J. & THOMPSON, I. D. 2013. Standard anatomical and visual space for the mouse retina: computational reconstruction and transformation of flattened retinae with the Retistruct package. *PLoS Comput Biol,* 9**,** e1002921.

TANG, I. H., MURAKAMI, D. M. & FULLER, C. A. 2002. Unilateral optic nerve transection alters light response of suprachiasmatic nucleus and intergeniculate leaflet. *Am J Physiol Regul Integr Comp Physiol,* 282**,** R569-77.

VAN DIEPEN, H. C., RAMKISOENSING, A., PEIRSON, S. N., FOSTER, R. G. & MEIJER, J. H. 2013. Irradiance encoding in the suprachiasmatic nuclei by rod and cone photoreceptors. *FASEB J,* 27**,** 4204-12.

VAN OOSTERHOUT, F., FISHER, S. P., VAN DIEPEN, H. C., WATSON, T. S., HOUBEN, T., VANDERLEEST, H. T., THOMPSON, S., PEIRSON, S. N., FOSTER, R. G. & MEIJER, J. H. 2012. Ultraviolet light provides a major input to non-image-forming light detection in mice. *Curr Biol,* 22**,** 1397-402.

VANDERLEEST, H. T., HOUBEN, T., MICHEL, S., DEBOER, T., ALBUS, H., VANSTEENSEL, M. J., BLOCK, G. D. & MEIJER, J. H. 2007. Seasonal encoding by the circadian pacemaker of the SCN. *Curr Biol,* 17**,** 468-73.

VIDAL, L. & MORIN, L. P. 2007. Absence of normal photic integration in the circadian visual system: response to millisecond light flashes. *J Neurosci,* 27**,** 3375-82.

Chapter 3: Colour as a Signal for Entraining the Mammalian Circadian Clock

(Adapted from the published article in PLoS Biology, April 2015)

3.1 Abstract

Although the daily solar cycle is the dominant environmental signal regulating mammalian circadian timing, our understanding of how specific features of the light environment contribute to photoentrainment is incomplete. Twilight is characterised by changes in irradiance (the quantity of light) occurring alongside changes in the spectral composition (colour) of light. The ability of the circadian system to use variations in irradiance to align its physiological processes with environmental time is well documented; however, the extent to which changes in the colour of ambient illumination could provide important timing cues remains unknown. Here, we address this using a combination of analytical and simulated natural visual stimuli based on spectral irradiance field recordings collected across many days.

Firstly, using stimuli designed to selectively modulate mouse short and long wavelength sensitive cones, we identify a subset (~20%) of SCN neurons exhibiting the spectrally-opponent (blue-yellow) responses required to extract this colour information from the twilight environment. Next, using visual stimuli designed to recreate various stages of twilight for the mouse visual system, we show that the firing rates of these spectrally-opponent SCN cells reliably track a wide range of solar angles (a property that is deficient in non-opponent SCN cells).

Finally, using in vivo monitoring of photoentrainment to simulated twilight, we show that chromatic signals detected by cone photoreceptors significantly influence circadian phase, allowing mice to appropriately time their activity to the middle of the night. Together, these findings reveal a new sensory mechanism for estimating time of day that would be available to most mammalian species capable of colour vision.

3.2 Introduction

The mammalian brain 'clock', the superchiasmatic nucleus (SCN), is responsible for synchronising physiological functions to environmental time. In order to carry out this function, it must receive input from the environment to accurately determine time of day. The diurnal changes in irradiance associated with the day/night cycle have long been considered to be the principal entraining time cue for the circadian clock (Lucas et al., 2012)

Photic information is relayed to the SCN from the retina via the retinohypothalamic tract (RHT), formed by axons of intrinsically photosensitive retinal ganglion cells (ipRGCs) expressing the photopigment melanopsin (Baver et al., 2008, Hattar et al., 2002). These ipRGCs are capable of responding directly to light even when isolated from the rest of the retina (Berson et al., 2002). Although melanopsin is sufficient for entrainment, ipRGCs are known to receive input from retinal circuitry associated with rods and cones (Belenky et al., 2003, Østergaard et al., 2007, Perez-Leon et al., 2006, Viney et al., 2007). However, selective ablation of ipRGCs blocks entrainment (Göz et al., 2008, Guler et al., 2008) and so ipRGCs are the principal route through which all light signals travel to reach the clock.

To date, entrainment has been understood in terms of measuring brightness through the action of SCN cells acting as luminance encoders (Meijer et al., 1986). Rods and melanopsin (Brown et al., 2011, Altimus et al., 2010, Lall et al., 2010) are known to be important for this, but cones are not considered to play much of a role in entrainment as 'cone only' mice fail to reliably entrain to light-dark cycles (Mrosovsky and Hattar, 2005) and entrainment persists after substantial cone degeneration (Freedman et al., 1999). The established view, is that cones enable the SCN to respond to rapid changes in irradiance (Brown et al., 2011), a signal that would theoretically be of minimal use to the circadian clock.

However, one of the unique contributions of cones in most mammals is that these allow for colour discrimination. It has long been known that, as the sun falls below the horizon the

spectral composition of ambient illumination changes. During 'twilight' there is an increase in the availability of short wavelength light, due to ozone filtering (Hulbert, 1953). Most mammals possess a short and a mid/long wavelength cone opsin allowing spectral comparisons along the blue-yellow axis (Peichl, 2005, Jacobs, 2013) and so this change should theoretically be detectable by the mammalian visual system. Since this change in spectral composition should be relatively unaffected by cloud cover, in principle measuring colour could provide the mammalian clock with useful additional information about time of day. This possibility was suggested many years ago (Roenneberg and Foster, 1997) and has been investigated in the context of the fish circadian system (Pauers et al., 2012). To date, however, it has not been investigated in mammals.

Leading up to this work, our recent study systematically evaluated the extent to which changes in apparent colour associated with the sun position could indeed provide useful timing information to the mouse clock (Walmsley et al., 2015). Using the mouse as a model organism, this theoretical work revealed a robust change in the ratio of excitation between the short and longwave mouse opsins that would constitute substantial changes in apparent colour to the mouse visual system. This colour signal was more predictive of solar angle across twilight than irradiance. Measuring wavelength could therefore provide the circadian clock with a more reliable estimate about time of day than relying on irradiance alone.

In mice it is difficult to study the relative contributions of the three types of photoreceptors to photoentrainment as rods, M-cone opsin (green-cones) and melanopsin all possess similar spectral sensitivities and it is therefore impossible to stimulate opsins individually without also introducing changes for rods and melanopsin. Therefore, in order to combat this, experiments are conducted in transgenic red cone knock-in (*Opn1mw*^{R}) mice, a well-validated model, in which the mouse medium wavelength (MWS) opsin has been replaced by the human red cone opsin (LWS) (Brown et al., 2011, Lall et al., 2010, Brown et al., 2013, Smallwood et al., 2003). The absorption of the cone opsin is lengthened so as to render the spectral sensitivities of rods, cones and melanopsin to be sufficiently different to allow differential stimulation of the different types of receptors.

3.3 Methods

3.3.1 *in vivo* electrophysiological recordings

3.3.1.1 Animals

All animal use was in accordance with the Animals (Scientific Procedures) Act of 1986 (United Kingdom). Electrophysiology experiments were performed under urethane anaesthesia; other procedures were conducted under isfluorane anaesthesia. Unless otherwise stated, animals used in this study (homozygous Opn1mw^{R} and Cnga3$^{-/-}$ mice) were housed under a 12-h dark/light cycle at a temperature of 22°C with food and water available ad libitum.

3.3.1.2 Surgical techniques

Adult (60–120 d) male Opn1mw^{R} mice were anaesthetised by intraperitoneal injection of urethane (1.55 g/kg) and placed into a stereotaxic frame (SR-15M; Narishage International) to hold the skull fixed in place for surgery. The surface of the skull was exposed using a scalpel incision and a hole was drilled using stereotaxic co-ordinates (0.98mm lateral to and 0.3mm posterior to Bregma) obtained from the stereotaxic mouse atlas (Paxinos and Franklin, 2001). The contralateral pupil was dilated with 1% atropine (Sigma Aldrich) and mineral oil (Sigma-Aldrich) added to prevent drying of the cornea.

Recording probes (Buszaki 32L; Neuronexus, MI, US) consisting of four shanks (spaced 200µm), each with eight closely spaced recordings sites in diamond formation (intersite distance 20–34µm) were coated with fluorescent dye (CM-DiI; Invitrogen, Paisley, UK) and then inserted into the brain 1 mm lateral and 0.3 mm caudal to bregma at an angle of 9° relative to the dorsal-ventral axis. Electrodes were then lowered to the level of the SCN using a fluid-filled micromanipulator (MO-10, Narishige International Ltd., London, UK).

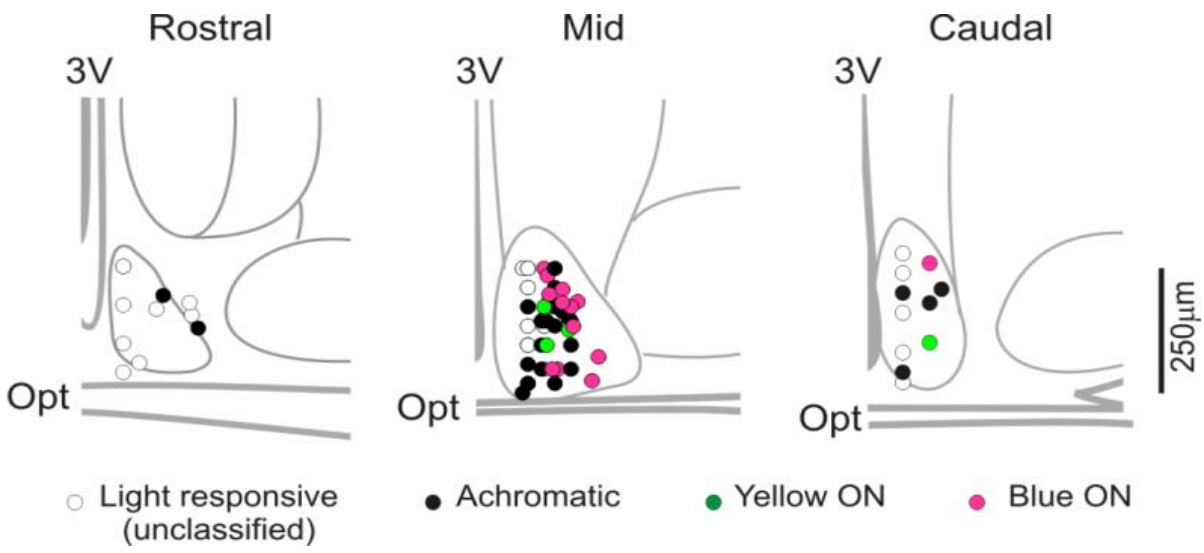

Figure 3.1: Anatomical locations of visually responsive cells types in the suprachiasmatic nucleus.

Projected anatomical locations of the visually responsive SCN cells reported in this study split according to response type. The unclassified population corresponds to cells that responded to light steps from darkness but not cone-isolating stimuli.

After allowing 30 min for neural activity to stabilise following probe insertion, wideband neural signals were acquired using a Recorder64 system (Plexon, TX, US), amplified (x3000) and digitized at 40 kHz. Surgical procedures were completed 1–2 h before the end of the home cage light phase, such that electrophysiological recordings spanned the late projected day-early projected night, when the SCN light response is most sensitive. Throughout the experiment, the animals temperature was maintained at 37˚C using a homeothermic mat (Harvard Apparatus, UK).

In order to isolate single-unit activity, the broadband neural signals data were high pass filtered (300Hz) and negative-going spikes with amplitudes >40µV extracted as 'virtual' waveforms using a custom-written program in MATLAB R2012a (The Mathsworks Inc., M, USA). Tetrodes were created by grouping 4 overlapping adjacent channels, resulting in a total of 12 tetrodes for the electrode. As the tetrodes contained data from overlapping channels, special care was taken to ensure that units were not isolated twice. To do this, after removing artefacts, spikes were sorted manually using commercial principle components based software (Offline sorter, Plexon, TX, USA) only on the channels that were unique to each tetrode. Single units were identifiable as a distinct cluster of spikes in principal component space. Following spike sorting, single units were exported to Neuroexplorer (Nex Technologies, MA, USA) and back into MATLAB for further analysis.

Following the experiment, accurate electrode placement was confirmed histologically. Projected anatomical locations of light response units reported in this study are presented in figure 3.1.

3.3.2 Visual Stimuli

All visual stimuli were delivered in a darkened chamber and generated using a custom-made light source (Cairn Research Ltd, Faversham, UK) consisting of independently controlled UV (λmax: 365nm), blue (λmax: 460nm) and amber (λmax: 600nm) LEDs. The light from the individual LEDs was combined using a series of dichromatic mirrors, passed through a filter wheel containing various neutral density (ND) filters (Cairn Research Ltd,

Faversham, UK), and focussed onto a 5mm circle of opal diffusing glass (Edmund Optics Inc., New York) positioned over the eye contralateral to the recording site. The light was centred on the middle of the eye so that light would be evenly distributed across the whole retina. LED intensity and the filter wheel position were both controlled by a PC running Labview 8.6 (National Instruments, Austin, TX, USA). Throughout these experiments, the ipsilateral eye was left uncovered.

Light measurements were performed using a calibrated spectroradiometer (Bentham instruments, Reading, UK). Using photopigment spectral absorbance data and allowing correction for pre-receptoral filtering (Govardovskii et al., 2000, Jacobs and Williams, 2007), LED intensity was initially calibrated to recreate for Opn1mw^{R} individuals the effective rod, cone and melanopsin excitation experienced by a wild-type (green cone) mouse visual system under typical natural daylight (average values from our environmental data at a solar angle 3° above the horizon; Figure 3.2, A).

We next calibrated manipulations of this background lighting condition to produce 4 pairs of stimuli that independently varied in apparent brightness for one or both cone opsin classes (either in unison or antiphase) with no apparent change in rod or melanopsin excitation (Figure 3.2, B). In each case, brightness for the stimulated opsin was varied by ±70%, to produce an overall 4.7-fold increase in intensity of between “bright” and “dim” phases of the stimulus. Transitions between the two stimulus phases occurred smoothly over 50ms.

An additional consideration when interpreting responses to these stimuli is that most mouse cones co-express varying proportions of both LWS and UVS opsin (Applebury et al., 2000). Since within a single cone photoreceptor the light-adaptation machinery must effectively integrate over all photons detected (regardless of which opsin detected them), for these co-expressing cones the effective contrast of our LWS/UVS-isolating stimuli will vary as a function of (a) the proportion of each opsin within the cone cell and (b) the background photon flux available to each of the two opsins (Figure 3.3). Importantly, since the background activation of UVS opsin ($2.14x10^{14}$ photons/cm^2/s) somewhat less than that

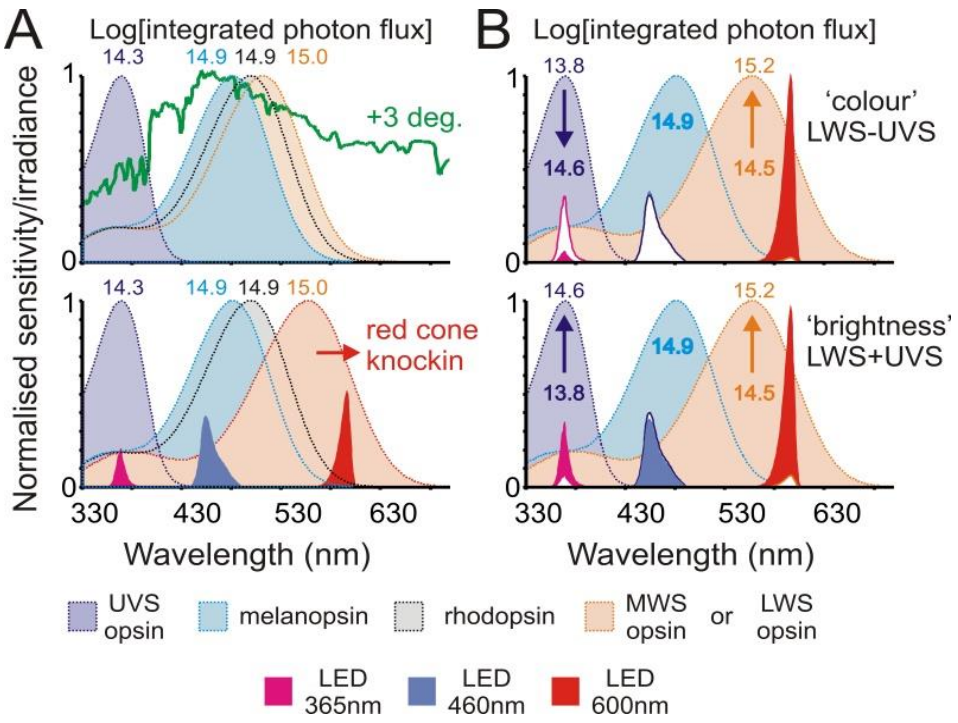

Figure 3.2: Selective modulation of colour and brightness in red cone knock-in mice.

(A) Top panel shows normalised spectral profile of daytime ambient illumination (green line; +3°) alongside sensitivity profiles for native mouse opsins. Numbers above traces indicate the calculated photon flux for each photoreceptor class (log photons/cm^2/s). Bottom panel shows spectral profile of three-primary LED system used used to recreate natural daylight from red cone knock-in mice (Opn1mw^R). Note the shift in cone sensitivity from MWS (top panel) to LWS (bottom panel): the photon flux experienced by wild-type mouse MWS cones (15 log photons/cm^2/s) is translated here into an equivalent photon flux for the LWS cone knock-in. (B) Illustration of spectral modulations used to selectively evoke changes in relative ("colour"; top) or absolute ("brightness"; bottom) activation of UV and long-wavelength sensitive (UVS/LWS) cone opsins. Numbers on traces reflect Log photon flux at blue versus yellow (top panel) or dim versus bright (bottom panel) stimulus phases. These equate to 4.7-fold changes (70% Michelson contrast) in cone opsin activation with essentially no effective change in melanopsin excitation (<1% Michelson). Effective changes in rod excitation are omitted for clarity but are also very small (6.5% and 4.5% Michelson for "brightness" and "colour" respectively), however, owing to the overall intensity of the stimuli, it is highly unlikely that rods could contribute to any response even with much larger contrasts.

		Photons/cm^2/s at 'high'				Photons/cm^2/s at 'low'				% Contrast			
Background	Condition	L-cone	S-cone	Rod	Mel	L-cone	S-cone	Rod	Mel	L-cone	S-cone	Rod	Mel
1	Mel	$1.03x10^{15}$	$2.14x10^{14}$	$1.32x10^{15}$	$1.63x10^{15}$	$1.03x10^{15}$	$2.14x10^{14}$	$1.12x10^{14}$	$6.79x10^{13}$	0	0	84.37	92.00
	L+S	$1.75x10^{15}$	$3.63x10^{14}$	$7.66x10^{14}$	$8.55x10^{14}$	$3.11x10^{14}$	$6.45x10^{13}$	$6.72x10^{14}$	$8.42x10^{14}$	69.79	69.80	6.54	0.82
	L	$1.75x10^{15}$	$2.14x10^{14}$	$7.62x10^{14}$	$8.56x10^{14}$	$3.11x10^{14}$	$2.14x10^{14}$	$6.75x10^{14}$	$8.41x10^{14}$	69.80	0	6.06	0.91
	S	$1.03x10^{15}$	$3.63x10^{14}$	$7.23x10^{14}$	$8.49x10^{14}$	$1.03x10^{15}$	$6.45x10^{13}$	$7.14x10^{14}$	$8.49x10^{14}$	0.04	69.80	0.57	0
	L-S	$1.75x10^{15}$	$6.45x10^{13}$	$7.52x10^{14}$	$8.49x10^{14}$	$3.11x10^{14}$	$3.63x10^{14}$	$6.85x10^{14}$	$8.48x10^{14}$	69.80	-69.80	4.68	0.02
	L+M+S	$1.75x10^{15}$	$3.63x10^{14}$	$1.22x10^{15}$	$1.44x10^{15}$	$3.11x10^{14}$	$6.45x10^{13}$	$2.17x10^{14}$	$2.56x10^{14}$	69.80	69.80	69.80	69.80
2	L+S	$4.93x10^{14}$	$4.95x10^{14}$	$1.74x10^{14}$	$1.73x10^{14}$	$8.77x10^{13}$	$8.80x10^{13}$	$1.42x10^{14}$	$1.73x10^{14}$	69.80	69.80	10.16	0
	L	$4.93x10^{14}$	$2.91x10^{14}$	$1.69x10^{14}$	$1.74x10^{14}$	$8.77x10^{13}$	$2.91x10^{14}$	$1.47x10^{14}$	$1.73x10^{14}$	69.80	0.01	6.89	0.10
	S	$2.90x10^{14}$	$4.95x10^{14}$	$1.64x10^{14}$	$1.73x10^{14}$	$2.90x10^{14}$	$8.80x10^{13}$	$1.53x10^{14}$	$1.73x10^{14}$	0.01	69.80	3.36	0.01
	L+M+S	$4.93x10^{14}$	$4.95x10^{14}$	$2.69x10^{14}$	$2.94x10^{14}$	$8.77x10^{13}$	$8.80x10^{13}$	$4.78x10^{13}$	$5.24x10^{13}$	69.80	69.8	69.80	69.80

Table 3.1: Calculated photon fluxes for each photoreceptor class in the silent substitution stimuli

The photon flux of each photoreceptor (photons/cm^2/s) at each background ('low' condition) and during the light step ('high' condition) within the silent substitution stimuli designed to selectively modulate each of the photoreceptor classes. The relative contrast of the steps at each background is also shown for each stimulus.

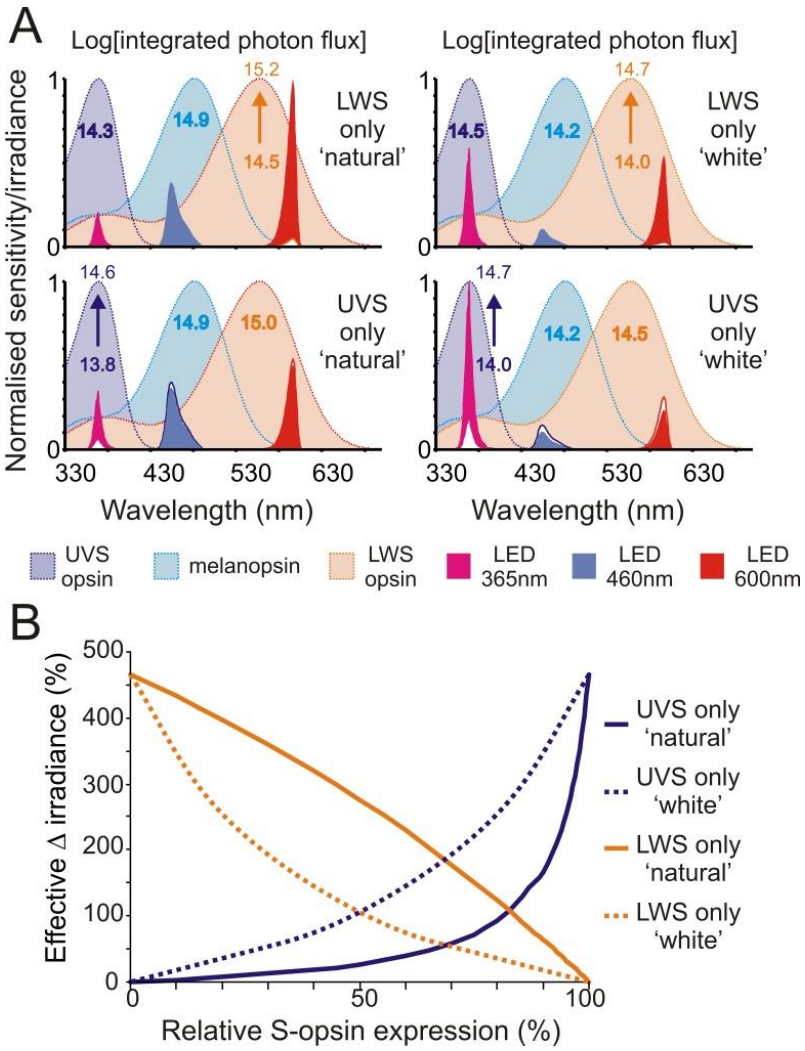

Figure 3.3: Background spectra.

Background spectra (A) Spectral modulations used to selectively evoke changes in LWS (top) or UVS (bottom) opsin excitation under 'natural' daylight and a 'white' background where basal activation of LWS and UVS are equal. In each case, effective change for the modulated opsin is 70% Michelson contrast (non-modulated ('silent') opsins <1% Michelson). Note that, since most mouse cones co-express both opsins (and must sum over all photons detected), the net change in cone photon flux presented by these stimuli is influenced by both the relative background photon flux photon flux at each of the two opsin classes and by the degree of co-expression in each cone. (B) Model of the effective change in irradiance presented by cone opsin-isolating stimuli, as a function of relative opsin co-expression, under 'natural' and 'white' backgrounds.

of LWS ($1.03x10^{15}$ photons/cm^2/s) under natural daylight responses to our cone-isolating stimuli will be skewed in favour of those originating with LWS cone opsin (Figure 3.3, A). To provide an unbiased assessment of the magnitude of responses driven by either opsin we also calibrated a second background lighting condition where baseline activation of the two cone opsins was identical (termed here 'white'; $2.9x10^{14}$ photons/cm^2/s; Figure 3.3). To identify the origin of cone responses, photoreceptor-isolating stimuli were presented as 10s steps in light intensity, alternating with 30 seconds of 'background' illumination (90s for melanopsin isolating stimuli).

We also applied stimuli that selectively modulated melanopsin excitation (±92%), without changing effective cone excitation. These steps were only applied on the natural background as the configuration of white background did not allow us to produce large melanopsin contrasts. These melanopsin stimuli additionally modulated apparent brightness for rod photoreceptors (±84%), however, due to the high background light levels (14.9 rod effective photons/cm^2/s) and previous work suggesting that rods have little influence on acute electrophysiological light responses in the SCN (Brown et al., 2011), we think that rods do not contribute to responses to these stimuli. Additionally, similar stimuli evoke very little response in the lateral geniculate nuclei (LGN) of melanopsin knockout animals (Brown et al., 2012).

In a subset of experiments (7/15) we also applied a second set of stimuli designed to recreate various stages of twilight, using our calculations of the effective photon fluxes experienced by mouse opsins at solar angles between -7 and 3° relative to the horizon (Figure 3.4, A). These were applied as discrete light steps (30 s) from darkness in random sequence with an interstimulus interval of 2 min.

To confirm whether elements of the resulting responses were dependent on spectral composition, these stimuli were interspersed with two additional stimulus sets (Figure 3.4, B, C) which were identical except that irradiance for the UVS opsin was fixed at a constant ratio relative to LWS (mimicking either day or night spectral composition).

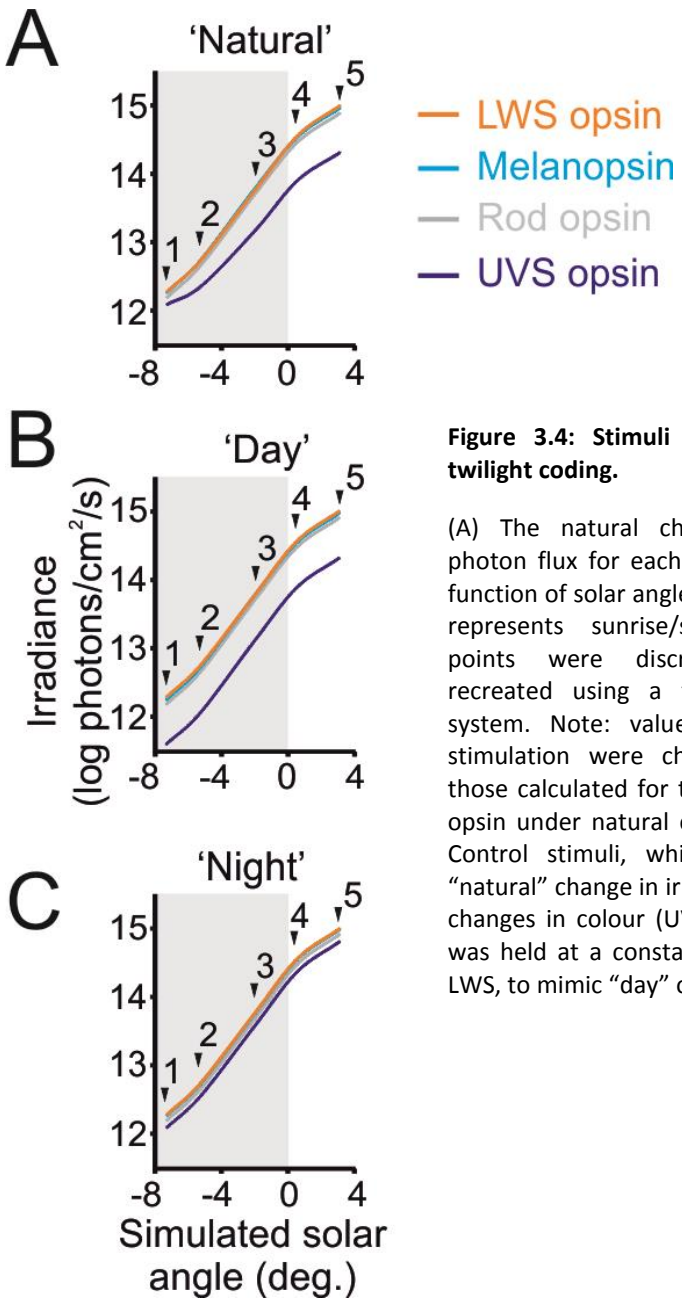

Figure 3.4: Stimuli used to examine twilight coding.

(A) The natural change in effective photon flux for each mouse opsin as a function of solar angle during twilight (0° represents sunrise/sunset). Indicated points were discrete light steps recreated using a three-primary LED system. Note: values for LWS opsin stimulation were chosen to replicate those calculated for the wild-type MWS opsin under natural conditions. (B & C) Control stimuli, which replicated the "natural" change in irradiance but lacked changes in colour (UVS opsin excitation was held at a constant ratio relative to LWS, to mimic "day" or "night" spectra).

3.3.3 Twilight Entrainment study

For behavioural experiments, we generated photoperiods that smoothly recreated measured changes in twilight illumination (Walmsley et al., 2015), with ("natural") or without the associated change in spectral composition (irradiance-only: spectra fixed to mimic "night") (Figure 3.5, B). Stimuli were generated by an array of three violet (400 nm) and three amber (590nm) high-power LEDs (LED Engin Inc., San Jose CA, US) placed behind a polypropylene diffusing screen covering the top of the cage. The combination of multiple LEDs allowed a larger range of brightness (from dark up to approximately 25 W/m^2 for the violet and 10 W/m^2 for the amber). Intensity of each LED was independently controlled by a voltage controlled driver (Thorlabs Inc., Newton NJ, US). The light intensity modulation signals were provided by a PC running Labview through a voltage output module (National Instruments), and followed a temporal profile that recreated the sun's progression during a northern latitude summer (calculations based on Stockholm, Sweden; Lat: 59, Long: 18, Elevation 76 m, 20 June 2013; total twilight duration = 2.3 h).

To determine the impact of twilight spectral changes on mouse entrainment, female $Opn1mw^R$ and $Cnga3^{-/-}$ (coneless) mice (housed under an 18:6 light–dark [LD] cycle) were first implanted with iButton temperature loggers (Maxim, DS1922L-F5#). To reduce weight and size, these were de-housed and encapsulated in a 20% Poly(ethylene-co-vinyl acetate) and 80% paraffin mixture as described by Lovegrove (Lovegrove, 2009). For implantation, mice were anaesthetised with isoflurane (1%–5% in O2) and the temperature logger implanted into the peritoneal cavity. Following surgery, animals were given a 0.03 mg/kg subcutaneous dose of buprenorphine and allowed to recover for at least 9 days in 18:6 LD before the start of the experiment.

The timing of lights off under this cycle was designated as Zeitgeber time (ZT12) and the timing of experimental photoperiods were set to align their midnight (ZT15) with this square wave LD cycle (Figure 3.5, C). Following recovery, group housed mice (five per cage) were transferred to the natural twilight photoperiod. The cage environment contained an opaque plastic hide, allowing the animals to choose their own light sampling regime (experimental set-up illustrated in Figure 3.5, A). After 14 days, mice were then returned to

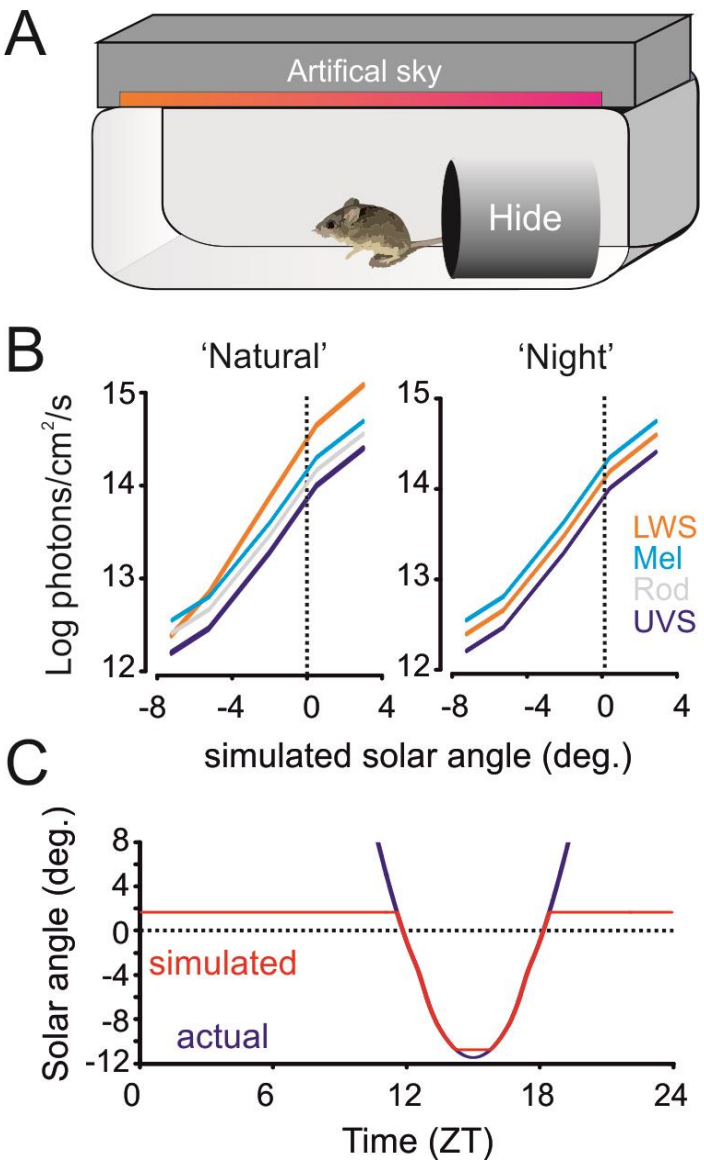

Figure 3.5: Assessing influences of twilight spectra on circadian entrainment.

(A) Schematic of housing conditions for experiments assessing the influence of twilight spectra. Mice (with temperature sensors implanted i.p.) were group housed (5/cage) and uniform illumination applied across the entire top surface of the cage via an artificial sky (comprising multiple amber and violet LEDs controlled by pulse width modulation). Mice could freely move between the open cage and an opaque plastic hide, allowing individuals to choose their own light sampling regimen. (B) Artificial sky was calibrated to replicate, for Opn1mw^{R} individuals, a wild-type mouse's experience of twilight (left: "natural"). A second, analytical twilight stimulus was calibrated to match the natural change in irradiance but with relative activation of cone opsins fixed to match the night spectra (right: "night"). (C) To maximise our ability to distinguish differences in phase of entrainment under the above conditions, twilight stimuli were set to a cycle that simulated the sun's progression during a northern latitude summer (calculations based on Stockholm, Sweden; Lat.: 59, Long.: 18, Elevation 76 m, 20 June 2013) for a total ""twilight"" duration of 2.3 h.

18:6 LD for a further 14 days and finally transferred to the “irradiance-only” twilight photoperiod.

At the end of the experiment, mice were culled by cervical dislocation and temperature loggers recovered. Temperature data (recorded in 30 min time bins) was processed by upsampling to 5 min resolution (cubic spline interpolation), Gaussian smoothing (SD = 45 min), and normalisation as a fraction of daily temperature range. Phase of entrainment was estimated as the timing of peak body temperature from that individual’s daily average profile (calculated from the last 9 days in each photoperiod).

3.4 Results

3.4.1 Colour coding in the SCN

Modelling based on field measurements of spectral irradiance indicates that blue-yellow colour, as detected by the mouse visual system, provides highly reliable information about sun position that the clock could use to estimate time of day. Accordingly, we first set out to determine whether SCN neurons are sensitive to changes in colour using extracellular electrophysiological recordings to monitor visually evoked changes in SCN firing in anaesthetised mice.

In order to separate out the relative contributions of brightness and colour to the responses of SCN neurons, experiments were performed in Opn1mw^{R} animals using a set of visual stimuli designed to selectively manipulate cone photoreception under lighting conditions that resembled natural daylight (see methods for details; Figure 3.3 & Table 3.1). In particular, cells were classified as colour sensitive when they (a) exhibited opposite changes in firing to stimulation of UVS vs. LWS opsin (i.e. spectral opponency) and (b) exhibited larger responses to chromatic vs. achromatic changes in cone excitation (UVS/LWS opsin stimulated in antiphase vs. in unison).

The largest possible change in blue-yellow colour we could generate involved selectively activating UVS and LWS in antiphase ('colour'). We first compared responses to this stimulus to those elicited by an identical magnitude stimulation of UWS and LWS opsin in unison (producing an achromatic change in 'brightness'). Any spectrally opponent cells should thus respond better to the 'colour' rather than 'brightness' condition. We found 17/43 SCN units (from 15 mice) that showed a preference to the 'colour' stimulus (Figure 3.6 - A & B; paired *t*-test, $p<0.05$, $n = 17$). There were an additional 26 visually responsive units that did not respond to either of these analytical stimuli (paired *t*-tests, $p>0.05$), and therefore at least one quarter of light-responsive SCN neurones exhibit chromatic opponency.

To confirm that the stimuli employed above truly distinguished subsets of SCN cells sensitive to colour, we next selectively modulated activation of either UVS or LWS opsin in isolation. Of the 26 SCN neurons which showed a measureable preference for achromatic changes in cone excitation we found substantial variation in response, with some cells responding only to activation of one opsin class and others showing clear responses to activation of either. Importantly, however, cone driven responses across this population were exclusively of the ON variety with no cells showing any evidence of OFF responses.

In contrast, SCN cells exhibiting a preference of chromatic modulation in cone excitation reliably exhibited responses of opposite sign to stimulation of either opsin class (i.e. colour-opponency). For the vast majority of such cells, this took the form of a blue-ON yellow-OFF response (Figure 3.6, A, C; pink traces; n= 13/17). Thus, the spiking activity of these cells was consistently high following increased UVS opsin stimulation and low following LWS opsin stimulation. We also found a small minority of cells (n= 4/17) that exhibited the opposite response profile, however (yellow-ON, blue- OFF; Fig 3.6 C). Interestingly, we also found that cone inputs exerted a much more powerful influence over the firing activity of chromatic cells relative to achromatic cells (Figure 3.6, B; absolute change for responses of chromatic cells = 8.1 ± 2.3 spikes/s versus 1.9 ± 0.5 spikes/s for achromatic cells, $n = 17$ and 26 respectively; *t*-test: $p<0.01$).

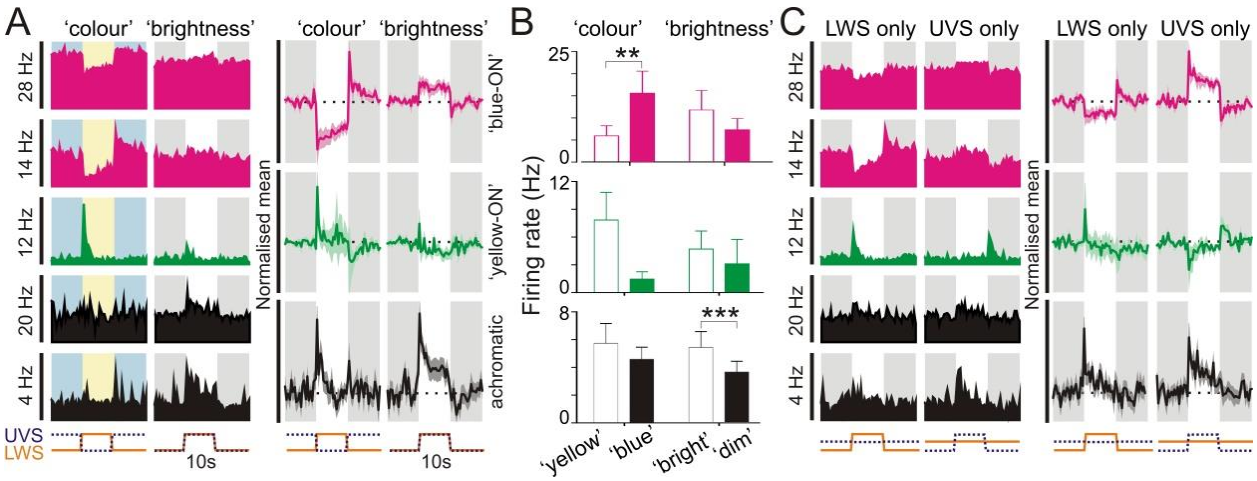

Figure 3.6: Colour opponent responses in suprachiasmatic neurons.

(A: left) Example responses of 5 SCN neurons to stimuli modulating UVS and LWS opsin excitation in antiphase ('colour') or in unison ('brightness'; both 70% Michelson contrast). Individual cells were preferentially excited by blue-yellow transitions ('blue ON'; pink traces), yellow-blue transitions ('yellow ON; green traces) or dim-bright transitions ('achromatic'; black traces). Shaded areas represent blue/yellow or dim/bright stimulus phase, Y Scale bars reflects peak firing rate in spikes/s, X scale bars indicate temporal profile of UVS/LWS opsin excitation. (A: right) Normalised mean (±SEM) change in firing for cells classified as 'blue-ON', 'yellow-ON' or achromatic (n=13, 4 &26 respectively). Conventions as above. (B) Mean (±SEM) firing rates of SCN cell populations tested with colour and brightness stimuli immediately following transitions (0-500ms) from 'blue'-'yellow'/'dim'-'bright' or vice versa. Data were analysed by paired t-test; ***=p<0.001, **=p<0.01. (C: left) Responses of cells from A to selective modulation of LWS or UVS opsin excitation, indicating 'blue'-ON/'yellow-OFF', 'yellow-ON'/'blue-OFF' or non-opponent responses (conventions as in A). (C: right) Normalised mean (±SEM) change in firing for SCN cell populations evoked by LWS and UVS opsin isolating stimuli. Note, normalisation and scaling for data in A and C is identical.

We next sought to better understand how the spectrally opponent responses of SCN neurons were generated. Most mouse cones co-express both UVS and MWS opsin (Applebury et al., 2000). The exceptions are rare "primordial S-cones" that only express UVS opsin (Haverkamp et al., 2005) and peripheral cones that may express either pigment alone (Nikonov et al., 2006). Chromatic opponency could arise either from a comparison between these rare single-opsin expressing cones or from cones expressing both opsins.

In order to distinguish between these two potential origins for chromatic responses, we exploited the fact that, for opsin co-expressing cones, the magnitude of responses to our cone isolating stimuli should be substantially altered by changes in the background spectra (see methods for details), whereas those originating with single opsin cones would not. Accordingly, we next compared responses to UVS and LWS isolating stimuli measured under conditions that resembled natural daylight with those presented under a background lighting condition with altered spectral composition ('white'; irradiance matched for LWS- and UVS- opsin). This analysis revealed substantial differences in responses to LWS and UVS contrast under the two backgrounds (Figure 3.7, A), indicating involvement of the more common opsin co-expressing cones in the chromatic responses of SCN neurons. Similarly, achromatic SCN cells showed little bias towards UVS and LWS opsin responses under 'natural' background illumination (Figure 3.7, B), but when stimuli were presented at the opsin-matched 'white' background, responses were skewed towards UVS opsin (as predicated for the contribution of cones expressing both opsins).

We next asked whether cells exhibiting colour opponency receive irradiance information from melanopsin. To this end, we modulated the spectral composition of our natural background lighting condition to produce large changes in melanopsin excitation (92% Michelson contrast) without any associated change in cone activation. When presented with these melanopsin isolating steps, 'blue'-ON cells exhibited slow, sustained increases in firing (Figure 3.8, A top: peak response = 3.2 ± 0.8 spikes/s above baseline; paired *t*-test $p<0.01$, n=13), as have been previously described for melanopsin-driven responses (Berson et al., 2002, Brown et al., 2010, Brown et al., 2011).

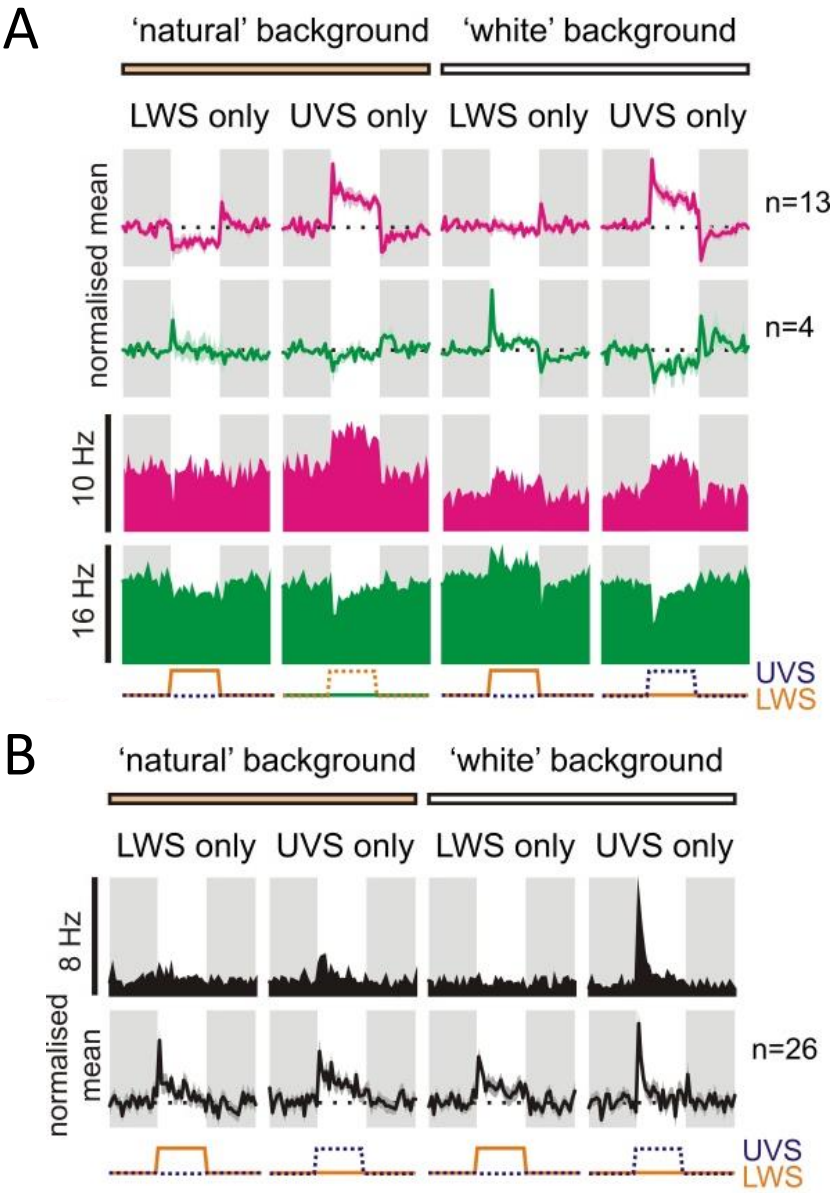

Figure 3.7: Effect of background on SCN responses.

(A: top) Normalised mean (±SEM) responses to UVS/LWS contrast under natural and white background spectra for all blue-ON and yellow-ON cells (n = 13 and 4 respectively). Shading indicates "dim" to "bright" transition, x-axis scale bars indicate temporal profile of UVS/LWS opsin excitation. Note, LWS and UVS opsin specific responses are modulated by changes in background spectra consistent with the involvement of cone that co-express both opsins. (A: bottom) Example responses of two colour-sensitive cells whose opponency was highly dependent on background spectra (one other blue-ON cell exhibited similar behaviour, not shown). Y-axis scale bar indicates firing frequency in spikes/s. (B) Example achromatic cell response (top) and normalised population mean (±SEM; bottom) for UVS and LWS contrast under the two backgrounds.

The responses of colour-insensitive (achromatic) cells also exhibited the expected response profile (Figure 3.8, A bottom: peak response = 1.8 ± 0.2 spikes/s above baseline; paired *t*-test $p<0.01$, n=26). The responses of the rare 'yellow'-ON cells (n=4) was variable (Figure 3.9, B; top), with 1 cell exhibiting an increase in firing (Figure 3.8, B; top), 1 cell exhibiting a reduction (Figure 3.8, B; bottom) in firing and 2 cells displaying no obvious response (not shown).

Given that both achromatic and chromatic cells clearly receive melanopsin-dependent irradiance information, we next investigated who these two signals interact in response to the modest variations in irradiance likely to be commonly encountered during active vision. In particular, we compared responses evoked by cone-selective changes in brightness (LWS+UVS) to those evoked by a spectrally neutral increase in brightness ('energy; LWS+UVS+Melanopsin), steps both stimuli providing 70% Michelson contrast to each receptor. Under these conditions, we found that the inclusion of melanopsin modulations produced very little change in the responses of either colour-opponent or achromatic cells when compared to those produced by the cone selective change in brightness (Figure 3.8, A; subtraction). Accordingly, these data suggest that for modest changes in irradiance the SCN response is in fact dominated by the influence of cone photoreception.

3.4.2 SCN responses to twilight stimuli

If cells are receiving both melanopsin independent irradiance signals and information about wavelength via cone opsins, how do these two signals combine to encode time of day under more natural conditions? To address this we generated stimuli that recreated for *Opn1mw*^{R} mice, the changes in irradiance and wavelength experienced by wildtype animals across the twilight to day transition (Figure 3.9, A). These were delivered as discrete light steps from darkness to simulate a rodent sampling light from an underground burrow.

'Blue'-ON cells exhibited a near linear increase in firing rate as a function of solar angle (Figure 3.9, B; n=9 from 7 mice), indicating that their activity fairly directly reports sun position across the twilight period. Conversely, responses of achromatic cells (Figure 3.9,

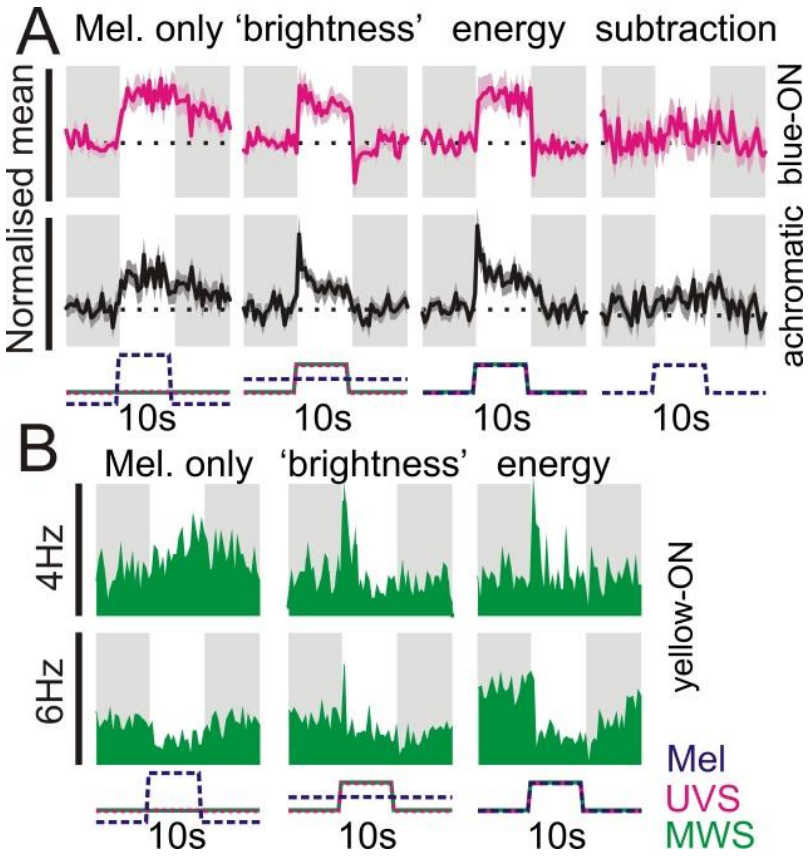

Figure 3.8: Melanopsin signals influence both colour- and brightness- sensitive cells.

(A) Normalised mean (±SEM) response of blue-ON colour-sensitive (n = 13) and achromatic cells (n = 23 tested) to stimuli targeting melanopsin and/or cones. Melanopsin-isolating stimuli presented a 92% Michelson contrast change (~1.4 log units), all other stimuli were 70% Michelson contrast. The energy condition reflects a spectrally neutral modulation in light intensity, providing 70% Michelson contrast for all retinal opsins. Far right panels reflect the predicted melanopsin contribution to the 70% energy condition (obtained by subtracting the responses to UVS + LWS only –"brightness"). Responses were normalised on a within-cell basis across all three stimulus conditions and are plotted on the same scale to highlight relative response amplitude. X-axis scale bars indicate temporal profile of UVS/LWS opsin and melanopsin excitation. (B) Example responses of yellow-ON colour-sensitive cells (bottom panels) to stimuli targeting melanopsin and/or cones or melanopsin. Melanopsin-isolating contrast had more heterogeneous effects in yellow-ON cells, with 1/4 cells exhibiting a reduction in firing and 2 cells displaying no obvious response (not shown). Conventions as above except that data are presented as raw firing rates. Y-axis scale bars represent peak firing in spikes/s.

D; n=8) saturated at solar angles corresponding to sunrise, indicating that they provide more limited information about sun position relative to blue-ON cells.

Although it is clear from the data above that 'blue'-ON cells effectively track irradiance across the twilight period, determining the specific contribution of the colour opponent mechanism to those properties requires additional information. To obtain this we also measured responses to two sets of analytical stimuli that replicated the natural change in irradiance but lacked changes in spectral composition (Figure 3.9, A). Instead, spectra were fixed at either the lowest solar angle for which data was available ('night') or to data recorded in daylight ('day'). Firing rate for 'blue'-ON cells was consistently higher for the 'night' stimulus and lower for the 'day' conditions (Figure 3.9, B; F-test, p=0.009), illustrating that the responses of these cells are highly sensitive to the changes in spectral composition that occur over the course of twilight. Conversely, achromatic cells were unable to distinguish between any of the 3 stimulus sets we tested (Figure 3.9, D; F-test, p=0.72). Thus, under the conditions tested here responses of the achromatic cell population as essentially entirely driven by irradiance as experienced by rods/melanopsin photoreception.

3.4.3 Colour sets circadian phase

The electrophysiological data above indicate that the subsets of SCN neurons are able to track changes in colour and/or irradiance occurring across twilight transitions..

We hypothesised, therefore, that the clock would use information about the change in colour occurring during natural twilight to determine phase of entrainment at the whole organism level. To investigate, this we scaled up our twilight stimuli to form an artificial sky that could be presented to freely moving mice. Stimuli were modelled upon a northern latitude summer, with an extended twilight period. As in the electrophysiological experiments, *Opn1mw*^{R} mice were used, but stimuli were designed to re-create changes in colour and irradiance as would be seen by wild-type mice.

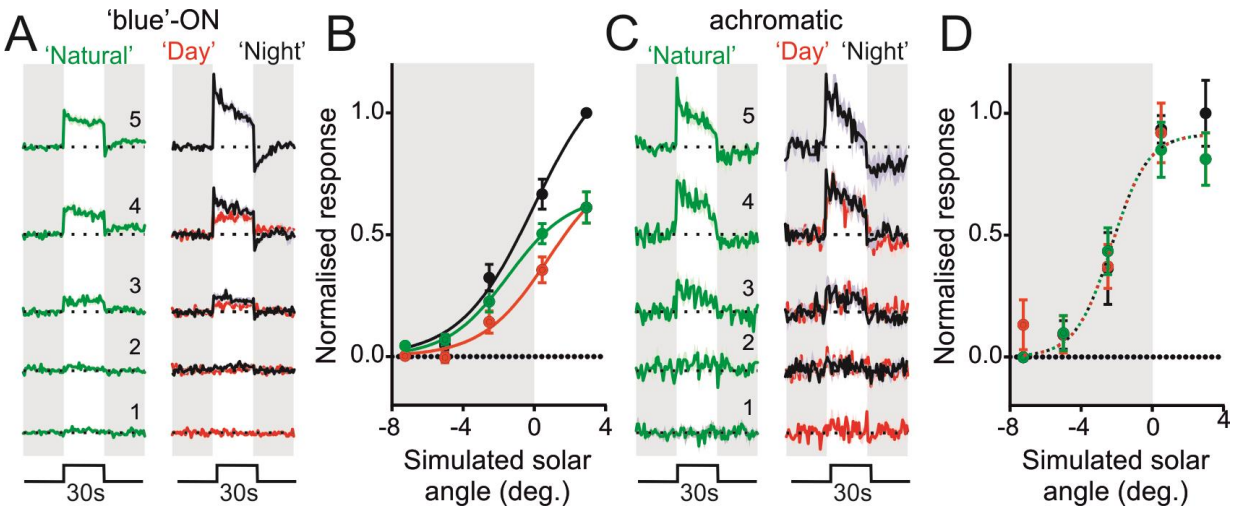

Figure 3.9: Colour signals control irradiance coding in suprachiasmatic neurons.

(A) Mean (±SEM) normalised responses of blue-ON cells (n = 9) to 30s light steps recreating the indicated stages of twilight. Responses were normalised on a within-cell basis according to the largest response observed across all three stimulus sets. (B) Initial (0–10 s) responses of cells from A as a function of simulated solar angle, fit with four-parameter sigmoid curves. Note: the influence of twilight spectral composition on the solar angle response curve (F-test for difference in curve parameters; p=0.009; direct comparisons between each pair of curves also revealed significant differences p<0.05). (C&D) Responses of achromatic cells (n = 8), conventions as in A and B. Achromatic cell responses to the three stimulus sets were statistically indistinguishable (F-test; p=0.72).

For these experiments, we compared the phase of circadian rhythms (obtained via body temperature telemetry) under exposure to light that recreated natural dawn/dusk transitions to an irradiance only stimulus with a fixed 'night' spectral composition. Peak body temperature occurred consistently later (Figure 3.10, A; 31±8mins, paired *t*-test, p=0.003; n=10) during the 'natural' twilight including both colour and irradiance signals than in the irradiance only 'night' twilight condition.

To confirm that this effect truly reflected the influence of cone photoreception and not some unintended difference in the apparent brightness of these two conditions we also performed the same experiment in Cnga3$^{-/-}$ mice lacking functional cone photoreception (Biel et al., 1999). The adjustment in phase seen in *Opn1mw*^{R} was absent in these mice (Figure 3.10, B; 6±9mins, paired *t*-test, p=0.51, n=9), confirming that it is the presence of cone signalling that is responsible for phase adjustment.

3.5 Discussion

Our findings demonstrate that the mammalian circadian clock is able to access information about both the irradiance and spectral composition of light in order to accurately encode time of day. This latter property relies on the action of a subset of cells within the SCN that receive opponent input from LWS and UVS-sensitive cones, allowing them to report changes along the blue-yellow colour axis.

The idea that changes in spectral composition of light could provide important signals to the circadian clock is not new, dating back to primitive mechanisms of archaebacteria (Roenneberg, 1996) and are thought to have evolved as a mechanism for early organisms to avoid high levels of harmful UV radiation during the day (Pittendrigh, 1993).

Changes in spectral composition of light have already been suggested to play a role in circadian entrainment in environments with little overall changes in irradiance, for example during artic summertime (Pohl, 1999). Particular importance has been placed in changes in

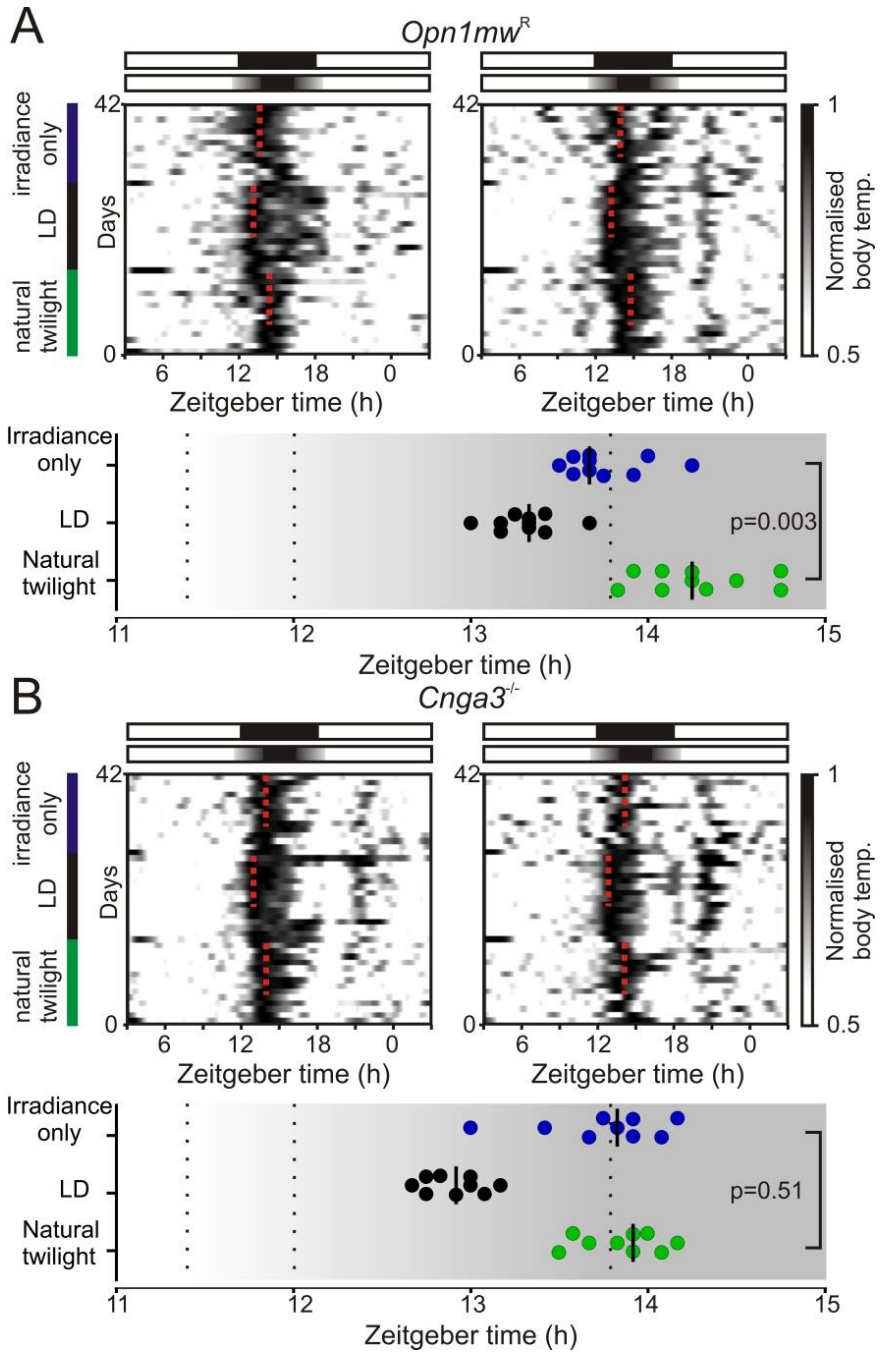

Figure 3.10: Colour changes associated with natural twilight influence circadian entrainment.

(A) Top: Example body temperature traces from two Opn1mw^R mice. Mice were exposed to sequential 14 d epochs of (i) simulated "natural" twilight (replicating natural changes in irradiance and colour during a northern-latitude summer), (ii) 18:6 square wave LD cycle, and (iii) a twilight photoperiod which lacked changes in colour (irradiance profile identical to "natural" but relative cone opsin excitation fixed to mimic night spectra). Dotted red lines indicate timing of peak body temperature from last 9 d in each photoperiod. Bottom plot indicates timing of peak body temperature for each individual (n = 10); bars represent median. Temperature cycles were significantly phase-advanced under the irradiance-only versus natural twilight (paired t test; p = 0.003). (B) Mice lacking functional cone phototransduction (Cnga3-/-) exhibit identical phase of entrainment under both photoperiods (conventions as in A; paired t test; p = 0.51, n = 9) with peak body temperature occurring significantly earlier versus wild-type mice under natural but not irradiance-only twilight (unpaired t tests, p = 0.005 and 0.91 respectively).

light at twilight as it is the time where most animals are active (Roenneberg and Foster, 1997), and colour opponent mechanisms in lizards have been implicated in enhanced perception of dawn and dusk (Solessio and Engbretson, 1993). Earlier studies have identified the capacity for blue-yellow colour discrimination as described here in the pineal/parietal organs of non-mammalian vertebrates such as frogs and lizards (Dodt and Meissl, 1982) and the effects of naturalistic spectral changes on the circadian system have been examined in fish (Pauers et al., 2012). However, although changes in colour have been implicated in assisting circadian entrainment, until now, no studies have been sufficiently controlled in order to specifically separate out the influences of irradiance and wavelength on the circadian system. Most importantly, the possibility that colour could be important in mammals has never, until now, been investigated.

The method of extracting information about changes in spectral composition of light that we have described here should be available to many mammals as the majority of species (around 90%) have retained the required functional short and medium/long wavelength photopigments (Jacobs, 2013). Naturally, this property extends the human visual system and may thus provide an explanation for previous reports of subadditive melatonin suppression in response to polychromatic light stimulation (Figueiro et al., 2004, Revell et al., 2010).

It is clear that colour signals are not necessary for entrainment as animals are perfectly able to entrain to standard LD cycles employed within the laboratory environment. However, our data clearly shows that most mammals should be able to use colour information from the environment to gain a more accurate measurement of sun position than simply measuring irradiance alone. Under natural conditions measuring colour could play a major role in negating the effect of changing weather patterns and cloud cover that can vary the actual irradiance of daylight significantly. If this is taken under consideration, it could be that our experiments have underestimated the importance of spectral composition to the clock as our light stimuli lacked these daily variations. Regardless of this limitation, we still see that changes in spectral composition alters the phase of circadian entrainment, with colour opponency providing a mechanism by which the SCN can fine tune the timings of behavioural/physiological processes to better align them with the solar day.

Further confirmation of this effect of colour on the timing of physiological rhythms reflects a genuine effect on the timing of SCN clock output can been found in *ex vivo* multiunit recordings of mice house under 'natural' and 'irradiance only' conditions (Walmsley et al., 2015). In line with our body temperature data, peak firing times of SCN neurons in *Opn1mw*^{R} mice align with the centre of the day when housed under a natural stimulus. Similarly, peak firing times across the SCN shift substantially earlier when housed under photoperiods that lack changes in colour.

SCN neurons receive input from all known classes of photoreceptor (Lucas et al., 2012, Brown et al., 2011, van Oosterhout et al., 2012, Dkhissi-Benyahya et al., 2007, Altimus et al., 2010, Lall et al., 2010, van Diepen et al., 2013). However, the conventional view is that photoentrainment is primarily driven by rod and melanopsin input (Altimus et al., 2010, Lall et al., 2010). Cones are associated with encoding rapid changes in irradiance, typically within the first few seconds of a light pulse (Brown et al., 2011, Lucas et al., 2012) a signal which seemingly would be of little use to the circadian system. In line with this view, cone-only mice fail to entrain to laboratory LD cycles (Mrosovsky and Hattar, 2005). Our work thus provides a new explanation for why cone inputs are included in the photoreceptive pathways innervating the SCN, acting as important regulators of circadian timing under natural conditions where both colour and irradiance vary dynamically across the day.

One question that is unresolved by this work is the precise mechanism by which SCN neurons receive colour input. The simplest way is via ipRGCs themselves, as we know that cones do transmit signals to the ipRGCs forming the RHT (Sharpe and Stockman, 1999, Belenky et al., 2003, Østergaard et al., 2007). However, colour opponency has not been documented before in mouse ipRGCs (Weng et al., 2013) but has previously described in primates (Dacey et al., 2005). The presence of melanopsin signals in our cells indicates that ipRGCs could indeed be the source of this colour input to the SCN, however, the role of melanopsin in the SCN response to 'energy' steps (L+S+Mel) is minor in comparison to that of cones and so it remains a possibility there is convergent input from ipRGC and non-ipRGCs.

Although ipRGCs do seem a logical source of colour input to the clock, the SCN is does not function autonomously. In addition to receiving direct RHT input from the retina, a second indirect pathway for photic information via the Intergeniculate leaflet (IGL) and associated geniculohypothalamic tract (GHT) (Moore and Card, 1994) is known to have a modulatory effect upon the SCN response. Additionally the OPN (most commonly known for its involvement in the pupillary light reflex) also possesses anatomical connections to the SCN (Moga and Moore, 1997) and the IGL (Moore et al., 2000) suggesting an additional third pathway for light input into the SCN. Therefore, network interactions between brain regions involved in the network could be involved in generating/regulating colour-opponent input to the clock.

The vast majority of the colour opponent cells we found in the mouse SCN are of the 'blue'-ON, 'yellow'-OFF phenotype, the complete opposite of those found in the primate retina (Dacey et al., 2005). However, Dacey and colleagues did not record from SCN-projecting mRGCs. Although ipRGCs with blue-ON properties have not yet been described, Dacey only recorded a small number of cells, and therefore primates almost certainly will possess blue-ON RGCs. The question remaining is whether primate blue-ON RGCs will express the photopigment melanopsin. This does not exclude the possibility of twilight chromatic signals from affecting primate circadian system. In fact, the human melatonin regulation system is evidence for the contrary as it displays a distinct bias towards short wavelengths of light (Thapan et al., 2001). However, we did also find a small number of 'yellow'-ON cells within the SCN that exhibit inhibitory responses to melanopsin stimulation.

Although the biological mechanisms from which these chromatic signals are derived remains elusive, the present findings convincingly show that these signals provide important additional information about time of day, allowing the SCN to calculate a more reliable measurement of solar angle than if using irradiance alone.

3.6 References

ALTIMUS, C. M., GULER, A. D., ALAM, N. M., ARMAN, A. C., PRUSKY, G. T., SAMPATH, A. P. & HATTAR, S. 2010. Rod photoreceptors drive circadian photoentrainment across a wide range of light intensities. *Nat Neurosci,* 13**,** 1107-12.

APPLEBURY, M. L., ANTOCH, M. P., BAXTER, L. C., CHUN, L. L., FALK, J. D., FARHANGFAR, F., KAGE, K., KRZYSTOLIK, M. G., LYASS, L. A. & ROBBINS, J. T. 2000. The murine cone photoreceptor: a single cone type expresses both S and M opsins with retinal spatial patterning. *Neuron,* 27**,** 513-23.

BAVER, S. B., PICKARD, G. E. & SOLLARS, P. J. 2008. Two types of melanopsin retinal ganglion cell differentially innervate the hypothalamic suprachiasmatic nucleus and the olivary pretectal nucleus. *Eur J Neurosci,* 27**,** 1763-70.

BELENKY, M. A., SMERASKI, C. A., PROVENCIO, I., SOLLARS, P. J. & PICKARD, G. E. 2003. Melanopsin retinal ganglion cells receive bipolar and amacrine cell synapses. *J Comp Neurol,* 460**,** 380-93.

BERSON, D. M., DUNN, F. A. & TAKAO, M. 2002. Phototransduction by retinal ganglion cells that set the circadian clock. *Science,* 295**,** 1070-3.

BIEL, M., SEELIGER, M., PFEIFER, A., KOHLER, K., GERSTNER, A., LUDWIG, A., JAISSLE, G., FAUSER, S., ZRENNER, E. & HOFMANN, F. 1999. Selective loss of cone function in mice lacking the cyclic nucleotide-gated channel CNG3. *Proc Natl Acad Sci U S A,* 96**,** 7553-7.

BROWN, T. M., ALLEN, A. E., AL-ENEZI, J., WYNNE, J., SCHLANGEN, L., HOMMES, V. & LUCAS, R. J. 2013. The melanopic sensitivity function accounts for melanopsin-driven responses in mice under diverse lighting conditions. *PLoS One,* 8**,** e53583.

BROWN, T. M., GIAS, C., HATORI, M., KEDING, S. R., SEMO, M., COFFEY, P. J., GIGG, J., PIGGINS, H. D., PANDA, S. & LUCAS, R. J. 2010. Melanopsin contributions to irradiance coding in the thalamo-cortical visual system. *PLoS Biol,* 8**,** e1000558.

BROWN, T. M., TSUJIMURA, S., ALLEN, A. E., WYNNE, J., BEDFORD, R., VICKERY, G., VUGLER, A. & LUCAS, R. J. 2012. Melanopsin-based brightness discrimination in mice and humans. *Curr Biol,* 22**,** 1134-41.

BROWN, T. M., WYNNE, J., PIGGINS, H. D. & LUCAS, R. J. 2011. Multiple hypothalamic cell populations encoding distinct visual information. *J Physiol,* 589**,** 1173-94.

DACEY, D. M., LIAO, H. W., PETERSON, B. B., ROBINSON, F. R., SMITH, V. C., POKORNY, J., YAU, K. W. & GAMLIN, P. D. 2005. Melanopsin-expressing ganglion cells in primate retina signal colour and irradiance and project to the LGN. *Nature,* 433**,** 749-54.

DKHISSI-BENYAHYA, O., GRONFIER, C., DE VANSSAY, W., FLAMANT, F. & COOPER, H. M. 2007. Modeling the role of mid-wavelength cones in circadian responses to light. *Neuron,* 53**,** 677-87.

DODT, E. & MEISSL, H. 1982. The pineal and parietal organs of lower invertebrates. *Experientia,* 38**,** 996-1000.

FIGUEIRO, M. G., BULLOUGH, J. D., PARSONS, R. H. & REA, M. S. 2004. Preliminary evidence for spectral opponency in the suppression of melatonin by light in humans. *Neuroreport,* 15**,** 313-6.

FREEDMAN, M. S., LUCAS, R. J., SONI, B., VON SCHANTZ, M., MUNOZ, M., DAVID-GRAY, Z. & FOSTER, R. 1999. Regulation of mammalian circadian behavior by non-rod, non-cone, ocular photoreceptors. *Science,* 284**,** 502-4.

GOVARDOVSKII, V. I., FYHRQUIST, N., REUTER, T., KUZMIN, D. G. & DONNER, K. 2000. In search of the visual pigment template. *Vis Neurosci,* 17**,** 509-28.

GULER, A. D., ECKER, J. L., LALL, G. S., HAQ, S., ALTIMUS, C. M., LIAO, H. W., BARNARD, A. R., CAHILL, H., BADEA, T. C., ZHAO, H., HANKINS, M. W., BERSON, D. M., LUCAS, R. J.,

YAU, K. W. & HATTAR, S. 2008. Melanopsin cells are the principal conduits for rod-cone input to non-image-forming vision. *Nature,* 453**,** 102-5.
GÖZ, D., STUDHOLME, K., LAPPI, D. A., ROLLAG, M. D., PROVENCIO, I. & MORIN, L. P. 2008. Targeted destruction of photosensitive retinal ganglion cells with a saporin conjugate alters the effects of light on mouse circadian rhythms. *PLoS One,* 3**,** e3153.
HATTAR, S., LIAO, H. W., TAKAO, M., BERSON, D. M. & YAU, K. W. 2002. Melanopsin-containing retinal ganglion cells: architecture, projections, and intrinsic photosensitivity. *Science,* 295**,** 1065-70.
HAVERKAMP, S., WÄSSLE, H., DUEBEL, J., KUNER, T., AUGUSTINE, G. J., FENG, G. & EULER, T. 2005. The primordial, blue-cone color system of the mouse retina. *J Neurosci,* 25**,** 5438-45.
HULBERT, E. 1953. Explanation of the Brightness and Color of the Sky, Particularly the Twilight Sky.: The Journal of the Optical Society of America.
JACOBS, G. H. 2013. Losses of functional opsin genes, short-wavelength cone photopigments, and color vision--a significant trend in the evolution of mammalian vision. *Vis Neurosci,* 30**,** 39-53.
JACOBS, G. H. & WILLIAMS, G. A. 2007. Contributions of the mouse UV photopigment to the ERG and to vision. *Doc Ophthalmol,* 115**,** 137-44.
LALL, G. S., REVELL, V. L., MOMIJI, H., AL ENEZI, J., ALTIMUS, C. M., GULER, A. D., AGUILAR, C., CAMERON, M. A., ALLENDER, S., HANKINS, M. W. & LUCAS, R. J. 2010. Distinct contributions of rod, cone, and melanopsin photoreceptors to encoding irradiance. *Neuron,* 66**,** 417-28.
LOVEGROVE, B. G. 2009. Modification and miniaturization of Thermochron iButtons for surgical implantation into small animals. *J Comp Physiol B,* 179**,** 451-8.
LUCAS, R. J., LALL, G. S., ALLEN, A. E. & BROWN, T. M. 2012. How rod, cone, and melanopsin photoreceptors come together to enlighten the mammalian circadian clock. *Prog Brain Res,* 199**,** 1-18.
MEIJER, J. H., GROOS, G. A. & RUSAK, B. 1986. Luminance coding in a circadian pacemaker: the suprachiasmatic nucleus of the rat and the hamster. *Brain Res,* 382**,** 109-18.
MOGA, M. M. & MOORE, R. Y. 1997. Organization of neural inputs to the suprachiasmatic nucleus in the rat. *J Comp Neurol,* 389**,** 508-34.
MOORE, R. Y., WEIS, R. & MOGA, M. M. 2000. Efferent projections of the intergeniculate leaflet and the ventral lateral geniculate nucleus in the rat. *J Comp Neurol,* 420**,** 398-418.
MROSOVSKY, N. & HATTAR, S. 2005. Diurnal mice (Mus musculus) and other examples of temporal niche switching. *J Comp Physiol A Neuroethol Sens Neural Behav Physiol,* 191**,** 1011-24.
NIKONOV, S. S., KHOLODENKO, R., LEM, J. & PUGH, E. N. 2006. Physiological features of the S- and M-cone photoreceptors of wild-type mice from single-cell recordings. *J Gen Physiol,* 127**,** 359-74.
PAUERS, M. J., KUCHENBECKER, J. A., NEITZ, M. & NEITZ, J. 2012. Changes in the colour of light cue circadian activity. *Anim Behav,* 83**,** 1143-1151.
PAXINOS, G. & FRANKLIN, K. 2001. *The Mouse Brain in Stereotaxic Coordinates,* San Diego, Academic Press.
PEICHL, L. 2005. Diversity of mammalian photoreceptor properties: adaptations to habitat and lifestyle? *Anat Rec A Discov Mol Cell Evol Biol,* 287**,** 1001-12.
PEREZ-LEON, J. A., WARREN, E. J., ALLEN, C. N., ROBINSON, D. W. & BROWN, R. L. 2006. Synaptic inputs to retinal ganglion cells that set the circadian clock. *Eur J Neurosci,* 24**,** 1117-23.

PITTENDRIGH, C. S. 1993. Temporal organization: reflections of a Darwinian clock-watcher. *Annu Rev Physiol,* 55**,** 16-54.

POHL, H. 1999. Spectral composition of light as a Zeitgeber for birds living in the high arctic summer. *Physiol Behav,* 67**,** 327-37.

REVELL, V. L., BARRETT, D. C., SCHLANGEN, L. J. & SKENE, D. J. 2010. Predicting human nocturnal nonvisual responses to monochromatic and polychromatic light with a melanopsin photosensitivity function. *Chronobiol Int,* 27**,** 1762-77.

ROENNEBERG, T. 1996. The complex circadian system of *Gonyaulax polyedra*. *Physiologica Plantarum,* 96**,** 733-737.

ROENNEBERG, T. & FOSTER, R. G. 1997. Twilight times: light and the circadian system. *Photochem Photobiol,* 66**,** 549-61.

SHARPE, L. T. & STOCKMAN, A. 1999. Rod pathways: the importance of seeing nothing. *Trends Neurosci,* 22**,** 497-504.

SMALLWOOD, P. M., OLVECZKY, B. P., WILLIAMS, G. L., JACOBS, G. H., REESE, B. E., MEISTER, M. & NATHANS, J. 2003. Genetically engineered mice with an additional class of cone photoreceptors: implications for the evolution of color vision. *Proc Natl Acad Sci U S A,* 100**,** 11706-11.

SOLESSIO, E. & ENGBRETSON, G. A. 1993. Antagonistic chromatic mechanisms in photoreceptors of the parietal eye of lizards. *Nature,* 364**,** 442-5.

THAPAN, K., ARENDT, J. & SKENE, D. J. 2001. An action spectrum for melatonin suppression: evidence for a novel non-rod, non-cone photoreceptor system in humans. *J Physiol,* 535**,** 261-7.

VAN DIEPEN, H., RAMKISOENSING, A., PEIRSON, S. N., FOSTER, R. G. & MEIJER, J. H. 2013. Irradiance encoding in the suprachiasmatic nuclei by rod and cone photoreceptors. *The FASEB Journal,* Epub ahead of print.

VAN OOSTERHOUT, F., FISHER, S. P., VAN DIEPEN, H. C., WATSON, T. S., HOUBEN, T., VANDERLEEST, H. T., THOMPSON, S., PEIRSON, S. N., FOSTER, R. G. & MEIJER, J. H. 2012. Ultraviolet light provides a major input to non-image-forming light detection in mice. *Curr Biol,* 22**,** 1397-402.

VINEY, T. J., BALINT, K., HILLIER, D., SIEGERT, S., BOLDOGKOI, Z., ENQUIST, L. W., MEISTER, M., CEPKO, C. L. & ROSKA, B. 2007. Local retinal circuits of melanopsin-containing ganglion cells identified by transsynaptic viral tracing. *Curr Biol,* 17**,** 981-8.

WALMSLEY, L., HANNA, L., MOULAND, J., MARTIAL, F., WEST, A., SMEDLEY, A. R., BECHTOLD, D. A., WEBB, A. R., LUCAS, R. J. & BROWN, T. M. 2015. Colour as a signal for entraining the mammalian circadian clock. *PLoS Biol,* 13**,** e1002127.

WENG, S., ESTEVEZ, M. E. & BERSON, D. M. 2013. Mouse ganglion-cell photoreceptors are driven by the most sensitive rod pathway and by both types of cones. *PLoS One,* 8**,** e66480.

ØSTERGAARD, J., HANNIBAL, J. & FAHRENKRUG, J. 2007. Synaptic contact between melanopsin-containing retinal ganglion cells and rod bipolar cells. *Invest Ophthalmol Vis Sci,* 48**,** 3812-20.

Chapter 4: Selective manipulation of cone inputs to optogenetically-identified mouse visual neurons

4.1 Abstract

Understanding how distinct populations of retinal and central neurons interact to coordinate behavioural and physiological responses to visual stimuli is a key goal for sensory biology. While the sophisticated range of mouse genetic tools available now make this goal attainable, certain aspects of visual discrimination are challenging to study in mice. For example, the close spectral sensitivity of most mouse photoreceptors makes it hard to distinguish visual responses that are dependent on the chromaticity vs. brightness of a given stimulus. We have previously employed mice with altered cone spectral sensitivity to overcome this issue, using multispectral stimuli to show that both brightness and colour contribute to circadian photoentrainment. We now validate a modification of our original 'silent-substitution' approach for use in wildtype mice, facilitating application of the technique alongside the wide range of new tools for cell-specific identification and circuit manipulation.

Using multielectrode recordings from the lateral geniculate nuclei (LGN) of wildtype and coneless mice, we first show that our silent-substitution protocols allow for robust and selective activation of both mouse cone types (either singly, in unison or in antiphase). We next show the utility of this approach alongside optogenetic-based cell identification, using 'optrode' recordings from mice with Channelrhodopsin2-directed to GABAergic neurons (Ai32; GAD2-Cre). These recordings indicate that chromatic sensitivity is rare or absent across GABA-positive intergeniculate leaflet/ventral LGN cells, suggesting that these thalamic nuclei are unlikely to provide a direct source of chromatic signals for circadian photoentrainment. In summary, we have established a useful new approach for investigating cone photoreception and colour discrimination in mice with wide-ranging utility alongside the ever-expanding mouse genetic toolbox.

4.2 Introduction

Visual nuclei across the brain contain heterogeneous populations of neurons, varying in functional properties, anatomical connectivity and the expression of neurochemical messengers (Maturana and Varela, 1982, Harrington and Rusak, 1989, Harrington, 1997, Howarth et al., 2014). Advances in mouse genetics offer new exciting ways to investigate the functional organisation of such circuits (Soden et al., 2014). For example, the ability to target exogenous proteins (e.g. optogenetic actuators) to specific cell types provides the opportunity to define how identified neuronal populations communicate with one another and/or to establish how the functional properties of cells vary according to neurochemical phenotype. Given the unprecedented insights that are thus available from this new generation of mouse genetic tools, it is no surprise that recent years have seen a dramatic increase in the use of mice for studying visual circuits (See Huberman and Niell, 2011 for review). Unfortunately, one area that has remained relatively poorly understood is how the mouse visual system processes chromatic information.

Mice possess two classes of cone opsin, maximally sensitive to shortwavelength (S-opsin; λmax=360nm) or green light (M-opsin; λmax=511nm) (Calderone and Jacobs, 1995, Szél et al., 1992, Lall et al., 2010), together allowing for a form of dichromatic ('blue-yellow') colour vision analogous to that found in most other mammals (See Jacobs, 2013 for review). While at first glance it may seem relatively straightforward to identify colour sensitive neurons, based on responses of opposite sign to UV and green light (i.e. ON vs. OFF), two features of the mouse visual system make this challenging. Firstly, all mouse opsins retain high sensitivity in the UV part of the spectrum (Figure 4.1), making it challenging to activate S-opsin without the confounding influence of other photoreceptive systems. Secondly, the spectral sensitivity of the mouse M-opsin is very similar to that of rod and melanopsin photoreception (λmax=498nm and 480nm respectively; Figure 4.1: A). Although a possible confounding influence of rod stimulation here can be ameliorated by working under very high background light levels, the possibility of activating melanopsin under such conditions makes it hard to confidently ascribe response components to M-opsin. Given that melanopsin signals are widespread throughout the mouse visual system (Brown et al., 2010, Ecker et al., 2010, Allen et al., 2014, Storchi et al., 2015) this is a

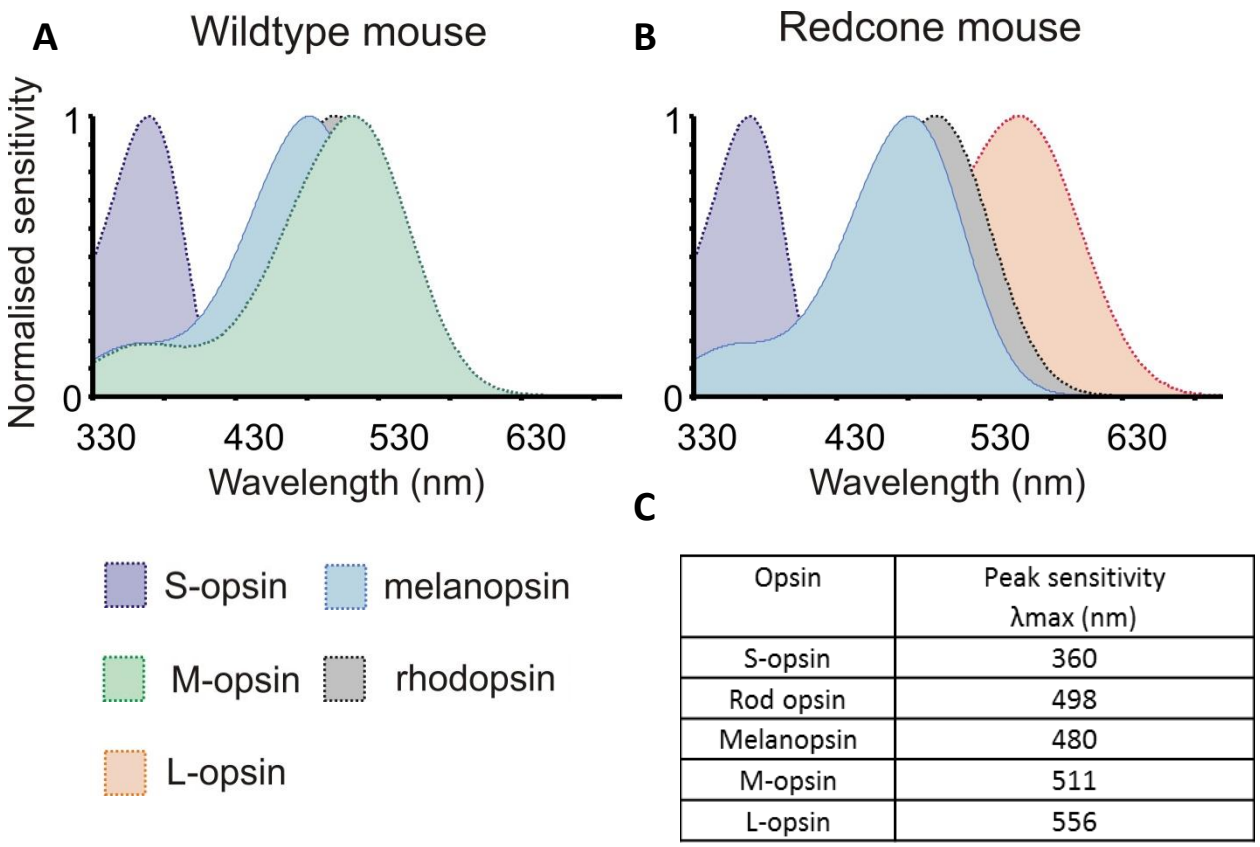

C

Opsin	Peak sensitivity λmax (nm)
S-opsin	360
Rod opsin	498
Melanopsin	480
M-opsin	511
L-opsin	556

Figure 4.1: Absorbance profiles of photopigments in wildtype and red cone mice.

Wildtype mice (A) possess two cone opsins: S-opsin that maximally absorbs light in the UV range (purple trace; λmax=360nm) and M-opsin that maximally absorb light within the green portion of the spectra (green trace; λmax=511nm). The absorbances of M-opsin, rod opsin and melanopsin (λmax=511nm, 498nm and 480nm respectively) are close within the light spectra which makes it difficult to separate out their relative contributions to the circadian light response. To make this easier, experiments that study photopigment contributions are carried out in red cone (*Opn1mw*^{R}*)* mice (B). Red cone mice possess the human red cone opsin (red trace; λmax=556nm) in place of the mouse M-cone opsin (left; green), rendering the absorbancies of the photoreceptors sufficiently different to facilitate the generation of cone-isolating stimuli. The peak absorbance of each of the photopigments is listed in (C). Adapted from Walmsley et al (2015).

significant drawback, especially when the regions studied receive the majority of their visual input from melanopsin expressing cells (e.g. the suprachiasmatic nucleus; SCN).

To overcome these issues, we have previously employed carefully calibrated polychromatic lighting to isolate cone and/or melanopsin signals ('silent-substitution'), allowing us to show that colour provides a key source of information to the mouse SCN circadian clock (Walmsley et al., 2015). While effective, this earlier approach relied on the use of a transgenic 'red cone' mouse model (Figure 4.1, B) in which the native mouse M-opsin is replaced by the human longwavelength sensitive L-opsin (Smallwood et al., 2003, Lall et al., 2010, Walmsley et al., 2015). This requirement thus presents a barrier to applying our methodology alongside other genetic tools (e.g. cell-selective optogenetics) which could help determine which SCN neuron types process colour signals and/or whether such responses rely on input from other visual structures (e.g. the intergeniculate leaflet/ventral lateral geniculate nucleus; IGL/vLGN). To avoid the logistical/financial drawbacks associated with incorporating the cone transgenics alongside genetic tools for circuit mapping, here we set out to validate a modification of the silent substitution approach suitable for studying cone signalling in wildtype (M-opsin-expressing) mice. We also aimed to demonstrate the utility of this approach alongside cell-type specific optogenetic-based cell identification and thus obtain new insights into the sensory properties of IGL/vLGN cell populations.

4.3 Methods

4.3.1 *in vivo* electrophysiological recordings

4.3.1.1 Animals

All animal use was in accordance with the Animals (Scientific Procedures) Act of 1986 (United Kingdom). Preliminary LGN experiments were performed on wildtype (C57BL/6J background; n=6) and coneless ($Cnga3^{-/-}$; n=8) mice. For optogenetic experiments, recordings (n=6) were performed in Ai32; GAD2-Cre mice. In these mice

Channelrhodopsin2:EYFP is selectively directed to GABAergic neurons via Cre recombinase (flox-STOP system), whose expression is under control of the glutamate decarboxylase 2 (GAD2) enzyme (Madisen et al., 2012, Taniguchi et al., 2011). All mice were housed under a 12-h dark/light cycle at a temperature of 22°C with food and water available ad libitum.

4.3.1.2 Surgical techniques

Adult male mice were anaesthetised by intraperitoneal injection of urethane (1.5g/kg) and placed into a stereotaxic frame (SR-15M; Narishige International) to hold the skull fixed in place for surgery. The surface of the skull was exposed using a scalpel incision and a hole was drilled using stereotaxic co-ordinates (2.5mm lateral to and 2.25mm posterior to Bregma) obtained from the stereotaxic mouse atlas (Paxinos and Franklin, 2001). Pupils were dilated with 1% atropine (Sigma Aldrich) and mineral oil (Sigma-Aldrich) added to prevent drying of the cornea.

For preliminary LGN experiments, a recording probe (A4X8-5mm-50-200-177; Neuronexus, MI, USA) consisting of 4 shanks (spaced 200µm), each with 8 recordings sites (spaced 50µm) was coated with fluorescent dye (CM-DiI; Invitrogen, Paisley, UK) and then inserted into the brain 2.5mm lateral and 2.25mm caudal to bregma. The electrode was then lowered to the level of the LGN using a fluid-filled micromanipulator (MO-10, Narishige International Ltd., London, UK). To maximise the number of light responsive units obtained from each experiment, after running through the light protocol, the probe was moved up 200µm and the light protocol repeated.

For IGL optogenetic experiments, a recording probe with attached optical fibre (A1x32-Poly3-10mm-50-177) was coated with fluorescent dye (CM-DiI; Invitrogen, Paisley, UK) and then inserted vertically into the brain 2.4mm lateral and 2.5mm caudal to bregma. The electrode was then lowered to the level of the IGL using a fluid-filled micromanipulator (MO-10, Narishige International Ltd., London, UK).

After allowing 30 min for neural activity to stabilise following probe insertion, wideband neural signals were acquired using a Recorder64 system (Plexon, TX, US), amplified (x3000) and digitized at 40 kHz. Surgical procedures were completed 1–2 h before the end of the home cage light phase, such that electrophysiological recordings spanned the late projected day-early projected night. Throughout the experiment, the animal's temperature was maintained at 37˚C using a homeothermic heat mat (Harvard Apparatus).

4.3.2 Generation of cone-isolating visual stimuli for wildtype mice

We have previously used polychromatic (3-primary) illumination systems to selectively manipulate cone photoreception in *Opn1mw*^{R} animals, with negligible effective contrast for rod or melanopsin photoreceptors (Brown et al., 2013, Allen et al., 2014, Walmsley et al., 2015). Given the very close spectral sensitivity of rhodopsin and the wildtype mouse M-cone opsin (Figure 4.1), it is not possible to generate equivalent high contrast cone modulating stimuli for wildtype animals that are also rod and melanopsin silent. We reasoned, however, that producing effective cone-isolating stimuli for wildtype mice is possible, provided that we work under high enough background light levels to silence rods. Indeed, we have previously used a similar approach to generate melanopsin-isolating stimuli for *Opn1mw*^{R} mice and validated that the relatively high rod contrast these provided (~67%) was insufficient to evoke noticeable responses under background illumination >10^{14} photons/cm^{2}/s (Brown et al., 2012).

Using MATLAB modelling (Mathworks, MA, USA) of commercially available high power LEDs, we determined that a combination of red (λmax: 617nm), blue (470nm) and ultraviolet (UV; 405nm) LEDs (Thorlabs, NJ, USA) provided a good compromise between the ability to produce high contrast manipulation of M- and S-cone opsin with no effective contrast for melanopsin (and relatively modest effective rod contrasts). Accordingly, we established a three primary illumination system, using dichroic mirrors (Thorlabs) to combine illumination from these three LEDs which was then focused onto the end of a 7mm diameter flexible fibre optic light guide (Edmund Optics; York, UK) terminating in an internally reflective plastic cone that could be positioned snugly over the animals eye.

Light measurements were performed at the aperture of the illumination system, via a calibrated spectroradiometer (Bentham instruments, Reading, UK). Using photopigment spectral absorbance data and allowing correction for pre-receptoral filtering (Govardovskii et al., 2000, Jacobs and Williams, 2007), pairs of metameric stimuli were then designed that selectively differed in activation of M- and S opsins (individually, in tandem (M+S) and in antiphase (M-S); 63% Michelson contrast). The effective melanopsin contrast for all these stimuli was negligible (~3%) while the effective rod contrast ranged from 1.8-35%, with a minimum effective rod photon flux $>10^{14}$ (Table 4.1). As controls, we also generated spectrally neutral stimulus pairs ('energy' stimuli: 20, 40, 63, 75, 90 & 96% Michelson contrast) and cone-silent stimuli that provided modest contrast for melanopsin and rods (36 & 21% Micheslon respectively).

For stimulus presentation, LED intensity was controlled using custom-written programs in LabView 8.6 (National Instruments). Our stimuli were carefully designed such that the 'background' for each (i.e. the average of 'bright' and 'dim' stimulus pairs) was identical. This allowed us to interleave blocks of stimulus presentation without confounding effects of adaptation to changes in background photon flux for one or more photoreceptors. Each metameric pair was delivered as 6-cycle blocks of square-wave modulations from the common background at 0.25Hz in a predefined sequence (ordered based on effective rod contrast). The full battery of test stimuli was then repeated multiple times (5-10) over the course of the experiment to allow us to track changes in responsiveness over time.

4.3.3 Optogenetic stimuli

Optogenetic stimuli (634mW/mm^2 at the tip of the 200µm fibre) of between 10 and 300ms duration were generated using a Blue (465nm) table-top PlexBright LED module (Plexon, TX, USA) and controlled via custom-written programs in via LabVIEW (National Instruments, TX, USA). Optogenetic stimuli were delivered directly to the brain through optical fibre, terminating 200µm above the location of the electrode sites.

	Photons/cm^2/s at 'high'				Photons/cm^2/s at 'low'				Michelson contrast (%)			
Condition	**M-cone**	**S-cone**	**Rod**	**Mel**	**M-cone**	**S-cone**	**Rod**	**Mel**	**M-cone**	**S-cone**	**Rod**	**Mel**
M	$4.5x10^{14}$	$4.3x10^{13}$	$2.1x10^{14}$	$1.5x10^{14}$	$1.0x10^{14}$	$4.3x10^{13}$	$1.1x10^{14}$	$1.4x10^{14}$	63.0	-0.3	31.1	3.3
S	$2.8x10^{14}$	$7.0x10^{13}$	$1.6x10^{14}$	$1.5x10^{14}$	$2.8x10^{14}$	$1.6x10^{13}$	$1.7x10^{14}$	$1.4x10^{14}$	-0.2	63.0	-1.8	3.0
M-S	$4.5x10^{14}$	$1.6x10^{13}$	$2.2x10^{14}$	$1.5x10^{14}$	$1.0x10^{14}$	$7.0x10^{13}$	$1.1x10^{14}$	$1.4x10^{14}$	62.9	-63.0	34.5	3.2
M+S	$4.5x10^{14}$	$7.0x10^{13}$	$2.1x10^{14}$	$1.5x10^{14}$	$1.0x10^{14}$	$1.6x10^{13}$	$1.2x10^{14}$	$1.4x10^{14}$	63.0	62.9	27.8	3.5
Energy	$4.5x10^{14}$	$7.0x10^{13}$	$2.7x10^{14}$	$2.4x10^{14}$	$1.0x10^{14}$	$1.6x10^{13}$	$6.0x10^{13}$	$5.4x10^{13}$	63.0	63.0	63.0	63.0
Rod/Mel	$2.8x10^{14}$	$4.3x10^{13}$	$2.0x10^{14}$	$2.0x10^{14}$	$2.8x10^{14}$	$4.3x10^{13}$	$1.3x10^{14}$	$9.4x10^{13}$	0.0	0.0	21.3	36.0

Table 4.1: Calculated photon fluxes for each photoreceptor class in the silent substitution stimuli.

The photon flux of each photoreceptor (photons/cm^2/s) at each background ('low' condition) and during the light step ('high' condition) within the silent substitution stimuli designed to selectively modulate each of the photoreceptor classes. The relative contrast of the steps at each background is also shown for each stimulus.

4.3.4 Histology

At the end of each experiment the brain was removed and post-fixed in 4% paraformaldehyde overnight and then cryoprotected in 30% sucrose. The following day, brains were sectioned at 100µm on a freezing sledge microtome and mounted onto slides using Vectasheild (Vectorlaboratories Ltd., Peterbourogh, UK).

After mounting DiI-labelled probe placements were visualised under a fluorescent microscope (Olympus BX51) with appropriate filter sets. Resulting images were then compared with appropriate stereotaxic atlas figures (Paxinos, 2001), to confirm appropriate probe placement.

4.3.5 Data Analysis

Responses to silent substitution and optogenetic stimuli were analysed by custom written programs in MATLAB R2014a. Where appropriate, firing rate modulations evoked by silent substitution stimuli were deemed significant using χ^2-peridogram. Graphs were produced in GraphPad prism 6.04 and Neuroexplorer (Version 4.133; Nex Technologies, AL, USA). Statistical tests were carried out in GraphPad prism 6.04. Single cell/channel example responses are presented as the mean ± SEM change in firing across all trials relative to baseline. Where average population data is presented, data was baseline subtracted to calculate the change in firing and presented as the mean ± SEM change in firing, as above.

4.4 Results

4.4.1 Validation of the green cone silent substitution protocol

We first set out to confirm that the metameric cone-isolating stimuli we designed were indeed effectively silent for rod and melanopsin photoreception. In particular, it was important to establish that the modest rod contrasts (<35% Michelson; Table 4.1) these stimuli produced were insufficient to activate rods under our experimental conditions

(effective rod flux= 14.2 log photons/cm^2/s). To this end, we initially performed in vivo multielectrode recordings in the LGN of male 'coneless' mice (Cnga3$^{-/-}$; n=8 recordings). Since these mice lack cone phototransduction, any LGN response to retinal illumination in these animals must originate with rods or melanopsin. However, since even very high contrast changes in melanopsin activation do not seem to translate to noticeable changes in neuronal firing at the temporal frequencies (0.25Hz) we employed here (Brown et al., 2013, Procyk et al., 2015), we predicted that responses in the coneless mice (if present) could be ascribed to rods. On that basis, we specifically chose to perform these recordings in the LGN because previous work indicates that rod-driven responses are more robust in this region than in other visual nuclei (Brown et al., 2011).

To help define the amount of rod contrast that could be safely applied without risk of actually recruiting rod responses under our experimental conditions, alongside our cone-isolating stimuli, we also tested LGN multiunit responses (n=152 recording sites) to a rod/melanopsin isolating stimulus and spectrally neutral 'energy' modulations of varying contrasts (20, 40, 63, 75, 90 and 95%). In line with our predictions, above, we found that very few channels exhibited significant modulations in firing rate to any of our cone-isolating stimuli but that responses became more noticeable with increasing rod contrast (Figure 4.2, A).

As expected for our experimental conditions, the modulations in multiunit firing rate we observed we typically small even for very large rod contrasts (Figure 4.2, C, D). Somewhat surprisingly, however, we did observe a modest number electrode sites that exhibited significant modulations to our cone-selective stimuli (Figure 4.2, A, B). This was most evident for the M-S modulating stimuli (which provided the highest rod contrast: 35% Michelson), where ~11% of cells exhibited a significant modulation in firing rate. Upon closer inspection, we noticed that overt responses to these cone-isolating/low rod contrast stimuli were entirely absent during early parts of our experiment and then gradually appeared after extended recording epochs (Figure 4.2, D). These data suggest then that despite the relatively high background light levels we employed, after extended epochs of adaptation rods regain enough sensitivity to drive responses to modest contrasts (>30%) in a subset of cells.

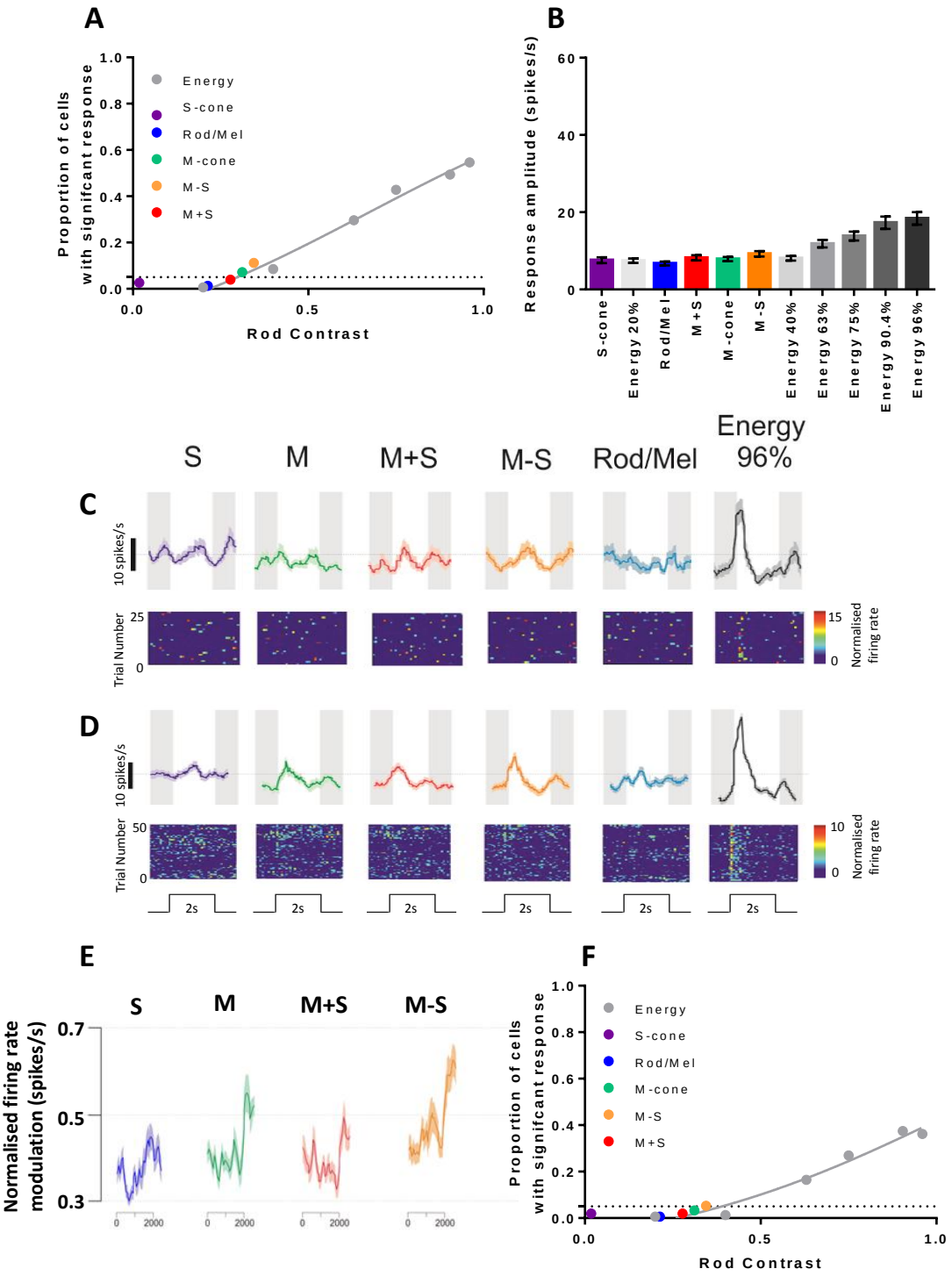

Figure 4.2: LGN multiunit responses of coneless mice to silent substitution stimuli.

(A) The proportions of multiunit channels that have a significant response to each of the 7 silent substitution stimuli in coneless mice, plotted in relation to their rod contrast. Grey points indicate proportions of cells responding to energy steps. (B) The average firing rate modulation across all channels exhibiting significant responses to the 96% energy step (n=82 channels). (C&D) Example responses and associated trial bin counts of coneless mice to a 2s stimulus (represented by the unshaded area), expressed in terms of their rod contrast. (C) An example response from a channel that only responds to an energy step. (D) An example of a coneless channel that develops responses to M-opsin and M-S stimuli partway through the experiment. Conventions as in C. (E) Normalised 'response' to S- and M-cone modulating stimuli over time (10 trial running average). (F) Proportion of cells with a significant response to presentations of each of the individual stimuli that occur within 2000 seconds of beginning the protocol. Conventions as in A.

Accordingly, we next aimed to determine over what timescales it was possible to employ our cone-isolating stimuli with negligible risk of beginning to also evoke rod-based responses. To address this, we examined the stimulus-response relationships for responding cells across individual blocks of stimulus presentation (see methods) throughout the experiment (Figure 4.2, E). This analysis indicated that, among the population of cells that regain sensitivity to low rod contrasts, nominal response amplitude (peak-trough difference in firing rate) quite consistently began to increase ~2000s after start of stimulus presentation. Accordingly, we reanalysed our data above, restricting analysis to stimuli presented <2000 seconds of the start of the protocol. Under these conditions we found that the proportions of recordings exhibiting statistical significant modulations to cone isolating stimuli fell to at or below chance (p=0.05), even for the stimulus condition producing the highest rod contrast (M-S; Figure 4.2, F).

Having established conditions under which our cone-isolating stimuli were effectively silent for rods and melanopsin, we next aimed to confirm that these stimuli were indeed sufficient to drive cone-based responses in wildtype mice. To this end, we then carried out in vivo multiunit recordings in the LGN region of male wildtype mice (C57BL/6J background; n=6). As expected for these wildtype LGN recordings, stimulus response relationships no longer reflected the effective rod contrast they provided (Figure 4.3, A, B). Indeed, we now observed robust multiunit responses (n=107 light responsive channels) to each of our cone-isolating stimuli (Figure 4.3, A), with large proportions of channels (~80%) responding to at least some conditions (Figure 4.3, B). Moreover, multiunit response amplitudes were substantially higher (~10 times) than those observed among the small subset of coneless recordings where we could detect rod responses after extended adaptation (compare Figure 4.2 and 4.3). Interestingly, while we didn't here seek to characterise responses across individual cells, even at the multiunit level we were able to identify clear evidence of both chromatic (Figure 4.3, C) and achromatic (Figure 4.3, D) cone signalling. On that basis we conclude that our approach is suitable for studying cone signalling/colour processing in the mouse visual system.

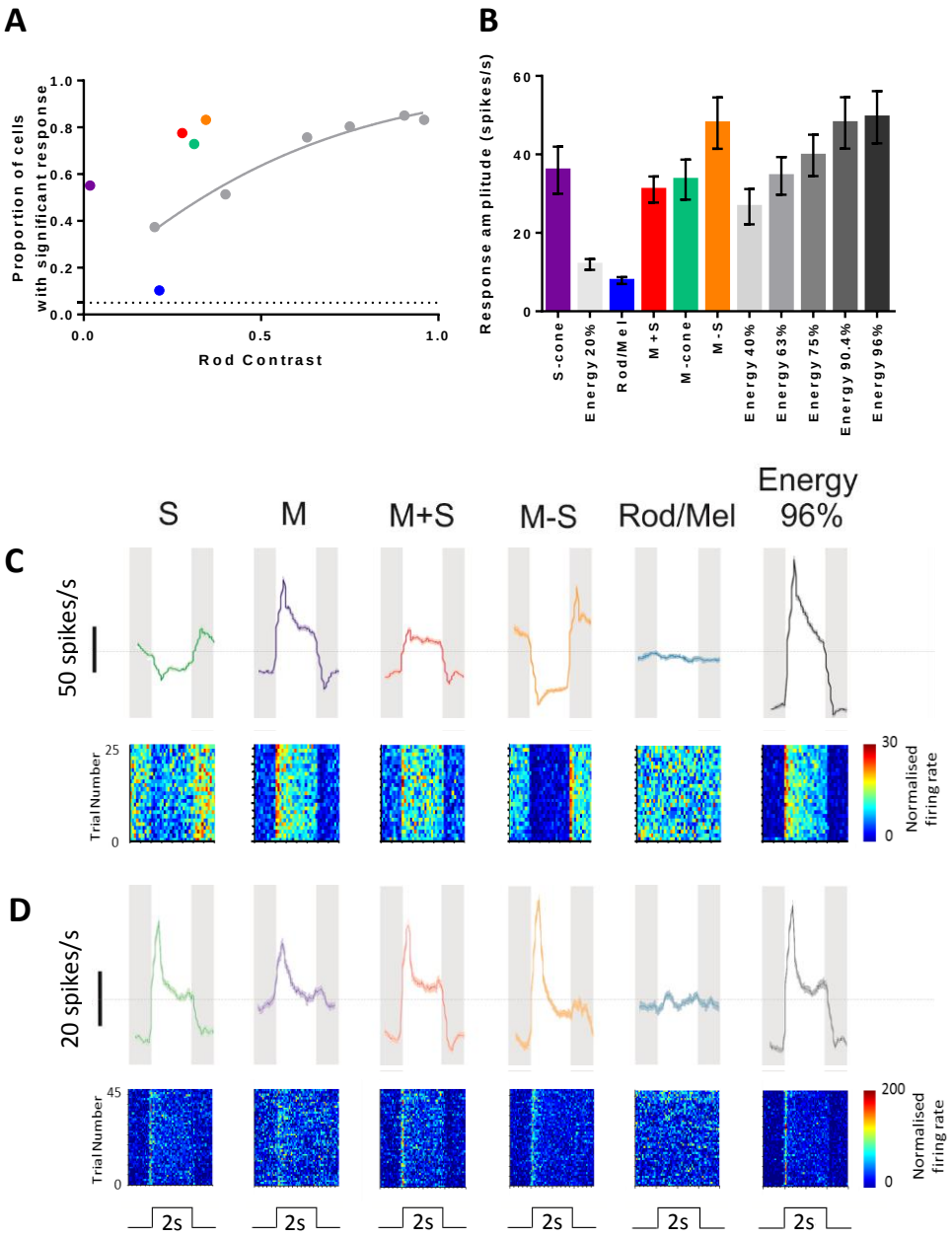

Figure 4.3: LGN multiunit responses of wildtype mice to the individual silent substitution stimuli.

(A) The proportions of multiunit channels that have a significant response to each of the 7 silent substitution stimuli in wildtype mice. (B) The average response amplitudes of channels that have significant responses to each of the individual stimuli. (C&D) Example responses and associated trial bin counts of wildtype mice to a 2s stimulus (represented by the unshaded area), expressed in terms of their rod contrast. (C) An example of a chromatic channel with opponent responses to activation of M-and S-opsins. (D) The response of an achromatic channel that responds to the stimulation of either M-or S-opsin only.

4.4.2 The identification of and characterisation of GABA-expressing cells in the IGL/LGN

We next set out to demonstrate the utility of the silent-substitution approach outlined above, alongside cell-specific optogenetic identification/manipulation. In particular we set out to employ this approach to determine whether the LGN-cell groups providing input to the circadian system (GABAergic IGL/vLGN cells) might convey colour signals. To this end, we next performed 'optrode' recordings (n=6) in Ai32; GAD2-Cre mice. In these animals channelrhodopsin2 is specifically directed to neurons expressing the GABA synthetic enzyme GAD2 (Madisen et al., 2012, Taniguchi et al., 2011), allowing ready identification of GABA cells on the basis of intrinsic photosensitivity. Of note, since GAD2 is only expressed in a very small minority of dLGN cells (Hammer et al., 2014), this approach also provides a useful marker to distinguish putative IGL cells detected during these multielectrode recordings from those in the neighbouring dorsal LGN.

We first examined multiunit responses to 5s steps of retinal illumination (405nm; 15.3 log photons/cm^2/s) and local light flashes (100ms, 465nm; ~600mW/mm^2 at fibre tip) across the LGN (Figure 4.4). As expected, while high amplitude visual responses were present across the entirety of the LGN (Figure 4.4, B), responses to optogenetic activation of GABA neurons were much larger at recordings sites located in the IGL/vLGN region (Figure 4.4, C).

An important consideration in using optogenetic-based cell identification strategies is that these require high light levels (See Häusser (2014) for review). Our identification of robust responses to intraneural light delivery suggests our stimuli were easily sufficient to drive optogenetic responses, even at recording sites most distant from the optical fibre (Figure 4.4). Nonetheless, we were keen to directly confirm that, under our experimental conditions, anatomical variations in light penetration did not bias our identification of GABAergic cells in any way. To this end, we utilised the precise geometry of our optrode arrays to calculate mean response amplitude to our optogenetic stimuli as a function of distance from the fibre tip. To account for difference in GABA neuron number, we analysed these data separately for recording sites predicted to lie within the IGL/vLGN (n=74) and the dLGN (n=34) regions.

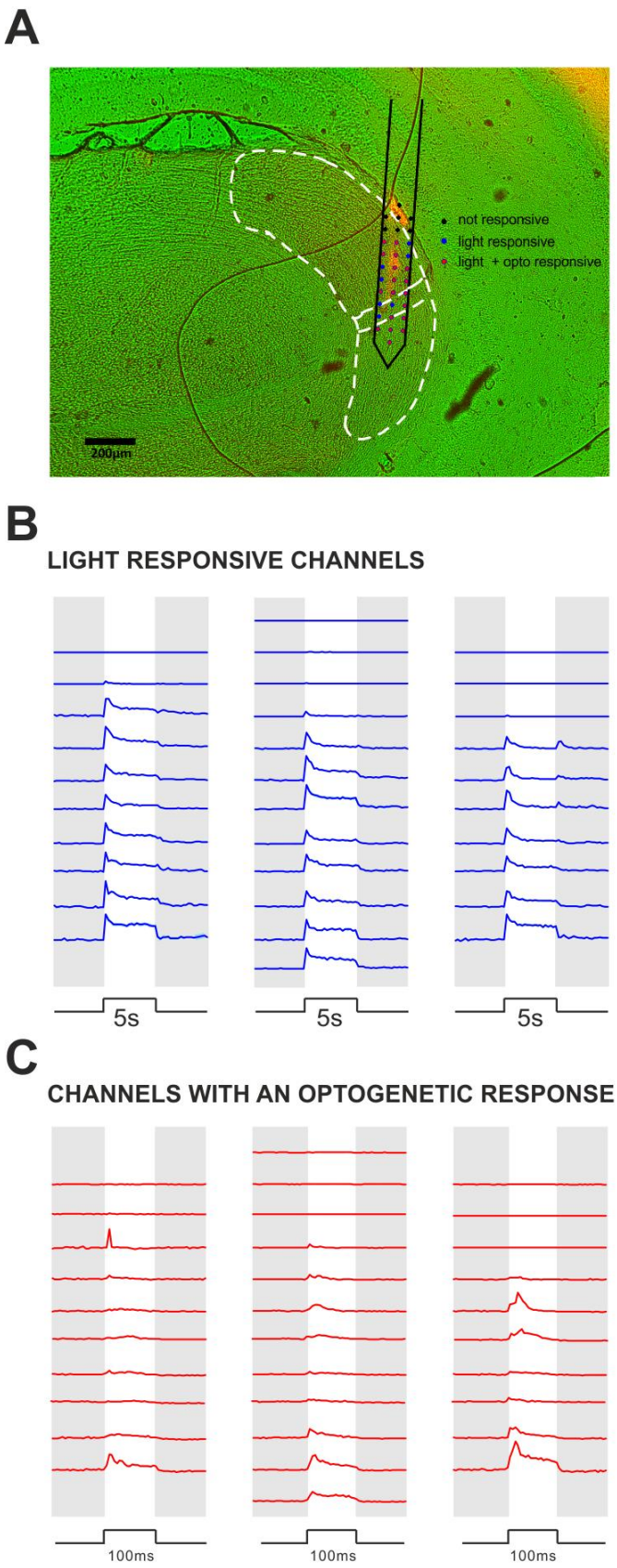

Figure 4.4: The locations of optogenetic and light responsive multiunit channels within the visual thalamus.

An example experiment, highlighting the position of the 32 electrode sites within dLGN and IGL/vLGN regions (A). Blue circles correspond to sites that show a response to a 5s full field light flash. Red circles with blue outline correspond to channels that respond to both a 5s light stimulation and a 100ms optogenetic pulse. Black channels did not respond to any of the stimuli. Light responses are shown in B, and optogenetic responses are shown in C. We were unable to identify any non-light responsive channels that responded to optogenetic stimulation.

Analysed in this manner, we could not detect any obvious relationship between anatomical distance from the fibre tip and response amplitude in either the IGL/vLGN (Figure 4.5, A) or dLGN (Figure 4.5, B). We conclude then that our stimuli are sufficiently bright to reliably activate GABA neurons, even when these are located 600µm distal from our optical fibre and/or we apply very brief (10ms) light steps (Figure 4.5, C). As indicated above, however, we did find that optogenetically evoked spiking response were reliably larger in the IGL/vLGN vs. dLGN (Figure 4.5, D). Thus, while response amplitude increased as a function of flash duration in both regions, average response amplitudes were 2-3 times higher in the IGL/vLGN, in line with the lower proportion of GABA cells in the dLGN.

Having established that our optogenetic stimuli robustly activate GABAergic neurons, we next set out to specifically evaluate the sensory properties of IGL/vLGN GABA cells. From our multiunit recordings at electrode sites within or neighbouring the IGL/vlGN region we were able to isolate 30 single units. All of these cells responded to visual stimuli (Figure 4.6, B&C: left) and 21/30 (70%) were also responsive to optogenetic stimulation ('GABA+'; Figure 4.6, C: bottom), consistent with the high proportion of GABA-expressing neurons in the IGL/vLGN. Of note, cells lacking optogenetic responses were typically detected intermingled with other neurons that robustly responded to optogenetic activation. As expected based on our previous work (Howarth et al., 2014), all but one of these cells exhibited monocular responses driven by the contralateral retina (one GABA+ cell displayed binocular responses). The vast majority of monocular cells (23/29) exhibited sustained responses to illumination of the contralateral eye. The remaining 6 neurons exhibited excitatory responses to both steps up and steps down in light intensity (ON/OFF responses).

In response to cone-isolating stimuli, we observed heterogeneity among IGL/vLGN cell populations (Figure 4.6, D). Thus a subset of both GABA+ and GABA- cells lacked detectable response to all these stimuli (n=8/21 and 1/9 respectively) suggesting that either their sensitivity to full field changes in illumination is low or that such cells exclusively receive rod inputs. Among the remaining cells, we also observed substantial variability in the relative magnitude of responses to M vs. S-opsin stimulation, with all cells exhibiting at least some response to M-opsin isolating stimuli. In addition, we found very little evidence

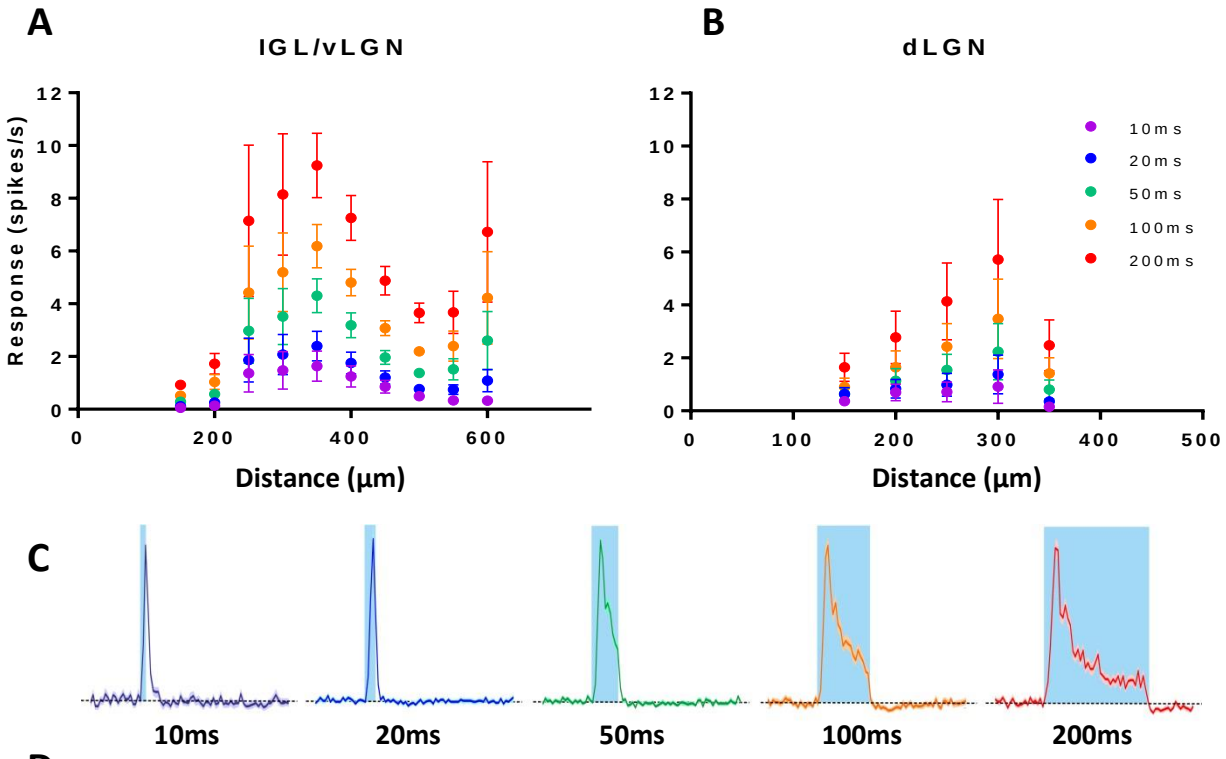

Figure 4.5: The magnitude of optogenetic responses within the IGL/vLGN region does not vary in accordance to their distance from the tip of the optical fibre.

Mean±SEM response of all multiunit channels (n=111 channels) within the IGL/vLGN (n=74 channels) and dLGN (n=37) thalamic regions. The amplitude of optogenetic responses within the IGL/vLGN (A) remains substantial at sites near the tip of the electrode (600µm). Within the dLGN (B), responses are substantial at all distances measured. (C) Example multiunit channel responses to optogenetic stimuli of various durations (10, 20, 50 100 and 200ms; represented by the blue shaded areas) at a distance of 600µm from the fibre optic tip are shown in (D). The amplitude of responses within the IGL/vLGN region are significantly higher than the LGN at all durations of stimuli >10ms. **=p<0.01, ***=p<0.001, ****=p<0.0001.

for direct chromatic response across the IGL/vLGN region. Indeed, just 1 cell (GABA-ve) displayed colour-opponent responses (S-ON/M-OFF). Together then, these data indicate that IGL/vLGN cells primarily convey achromatic signals and receive little input from the 'primordial' S-cones that appear to be important for responses in other non-image forming nuclei such as the OPN (Allen et al., 2011).

4.5 Discussion

Here we describe and validate a silent substitution approach that allows for selective modulation of cone photoreception in mice. These findings build on our previous application of this technology in mice with altered cone sensitivity (Walmsley et al., 2015), facilitating application of this important new tool alongside the full mouse genetic toolbox for mapping the neural circuits. Accordingly, here we apply this technique alongside optogenetic-based identification of GABA neurons in the IGL/vLGN to show that the majority of cells in this thalamic component of the extended circadian system convey achromatic signals derived from M-/S-opsin co-expressing cones.

One of the key questions arising from our previous report that colour influences circadian timing (Walmsley et al., 2015) was whether SCN neurons received colour opponent input directly from the retina or via indirect inputs from the thalamus. In fact, we found that colour-opponent responses were extremely rare within the IGL/vLGN (<5% of the cells we recorded). Moreover the one colour sensitive cell we detected in the vLGN in fact lacked optogenetic responses, suggesting it was unlikely to form part of the GABAergic projection to the SCN (Moore and Speh, 1993). Accordingly we think it unlikely that colour sensitive responses in the SCN are directly driven by the geniculohypothalamic projection. On the other hand, we cannot at present rule out the possibility that the M-OFF component of SCN chromatic responses derives from inhibitory GABAergic input from IGL/vLGN cells. Indeed, across our sample we found a substantial proportion of M-opsin biased GABA+ neurons in these regions.

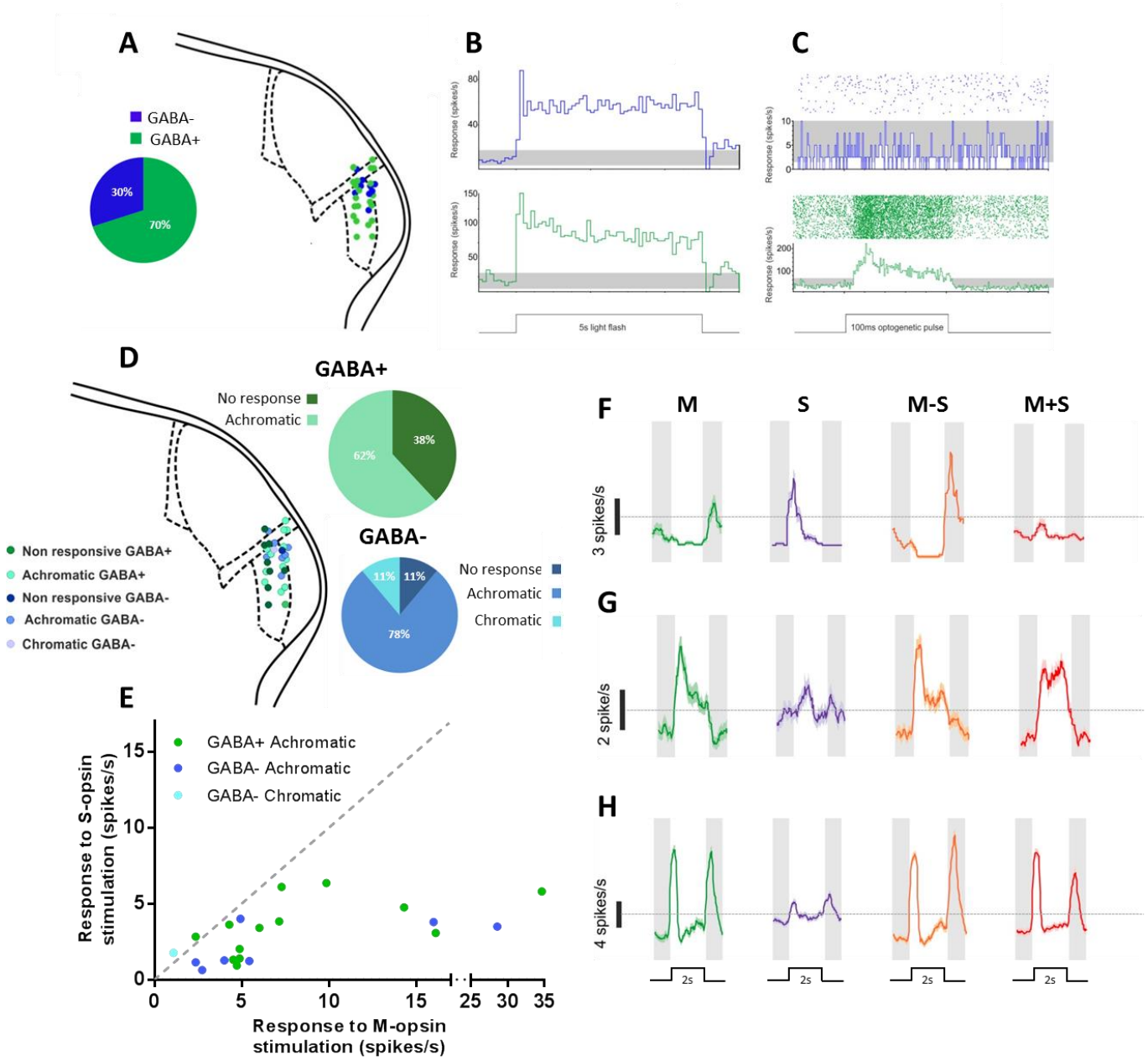

Figure 4.6: The locations of optogenetic and light responsive single neurons within the IGL/LGN.

Light responsive single neurons (n=30) fall into one of two categories: cells that respond to light but not optogenetic stimuli (blue; n=9) and cells that respond to both light and optogenetic stimulation (green; n=21). The locations of these neurons within the visual thalamus are shown in A. Example responses of each of the cell types to a 5s binocular light stimulus are shown as a histogram in B. Responses to a 100ms optogenetic pulse are shown as raster plots with associated histograms in C. A neuron that responds to only photic stimulation is shown in blue (B&C; top) and a neuron that responds to both photic and optogenetic stimuli is shown in green (B&C; bottom). There is no association between the location of a light responsive cell and its response to metameric stimuli (D). GABA+ (n=21) cells consist of 2 subpopulations: 62% are achromatic (exhibit 'ON' responses to M- and/or S-opsin) whilst the remaining 38% do not respond to metameric stimuli. For GABA- cells (n=9): 1 cell did not respond to metameric stimuli, 7/9 exhibited achromatic responses and 1 cell exhibited chromatic (colour-opponent) responses. Across the IGL/vLGN region the majority of cells exhibit greater responses to the stimulation of M-opsin than S-opsin (E). This can also be seen on individual cell basis (F-G). The one chromatic cell (F) and two achromatic cells (G&H) are shown as example responses. Within the IGL/vLGN region a large proportion of neurons exhibit excitatory responses to both steps up and steps down in light intensity (H).

It is also worth noting here that both the SCN and IGL/vLGN are heavily targeted by M1-type mRGCs (Hattar et al., 2006). Indeed, at least some of the same cells that target the SCN also project to the IGL (Morin et al., 2003). On that basis, the very low proportion of colour sensitive cells we identify here relative to the SCN (~25%) suggests that colour responses are unlikely to originate within M1 mRGCs. Consistent with that view, previous direct investigations of mouse mRGCs did not find evidence for colour opponent responses (Weng et al., 2013). Together then we suspect that if circadian responses to colour originate entirely within the retina this involves a rare subtype of mRGC that targets the SCN but provides little input to the IGL/vLGN. This situation would thus reflect a substantive difference relative to previous suggestions that mRGC projections to the primate LGN convey chromatic information (Dacey et al., 2005).

Insofar as our cone-isolating stimuli rely on the use of high background light levels to silence rods, our use of coneless mice here also constitutes an important source of information about the conditions under which this requirement is met. A somewhat surprising outcome of these experiments was that we found evidence that rod responses appear in a subset of LGN cells following lengthy (>30min) adaptation to a bright background light. Previous work suggests that rod responses typically saturate at light levels 1-2 orders of magnitude lower than the background light (10^{14} photons/cm^2/s) we employed here (Pang et al., 2004). Consistent with these findings, previous applications of the silent substitution approach under broadly similar background light levels did not detect substantial evidence of rod-derived responses to relatively high contrast (~67%) stimuli (Brown et al., 2012). We assume this relates to differences in stimulus protocols, since this earlier study did not monitor responses for such extended epochs as those used here.

On balance then, while we confirm that our approach can be used to effectively isolate M- and S-opsin derived signals, we recommend that the possibility of rod intrusion be carefully considered if the experimental protocol differs substantially from that used here. In line with this view, previous work indicates that the experimentally determined saturation point for rods is substantially influenced depending upon experimental conditions (Azevedo and Rieke, 2011), prior light exposure (Adelson, 1982) and according to the species studied

(Nakatani et al., 1991). Most importantly, there is in fact good evidence to suggest that rods are capable of responding under any level of illumination following sufficient adaptation (Naarendorp et al., 2001, Szikra et al., 2014). For example, while severely attenuated, some visually-guided navigation persists in mice without functional cone phototransduction under light levels 10 x brighter than those used here (Nathan et al., 2006). Accordingly, maintaining effective rod contrasts as low as is practical is a key consideration for the effective use of cone-isolating stimuli.

A second factor to consider when interpreting data generated using cone-isolating stimuli relates to interpreting a lack of response. For example, here we identified a sizeable proportion of IGL/vLGN cells (33%) that did not exhibit reliable changes in firing rate to any of our cone-isolating stimuli (but did respond to light steps under dark adapted conditions). In principle there are two explanations for such data, either such cells receive input solely from rods or their contrast sensitivity (at least for full field steps) is very low. In this regard it is worth noting that, based on published data for spatially patterned stimuli, the contrasts applied here (63%) should be sufficient to evoke very robust responses from all LGN cells (Grubb and Thompson, 2003). Contrast sensitivity has not, to our knowledge, been extensively investigated for full field stimuli, although our previous work (Howarth et al., 2014) suggests this may be substantially lower than for the patterned stimuli mentioned above. Modifications to our approach to increase effective contrast (by adding 1 or more wavelengths) and/or to produce photoreceptor-isolating spatial patterns (e.g. Allen et al., 2014) are certainly achievable, however, providing a means of addressing this question where necessary.

In summary, we have developed and validated a silent-substitution based approach enabling selective modulation of individual cone opsins in the wildtype retina. In combination with the sophisticated mouse genetic tools now available, this approach should prove highly useful in dissecting the organisation and properties of visual pathways responsible for chromatic processing in the mammalian brain and retina.

4.6 References

ADELSON, E. H. 1982. Saturation and adaptation in the rod system. *Vision Res,* 22**,** 1299-312.

ALLEN, A. E., BROWN, T. M. & LUCAS, R. J. 2011. A distinct contribution of short-wavelength-sensitive cones to light-evoked activity in the mouse pretectal olivary nucleus. *J Neurosci,* 31**,** 16833-43.

ALLEN, A. E., STORCHI, R., MARTIAL, F. P., PETERSEN, R. S., MONTEMURRO, M. A., BROWN, T. M. & LUCAS, R. J. 2014. Melanopsin-driven light adaptation in mouse vision. *Curr Biol,* 24**,** 2481-90.

AZEVEDO, A. W. & RIEKE, F. 2011. Experimental protocols alter phototransduction: the implications for retinal processing at visual threshold. *J Neurosci,* 31**,** 3670-82.

BROWN, T. M., ALLEN, A. E., AL-ENEZI, J., WYNNE, J., SCHLANGEN, L., HOMMES, V. & LUCAS, R. J. 2013. The melanopic sensitivity function accounts for melanopsin-driven responses in mice under diverse lighting conditions. *PLoS One,* 8**,** e53583.

BROWN, T. M., GIAS, C., HATORI, M., KEDING, S. R., SEMO, M., COFFEY, P. J., GIGG, J., PIGGINS, H. D., PANDA, S. & LUCAS, R. J. 2010. Melanopsin contributions to irradiance coding in the thalamo-cortical visual system. *PLoS Biol,* 8**,** e1000558.

BROWN, T. M., TSUJIMURA, S., ALLEN, A. E., WYNNE, J., BEDFORD, R., VICKERY, G., VUGLER, A. & LUCAS, R. J. 2012. Melanopsin-based brightness discrimination in mice and humans. *Curr Biol,* 22**,** 1134-41.

BROWN, T. M., WYNNE, J., PIGGINS, H. D. & LUCAS, R. J. 2011. Multiple hypothalamic cell populations encoding distinct visual information. *J Physiol,* 589**,** 1173-94.

CALDERONE, J. B. & JACOBS, G. H. 1995. Regional variations in the relative sensitivity to UV light in the mouse retina. *Vis Neurosci,* 12**,** 463-8.

DACEY, D. M., LIAO, H. W., PETERSON, B. B., ROBINSON, F. R., SMITH, V. C., POKORNY, J., YAU, K. W. & GAMLIN, P. D. 2005. Melanopsin-expressing ganglion cells in primate retina signal colour and irradiance and project to the LGN. *Nature,* 433**,** 749-54.

ECKER, J. L., DUMITRESCU, O. N., WONG, K. Y., ALAM, N. M., CHEN, S. K., LEGATES, T., RENNA, J. M., PRUSKY, G. T., BERSON, D. M. & HATTAR, S. 2010. Melanopsin-expressing retinal ganglion-cell photoreceptors: cellular diversity and role in pattern vision. *Neuron,* 67**,** 49-60.

GOVARDOVSKII, V. I., FYHRQUIST, N., REUTER, T., KUZMIN, D. G. & DONNER, K. 2000. In search of the visual pigment template. *Vis Neurosci,* 17**,** 509-28.

GRUBB, M. S. & THOMPSON, I. D. 2003. Quantitative characterization of visual response properties in the mouse dorsal lateral geniculate nucleus. *J Neurophysiol,* 90**,** 3594-607.

HAMMER, S., CARRILLO, G. L., GOVINDAIAH, G., MONAVARFESHANI, A., BIRCHER, J. S., SU, J., GUIDO, W. & FOX, M. A. 2014. Nuclei-specific differences in nerve terminal distribution, morphology, and development in mouse visual thalamus. *Neural Dev,* 9**,** 16.

HARRINGTON, M. & RUSAK, B. 1989. Photic responses of geniculo-hypothalamic tract neurons in the Syrian hamster. *Visual Neuroscience,* 2.

HARRINGTON, M. E. 1997. The ventral lateral geniculate nucleus and the intergeniculate leaflet: interrelated structures in the visual and circadian systems. *Neurosci Biobehav Rev,* 21**,** 705-27.

HATTAR, S., KUMAR, M., PARK, A., TONG, P., TUNG, J., YAU, K. W. & BERSON, D. M. 2006. Central projections of melanopsin-expressing retinal ganglion cells in the mouse. *J Comp Neurol,* 497**,** 326-49.

HOWARTH, M., WALMSLEY, L. & BROWN, T. M. 2014. Binocular integration in the mouse lateral geniculate nuclei. *Curr Biol,* 24**,** 1241-7.
HUBERMAN, A. D. & NIELL, C. M. 2011. What can mice tell us about how vision works? *Trends Neurosci,* 34**,** 464-73.
HÄUSSER, M. 2014. Optogenetics: the age of light. *Nat Methods,* 11**,** 1012-4.
JACOBS, G. H. 2013. Losses of functional opsin genes, short-wavelength cone photopigments, and color vision--a significant trend in the evolution of mammalian vision. *Vis Neurosci,* 30**,** 39-53.
JACOBS, G. H. & WILLIAMS, G. A. 2007. Contributions of the mouse UV photopigment to the ERG and to vision. *Doc Ophthalmol,* 115**,** 137-44.
LALL, G. S., REVELL, V. L., MOMIJI, H., AL ENEZI, J., ALTIMUS, C. M., GULER, A. D., AGUILAR, C., CAMERON, M. A., ALLENDER, S., HANKINS, M. W. & LUCAS, R. J. 2010. Distinct contributions of rod, cone, and melanopsin photoreceptors to encoding irradiance. *Neuron,* 66**,** 417-28.
MADISEN, L., MAO, T., KOCH, H., ZHUO, J. M., BERENYI, A., FUJISAWA, S., HSU, Y. W., GARCIA, A. J., GU, X., ZANELLA, S., KIDNEY, J., GU, H., MAO, Y., HOOKS, B. M., BOYDEN, E. S., BUZSÁKI, G., RAMIREZ, J. M., JONES, A. R., SVOBODA, K., HAN, X., TURNER, E. E. & ZENG, H. 2012. A toolbox of Cre-dependent optogenetic transgenic mice for light-induced activation and silencing. *Nat Neurosci,* 15**,** 793-802.
MATURANA, H. R. & VARELA, F. J. 1982. Color-opponent responses in the avian lateral geniculate: a study in the quail (Coturnix coturnix japonica). *Brain Res,* 247**,** 227-41.
MOORE, R. Y. & SPEH, J. C. 1993. GABA is the principal neurotransmitter of the circadian system. *Neurosci Lett,* 150**,** 112-6.
MORIN, L. P., BLANCHARD, J. H. & PROVENCIO, I. 2003. Retinal ganglion cell projections to the hamster suprachiasmatic nucleus, intergeniculate leaflet, and visual midbrain: bifurcation and melanopsin immunoreactivity. *J Comp Neurol,* 465**,** 401-16.
NAARENDORP, F., SATO, Y., CAJDRIC, A. & HUBBARD, N. P. 2001. Absolute and relative sensitivity of the scotopic system of rat: electroretinography and behavior. *Vis Neurosci,* 18**,** 641-56.
NAKATANI, K., TAMURA, T. & YAU, K. W. 1991. Light adaptation in retinal rods of the rabbit and two other nonprimate mammals. *J Gen Physiol,* 97**,** 413-35.
NATHAN, J., REH, R., ANKOUDINOVA, I., ANKOUDINOVA, G., CHANG, B., HECKENLIVELY, J. & HURLEY, J. B. 2006. Scotopic and photopic visual thresholds and spatial and temporal discrimination evaluated by behavior of mice in a water maze. *Photochem Photobiol,* 82**,** 1489-94.
PANG, J. J., GAO, F. & WU, S. M. 2004. Light-evoked current responses in rod bipolar cells, cone depolarizing bipolar cells and AII amacrine cells in dark-adapted mouse retina. *J Physiol,* 558**,** 897-912.
PAXINOS, G. & FRANKLIN, K. 2001. *The Mouse Brain in Stereotaxic Coordinates,* San Diego, Academic Press.
PAXINOS, G. F., K.B.J. 2001. *The mouse brain in stereotaxic coordinates: Second Edition,* San Diego, Academic Press.
PROCYK, C. A., ELEFTHERIOU, C. G., STORCHI, R., ALLEN, A. E., MILOSAVLJEVIC, N., BROWN, T. M. & LUCAS, R. J. 2015. Spatial receptive fields in the retina and dorsal lateral geniculate nucleus of mice lacking rods and cones. *J Neurophysiol,* 114**,** 1321-30.
SMALLWOOD, P. M., OLVECZKY, B. P., WILLIAMS, G. L., JACOBS, G. H., REESE, B. E., MEISTER, M. & NATHANS, J. 2003. Genetically engineered mice with an additional class of cone photoreceptors: implications for the evolution of color vision. *Proc Natl Acad Sci U S A,* 100**,** 11706-11.
SODEN, M. E., GORE, B. B. & ZWEIFEL, L. S. 2014. Defining functional gene-circuit interfaces in the mouse nervous system. *Genes Brain Behav,* 13**,** 2-12.

STORCHI, R., MILOSAVLJEVIC, N., ELEFTHERIOU, C. G., MARTIAL, F. P., ORLOWSKA-FEUER, P., BEDFORD, R. A., BROWN, T. M., MONTEMURRO, M. A., PETERSEN, R. S. & LUCAS, R. J. 2015. Melanopsin-driven increases in maintained activity enhance thalamic visual response reliability across a simulated dawn. *Proc Natl Acad Sci U S A,* 112**,** E5734-43.

SZIKRA, T., TRENHOLM, S., DRINNENBERG, A., JÜTTNER, J., RAICS, Z., FARROW, K., BIEL, M., AWATRAMANI, G., CLARK, D. A., SAHEL, J. A., DA SILVEIRA, R. A. & ROSKA, B. 2014. Rods in daylight act as relay cells for cone-driven horizontal cell-mediated surround inhibition. *Nat Neurosci,* 17**,** 1728-35.

SZÉL, A., RÖHLICH, P., CAFFÉ, A. R., JULIUSSON, B., AGUIRRE, G. & VAN VEEN, T. 1992. Unique topographic separation of two spectral classes of cones in the mouse retina. *J Comp Neurol,* 325**,** 327-42.

TANIGUCHI, H., HE, M., WU, P., KIM, S., PAIK, R., SUGINO, K., KVITSIANI, D., KVITSANI, D., FU, Y., LU, J., LIN, Y., MIYOSHI, G., SHIMA, Y., FISHELL, G., NELSON, S. B. & HUANG, Z. J. 2011. A resource of Cre driver lines for genetic targeting of GABAergic neurons in cerebral cortex. *Neuron,* 71**,** 995-1013.

WALMSLEY, L., HANNA, L., MOULAND, J., MARTIAL, F., WEST, A., SMEDLEY, A. R., BECHTOLD, D. A., WEBB, A. R., LUCAS, R. J. & BROWN, T. M. 2015. Colour as a signal for entraining the mammalian circadian clock. *PLoS Biol,* 13**,** e1002127.

WENG, S., ESTEVEZ, M. E. & BERSON, D. M. 2013. Mouse ganglion-cell photoreceptors are driven by the most sensitive rod pathway and by both types of cones. *PLoS One,* 8**,** e66480.

Chapter 5: Influence of the Intergeniculate leaflet on SCN light responses

5.1 Abstract

Information about the spectral composition ('colour') and amount ('brightness') of external illumination form important temporal cues used by mammals to synchronise their circadian system to the environment. Visual information reaches the master circadian pacemaker, the suprachiasmatic nucleus (SCN), both directly via the retinohypothalamic tract and indirectly via intergeniculate leaflet (IGL) cells forming the geniculohypothalamic tract (GHT). At present, however, the contribution of GHT inputs to the colour and/or brightness coding properties of SCN neurons are unknown. To investigate this issue, we performed *in vivo* electrophysiological recordings from the SCN of anaesthetised mice in conjunction with electrical stimulation or pharmacological inhibition (via local muscimol injection) of GHT activity.

Electrical stimulation of the IGL region drove inhibitory responses that were almost exclusively restricted to regions of the hypothalamus displaying visual responses. Subsequent analysis of single cell responses indicated that both colour sensitive and non-colour sensitive SCN cells received inhibitory input via the GHT. Moreover, unilateral inactivation of the IGL and surrounding visual thalamus increased responses of the SCN to stimulation of the opposing (contralateral) eye alongside a significant increase in baseline firing rate. Of note, we also found evidence that S-opsin driven responses were preferentially enhanced relative to those originating with L-opsin following removal of GHT inputs. By contrast, ipsilateral visual responses and light evoked activity of contralateral SCN were largely unaffected by these manipulations. Together these data indicate that GHT afferents convey inhibitory visual signals to the ipsilateral SCN, primarily originating with crossed retinal projections.

5.2 Introduction

Photic information from the environment is transmitted to the SCN via two distinct pathways. The principal pathway for light input is the retinohypothalamic tract (RHT), which transmits photic information from intrinsically photosensitive retinal ganglion cells (ipRGCs) in the retina directly to the SCN (Morin et al., 2003). The SCN can also receive visual signals indirectly via intergeniculate leaflet (IGL) cells that form the geniculohypothalamic tract (GHT) (Moore and Card, 1994). The GHT originates in neurons throughout the IGL (Card and Moore, 1989), providing a primarily ipsilateral monosynaptic projection to the SCN (Harrington and Rusak, 1989, Card and Moore, 1989). In mice, both RHT and GHT terminal fields are found intermingled throughout the SCN (Morin and Blanchard, 2001, Morin et al., 2006, Morin, 2013), suggesting that individual SCN cells may integrate both direct and indirect visual signals.

In line with a functional role for the GHT in regulating the circadian photoentrainment, lesions to the IGL inhibit the period lengthening effects of constant light (Harrington and Rusak, 1986). IGL-lesioned hamsters also exhibit smaller phase advances and larger phase delays to photic stimulation (Pickard et al., 1987), and lengthened free-running periods in constant darkness (DD) (Pickard, 1994). Taken together, these data indicate that while GHT input is not essential for photoentrainment, IGL neurons certainly appear to play a modulatory role in circadian responses to light.

Consistent with anatomical data indicating dense ipRGC projections to the IGL (Hattar et al., 2006), electrophysiological studies have shown that many IGL neurons exhibit sustained ON responses to retinal illumination, indicating that they encode irradiance (Harrington and Rusak, 1989, Howarth et al., 2014). IGL neurons are also known to exhibit various kinds of binocular interaction, including the presence of cells that selectively respond to interocular differences in irradiance (Harrington and Rusak, 1989, Howarth et al., 2014). Moreover, previous work suggests that a subset of IGL neurons in birds are colour sensitive (Maturana and Varela, 1982), and our recent work (see chapter 4) indicates that this is also true of at least some mouse IGL cells. It is clear then that IGL neurons are a heterogeneous population with respect to their sensory properties (Harrington, 1997).

In line with the functional heterogeneity outlined above, IGL neurons are also neuroanatomically diverse, innervating a large number of other brain nuclei and expressing a number of different neuromodulators (Harrington, 1997, Morin, 2013). Although the precise relationship between functional and neuroanatomical properties of IGL cells is still poorly defined, a major population of cells forming the GHT co-express neuropeptide Y (NPY) and GABA (Moore and Speh, 1993). Both GABA (Wagner et al., 1997, De Jeu and Pennartz, 2002, Choi et al., 2008) and NPY (Mason et al., 1987, Liou and Albers, 1991) have been reported to exert mixed inhibitory/excitatory effects on SCN neurons, although electrical stimulation studies suggest that the GHT exerts a predominantly inhibitory influence on SCN firing activity (Roig et al., 1997). Unfortunately, the nature of the sensory signals supplied to the SCN via NPY cells is unknown. Thus, there are conflicting reports as to whether NPY-expressing neurons in the IGL actually receive direct retinal input (Thankachan and Rusak, 2005, Morin, 2013, Takatsuji et al., 1991). Moreover, NPY cells in the IGL reportedly lack light-induced c-Fos expression (Juhl et al., 2007). In contrast, studies using antidromic activation have indicated at least some SCN-projecting IGL cells are light sensitive, although it is unclear if these are NPY cells or precisely what kind of signals they send to the SCN (Blasiak and Lewandowski, 2013, Zhang and Rusak, 1989).

A second subset of IGL neurons project to the contralateral IGL and can be distinguished from SCN-projecting neurons by their expression the neurotransmitter Enkephalin (ENK) (Moore and Speh, 1993, Blasiak and Lewandowski, 2013). Existing work suggests that the visual response properties of these geniculogeniculate-projecting cells may differ from those of IGL cells that project to the SCN (Blasiak and Lewandowski, 2013). These data thus provide a further indication that the functional heterogeneity in IGL visual responses (discussed above) reflects cells with differing anatomical connectivity/functional roles. Importantly, however, these data also then indicate that it is impossible to infer what kinds of signals the GHT might send to the SCN simply by investigating the sensory properties of IGL neurons. Moreover, since none of the previous studies targeting specific IGL-cell populations have investigated their sensory properties in any detail, the contribution of GHT inputs to SCN light responses is still essentially unknown. In light of this uncertainty regarding how GHT input contributes to visual processing in the SCN, here we set out to investigate this question directly using a combination of electrical stimulation and pharmacological inhibition of GHT activity. By using these approaches alongside a

comprehensive characterisation of SCN sensory properties, we hoped to define the extent to which colour and/or brightness coding properties in the SCN are modulated by visual signals originating from the GHT.

5.3 Methods

5.3.1 Animals

All animal use was in accordance with the Animals (Scientific Procedures) Act of 1986 (United Kingdom). Experiments were performed on adult male wild-type mice (C57BL/6J background) under urethane anaesthesia. Before surgery, mice were housed under a 12-h dark/light cycle at a temperature of 22°C with food and water available ad libitum.

5.3.2 *in vivo* electrophysiology

Mice were anaesthetised by intraperitoneal injection of urethane (1.5 g/kg) and placed into a stereotaxic frame (SR-15M; Narishage International) to hold the skull fixed in place for surgery. The surface of the skull was exposed using a scalpel incision and 2 holes were drilled using stereotaxic co-ordinates (0.95mm lateral to and 0.3mm posterior to Bregma for SCN probe; 2.3 mm lateral to and 3.5mm posterior to Bregma for IGL probe) obtained from the stereotaxic mouse atlas (Paxinos and Franklin, 2001). Pupils were dilated with 1% atropine (Sigma-Aldrich, Dorset, UK) and mineral oil (Sigma-Aldrich, Dorset, UK) added to prevent drying of the cornea.

A recording probe (Buszaki 32L; Neuronexus, MI, US) consisting of four shanks (spaced 200µm), each with eight closely spaced recordings sites in diamond formation (intersite distance 20–34µm) was coated with fluorescent dye (CM-DiI; Invitrogen, Paisley, UK) and then inserted into the brain 0.95 mm lateral and 0.3 mm caudal to bregma at an angle of 9° relative to the dorsal-ventral axis, to target the SCN.

A second electrode was then inserted into the brain 2.3mm lateral and 3.5mm caudal to bregma at an angle of 16° relative to the dorsal-ventral axis to target the IGL-region. For experiments involving pharmacological manipulation of GHT activity, this was a recording electrode with attached drug cannula (E16-20mm-100-177; Neuronexus, MI, US). In stimulation experiments, the second probe was a stimulation electrode (A4x4-4mm-200-200-1250; Neuronexus, MI, US) consisting of four shanks (spaced 200µm), each with four stimulation sites (intersite distance 200µm). Electrodes were then lowered to the levels of the SCN and IGL using a fluid-filled micromanipulator (MO-10, Narishige International Ltd., London, UK).

After allowing 30 min for neural activity to stabilise following probe insertion, wideband neural signals were acquired using a Recorder64 system (Plexon, TX, US), amplified (x3000) and digitized at 40 kHz. Throughout the experiment, the animals temperature was maintained at 37˚C using a homeothermic mat (Harvard Apparatus, UK).

5.3.2.1 Pharmacological inhibition of the visual thalamus using muscimol

For these experiments, the drug cannula attached to the recording probe was connected to a syringe filled with muscimol (1mM; Sigma-Aldrich, Dorset, UK). Muscimol was injected through the cannula into the IGL at a rate of 1µl/min, a minute at a time using a pump (Harvard Apparatus, Cambridge, UK). In order to be confident that GHT activity was robustly inhibited by this manipulation, between infusions, a 2s light step was used to verify response magnitude across the visual thalamus. This was process was repeated 2-4 times until no light responses were detected at any recording sites. We thus provided relatively large drug injections predicted to encompass the majority of the lateral geniculate nuclei. Visual stimuli were given before and after muscimol infusion to allow comparison.

5.3.2.2 Electrical stimulation

Electrical stimuli consisted of a biphasic bipolar square wave pulse (100µV/100µs per phase), generated by a PlexStim 2.0 stimulation box (Plexon, TX, US) and controlled via a custom written program in LabVIEW (National Instruments, TX, USA).

Stimulation sites on the electrode are large (1250µm^2) and were activated to increase their conductance of current before each experiment by the application of an iridium oxide coating to the electrode surface (niPOD, Neuronexus). After placement of the probe, the current output of each channel was monitored to ensure that all of the channels used to deliver the stimuli were capable of delivering the correct amount of current. Typically groups of channels were used as positive and negative poles for the stimulus (4 sites each), to allow the conductance of stimulating current across large areas of the visual thalamus.

5.3.3 Visual Stimuli

Light measurements for both eye-specific and cone-isolating stimuli were performed using a calibrated spectroradiometer (Bentham instruments, Reading, UK).

5.3.3.1 Eye-specific stimuli

Full field visual stimuli were generated via two LEDs (λmax 410nm; half-width: ±7nm; Thorlabs, NJ, USA) independently controlled via LabVIEW (National Instruments, TX, USA) and neutral density filter wheels (Thorlabs). Light was supplied to the subject via 7mm diameter flexible fibre optic light guides (Edmund Optics; York, UK), positioned 5mm from each eye and enclosed within internally reflective plastic cones that fit snugly over each eye to prevent off-target effects due to scattered light.

To determine the relative magnitude and sensitivity of eye specific responses in SCN neurons, mice were maintained in darkness and 5s light steps were applied in an interleaved fashion to contra- and/or ipsilateral eyes for a total of 10 repeats at logarithmically increasing intensities spanning 11.8-15.8 log photons/cm^2/s (interstimulus interval 20s). Because all mouse photoreceptors display similar sensitivity to the wavelengths contained in our stimuli (Brown et al., 2013, Brown et al., 2012), after correction for pre-receptoral filtering (Govardovskii et al., 2000, Jacobs and Williams, 2007), effective photon fluxes for each mouse opsin were between 0.5 (M- and S-cone opsins) and 0.3 log units (melanopsin) dimmer than this value. Intensities reported in the manuscript reflect effective irradiance for rod opsin, which is intermediate between these extremes (11.4-15.4 log photons/cm^2/s).

5.3.3.2 Cone-isolating visual stimuli

To assess the chromatic input to the SCN, metameric stimuli were designed that selectively modulates the activation of M- and S- opsins individually, in tandem and in antiphase and lacked any effective change in melanopsin and rod excitation.

Cone-isolating stimuli were generated using independently controlled red (λmax: 617nm), blue (λmax: 470nm) and ultraviolet (UV) (λmax: 405nm) LEDs. The intensity of the three LEDs was controlled using custom-written programs in LabView 8.6 (National Instruments). The stimuli were delivered from a background as a 0.25Hz square-wave stimulus. The stimulus consisted of 2s step up in light intensity from a 'dim' condition (background) to a 'bright' condition (stimulus). Irradiance for the stimulated cone opsins was varied by ±63%, to produce an overall 4.4 fold increase in intensity between 'bright' and 'dim' phases. A stimulus that activates all photoreceptors simultaneously (energy steps; ±63%) was also included. The effective photon fluxes of each of these stimuli have been reported previously (Table 4.1).

5.3.4 Histology

At the end of each experiment the brain was removed and post-fixed in 4% paraformaldehyde overnight and then cryoprotected in 30% sucrose. The following day, brains were sectioned at 100µm on a freezing sledge microtome and mounted onto slides using Vectashield (Vectorlaboratories Ltd., Peterbourogh, UK).

After mounting, DiI-labelled probe placements were visualised under a fluorescent microscope (Olympus BX51) with appropriate filter sets. Resulting images were then compared with appropriate stereotaxic atlas figures (Paxinos, 2001) to verify appropriate SCN and LGN probe placement.

5.4 Results

5.4.1 Influence of GHT stimulation on SCN activity

In order to determine the functional impact of GHT input to the SCN, we first applied electrical microstimulation to the IGL region of a subset (n=7) of mice. Visual stimuli (full field light steps) were then used to classify the responses of these cells.

In total, we identified light-dependent changes in firing at 130/224 recording sites located in and around the SCN (Figure 5.1, A: left). Out of these light-responsive multiunit recording sites, 16% (n=21) also showed changes in firing activity following IGL microstimulation, with the vast majority (20/21) exhibiting inhibitory responses (Figure 5.1, B). Thus, only 1 multiunit recording site showed increased firing in response to GHT activation (Figure 5.1, C). The remainder of our recordings (94 sites) were located in the periSCN region but did not respond to any of our light stimuli (Figure 5.1, A: right) so indicating that the neighbouring cells were very unlikely to have received direct retinal input. Electrical stimulation of the IGL elicited no response in 99% (n=93) of these visually insensitive recording regions, with the sole responding site exhibiting an inhibitory response.

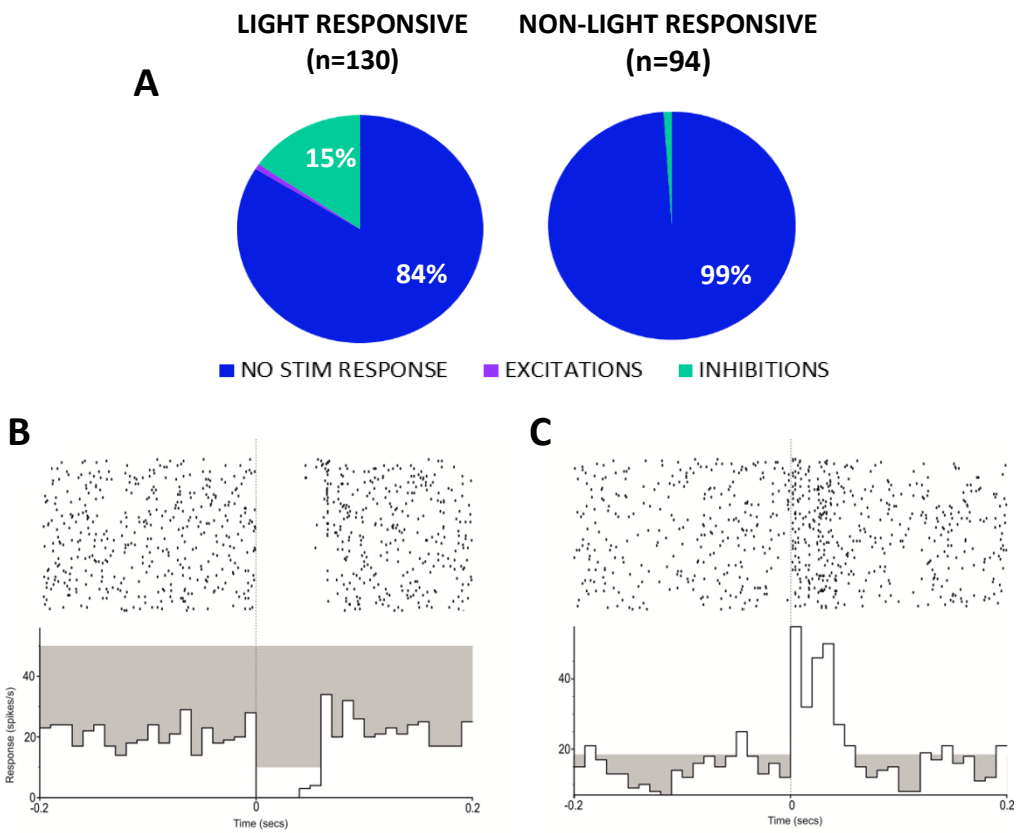

Figure 5.1: Responses to ipsilateral GHT stimulation across the SCN region.

(A) Proportions of SCN recording sites exhibiting excitatory or inhibitory responses to electrical stimulation of the IGL region (100-300µV biphasic dipolar stimulation; 100µs/phase). Left: proportions of channels that are light responsive. Right: proportions of responses from multiunit channels that did not respond to light flashes. (B) An example SCN channel receiving inhibitory input from the SCN. (C) An example channel receiving excitatory input from the IGL.

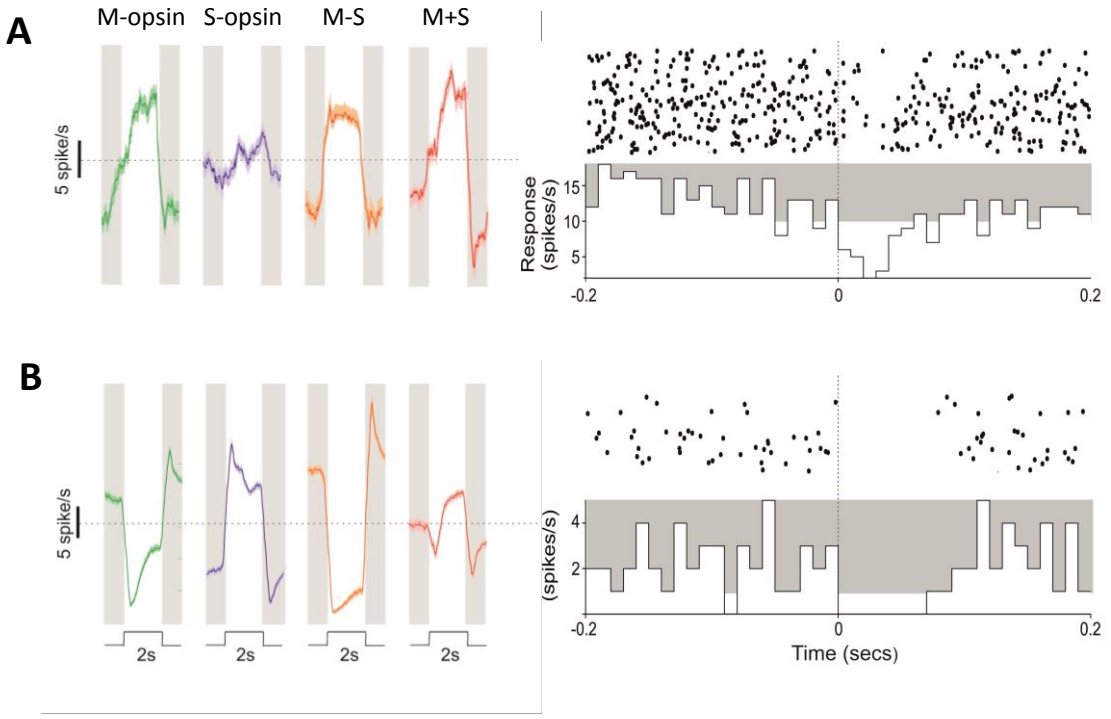

Figure 5.2: Inhibitory responses can be seen in both chromatic (colour-opponent) and achromatic cells within the SCN.

(A) An example of an achromatic SCN neuron. Left: The mean (±SEM) response to a 2s light stimuli designed to activate M-opsin and S-opsin individually, in tandem and in anti-phase. This cells response is primarily determined by the degree of M-opsin activation. Right: Raster plot (top) and perievent histogram (bottom) showing the inhibitory response to electrical stimulation within the IGL. (B) An example of a SCN neuron that receives colour-opponent information from the retina (M-OFF, S-ON). Conventions as in A.

Since individual SCN neurons can exhibit various different sensory properties, including cells that encode irradiance, colour or specifically respond to visual contrast (Walmsley et al., 2015, Walmsley and Brown, 2015), we next investigated whether GHT input might preferentially influence specific classes of visually sensitive SCN neurons. In total we isolated 9 single SCN cells from these recordings, all of which exhibited sustained monocular visual responses to 410nm light steps. To investigate chromatic sensitivity, we next presented photoreceptor-isolating stimuli to differentially activate M- and S-opsin.

Almost half (4/9) of the cells we isolated were confirmed as colour sensitive, exhibiting robust M-OFF, S-ON responses. Of the remaining cells, two were preferentially sensitive to M-opsin stimulation and the remainder lacked clear responses to selective cone activation. Consistent with our analysis of multiunit responses above, only a subset (2/9) of the single units we isolated responded to GHT activation, with 1 chromatic and 1 achromatic cell exhibiting pronounced inhibitory responses (Figure 5.2, A&B). These data thus establish that at least a subset of the colour and irradiance coding cell populations in the SCN receive inhibitory input from the GHT.

5.4.2 Contribution of GHT inputs to SCN light responses

We next set out to determine the functional contribution of GHT inputs to the SCN light responses. To this end, we set out to monitor SCN visual activity before and after pharmacological inhibition of IGL activity. This was achieved by microinjection of the $GABA_A$ antagonist muscimol (1mM) into the visual thalamus. Following large muscimol injections (2-4µL) light evoked (and spontaneous) activity was profoundly suppressed across the visual thalamus (Figure 5.3; top). Drug spread was calculated by identifying the electrode sites on which light responses were abolished (Figure 5.3), using the known inter-site distances from the manufacturer's specification. On this basis we estimated that activity was inhibited at sites located up to 850µm from the site of drug infusion, providing ample coverage to ensure complete removal of GHT inputs to the SCN, which was subsequently verified via post-hoc histological processing (Figure 5.3; bottom).

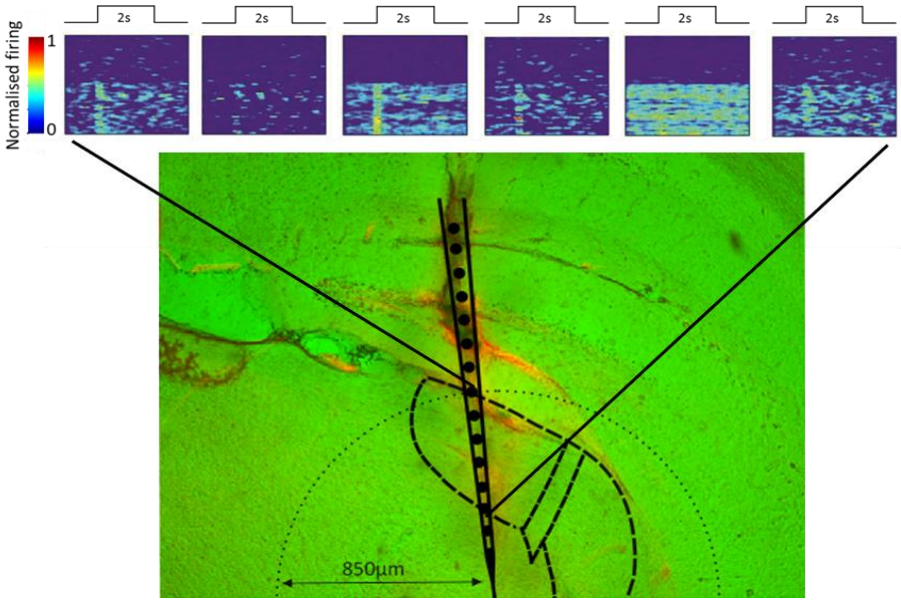

Figure 5.3: Microinjection of muscimol silences the visual thalamus.

Bottom: Histological verification of drug probe placement within the visual thalamus. Top: Trial bin counts for multiunit firing activity across repeated presentations of a 2s light step. Muscimol infusion rapidly abolishes spontaneous and visually evoked activity at sites located up to 850µm from the site of drug infusion

In total we examined the effect of GHT inhibition during multielectrode (32 channel) extracellular recordings from the SCN and surrounding hypothalamus of 8 mice. We first investigated the contribution of the GHT to irradiance coding in the SCN by applying full-field 410nm light steps of varying irradiance to one or both eyes. Importantly, since all mouse photoreceptor classes are equally sensitive in this part of the spectrum (see Methods), any heterogeneity in the photoreceptor populations driving specific responses (Brown et al., 2011, van Oosterhout et al., 2012) should not influence sensitivity as assessed under these conditions. These stimuli were presented before and after unilateral GHT inactivation to allow for comparison. Since IGL projections to the SCN are predominantly (but not exclusively) ipsilateral (Card and Moore, 1989) we independently evaluated the effect of both ipsilateral (n=5 mice) and contralateral (n=3 mice) GHT inactivation. To assess the impact of any GHT-independent changes in SCN responsiveness over the course of our experiment we also performed control recordings in 6 mice using an identical protocol (drug probe implanted but no muscimol administered).

In line with the anatomical arrangement of GHT inputs (Card and Moore, 1989), significant differences in light-evoked activity was only seen in the ipsilateral SCN (Figure 5.4). Thus, across the ipsilateral SCN, GHT inhibition significantly increased multiunit firing responses to stimulation of the contralateral eye (n=63 light responsive channels; Figure 5.4, A; F-test, F=4.67 p=0.001). A similar increase in multiunit firing was also evident when both eyes were stimulated (Figure 5.4, C; F-test, F=4.328 p=0.0018), whereas responses to stimulation of the ipsilateral eye were unchanged (Figure 5.4, B; F-test, F=1.849, p=0.1179). These data suggest, therefore, that the GHT primarily conveys signals from crossed retinal projections within the brain to the ipsilateral SCN.

In contrast with the above, removal of contralateral GHT activity (n=33 light responsive channels) had no significant effect upon stimulation of either eye (Figure 5.4, D-F; CONTRA: F-test, F=0.8715 p=0.4812; IPSI: F-test, F=2.277 p=0.0608), although there was a slight trend toward increased responses to stimulation of the ipsilateral eye. Moreover, visual responses obtained under control conditions (an identical visual stimulation protocol and time difference between the two sets of measurements; n=127 light responsive channels from 6 mice) exhibited no significant differences (Figure 5.4, G-I; CONTRA: F-test, F=1.35

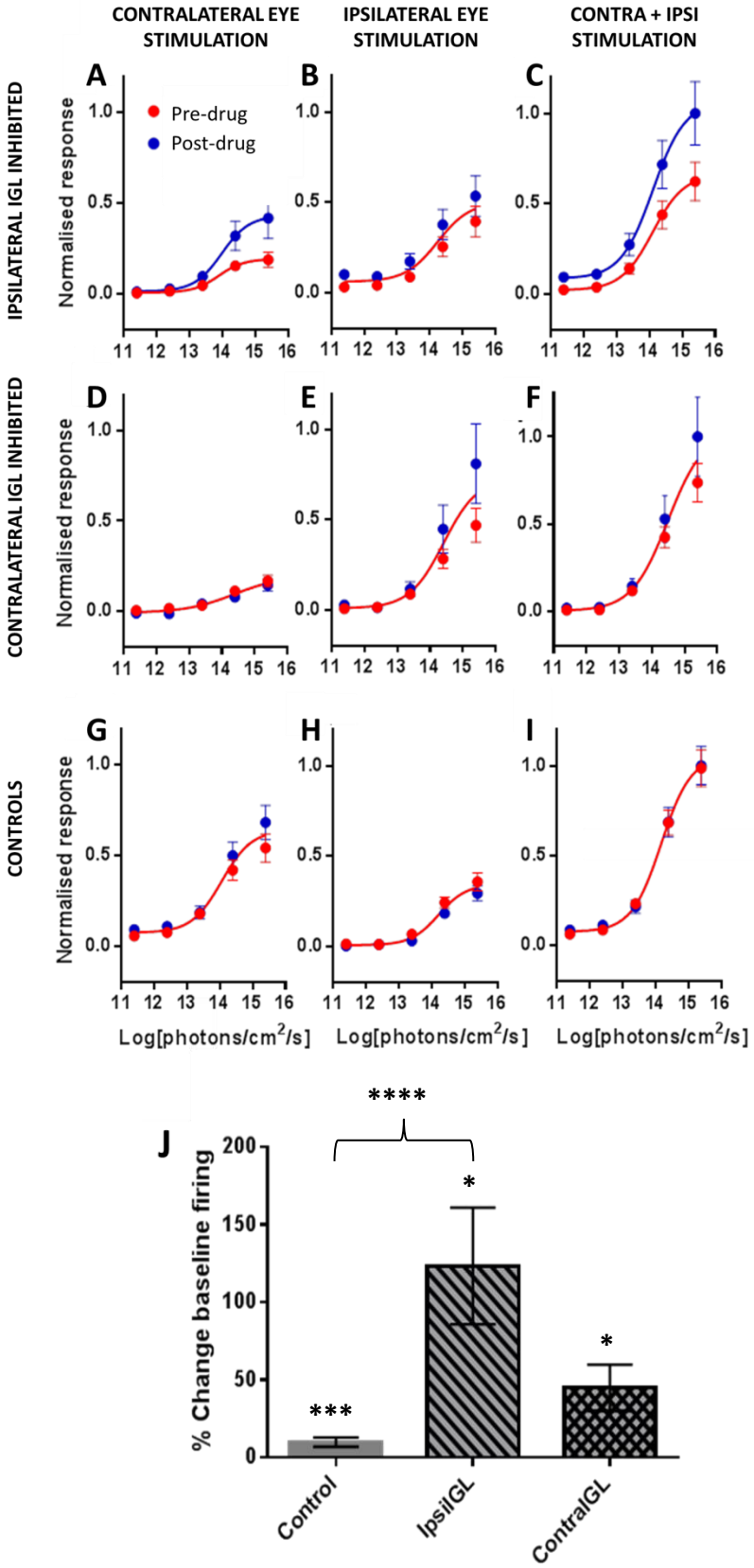

Figure 5.4: Effects of GHT inhibition on eye-specific responses within the SCN.

(A-I) Normalised multiunit SCN responses to contra-, ipsilateral and binocular (contra+ipsi) optical stimulation (5s flashes from dark; 410nm LED) before and after unilateral GHT inhibition via local injection of muscimol. When the ipsilateral GHT is inhibited (A-C) SCN responses to contralateral (A; p=0.01) and binocular (C; p=0.018) stimuli are enhanced. Inhibition of the contralateral GHT (D-F) has no effect on SCN responses to eye-specific stimuli. Under control conditions (G-I) there were no changes in visual responses. GHT inhibition significantly altered spontaneous activity within the SCN (J) in all three groups (paired *t*-tests: CONTRA p=0.0007, IPSI p=0.0119, CONTROLS p=0.0161). Spontaneous activity in the ipsilateral SCN increased significantly more than in the control group (1-way ANOVA, Dunnett's multiple comparisons test; p<0.0001).

p=0.2492; IPSI: F-test, F=1.943 p=0.1011). These data thus indicate that time-dependent changes in SCN firing could not explain the effects of muscimol application described above and that contralateral GHT projections do not exert a pronounced influence over SCN firing light responses.

We also found that GHT inhibition significantly altered spontaneous activity within the SCN. Thus, although paired t-tests indicated a significant increase in firing in all three groups (Figure 5.4, J; CONTRA p=0.0007, IPSI p=0.0119, CONTROLS p=0.0161), spontaneous activity in the ipsilateral SCN increased significantly more than in the control group (1-way ANOVA, Dunnett's multiple comparisons test; p<0.0001). The GHT therefore modulates both spontaneous firing and light-evoked aspects of the SCN light response.

In general agreement with the population responses described above, analysis of the modest sample of individual cells isolated from these recordings indicated that most contralaterally responsive neurons (3 out of 4) exhibited enhanced responses (p<0.05) after inhibition of the ipsilateral GHT (Figure 5.5, A: p<0.05). Interestingly, however, we also found that 2 out of 3 SCN cells that responded to ipsilateral visual stimuli exhibited enhanced responses following GHT inhibition, including one binocular cell, where both eye-specific response components displayed facilitation after ipsilateral IGL inhibition (Figure 5.5, B: p<0.05). Similarly, we also found that 2 out of 3 cells isolated from experiments using contralateral GHT inhibition exhibited significantly enhanced light responses post-drug. These results should be interpreted with some caution, since in our control experiments a subset of cells (n=3/10) exhibited spontaneous changes in response amplitude (p>0.05) over an equivalent time period to that used to evaluate drug effects. Nonetheless, while a larger sample size would be needed to draw firm conclusions, together these data suggest that the GHT may not exclusively modulate ipsilateral SCN responses to crossed retinal inputs.

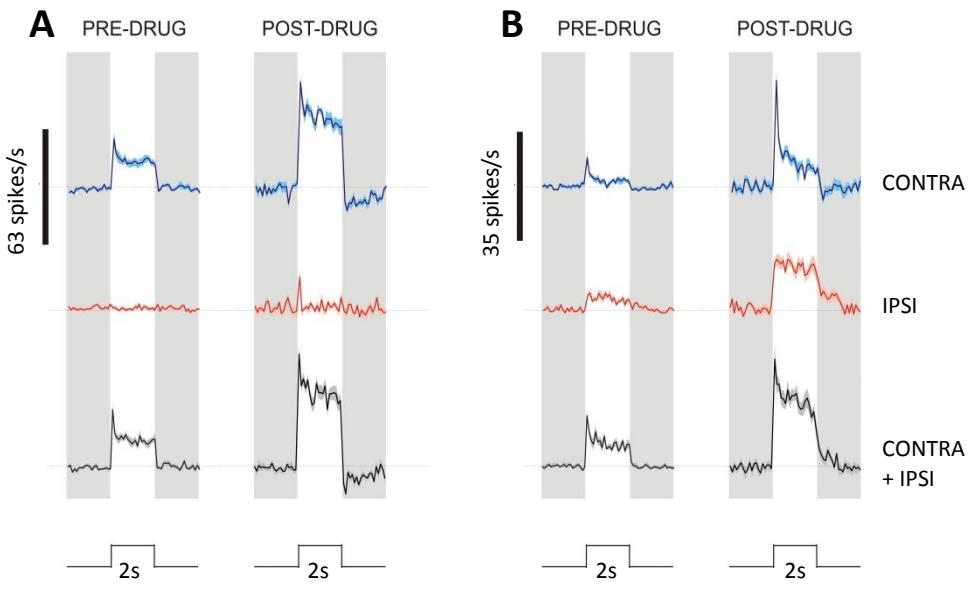

Figure 5.5: Effects of GHT inhibition on eye-specific responses within individual SCN neurons.

Example responses of single SCN neurons before and after inhibition of the ipsilateral IGL. The vast majority (3/4) of contralaterally responsive neurons exhibit enhanced responses to both monocular and binocular stimuli (A). A binocular cell receiving input from both eyes, exhibit enhanced responses to both ipsi- and contralateral stimuli (B).

5.4.3 The GHT reduces the sensitivity of SCN chromatic responses

We have previously established that the SCN receives information about colour from the retina (Walmsley et al., 2015). Since the origins of colour input to the SCN are currently unknown, and our electrical stimulation studies indicate that at least some colour sensitive SCN neurons receive GHT input, we next set out to assess their dependence on input from the GHT. As above then, we presented photoreceptor isolating stimuli to differentially activate M- and S-opsin before and after inactivation of the IGL. Due to constraints of the recording setup, chromatic stimuli were presented to the eye contralateral to the inhibited IGL only.

In order to ascertain whether GHT inputs differentially contribute to chromatic vs. achromatic responses within the SCN, we divided the multiunit population data recorded from the SCN into 2 groups: a 'chromatic' group containing channels (n=159) where firing activity was most responsive to coloured stimuli (significantly greater responses to stimuli that modulated M- and S-cone opsin in antiphase vs. in unison) stimuli and an 'achromatic' group (n=63) that exhibited greatest firing to simultaneous increases intensity for L and S cone opsin. Channels lacking significant responses to any of the stimuli we applied (i.e. those that did not receive input from the eye where stimuli were applied) were excluded from this analysis.

Analysis of post-treatment changes in SCN 'chromatic-population' responses to contralateral visual stimuli (Figure 5.6, A) revealed significant effects of stimulus type (2-Way ANOVA, $F_{3,117}$=4.1, p=0.009), group (ipsilateral GHT inhibition vs. control; $F_{1,39}$=6.4, p=0.016) and their interaction ($F_{3,117}$=2.8, p=0.044). Moreover, subsequent analysis revealed significant treatment-related changes in firing only in the ipsilateral GHT inhibition group (2-way ANOVA; Stimulus type x Treatment: $F_{3,51}$=3.3, p= 0.0275) with significant increases in response to S- and L-S opsin modulating stimuli ($p<0.01$ and $p<0.05$ respectively, Sidak post-test; controls all $p>0.05$). Together then, these data indicate that the ipsilateral GHT may selectively attenuate S-opsin driven responses in chromatic cells. As expected, we did not observe any significant changes in chromatic population responses to cone-isolating stimuli following inhibition of the contralateral GHT (Figure 5.6, B).

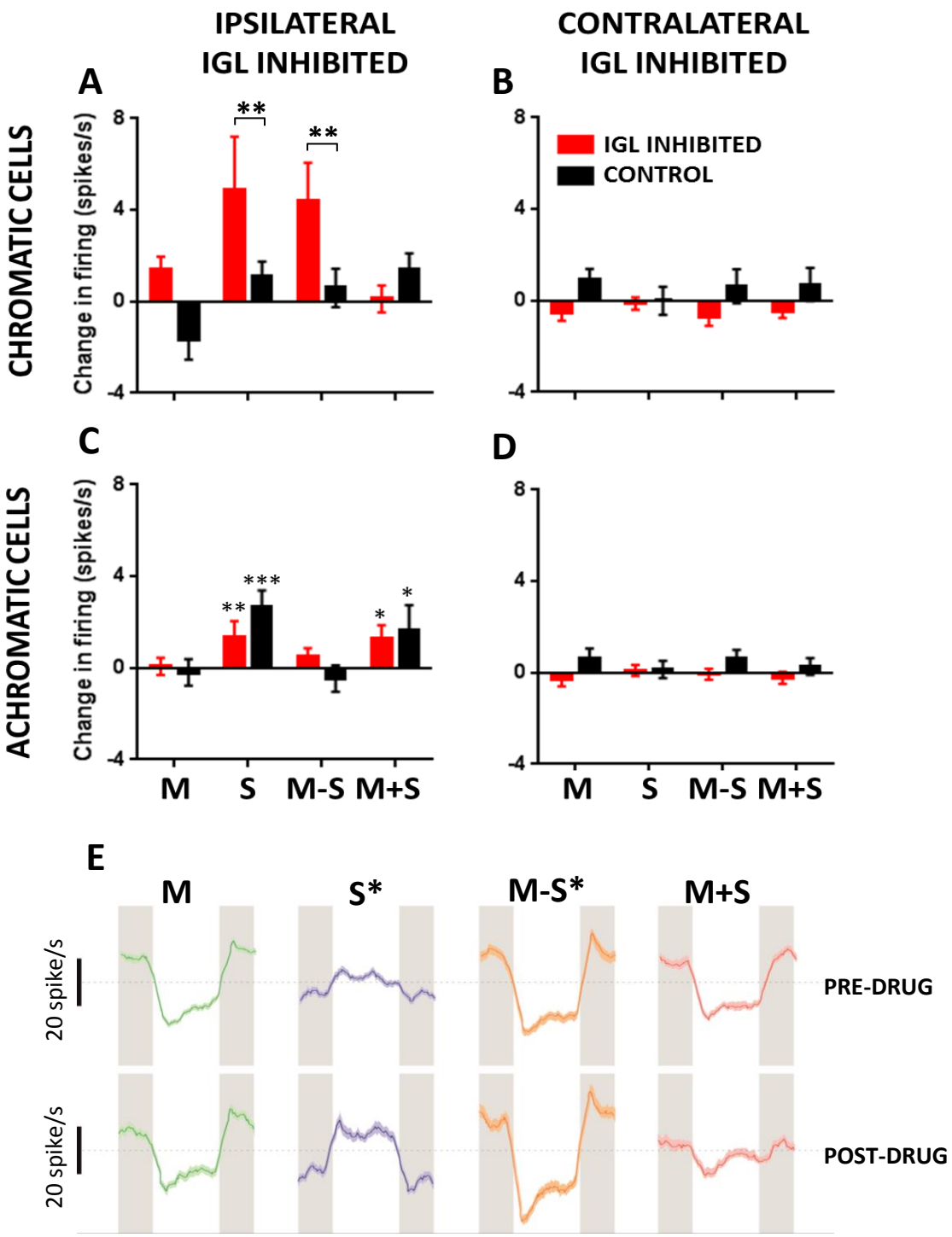

Figure 5.6: The GHT acts to reduce the sensitivity of SCN chromatic responses.

(A-D) Post-muscimol change in firing responses of chromatic (colour opponent) and achromatic (responsive to at least one opsin) multiunit channels relative to control conditions. (A) Removal of ipsilateral IGL input increases the response of chromatic channels to S- (p≤0.01) and L-S opsin (p≤0.01) stimuli; a change that is absent in control experiments (p=0.2505). (B) Removal of contralateral IGL input has no significant effect on SCN chromatic cell responses to colour stimuli. (C) Achromatic channels increased their responsiveness to S- (p≤0.01) and L+S (p≤0.05) opsin stimuli after ipsilateral IGL inhibition. Control experiments showed no significant change in response to the addition of drug (2-way ANOVA; p= 0.1079). However, they exhibited a stimulus-dependent effect of the drug (StimulusxDrug: $F_{3,141}$=5.747 P=0.001), with post hoc analysis revealing increases in response to S- (p≤0.0001) and L+S opsin stimulation (p≤0.01). (D) Removal of contralateral IGL input has no significant effect on SCN achromatic cell responses to colour stimuli. (E) After principal component analysis we found one example of a chromatic cell that exhibited the significant increase (p<0.05) in sensitivity to S and M-S stimuli.

Moreover, by contrast with the above, we did not observe any effect of group (ipsilateral GHT inhibition vs. control; $F_{1,917}$=0.02, p=0.88) or the interaction of stimulus type and group ($F_{3,273}$=1.7, p=0.198) for post-treatment changes in the responses of the achromatic SCN population. In fact, however, subsequent analysis revealed a significant effect of treatment in both ipsilateral GHT inhibition and control groups, with increased responsiveness to S- and L+S opsin modulating stimuli (Figure 5.6, C; 2-way ANOVA with sidak posthoc tests). Based on the relatively short time interval between pre- and post-treatments tests for these stimuli (~15min), we assume this observation reflects some form of network adaptation which results in enhanced cone driven responses across this group, unrelated to the specific effects of GHT inhibition. As above, there were no significant changes in achromatic population responses to cone-isolating stimuli following inhibition of the contralateral GHT (Figure 5.6, D). After principal component analysis, we were able to identify one example of a chromatic cell that exhibited a significant increases ($p<0.05$) in sensitivity to the S and L-S stimuli after the removal of ipsilateral IGL input (Figure 5.6, E).

5.5 Discussion

To date, the best known role for the GHT within the circadian system is in conveying arousal related information (Edmonds, 1977, Abe et al., 2007, Dudley et al., 1998, Grossman et al., 2000). While it is relatively well established that this pathway functionally opposes circadian resetting responses to light (van den Pol et al., 1996, Biello et al., 1997), the extent to which the GHT actually conveys visual information has remained controversial. Here we provide strong evidence that the GHT does directly convey visual signals and thus acts to tune the acute light-evoked activity of SCN neurons. Thus, we find that specific features of the acute SCN light response are modulated following inactivation of the GHT, including the balance of eye-specific visual responses and chromatic responses. Accordingly our data are compatible with the idea that not only do GHT signals directly influence the sensory properties of circadian responses to light, but also that the GHT might regulate other non-image forming light responses, such as suppression of melatonin secretion.

Following pharmacological inactivation of the ipsilateral LGN we primarily find an increase in contralateral, but not ipsilateral-driven visual responses within the SCN. These data suggest that the GHT primarily conveys inhibitory signals from IGL cells that are excited by crossed retinal projections. In line with this view, input to the IGL from the contralateral eye is at least twice as dense as that from the ipsilateral eye in all rodent species studied (Moore and Card, 1994, Tang et al., 2002, Hattar et al., 2006). Moreover, our previous work has shown that almost all cells in the mouse IGL/vLGN respond to contralateral visual signals, with less than 20% receiving ipsilateral input (Howarth et al., 2014). Our data also suggest that the functional influence of the GHT is primarily limited to cells in the ipsilateral SCN, since inhibition of the opposing GHT did not significantly change SCN visual responses. This finding is consistent with previous anatomical studies of the GHT in other rodent species indicating a predominantly ipsilateral projection (Card and Moore, 1989, Tang et al., 2002).

In addition to the above, we also found evidence that inactivating the GHT significantly increases colour-discrimination among a subset of SCN cells. This effect primarily derives from an increase in S-cone driven responses, suggesting that the GHT provides S-opsin biased inhibitory signals to chromatic cells. We should note, however, that S-cone driven responses for the achromatic cell population increased slightly following both ipsilateral GHT inhibition and under matched control recordings. Thus, network adaptation occurring across the timescale of our recordings appears to account for a treatment-independent change in responsiveness among achromatic cells. Despite this, our statistical analysis suggests the effect we see among the chromatic population is greater than could be simply explained by this kind of adaptation effect. On balance, then, we tentatively conclude that GHT inputs selectively alter chromatic sensitivity in the SCN.

Together, the data discussed above indicate that GHT inputs are preferentially activated by specific kinds of visual signals. In line with the idea that a primary role for the GHT is to modulate SCN visual responses, we also find that responses to electrical stimulation of the GHT are almost exclusively restricted to retinorecipient areas of the SCN. This finding is consistent with anatomical studies demonstrating that GHT terminals innervate the same areas of the SCN as the RHT (Harrington et al., 1985, Card and Moore, 1989), although one

previous study provided evidence that some non-retinorecipient SCN neurons in the rat also exhibit functional responses to GHT stimulation (Roig et al., 1997).

We do not here find evidence for substantial GHT input to non-retinorecipient regions of the SCN but, in other respects, our data align quite well with those of Roig and colleagues (1997). Hence we find that responses to GHT stimulation are almost exclusively inhibitory and are restricted to a subset (~20%) of retinorecipient SCN cells. It is currently unclear whether there are specific functional differences in the properties of these SCN cells that do vs. don't respond to activation of the GHT. Nonetheless, based on the small sample of single cells we isolated here, we can conclude that subsets of both colour sensitive and achromatic SCN neurons receive GHT input. It is important to also consider, however, that our electrical stimulation experiments may underestimate the proportion of SCN cells that receive GHT input, since inhibitory responses are hard to detect in cells with very low spontaneous firing rates. Indeed, we observed an average ~70% increase in multiunit light response magnitude following inhibition of the ipsilateral LGN, suggesting that GHT influences may in fact be quite widespread across SCN cells.

The predominantly inhibitory nature of GHT inputs we report above is not unexpected, given that the major neurotransmitters/modulators employed by GHT cells (GABA and NPY) are known to drive primarily inhibitory responses in the SCN (Liu and Reppert, 2000, Gribkoff et al., 1999, Gribkoff et al., 2003, Liou and Albers, 1991). Nonetheless, there have been reports of excitatory actions of both GABA (Wagner et al., 1997, De Jeu and Pennartz, 2002, Choi et al., 2008) and NPY (Mason et al., 1987) in the SCN under certain circumstances. Importantly, then, our data indicate these more unusual excitatory actions do not contribute significantly to the GHT-driven responses studied here (under more physiological conditions).

Given that NPY cells in the IGL form at least a major component of the GHT (and that we provide evidence indicating that the GHT conveys visual signals), one might conclude from our data that NPY cells are visually responsive. In this regard, anatomical studies have indeed shown that retinal fibres synapse onto NPY-expressing cells in both the rat (Takatsuji et al., 1991) and hamster IGL (Harrington et al., 1985). By contrast, functional

studies have suggested that NPY cells may not be visually responsive (Thankachan and Rusak, 2005, Morin, 2013, Takatsuji et al., 1991). Although our data cannot directly resolve this discrepancy, given existing data indicating that not all GHT cells contain NPY (Morin and Blanchard, 2001), we speculate that visual signals conveyed by the GHT may originate with non-NPY-expressing cells.

At present we can only speculate as to the functional significance of the GHT mediated modulation of SCN visual responsiveness we describe here. Given that the GHT is heavily implicated in regulating circadian responses to non-photic (arousal-related) stimuli (Edmonds, 1977, Abe et al., 2007, Dudley et al., 1998, Grossman et al., 2000), we assume that the GHT thus provides a means of modifying photic responses in the SCN based on arousal state. In this regard, the IGL receives substantial serotonergic (5-HT) innervation from the dorsal raphé nuclei (DRN) which drive a pronounced daily rhythm in 5-HT release, peaking during the night (Meyer-Bernstein and Morin, 1996, Vrang et al., 2003, Grossman et al., 2004). Since local application of serotonergic agonists robustly inhibit the photic responses of IGL neurons (Ying et al., 1993), we predict that this DRN input acts to switch off GHT-mediated inhibition of SCN visual responses during the night. This mechanism could thus contribute to the pronounced gating of circadian (Gillette and Mitchell, 2002) and acute (Brown et al., 2011) SCN visual responses that is essential for robust circadian entrainment.

In summary, our data provides new insights into the mechanisms through which the wider circadian network processes visual signals. Most notably, we show that the GHT modulates specific features of the acute light responses of SCN neurons and that one function of this input is to adjust chromatic sensitivity among colour-opponent neurons. Based on previous investigations of IGL-cell function we suggest this arrangement provides a mechanism by which the circadian and other non-image forming visual responses could be adjusted based on arousal state.

5.6 References

ABE, H., HONMA, S. & HONMA, K. 2007. Daily restricted feeding resets the circadian clock in the suprachiasmatic nucleus of CS mice. *Am J Physiol Regul Integr Comp Physiol,* 292**,** R607-15.

BIELLO, S. M., GOLOMBEK, D. A. & HARRINGTON, M. E. 1997. Neuropeptide Y and glutamate block each other's phase shifts in the suprachiasmatic nucleus in vitro. *Neuroscience,* 77**,** 1049-57.

BLASIAK, T. & LEWANDOWSKI, M. H. 2013. Differential firing pattern and response to lighting conditions of rat intergeniculate leaflet neurons projecting to suprachiasmatic nucleus or contralateral intergeniculate leaflet. *Neuroscience,* 228C**,** 315-324.

BROWN, T. M., ALLEN, A. E., AL-ENEZI, J., WYNNE, J., SCHLANGEN, L., HOMMES, V. & LUCAS, R. J. 2013. The melanopic sensitivity function accounts for melanopsin-driven responses in mice under diverse lighting conditions. *PLoS One,* 8**,** e53583.

BROWN, T. M., TSUJIMURA, S., ALLEN, A. E., WYNNE, J., BEDFORD, R., VICKERY, G., VUGLER, A. & LUCAS, R. J. 2012. Melanopsin-based brightness discrimination in mice and humans. *Curr Biol,* 22**,** 1134-41.

BROWN, T. M., WYNNE, J., PIGGINS, H. D. & LUCAS, R. J. 2011. Multiple hypothalamic cell populations encoding distinct visual information. *J Physiol,* 589**,** 1173-94.

CARD, J. P. & MOORE, R. Y. 1989. Organization of lateral geniculate-hypothalamic connections in the rat. *J Comp Neurol,* 284**,** 135-47.

CHOI, H. J., LEE, C. J., SCHROEDER, A., KIM, Y. S., JUNG, S. H., KIM, J. S., KIM, D. Y., SON, E. J., HAN, H. C., HONG, S. K., COLWELL, C. S. & KIM, Y. I. 2008. Excitatory actions of GABA in the suprachiasmatic nucleus. *J Neurosci,* 28**,** 5450-9.

DE JEU, M. & PENNARTZ, C. 2002. Circadian modulation of GABA function in the rat suprachiasmatic nucleus: excitatory effects during the night phase. *J Neurophysiol,* 87**,** 834-44.

DUDLEY, T. E., DINARDO, L. A. & GLASS, J. D. 1998. Endogenous regulation of serotonin release in the hamster suprachiasmatic nucleus. *J Neurosci,* 18**,** 5045-52.

EDMONDS, S. C. 1977. Food and light as entrainers of circadian running activity in the rat. *Physiol Behav,* 18**,** 915-9.

GILLETTE, M. U. & MITCHELL, J. W. 2002. Signaling in the suprachiasmatic nucleus: selectively responsive and integrative. *Cell Tissue Res,* 309**,** 99-107.

GOVARDOVSKII, V. I., FYHRQUIST, N., REUTER, T., KUZMIN, D. G. & DONNER, K. 2000. In search of the visual pigment template. *Vis Neurosci,* 17**,** 509-28.

GRIBKOFF, V. K., PIESCHL, R. L. & DUDEK, F. E. 2003. GABA receptor-mediated inhibition of neuronal activity in rat SCN in vitro: pharmacology and influence of circadian phase. *J Neurophysiol,* 90**,** 1438-48.

GRIBKOFF, V. K., PIESCHL, R. L., WISIALOWSKI, T. A., PARK, W. K., STRECKER, G. J., DE JEU, M. T., PENNARTZ, C. M. & DUDEK, F. E. 1999. A reexamination of the role of GABA in the mammalian suprachiasmatic nucleus. *J Biol Rhythms,* 14**,** 126-30.

GROSSMAN, G. H., FARNBAUCH, L. & GLASS, J. D. 2004. Regulation of serotonin release in the Syrian hamster intergeniculate leaflet region. *Neuroreport,* 15**,** 103-6.

GROSSMAN, G. H., MISTLBERGER, R. E., ANTLE, M. C., EHLEN, J. C. & GLASS, J. D. 2000. Sleep deprivation stimulates serotonin release in the suprachiasmatic nucleus. *Neuroreport,* 11**,** 1929-32.

HARRINGTON, M. & RUSAK, B. 1989. Photic responses of geniculo-hypothalamic tract neurons in the Syrian hamster. *Visual Neuroscience,* 2.

HARRINGTON, M. E. 1997. The ventral lateral geniculate nucleus and the intergeniculate leaflet: interrelated structures in the visual and circadian systems. *Neurosci Biobehav Rev,* 21**,** 705-27.
HARRINGTON, M. E., NANCE, D. M. & RUSAK, B. 1985. Neuropeptide Y immunoreactivity in the hamster geniculo-suprachiasmatic tract. *Brain Res Bull,* 15**,** 465-72.
HARRINGTON, M. E. & RUSAK, B. 1986. Lesions of the thalamic intergeniculate leaflet alter hamster circadian rhythms. *J Biol Rhythms,* 1**,** 309-25.
HATTAR, S., KUMAR, M., PARK, A., TONG, P., TUNG, J., YAU, K. W. & BERSON, D. M. 2006. Central projections of melanopsin-expressing retinal ganglion cells in the mouse. *J Comp Neurol,* 497**,** 326-49.
HOWARTH, M., WALMSLEY, L. & BROWN, T. M. 2014. Binocular integration in the mouse lateral geniculate nuclei. *Curr Biol,* 24**,** 1241-7.
JACOBS, G. H. & WILLIAMS, G. A. 2007. Contributions of the mouse UV photopigment to the ERG and to vision. *Doc Ophthalmol,* 115**,** 137-44.
JUHL, F., HANNIBAL, J. & FAHRENKRUG, J. 2007. Photic induction of c-Fos in enkephalin neurons of the rat intergeniculate leaflet innervated by retinal PACAP fibres. *Cell Tissue Res,* 329**,** 491-502.
LIOU, S. Y. & ALBERS, H. E. 1991. Single unit response of neurons within the hamster suprachiasmatic nucleus to neuropeptide Y. *Brain Res Bull,* 27**,** 825-8.
LIU, C. & REPPERT, S. M. 2000. GABA synchronizes clock cells within the suprachiasmatic circadian clock. *Neuron,* 25**,** 123-8.
MASON, R., HARRINGTON, M. E. & RUSAK, B. 1987. Electrophysiological responses of hamster suprachiasmatic neurones to neuropeptide Y in the hypothalamic slice preparation. *Neurosci Lett,* 80**,** 173-9.
MATURANA, H. R. & VARELA, F. J. 1982. Color-opponent responses in the avian lateral geniculate: a study in the quail (Coturnix coturnix japonica). *Brain Res,* 247**,** 227-41.
MEYER-BERNSTEIN, E. & MORIN, L. 1996. Differential serotonergic innervation of the suprachiasmatic nucleus and the intergeniculate leaflet and its role in circadian rhythm modulation. The Journal of Neuroscience.
MOORE, R. Y. & CARD, J. P. 1994. Intergeniculate leaflet: an anatomically and functionally distinct subdivision of the lateral geniculate complex. *J Comp Neurol,* 344**,** 403-30.
MOORE, R. Y. & SPEH, J. C. 1993. GABA is the principal neurotransmitter of the circadian system. *Neurosci Lett,* 150**,** 112-6.
MORIN, L. & BLANCHARD, J. 2001. Organization of the hamster intergeniculate leaflet: NPY and ENK projections to the suprachiasmatic nucleus,intergeniculate leaflet and posterior limitans nucleus. *Visual Neuroscience,* 12.
MORIN, L. P. 2013. Neuroanatomy of the extended circadian rhythm system. *Exp Neurol,* 243**,** 4-20.
MORIN, L. P., BLANCHARD, J. H. & PROVENCIO, I. 2003. Retinal ganglion cell projections to the hamster suprachiasmatic nucleus, intergeniculate leaflet, and visual midbrain: bifurcation and melanopsin immunoreactivity. *J Comp Neurol,* 465**,** 401-16.
MORIN, L. P., SHIVERS, K. Y., BLANCHARD, J. H. & MUSCAT, L. 2006. Complex organization of mouse and rat suprachiasmatic nucleus. *Neuroscience,* 137**,** 1285-97.
PAXINOS, G. & FRANKLIN, K. 2001. *The Mouse Brain in Stereotaxic Coordinates,* San Diego, Academic Press.
PAXINOS, G. F., K.B.J. 2001. *The mouse brain in stereotaxic coordinates: Second Edition,* San Diego, Academic Press.
PICKARD, G. E. 1994. Intergeniculate leaflet ablation alters circadian rhythms in the mouse. *Neuroreport,* 5**,** 2186-8.
PICKARD, G. E., RALPH, M. R. & MENAKER, M. 1987. The intergeniculate leaflet partially mediates effects of light on circadian rhythms. *J Biol Rhythms,* 2**,** 35-56.

ROIG, J. A., GRANADOS-FUENTES, D. & AGUILAR-ROBLERO, R. 1997. Neuronal subpopulations in the suprachiasmatic nuclei based on their response to retinal and intergeniculate leaflet stimulation. *Neuroreport,* 8**,** 885-9.

TAKATSUJI, K., MIGUEL-HIDALGO, J. J. & TOHYAMA, M. 1991. Retinal fibers make synaptic contact with neuropeptide Y and enkephalin immunoreactive neurons in the intergeniculate leaflet of the rat. *Neurosci Lett,* 125**,** 73-6.

TANG, I. H., MURAKAMI, D. M. & FULLER, C. A. 2002. Unilateral optic nerve transection alters light response of suprachiasmatic nucleus and intergeniculate leaflet. *Am J Physiol Regul Integr Comp Physiol,* 282**,** R569-77.

THANKACHAN, S. & RUSAK, B. 2005. Juxtacellular recording/labeling analysis of physiological and anatomical characteristics of rat intergeniculate leaflet neurons. *J Neurosci,* 25**,** 9195-204.

VAN DEN POL, A. N., OBRIETAN, K., CHEN, G. & BELOUSOV, A. B. 1996. Neuropeptide Y-mediated long-term depression of excitatory activity in suprachiasmatic nucleus neurons. *J Neurosci,* 16**,** 5883-95.

VAN OOSTERHOUT, F., FISHER, S. P., VAN DIEPEN, H. C., WATSON, T. S., HOUBEN, T., VANDERLEEST, H. T., THOMPSON, S., PEIRSON, S. N., FOSTER, R. G. & MEIJER, J. H. 2012. Ultraviolet light provides a major input to non-image-forming light detection in mice. *Curr Biol,* 22**,** 1397-402.

VRANG, N., MROSOVSKY, N. & MIKKELSEN, J. D. 2003. Afferent projections to the hamster intergeniculate leaflet demonstrated by retrograde and anterograde tracing. *Brain Res Bull,* 59**,** 267-88.

WAGNER, S., CASTEL, M., GAINER, H. & YAROM, Y. 1997. GABA in the mammalian suprachiasmatic nucleus and its role in diurnal rhythmicity. *Nature,* 387**,** 598-603.

WALMSLEY, L. & BROWN, T. M. 2015. Eye-specific visual processing in the mouse suprachiasmatic nuclei. *J Physiol,* 593**,** 1731-43.

WALMSLEY, L., HANNA, L., MOULAND, J., MARTIAL, F., WEST, A., SMEDLEY, A. R., BECHTOLD, D. A., WEBB, A. R., LUCAS, R. J. & BROWN, T. M. 2015. Colour as a signal for entraining the mammalian circadian clock. *PLoS Biol,* 13**,** e1002127.

YING, S. W., ZHANG, D. X. & RUSAK, B. 1993. Effects of serotonin agonists and melatonin on photic responses of hamster intergeniculate leaflet neurons. *Brain Res,* 628**,** 8-16.

ZHANG, D. & RUSAK, B. 1989. Photic sensitivity of geniculate neurons that project to the suprachiasmatic nuclei or the contralateral geniculate. *Brain Research,* 504**,** 161-164

Chapter 6: General Discussion

The aim of this thesis was to investigate how the circadian network integrates information from the photic environment, using primarily an electrophysiological approach. In doing so I generated several key findings that advance our understanding our how light is processed by the circadian system and regulates biological rhythms:

- Contrary to previous beliefs, SCN neural activity does not accurately measure global light levels at either the single cell or population levels (Chapter 2).
- The SCN contains colour sensitive neurons and uses information about spectral composition of light to fine tune circadian phase in accordance with natural changes in illumination across the solar day (Chapter 3).
- Inputs from the GHT modulate specific features of the SCN neuronal light response (Chapter 5).
- In addition, I established and validated an important new experimental approach that will prove invaluable for future studies of the neural circuitry responsible for chromatic processing in the mouse brain or retina (Chapter 4).

A discussion follows; drawing on these findings to highlight the implications and questions arising, provide a critical evaluation of the experimental strategies employed and to suggest possible future studies to build on the work presented here.

6.1 Implications of this work

6.1.1 SCN response heterogeneity and effects of local variations in illumination

The data presented in Chapter 2 indicates that SCN neurons do not receive input from across the whole visual scene; instead they at most sample light from within just one hemisphere. Based on the prevalence of cells exhibiting monocular vs. binocular responses, we estimate that SCN neurons may only receive input from very small number (~2) of RGCs.

Consistent with these findings, our preliminary data (Figure 6.1) and work from other collaborators (Mouland et al., 2015) indicate that at least some SCN neurons do indeed only respond to visual signals within restricted regions of visual space. Given the dense retinal projections spanning the entirety of the SCN, and the small size of the SCN, the expectation would be that the SCN would draw inputs from across the whole of the retina: we must therefore consider why this is not the case.

The most likely possibility seems to be that ability to sample restrictively from the retina serves some adaptive purpose. Indeed, such an arrangement is presumably important to allow for different populations of SCN neurons with distinct sensory properties, such as the blue-ON, yellow-ON and brightness-sensitive phenotypes we have identified in this thesis. However, if irradiance encoding is sufficient for photic entrainment, why do we need these different types of cells?

At present we know little of how neural changes in spiking are translated into changes in circadian phase, however previous work suggest a direct correlation between spiking and phase shifting (Brown et al., 2011) and that triggering SCN firing is sufficient to induce phase shifts (Jones et al., 2015). On that basis, we suggested in chapter 2 that SCN cells might in fact be independently reset according to which sorts of visual signals they receive, with whole animal changes in circadian phase reflecting the average change across all the relevant cellular oscillators. Consequently, both the position (i.e. looking at the ground/sky) and the properties (colour vs brightness sensitive) of a cell's receptive field (RF) could have a quite dramatic effect on the daily visual input received and thus resulting circadian phase. Such a mechanism could thus explain previous reports that the phasing of individual SCN cells is quite heterogeneous (Brown and Piggins, 2009) and is consistent with our data showing changes in the phase distributions of SCN cells under natural vs. brightness only photoperiods (Walmsley et al., 2015).

However, a related possibility is that different populations of cells drive distinct physiological outputs of the circadian clock (e.g. activity, hormone secretion etc.). Indeed, the idea that SCN cell groups with different phasing might control different output rhythms has been suggested previously (Kalsbeek et al., 2006). Consistent with this view, our

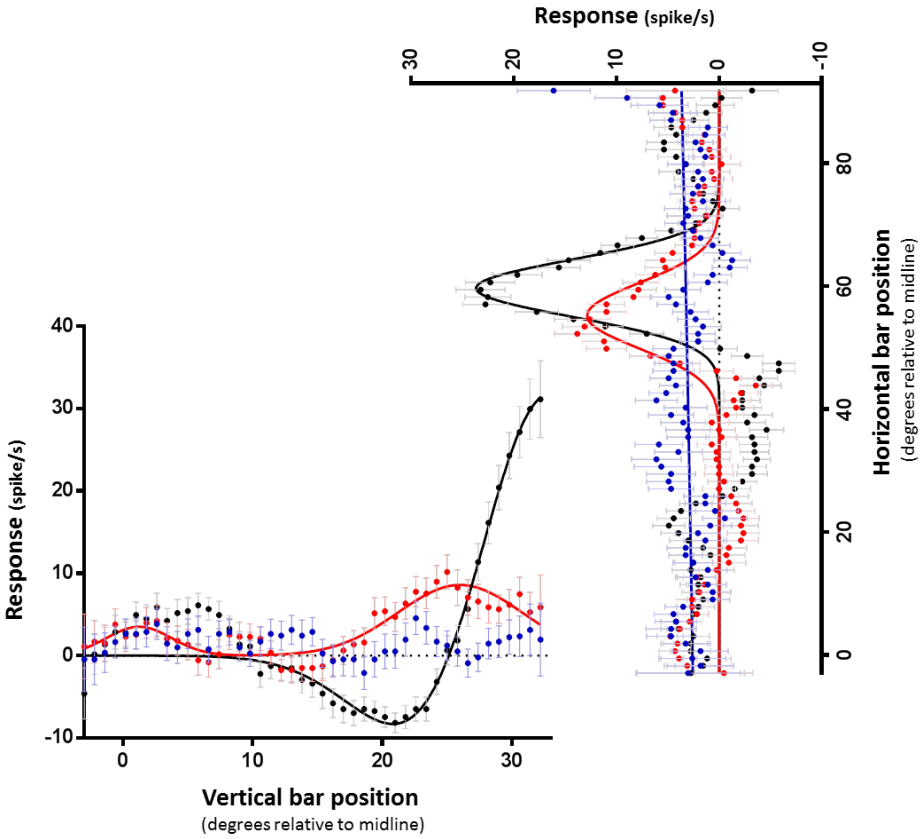

Figure 6.1: Some SCN neurons only respond to visual signals within restricted regions of visual space.

Receptive fields (RF) were mapped using horizontal and vertical flashing black/white bars under either monocular or binocular viewing conditions (ipsilateral stimulation: red, contralateral stimulation: blue, binocular stimulation: black). We were able to map receptive fields in in 33% (12/36) of SCN neurons tested. 5 of these had receptive fields occupying a small area of the visual field. The mean±SEM response (8 trials) of a neuron exhibiting one of these small receptive fields is shown above. Solid lines indicate Gaussian fit. All angles are expressed relative to the skull midpoint.

preliminary data suggests that changes in the spectral composition of light can desynchronise different clock controlled aspects of physiology in mice. Under light cycles that replicate natural twilight, mouse locomotor activity and core body temperature rhythms exhibit similar timing (Figure 6.2, A). However, when these mice are then transferred to light cycles that lack these changes in colour, activity rhythms are dramatically advanced relative to core body temperature (Figure 6.2, B), indicating that cell populations with specific sensory characteristics may indeed influence the timing of different aspects of an organism's physiology.

6.1.2 Neural origins of colour-dependent input to the circadian system

In Chapter 3, we demonstrate that a subpopulation of SCN neurons exhibit spectrally-opponent responses (either blue-ON/yellow-OFF or blue-OFF/ yellow-ON), rendering them able to detect differences in colour. More importantly, we demonstrate that mice can use this 'colour' signal as a circadian timing cue in order to more accurately judge time of day. As discussed previously, the simplest origin for this 'chromatic' input is that these responses are directly driven by a subset of mRGCs in the retina. However, the SCN resides at the centre of a network of brain structures (see Dibner et al., 2010 for review), giving rise to the alternative possibilities that this input arises due to local processing or inputs from other regions, such as the IGL.

The data in chapter 5 effectively rules out the IGL as the origin of these signals, as SCN responses to S- and M-opsin stimulation remain when IGL input is removed. This leaves us with one of two options, the first being that a subset of mRGCs directly convey chromatic input to the SCN. As SCN-projecting mRGCs also project to the IGL, one would expect significant numbers of colour responses within neurons in the IGL/vLGN. In fact, these seem very rare (Chapter 4), indicating that If SCN chromatic responses do arise directly from mRGCs, it must originate in a particular subtype that project to the SCN but not IGL/vLGN.

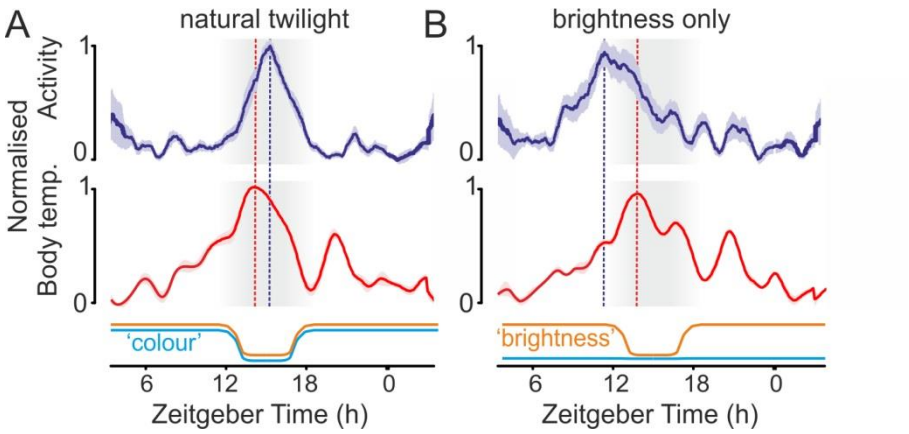

Figure 6.2: Differences in the spectral composition of light can desynchronise different clock controlled aspects of physiology.

Under light cycles that replicate natural twilight (A), mouse locomotor activity (detected by I.R. sensors) and core body temperature rhythms exhibit similar timing. When transferred to light cycles that lack changes in colour (brightness only; B), activity rhythms are dramatically advanced relative to core body temperature (group data from 5 co-housed mice of mixed genotype- chapter 3).

As discussed above, there are at least 5 known types of mRGCs. The RHT mainly consists of projections from mainly M1 mRGCs (Baver et al., 2008), but, the SCN is also innervated by some non-M1 Brn3b+ve mRGCs (Chen et al., 2011). Given that only 1/4 cells within the SCN are colour sensitive, we suspect that it must be these non-M1 mRGCs that conveys this chromatic information. If this population of chromatic mRGCs were rare, this may certainly explain why these did not show up in a previous investigation of mRGC responses to cone signals (Weng et al., 2013).

Although colour-opponent responses of SCN neurons could indeed be due to direct input from mRGCs (Figure 6.3, A), it is impossible for us to rule out alternative possibility that these properties arise via local differential processing of M- and S-cone opsin inputs. Indeed, since our data (chapter 2) indicates that at least some SCN cells get input from more than 1 RGC (i.e. binoculars cells), it is certainly possible that a single SCN neuron could combine inputs from one 'ON'-RGC and one 'OFF'-RGC with different chromatic preference (Figure 6.3, B). This is an important question for future studies (see below).

6.1.3 Implications for practical application of light to regulate circadian timing

Since the discovery of melanopsin, there has been increasing interest in using light to manipulate circadian timing to enhance human health. In particular, because of the relatively short wavelength sensitivity of melanopsin (~480nm), existing approaches work on the principle that by using low colour temperatures (i.e. making light more yellow), unwanted circadian responses can be reduced (e.g. during late evening working). Conversely, higher colour temperature (bluer) lighting is recommend for producing maximal effects on the circadian system (i.e. for use during daytime). Our identification of colour as an import source of circadian timing information (Chapter 3) provides important new data that may inform such practical lighting design. Consequently, while it is true that reducing melanopsin activation will reduce circadian responses, it is now readily achievable to adjust melanopsin activation without changing colour (e.g. as demonstrated in chapter 3). Therefore if we are also going to change colour; is blue or yellow better?

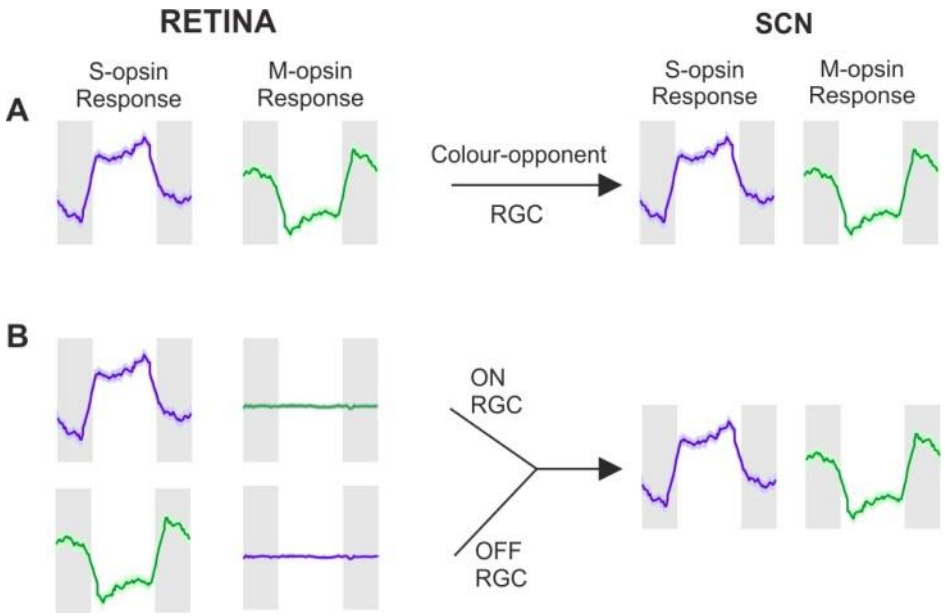

Figure 6.3: Retinal vs. local processing as the source of SCN colour opponent input.

Colour discrimination within the SCN is enabled by colour-opponent input to SCN neurons. This input may arise via direct input from the retina, via innervation by a colour-opponent RGC (A). It may instead involve local processing within the SCN neuron itself via the combination of antagonistic input from 2 achromatic RGCs that preferentially respond to the activation of M- and S- opsin (B).

Since daytime is in fact associated with more yellow light than is twilight (Walmsley et al., 2015), one might argue that bluer lights would have a weaker circadian effect at a fixed level of melanopic illuminance. Consistent with this, our mouse data show that physiological rhythms are phase advanced under photoperiods where light is maintained under constant 'night' spectra vs. when colour changes naturally (Chapter 3). This implies a weaker effect on the mouse circadian clock, which primarily relies on an evening delay for entrainment.

The argument above seems to run counter, however, to the greater prevalence of blue vs. yellow-ON cells in the SCN - since night spectra should overall evoke more SCN firing we would expect this to translate instead to a phase delay not advance. One possibility is that general positive relationship between firing and phase shifting (Brown et al., 2011) doesn't hold true for colour cells (e.g. blue-ON cells inhibit phase shifting). Or equally, that colour differentially contributes to advances vs. delays. Data in chapter 5 suggest that the IGL modulates chromatic sensitivity within the SCN, and preliminary data from the lab (unpublished) suggests that IGL responses themselves may undergo circadian variation. Therefore, the GHT could gate the chromatic sensitivity of the SCN across the circadian cycle. Addressing these questions is thus an especially important goal moving forward for any practical application of colour to manipulate circadian timing.

A final consideration that we must make is whether or not our findings in mice directly translate to humans. Alongside previous identification of colour opponent primate mRGCS (Dacey et al., 2005), a role for colour seems likely based on melatonin suppression data and pupillography. Primate mRGCs (Dacey et al., 2005) and the human PLR (Spitschan et al., 2014) exhibit blue-OFF/yellow-ON responses, whereas melatonin secretion is better supressed by short wavelengths suggesting a possible blue-ON input (Lockley et al., 2003). Although is melatonin secretion more directly related to circadian system, it is already clear that the spectral sensitivity of melatonin suppression and circadian phase shifts are different (Gooley et al., 2010). As such, it is currently unclear whether the effects of colour we see in mice will directly translate to humans. Resolving the specific effects of colour on the mouse circadian clock (and other NIF functions) is thus a key first step towards addressing this question.

6.2 Discussion of experimental strategies

6.2.1 Use of anaesthesia

The main experimental approach employed for this thesis was extracellular electrophysiological recordings from within the SCN of anaesthetised mice. All of our recordings were conducted under urethane anaesthesia, which enables stable recordings for prolonged periods of time (Maggi and Meli, 1986a) due to minimal effects on the cardiovascular system (Maggi and Meli, 1986b). Urethane action has only minor effects on GABAergic signalling (Maggi and Meli, 1986a, Hara and Harris, 2002) and is therefore useful for our studies as it maintains circadian network oscillations within the brain which rely on GABA (Buzsáki, 2002). However, brain activity under anaesthesia is certainly not identical to that of the awake animal, with behaviour playing a strong role in modulating the magnitude of visual responses (Chiappe et al., 2010, Maimon et al., 2010, Niell and Stryker, 2010). It is therefore important to consider the possibility that responses recorded under the experimental conditions employed in chapters 2-5 have been influenced by our choice of anaesthetic. Since, to date, there is little evidence that anaesthesia alters the fundamental sensory properties of visual neurons, one would imagine this is unlikely to have significantly skewed our conclusions. Consistent with this view, comparing the data from this thesis to that collected in freely-moving mice (van Diepen et al., 2013, van Oosterhout et al., 2012) indicates that the sensitivity of visual responses are not substantially altered by urethane anaesthesia.

Nonetheless, one potentially attractive alternative to the approach employed here is to use chronically implanted electrodes to record circadian light responses in awake, free-moving animals. In principle, this would enable us to track sensory properties of neurons across the circadian cycle and relate changes in neuronal activity to behaviour. It is also possible to combine chronic electrophysiological recordings with optogenetic manipulation of neurons, should this prove necessary for specific experiments (Anikeeva et al., 2012). However, whilst it is possible to deliver full-field stimuli to awake animals (van Diepen et al., 2013), employing carefully controlled visual stimuli under these conditions becomes much more challenging.

More significantly, our experience tells us that individual SCN cells are much harder to isolate than in other brain regions, even under the stable recording conditions provided by the anaesthetised preparation. Factoring in the added noise due to animal movement is likely to make this task even more difficult. Indeed, other groups that use chronic SCN recordings (van Diepen et al., 2013, van Oosterhout et al., 2012) do not routinely report the activities of isolated SCN single cells. Since the ability to define single cell responses is critical for many of our key questions moving forward, this represents is a significant drawback for the analysing the functional properties of non-image forming visual circuits.

Another alternative approach would be to record in awake but head-fixed animals (Schwarz et al., 2010). Such a setup would certainly allow for better control of visual stimuli. The major downfall of this technique, however, is that head fixation is a stressful procedure for mice and so it would not be possible to track neurons for extended periods of time. Since we think it unlikely that the sensory properties of SCN neurons would be dramatically different under awake vs. anaesthetised conditions, we think this kind of recording modality is unlikely to be especially useful here.

6.2.2 Localisation of neural recordings

In all of our experiments, we used DiI (and the precise geometry of our electrode arrays) to estimate the locations of the neurons we recorded (Figures 3.1 and 4.6). Based on our experience with this approach and analysis of spike waveforms detected across multiple sites of our electrode arrays (Howarth et al., 2014), we estimate the error associated with the resulting estimates to be <±75µm. Nonetheless, this level of resolution means that the technique is not well suited to distinguishing anatomical differences in sensory properties within small nuclei such as the SCN or between adjacent visual regions where electrode sites are located close to the borders.

This later issue can be, in part, ameliorated by combing DiI with other staining techniques to label specific brain structures. I demonstrate this in chapter 2 (Figure 3.1), using a marker of M1 melanopsin ganglion cell projections to define the boundaries of the

retinorecipient SCN region. A limitation of this technique, however, is that the washing and extended reaction steps required (~4h) reduced the intensity of the DiI signal.

The alternative and/or complementary approach we could have used is to electrolytically lesion a number of electrode sites to permanently mark their location in the brain. Such an approach is of course readily applicable alongside staining techniques to define the boundaries of particular brain structures. Lesioning in this manner could, in principle, be especially useful in the case of small structures like the IGL which are sandwiched between other visual nuclei; for example, used alongside immunohistochemistry for EYFP-labelled GABA cells in Ai32GAD mice (chapter 4). One major limitation to using the lesion method alongside multielectrode recording probes though is that applying lesioning current requires that the headstage first be removed carrying the risk of displacing and/or breaking the (expensive) electrode. Moreover, from past experience, controlling lesion size using these probes is challenging. In light of these drawbacks we thus consider the use of DiI-labelling preferable. Indeed, we find that the distribution of functional responses identified using this approach closely follows the anatomical boundaries of the visual regions we record from (Figures 2.1 and 4 .4). With the caveats highlighted above then, we considered the DiI-based strategy appropriate.

6.2.3 Use of red cone mice

In chapter 3, we used red cone mice (Smallwood et al., 2003) to determine colour input to the SCN. A fundamental assumption inherent in this approach is that the pattern of human L-opsin expression entirely recapitulates that which would occur for the native mouse M-cone opsin. While there is no existing data to suggest that this assumption is false, it remains a formal possibility that regulation of L-opsin expression is not entirely identical to the wildtype situation.

In chapter 4, we verified that it is possible to isolate cone signals using a silent substitution approach in wildtype mice. Importantly, our application of this approach to the mouse SCN revealed a similar mixture of colour-sensitive and achromatic cone-derived responses

(Chapter 5) to those we originally identified in red cone animals (Chapter 3). As such, we are confident that this earlier use of mice with altered cone sensitivity is unlikely to have substantially effected our conclusions.

6.2.4 Combining electrophysiological recording with local drug delivery or optogenetics

For the local drug delivery method we employed in chapter 5, we could use MUA recordings to confirm drug delivery by the complete abolition of multiunit light responses. We did however, find that the volume of drug required to evoke this effect varied considerably between experiments. We assume this reflects variable degrees of occlusion of the drug delivery cannula by tissue debris on route to target. As such, it is hard to accurately determine or control the volume of drug delivered using this approach. In the case of the experiments presented here, we do not consider this a significant barrier, insofar as we aimed to achieve relatively global inhibition of thalamic activity (and were able to verify that this occurred during the experiment). Nonetheless, our experience suggests that this technique is not well suited to more localised applications. Also the inhibition we can achieve using local muscimol application is essentially irreversible, making it hard to distinguish spontaneous changes from drug-evoked changes in SCN responses. Accordingly, we consider optogenetic-based circuit manipulation a more promising strategy for future experiments of this nature (e.g. using Archeo- or halorhodopsin; See Han (2012) for review).

In this regard, we have certainly confirmed that using a combination of optogenetic stimulation and electrophysiological recording to identify and manipulate specific cell types is readily achievable. Thus, in chapter 4 we use the Ai32; GAD2-Cre mouse line to drive channelrhodopsin-2 expression in cells throughout the CNS that express the biosynthetic enzyme for GABA, GAD2 (Madisen et al., 2012, Taniguchi et al., 2011). Although we readily identify subsets of optogenetically responsive cells using this mouse line (whose distribution matches that expected for GABA neurons), key considerations with this type of strategy are the specificity and penetrance of the targeting constructs.

In the case of the GAD2-Cre line used to drive channelrhodopsin-2 expression, specificity and penetrance are both high, with over 90% of cortical neurons examined immunopositive for GAD2 and over 90% of GAD2-immunopositive cells exhibiting Cre-driven reporter expression (Taniguchi et al. 2011). It is important to note however that two distinct enzymes catalyse GABA synthesis, GAD1 and GAD2. Although both enzymes are highly expressed across the mouse IGL/vLGN (Allen brain atlas, experiments: 479 and 79591669) there have been no direct studies of enzyme co-localisation in this region. Studies in other brain regions, however, suggest that the overwhelming majority (95-98%) of neurons that express GAD2 also express GAD1, (Zhao et al., 2013). By contrast, a somewhat larger proportion (5-14%) of GAD1 expressing neurons do not express GAD2 in the lateral septum (Zhao et al., 2013). On balance then, our use of the GAD2-Cre line may have led us to slightly underestimate the proportion of GABA+ neurons within our sample. However, based on Allen mouse brain atlas data (Lein et al., 2007), it appears that similar proportions (~70%) of IGL/vLGN neurons express GAD1 and/or GAD2, which is in line with the proportions of optogenetically-identifiable cells we found in chapter 4. Accordingly, we think it unlikely that the cell populations we identify are not at least highly enriched for GABA+ and GABA- cells.

6.3 Key areas for follow-up work

Based on the new findings presented in this thesis and the insights gained along the way, there are a number of important areas for immediate follow up study:

6.3.1 Role of IGL and other visual nuclei in modulating circadian responses

Based on pharmacological inhibition data, we speculate that the GHT may act to modulate SCN colour discrimination in a circadian/diurnal manner. However, it is currently unclear whether SCN colour responses vary in circadian manner or whether signals provided by the GHT do. Having established protocols to investigate sensory properties in detail (e.g. Chapters 2 and 4), the most effective way to investigate is using optogenetics:

Halorhodopsin (NpHR) is a light-sensitive chloride pump, that when stimulated by 580nm light hyperpolarises cells by pumping Cl^- ions into the cell, effectively switching off neurons (Zhang et al., 2007). If NpHR is expressed in GAD2-expressing cells in the IGL, the vast majority of neurons within the IGL can be switched off with high temporal precision, allowing us to assess sensory properties of SCN neurons in the presence and absence of GHT input. Such an approach will thus allow us to avoid the possible confound of circadian/light adaptation-driven changes in cellular responsiveness that potentially complicate interpretation of the pharmacological inhibition approaches we used in chapter 5. We could therefore record from SCN neurons at different points across the day and use optogenetic inhibition of IGL GABA cells to ascertain whether sensory properties vary in a circadian manner and whether this property relies on GHT inputs. We could also use more selective optogenetic labelling of key IGL cell populations (e.g NPY cells; Moore and Spech (1993)) to identify which sensory signals they convey and/or their specific roles in modulating SCN light responses.

Given the discussion above (6.2.1), we would originally propose to employ these experiments in anaesthetised mice. However, since GHT cells may be modulated by arousal stimuli, moving forward it would also be highly informative to do these experiments in freely moving animals. It would also be interesting to use similar approaches to investigate involvement of other sources of visual input to SCN e.g. OPN.

6.3.2 Origins of SCN colour discrimination

It is currently unclear whether colour-discrimination in SCN neurons is driven directly by mRGCs or whether it involves local network processing within the retina. There are a number of directions we could take in order to investigate this:

One option would be to perform *in vitro* electrophysiological recordings from the mouse retina on a multielectrode array (MEA). Using pharmacological blockade of rod/cone pathways, identifying mRGCs under these conditions is straightforward (Berson et al., 2002), while our development of metameric stimuli will provide a reliable way to assess

their chromatic sensitivity. Such approaches could also be combined with retrograde optogenetic labelling to specifically identify SCN projecting cells. An additional/alternative approach (e.g. if colour opponent mRGCS could not be identified) would be to employ spatially structured metameric stimuli (e.g. Allen et al., 2014) to define the chromatic RFs of SCN neurons. If these are directly driven by retinal input one would expect them to exhibit spatially localised and overlapping S- and M-opsin driven subunits. In contrast, if chromatic properties of SCN neurons rely heavily on central processing this is unlikely to be the case. Moreover, using the protocols employed in this thesis, these experiments could be combined with optogenetic-based cell identification to determine which of the key SCN cell populations process colour (e.g. VIP cells or AVP cells).

6.3.3 Influence of colour on circadian physiology

As discussed above, it is clear from my data that colour does influence circadian rhythms but the specific details of how it does so are currently unclear. One experiment to investigate this could involve measuring mouse behaviour (e.g. wheel running) and applying melanopsin isoluminant blue or yellow pulses in late evening and/or early night to determine if blue or yellow light exerts stronger influence on the circadian system, and whether this arrangement varies according to circadian phase.

Moreover, to investigate the possibility that different populations of SCN neurons control different physiological outputs (as suggested earlier) we could in principle use similar approaches alongside measures of other whole animal rhythms (e.g. body temperature, hormone secretion etc.). Should these experiments confirm that distinct physiological outputs are indeed differentially sensitive to brightness vs. colour, we could then use electrophysiological approaches to define the neural circuitry controlling those responses, e.g. using antidromic activation to identify and characterise the sensory properties of SCN neurons projecting to output regions such as the paraventricular nuclei or dorsomedial hypothalamus.

Chapter 7: References

References from chapters 1 and 6 are included below. References for chapters 2-5 are included at the end of individual chapters.

7.1 Introduction

ABE, H., HONMA, S. & HONMA, K. 2007. Daily restricted feeding resets the circadian clock in the suprachiasmatic nucleus of CS mice. *Am J Physiol Regul Integr Comp Physiol,* 292**,** R607-15.

ABRAHAMSON, E. E. & MOORE, R. Y. 2001. Suprachiasmatic nucleus in the mouse: retinal innervation, intrinsic organization and efferent projections. *Brain Res,* 916**,** 172-91.

AGGELOPOULOS, N. C. & MEISSL, H. 2000. Responses of neurones of the rat suprachiasmatic nucleus to retinal illumination under photopic and scotopic conditions. *J Physiol,* 523 Pt 1**,** 211-22.

AGOSTINO, P. V., FERREYRA, G. A., MURAD, A. D., WATANABE, Y. & GOLOMBEK, D. A. 2004. Diurnal, circadian and photic regulation of calcium/calmodulin-dependent kinase II and neuronal nitric oxide synthase in the hamster suprachiasmatic nuclei. *Neurochem Int,* 44**,** 617-25.

AHNELT, P. K. & KOLB, H. 2000. The mammalian photoreceptor mosaic-adaptive design. *Prog Retin Eye Res,* 19**,** 711-77.

AIDA, R., MORIYA, T., ARAKI, M., AKIYAMA, M., WADA, K., WADA, E. & SHIBATA, S. 2002. Gastrin-releasing peptide mediates photic entrainable signals to dorsal subsets of suprachiasmatic nucleus via induction of Period gene in mice. *Mol Pharmacol,* 61**,** 26-34.

AKASHI, M., TSUCHIYA, Y., YOSHINO, T. & NISHIDA, E. 2002. Control of intracellular dynamics of mammalian period proteins by casein kinase I epsilon (CKIepsilon) and CKIdelta in cultured cells. *Mol Cell Biol,* 22**,** 1693-703.

AKASU, T., SHOJI, S. & HASUO, H. 1993. Inward rectifier and low-threshold calcium currents contribute to the spontaneous firing mechanism in neurons of the rat suprachiasmatic nucleus. *Pflugers Arch,* 425**,** 109-16.

ALAMILLA, J., PEREZ-BURGOS, A., QUINTO, D. & AGUILAR-ROBLERO, R. 2014. Circadian modulation of the Cl(-) equilibrium potential in the rat suprachiasmatic nuclei. *Biomed Res Int,* 2014**,** 424982.

ALBERS, H. E., LIOU, S. Y., STOPA, E. G. & ZOELLER, R. T. 1991. Interaction of colocalized neuropeptides: functional significance in the circadian timing system. *J Neurosci,* 11**,** 846-51.

ALBERS, H. E., OTTENWELLER, J. E., LIOU, S. Y., LUMPKIN, M. D. & ANDERSON, E. R. 1990. Neuropeptide Y in the hypothalamus: effect on corticosterone and single-unit activity. *Am J Physiol,* 258**,** R376-82.

ALBUS, H., VANSTEENSEL, M. J., MICHEL, S., BLOCK, G. D. & MEIJER, J. H. 2005. A GABAergic mechanism is necessary for coupling dissociable ventral and dorsal regional oscillators within the circadian clock. *Curr Biol,* 15**,** 886-93.

ALLEN, A. E., BROWN, T. M. & LUCAS, R. J. 2011. A distinct contribution of short-wavelength-sensitive cones to light-evoked activity in the mouse pretectal olivary nucleus. *J Neurosci,* 31**,** 16833-43.

ALLEN, A. E., STORCHI, R., MARTIAL, F. P., PETERSEN, R. S., MONTEMURRO, M. A., BROWN, T. M. & LUCAS, R. J. 2014. Melanopsin-driven light adaptation in mouse vision. *Curr Biol,* 24**,** 2481-90.

ALTIMUS, C. M., GULER, A. D., ALAM, N. M., ARMAN, A. C., PRUSKY, G. T., SAMPATH, A. P. & HATTAR, S. 2010. Rod photoreceptors drive circadian photoentrainment across a wide range of light intensities. *Nat Neurosci,* 13**,** 1107-12.

ALVADO, L. & ALLEN, C. N. 2008. Tetraethylammonium (TEA) increases the inactivation time constant of the transient K+ current in suprachiasmatic nucleus neurons. *Brain Res,* 1221**,** 24-9.

AMES, A., LI, Y. Y., HEHER, E. C. & KIMBLE, C. R. 1992. Energy metabolism of rabbit retina as related to function: high cost of Na+ transport. *J Neurosci,* 12**,** 840-53.

AN, S., TSAI, C., RONECKER, J., BAYLY, A. & HERZOG, E. D. 2012. Spatiotemporal distribution of vasoactive intestinal polypeptide receptor 2 in mouse suprachiasmatic nucleus. *J Comp Neurol,* 520**,** 2730-41.

ANTLE, M., MARCHANT, E., NIEL, L. & MISTLBERGER, R. 1998. Serotonin antagonists do not attenuate activity-induced phase shifts of circadian rhythms in the Syrian hamster. *Brain Research,* 813**,** 139-149.

ANTLE, M. C., GLASS, J. D. & MISTLBERGER, R. E. 2000. 5-HT(1A) autoreceptor antagonist-induced 5-HT release in the hamster suprachiasmatic nuclei: effects on circadian clock resetting. *Neurosci Lett,* 282**,** 97-100.

ANTLE, M. C., KRIEGSFELD, L. J. & SILVER, R. 2005. Signaling within the master clock of the brain: localized activation of mitogen-activated protein kinase by gastrin-releasing peptide. *J Neurosci,* 25**,** 2447-54.

ANTLE, M. C. & SILVER, R. 2005. Orchestrating time: arrangements of the brain circadian clock. *Trends Neurosci,* 28**,** 145-51.

APPLEBURY, M. L., ANTOCH, M. P., BAXTER, L. C., CHUN, L. L., FALK, J. D., FARHANGFAR, F., KAGE, K., KRZYSTOLIK, M. G., LYASS, L. A. & ROBBINS, J. T. 2000. The murine cone photoreceptor: a single cone type expresses both S and M opsins with retinal spatial patterning. *Neuron,* 27**,** 513-23.

ASCHOFF, J. 1965. Circadian rhythms in man - a self sustained oscillator with an inherent frequency underlies human 24-hour periodicity. *Science,* 148**,** 1427-1432.

ATKINSON, S., MAYWOOD, E., CHESHAM, J., WOZNY, C., COLWELL, C., HASTINGS, M. & WILLIAMS, S. 2011. Cyclic AMP signaling control of action potential firing rate and molecular circadian pacemaking in the suprachiasmatic nucleus. *Journal of Biological Rhythms,* 26.

ATON, S. J., COLWELL, C. S., HARMAR, A. J., WASCHEK, J. & HERZOG, E. D. 2005. Vasoactive intestinal polypeptide mediates circadian rhythmicity and synchrony in mammalian clock neurons. *Nat Neurosci,* 8**,** 476-83.

ATON, S. J., HUETTNER, J. E., STRAUME, M. & HERZOG, E. D. 2006. GABA and Gi/o differentially control circadian rhythms and synchrony in clock neurons. *Proc Natl Acad Sci U S A,* 103**,** 19188-93.

BADEA, T. C. & NATHANS, J. 2004. Quantitative analysis of neuronal morphologies in the mouse retina visualized by using a genetically directed reporter. *J Comp Neurol,* 480**,** 331-51.

BARNES, S. & KELLY, M. E. 2002. Calcium channels at the photoreceptor synapse. *Adv Exp Med Biol,* 514**,** 465-76.

BAVER, S. B., PICKARD, G. E. & SOLLARS, P. J. 2008. Two types of melanopsin retinal ganglion cell differentially innervate the hypothalamic suprachiasmatic nucleus and the olivary pretectal nucleus. *Eur J Neurosci,* 27**,** 1763-70.

BAYLISS, D. A. & BARRETT, P. Q. 2008. Emerging roles for two-pore-domain potassium channels and their potential therapeutic impact. *Trends Pharmacol Sci,* 29**,** 566-75.

BAYLOR, D. 1996. How photons start vision. *Proc Natl Acad Sci U S A,* 93**,** 560-5.

BELENKY, M. A., SMERASKI, C. A., PROVENCIO, I., SOLLARS, P. J. & PICKARD, G. E. 2003. Melanopsin retinal ganglion cells receive bipolar and amacrine cell synapses. *J Comp Neurol,* 460**,** 380-93.

BELLE, M. D., DIEKMAN, C. O., FORGER, D. B. & PIGGINS, H. D. 2009. Daily electrical silencing in the mammalian circadian clock. *Science,* 326**,** 281-4.

BELLE, M. D., HUGHES, A. T., BECHTOLD, D. A., CUNNINGHAM, P., PIERUCCI, M., BURDAKOV, D. & PIGGINS, H. D. 2014. Acute suppressive and long-term phase modulation actions of orexin on the mammalian circadian clock. *J Neurosci,* 34**,** 3607-21.

BENNETT, N. & SITARAMAYYA, A. 1988. Inactivation of photoexcited rhodopsin in retinal rods: the roles of rhodopsin kinase and 48-kDa protein (arrestin). *Biochemistry,* 27**,** 1710-5.

BERSON, D. M. 2003. Strange vision: ganglion cells as circadian photoreceptors. *Trends Neurosci,* 26**,** 314-20.

BERSON, D. M., CASTRUCCI, A. M. & PROVENCIO, I. 2010. Morphology and mosaics of melanopsin-expressing retinal ganglion cell types in mice. *J Comp Neurol,* 518**,** 2405-22.

BERSON, D. M., DUNN, F. A. & TAKAO, M. 2002. Phototransduction by retinal ganglion cells that set the circadian clock. *Science,* 295**,** 1070-3.

BIEL, M., WAHL-SCHOTT, C., MICHALAKIS, S. & ZONG, X. 2009. Hyperpolarization-activated cation channels: from genes to function. *Physiol Rev,* 89**,** 847-85.

BIELLO, S. M., GOLOMBEK, D. A. & HARRINGTON, M. E. 1997. Neuropeptide Y and glutamate block each other's phase shifts in the suprachiasmatic nucleus in vitro. *Neuroscience,* 77**,** 1049-57.

BIELLO, S. M. & MROSOVSKY, N. 1996. Phase response curves to neuropeptide Y in wildtype and tau mutant hamsters. *J Biol Rhythms,* 11**,** 27-34.

BLASIAK, T. & LEWANDOWSKI, M. H. 2013. Differential firing pattern and response to lighting conditions of rat intergeniculate leaflet neurons projecting to suprachiasmatic nucleus or contralateral intergeniculate leaflet. *Neuroscience,* 228C**,** 315-324.

BLOOMFIELD, S. A. & DACHEUX, R. F. 2001. Rod vision: pathways and processing in the mammalian retina. *Prog Retin Eye Res,* 20**,** 351-84.

BOBRZYNSKA, K. J., VRANG, N. & MROSOVSKY, N. 1996. Persistence of nonphotic phase shifts in hamsters after serotonin depletion in the suprachiasmatic nucleus. *Brain Res,* 741**,** 205-14.

BORTOFF, A. 1964. Localization of slow potential responses in the Necturus retina. *Vision Res,* 4**,** 627-35.

BOS, N. P. & MIRMIRAN, M. 1993. Effects of excitatory and inhibitory amino acids on neuronal discharges in the cultured suprachiasmatic nucleus. *Brain Res Bull,* 31**,** 67-72.

BOUSKILA, Y. & DUDEK, F. E. 1995. A rapidly activating type of outward rectifier K+ current and A-current in rat suprachiasmatic nucleus neurones. *J Physiol,* 488 (Pt 2)**,** 339-50.

BOWNDS, D., DAWES, J., MILLER, J. & STAHLMAN, M. 1972. Phosphorylation of frog photoreceptor membranes induced by light. *Nat New Biol,* 237**,** 125-7.

BRANDSTÄTTER, J. H., KOULEN, P. & WÄSSLE, H. 1997. Selective synaptic distribution of kainate receptor subunits in the two plexiform layers of the rat retina. *J Neurosci,* 17**,** 9298-307.
BREDT, D. S., HWANG, P. M. & SNYDER, S. H. 1990. Localization of nitric oxide synthase indicating a neural role for nitric oxide. *Nature,* 347**,** 768-70.
BREDT, D. S. & SNYDER, S. H. 1992. Nitric oxide, a novel neuronal messenger. *Neuron,* 8**,** 3-11.
BREUNINGER, T., PULLER, C., HAVERKAMP, S. & EULER, T. 2011. Chromatic bipolar cell pathways in the mouse retina. *J Neurosci,* 31**,** 6504-17.
BROWN, D. L., FESKANICH, D., SÁNCHEZ, B. N., REXRODE, K. M., SCHERNHAMMER, E. S. & LISABETH, L. D. 2009. Rotating night shift work and the risk of ischemic stroke. *Am J Epidemiol,* 169**,** 1370-7.
BROWN, T. M., ALLEN, A. E., AL-ENEZI, J., WYNNE, J., SCHLANGEN, L., HOMMES, V. & LUCAS, R. J. 2013. The melanopic sensitivity function accounts for melanopsin-driven responses in mice under diverse lighting conditions. *PLoS One,* 8**,** e53583.
BROWN, T. M., COLWELL, C. S., WASCHEK, J. A. & PIGGINS, H. D. 2007. Disrupted neuronal activity rhythms in the suprachiasmatic nuclei of vasoactive intestinal polypeptide-deficient mice. *J Neurophysiol,* 97**,** 2553-8.
BROWN, T. M., HUGHES, A. T. & PIGGINS, H. D. 2005. Gastrin-releasing peptide promotes suprachiasmatic nuclei cellular rhythmicity in the absence of vasoactive intestinal polypeptide-VPAC2 receptor signaling. *J Neurosci,* 25**,** 11155-64.
BROWN, T. M. & PIGGINS, H. D. 2007. Electrophysiology of the suprachiasmatic circadian clock. *Prog Neurobiol,* 82**,** 229-55.
BROWN, T. M., TSUJIMURA, S., ALLEN, A. E., WYNNE, J., BEDFORD, R., VICKERY, G., VUGLER, A. & LUCAS, R. J. 2012. Melanopsin-based brightness discrimination in mice and humans. *Curr Biol,* 22**,** 1134-41.
BROWN, T. M., WYNNE, J., PIGGINS, H. D. & LUCAS, R. J. 2011. Multiple hypothalamic cell populations encoding distinct visual information. *J Physiol,* 589**,** 1173-94.
BURNS, M. E. & BAYLOR, D. A. 2001. Activation, deactivation, and adaptation in vertebrate photoreceptor cells. *Annu Rev Neurosci,* 24**,** 779-805.
CAHILL, G. M. & MENAKER, M. 1989. Effects of excitatory amino acid receptor antagonists and agonists on suprachiasmatic nucleus responses to retinohypothalamic tract volleys. *Brain Res,* 479**,** 76-82.
CALDERONE, J. B. & JACOBS, G. H. 1995. Regional variations in the relative sensitivity to UV light in the mouse retina. *Vis Neurosci,* 12**,** 463-8.
CAMPBELL, G. & LIEBERMAN, A. R. 1982. Synaptic organization in the olivary pretectal nucleus of the adult rat. *Neurosci Lett,* 28**,** 151-5.
CARD, J. P. & MOORE, R. Y. 1984. The suprachiasmatic nucleus of the golden hamster: immunohistochemical analysis of cell and fiber distribution. *Neuroscience,* 13**,** 415-31.
CARD, J. P. & MOORE, R. Y. 1989. Organization of lateral geniculate-hypothalamic connections in the rat. *J Comp Neurol,* 284**,** 135-47.
CARTER-DAWSON, L. D. & LAVAIL, M. M. 1979. Rods and cones in the mouse retina. I. Structural analysis using light and electron microscopy. *J Comp Neurol,* 188**,** 245-62.
CASSONE, V. M., SPEH, J. C., CARD, J. P. & MOORE, R. Y. 1988. Comparative anatomy of the mammalian hypothalamic suprachiasmatic nucleus. *J Biol Rhythms,* 3**,** 71-91.
CASTEL, M., BELENKY, M., COHEN, S., OTTERSEN, O. P. & STORM-MATHISEN, J. 1993. Glutamate-like immunoreactivity in retinal terminals of the mouse suprachiasmatic nucleus. *Eur J Neurosci,* 5**,** 368-81.

CERVETTO, L., LAGNADO, L., PERRY, R. J., ROBINSON, D. W. & MCNAUGHTON, P. A. 1989. Extrusion of calcium from rod outer segments is driven by both sodium and potassium gradients. *Nature,* 337**,** 740-3.

CHALLET, E., SCARBROUGH, K., PENEV, P. D. & TUREK, F. W. 1998. Roles of suprachiasmatic nuclei and intergeniculate leaflets in mediating the phase-shifting effects of a serotonergic agonist and their photic modulation during subjective day. *J Biol Rhythms,* 13**,** 410-21.

CHANG, L., BREUNINGER, T. & EULER, T. 2013. Chromatic coding from cone-type unselective circuits in the mouse retina. *Neuron,* 77**,** 559-71.

CHEN, C. K., WOODRUFF, M. L., CHEN, F. S., CHEN, D. & FAIN, G. L. 2010. Background light produces a recoverin-dependent modulation of activated-rhodopsin lifetime in mouse rods. *J Neurosci,* 30**,** 1213-20.

CHEN, D., BUCHANAN, G. F., DING, J. M., HANNIBAL, J. & GILLETTE, M. U. 1999. Pituitary adenylyl cyclase-activating peptide: a pivotal modulator of glutamatergic regulation of the suprachiasmatic circadian clock. *Proc Natl Acad Sci U S A,* 96**,** 13468-73.

CHEN, S. K., BADEA, T. C. & HATTAR, S. 2011. Photoentrainment and pupillary light reflex are mediated by distinct populations of ipRGCs. *Nature,* 476**,** 92-5.

CHEN, T., ILLING, M., MOLDAY, L., HSU, Y., YAU, K. & MOLDAY, R. 1994. Subunit 2 (or beta) of retinal rod cGMP-gated cation channel is a component of the 240-kDa channel-associatedprotein and mediates Ca(2+)-calmodulin modulation. *Proc Natl Acad Sci USA,* 91**,** 11757-61.

CHOI, H. J., LEE, C. J., SCHROEDER, A., KIM, Y. S., JUNG, S. H., KIM, J. S., KIM, D. Y., SON, E. J., HAN, H. C., HONG, S. K., COLWELL, C. S. & KIM, Y. I. 2008. Excitatory actions of GABA in the suprachiasmatic nucleus. *J Neurosci,* 28**,** 5450-9.

CHÁVEZ, A. E. & DIAMOND, J. S. 2008. Diverse mechanisms underlie glycinergic feedback transmission onto rod bipolar cells in rat retina. *J Neurosci,* 28**,** 7919-28.

CLARKE, R. J. & IKEDA, H. 1985. Luminance and darkness detectors in the olivary and posterior pretectal nuclei and their relationship to the pupillary light reflex in the rat. I. Studies with steady luminance levels. *Exp Brain Res,* 57**,** 224-32.

CLOUES, R. K. & SATHER, W. A. 2003. Afterhyperpolarization regulates firing rate in neurons of the suprachiasmatic nucleus. *J Neurosci,* 23**,** 1593-604.

COLWELL, C. 2001. NMDA-evoked calcium transients and currents in the suprachiasmatic nucleus: gating by the circadian system. *European Journal of Neuroscience,* 13**,** 1420-1428.

COLWELL, C. S. 2011. Linking neural activity and molecular oscillations in the SCN. *Nat Rev Neurosci,* 12**,** 553-69.

COLWELL, C. S., FOSTER, R. G. & MENAKER, M. 1991. NMDA receptor antagonists block the effects of light on circadian behavior in the mouse. *Brain Res,* 554**,** 105-10.

COLWELL, C. S., MICHEL, S., ITRI, J., RODRIGUEZ, W., TAM, J., LELIEVRE, V., HU, Z., LIU, X. & WASCHEK, J. A. 2003. Disrupted circadian rhythms in VIP- and PHI-deficient mice. *Am J Physiol Regul Integr Comp Physiol,* 285**,** R939-49.

COLWELL, C. S., MICHEL, S., ITRI, J., RODRIGUEZ, W., TAM, J., LELIÈVRE, V., HU, Z. & WASCHEK, J. A. 2004. Selective deficits in the circadian light response in mice lacking PACAP. *Am J Physiol Regul Integr Comp Physiol,* 287**,** R1194-201.

COLWELL, C. S., RALPH, M. R. & MENAKER, M. 1990. Do NMDA receptors mediate the effects of light on circadian behavior? *Brain Res,* 523**,** 117-20.

COOK, P. B. & MCREYNOLDS, J. S. 1998. Lateral inhibition in the inner retina is important for spatial tuning of ganglion cells. *Nat Neurosci,* 1**,** 714-9.

CROOKS, J. & KOLB, H. 1992. Localization of GABA, glycine, glutamate and tyrosine hydroxylase in the human retina. *J Comp Neurol,* 315**,** 287-302.

CROUCH, R. K., CHADER, G. J., WIGGERT, B. & PEPPERBERG, D. R. 1996. Retinoids and the visual process. *Photochem Photobiol,* 64**,** 613-21.

CUI, L. N. & DYBALL, R. E. 1996. Synaptic input from the retina to the suprachiasmatic nucleus changes with the light-dark cycle in the Syrian hamster. *J Physiol,* 497 (Pt 2)**,** 483-93.

CUTLER, D. J., HARAURA, M., REED, H. E., SHEN, S., SHEWARD, W. J., MORRISON, C. F., MARSTON, H. M., HARMAR, A. J. & PIGGINS, H. D. 2003. The mouse VPAC2 receptor confers suprachiasmatic nuclei cellular rhythmicity and responsiveness to vasoactive intestinal polypeptide in vitro. *Eur J Neurosci,* 17**,** 197-204.

CUTLER, D. J., PIGGINS, H. D., SELBIE, L. A. & MASON, R. 1998. Responses to neuropeptide Y in adult hamster suprachiasmatic nucleus neurones in vitro. *Eur J Pharmacol,* 345**,** 155-62.

DACEY, D. M. 1990. The dopaminergic amacrine cell. *J Comp Neurol,* 301**,** 461-89.

DACEY, D. M. 1999. Primate retina: cell types, circuits and color opponency. *Prog Retin Eye Res,* 18**,** 737-63.

DACEY, D. M., LIAO, H. W., PETERSON, B. B., ROBINSON, F. R., SMITH, V. C., POKORNY, J., YAU, K. W. & GAMLIN, P. D. 2005. Melanopsin-expressing ganglion cells in primate retina signal colour and irradiance and project to the LGN. *Nature,* 433**,** 749-54.

DAI, J., VAN DER VLIET, J., SWAAB, D. F. & BUIJS, R. M. 1998. Human retinohypothalamic tract as revealed by in vitro postmortem tracing. *J Comp Neurol,* 397**,** 357-70.

DE JEU, M. & PENNARTZ, C. 2002. Circadian modulation of GABA function in the rat suprachiasmatic nucleus: excitatory effects during the night phase. *J Neurophysiol,* 87**,** 834-44.

DE JEU, M. T. & PENNARTZ, C. M. 1997. Functional characterization of the H-current in SCN neurons in subjective day and night: a whole-cell patch-clamp study in acutely prepared brain slices. *Brain Res,* 767**,** 72-80.

DE VRIES, M. J., NUNES CARDOZO, B., VAN DER WANT, J., DE WOLF, A. & MEIJER, J. H. 1993. Glutamate immunoreactivity in terminals of the retinohypothalamic tract of the brown Norwegian rat. *Brain Res,* 612**,** 231-7.

DIBNER, C., SCHIBLER, U. & ALBRECHT, U. 2010. The mammalian circadian timing system: organization and coordination of central and peripheral clocks. *Annu Rev Physiol,* 72**,** 517-49.

DING, J. M., BUCHANAN, G. F., TISCHKAU, S. A., CHEN, D., KURIASHKINA, L., FAIMAN, L. E., ALSTER, J. M., MCPHERSON, P. S., CAMPBELL, K. P. & GILLETTE, M. U. 1998. A neuronal ryanodine receptor mediates light-induced phase delays of the circadian clock. *Nature,* 394**,** 381-4.

DING, J. M., CHEN, D., WEBER, E. T., FAIMAN, L. E., REA, M. A. & GILLETTE, M. U. 1994. Resetting the biological clock: mediation of nocturnal circadian shifts by glutamate and NO. *Science,* 266**,** 1713-7.

DKHISSI-BENYAHYA, O., GRONFIER, C., DE VANSSAY, W., FLAMANT, F. & COOPER, H. M. 2007. Modeling the role of mid-wavelength cones in circadian responses to light. *Neuron,* 53**,** 677-87.

DO, M. T., KANG, S. H., XUE, T., ZHONG, H., LIAO, H. W., BERGLES, D. E. & YAU, K. W. 2009. Photon capture and signalling by melanopsin retinal ganglion cells. *Nature,* 457**,** 281-7.

DOLLET, A., ALBRECHT, U., COOPER, H. M. & DKHISSI-BENYAHYA, O. 2010. Cones are required for normal temporal responses to light of phase shifts and clock gene expression. *Chronobiol Int,* 27**,** 768-81.

DRAGICH, J. M., LOH, D. H., WANG, L. M., VOSKO, A. M., KUDO, T., NAKAMURA, T. J., ODOM, I. H., TATEYAMA, S., HAGOPIAN, A., WASCHEK, J. A. & COLWELL, C. S. 2010.

The role of the neuropeptides PACAP and VIP in the photic regulation of gene expression in the suprachiasmatic nucleus. *Eur J Neurosci,* 31**,** 864-75.
DROUYER, E., RIEUX, C., HUT, R. A. & COOPER, H. M. 2007. Responses of suprachiasmatic nucleus neurons to light and dark adaptation: relative contributions of melanopsin and rod-cone inputs. *J Neurosci,* 27**,** 9623-31.
DUDLEY, T. E., DINARDO, L. A. & GLASS, J. D. 1998. Endogenous regulation of serotonin release in the hamster suprachiasmatic nucleus. *J Neurosci,* 18**,** 5045-52.
DZIEMA, H. & OBRIETAN, K. 2002. PACAP potentiates L-type calcium channel conductance in suprachiasmatic nucleus neurons by activating the MAPK pathway. *J Neurophysiol,* 88**,** 1374-86.
EARNEST, D. J. & SLADEK, C. D. 1986. Circadian rhythms of vasopressin release from individual rat suprachiasmatic explants in vitro. *Brain Res,* 382**,** 129-33.
EBLING, F. J. 1996. The role of glutamate in the photic regulation of the suprachiasmatic nucleus. *Prog Neurobiol,* 50**,** 109-32.
ECKER, J. L., DUMITRESCU, O. N., WONG, K. Y., ALAM, N. M., CHEN, S. K., LEGATES, T., RENNA, J. M., PRUSKY, G. T., BERSON, D. M. & HATTAR, S. 2010. Melanopsin-expressing retinal ganglion-cell photoreceptors: cellular diversity and role in pattern vision. *Neuron,* 67**,** 49-60.
EDMONDS, S. C. 1977. Food and light as entrainers of circadian running activity in the rat. *Physiol Behav,* 18**,** 915-9.
EHLEN, J. C., GROSSMAN, G. H. & GLASS, J. D. 2001. In vivo resetting of the hamster circadian clock by 5-HT7 receptors in the suprachiasmatic nucleus. *J Neurosci,* 21**,** 5351-7.
EKESTEN, B. & GOURAS, P. 2005. Cone and rod inputs to murine retinal ganglion cells: evidence of cone opsin specific channels. *Vis Neurosci,* 22**,** 893-903.
EMANUEL, A. J. & DO, M. T. 2015. Melanopsin tristability for sustained and broadband phototransduction. *Neuron,* 85**,** 1043-55.
ETCHEGARAY, J. P., MACHIDA, K. K., NOTON, E., CONSTANCE, C. M., DALLMANN, R., DI NAPOLI, M. N., DEBRUYNE, J. P., LAMBERT, C. M., YU, E. A., REPPERT, S. M. & WEAVER, D. R. 2009. Casein kinase 1 delta regulates the pace of the mammalian circadian clock. *Mol Cell Biol,* 29**,** 3853-66.
FARAHBAKHSH, Z. T., HIDEG, K. & HUBBELL, W. L. 1993. Photoactivated conformational changes in rhodopsin: a time-resolved spin label study. *Science,* 262**,** 1416-9.
FARBER, D. B. & LOLLEY, R. N. 1974. Cyclic guanosine monophosphate: elevation in degenerating photoreceptor cells of the C3H mouse retina. *Science,* 186**,** 449-51.
FARRENS, D. L., ALTENBACH, C., YANG, K., HUBBELL, W. L. & KHORANA, H. G. 1996. Requirement of rigid-body motion of transmembrane helices for light activation of rhodopsin. *Science,* 274**,** 768-70.
FESENKO, E. E., KOLESNIKOV, S. S. & LYUBARSKY, A. L. 1985. Induction by cyclic GMP of cationic conductance in plasma membrane of retinal rod outer segment. *Nature,* 313**,** 310-3.
FOSTER, R. G., ARGAMASO, S., COLEMAN, S., COLWELL, C. S., LEDERMAN, A. & PROVENCIO, I. 1993. Photoreceptors regulating circadian behavior: a mouse model. *J Biol Rhythms,* 8 Suppl**,** S17-23.
FOSTER, R. G., PROVENCIO, I., HUDSON, D., FISKE, S., DE GRIP, W. & MENAKER, M. 1991. Circadian photoreception in the retinally degenerate mouse (rd/rd). *J Comp Physiol A,* 169**,** 39-50.
FREDRIKSSON, R., LAGERSTRÖM, M. C., LUNDIN, L. G. & SCHIÖTH, H. B. 2003. The G-protein-coupled receptors in the human genome form five main families. Phylogenetic analysis, paralogon groups, and fingerprints. *Mol Pharmacol,* 63**,** 1256-72.

FREEDMAN, M. S., LUCAS, R. J., SONI, B., VON SCHANTZ, M., MUNOZ, M., DAVID-GRAY, Z. & FOSTER, R. 1999. Regulation of mammalian circadian behavior by non-rod, non-cone, ocular photoreceptors. *Science,* 284**,** 502-4.

FREEMAN, G. M., KROCK, R. M., ATON, S. J., THABEN, P. & HERZOG, E. D. 2013. GABA networks destabilize genetic oscillations in the circadian pacemaker. *Neuron,* 78**,** 799-806.

GAMBLE, K. L., ALLEN, G. C., ZHOU, T. & MCMAHON, D. G. 2007. Gastrin-releasing peptide mediates light-like resetting of the suprachiasmatic nucleus circadian pacemaker through cAMP response element-binding protein and Per1 activation. *J Neurosci,* 27**,** 12078-87.

GARTHWAITE, J. 1991. Glutamate, nitric oxide and cell-cell signalling in the nervous system. *Trends Neurosci,* 14**,** 60-7.

GEKAKIS, N., STAKNIS, D., NGUYEN, H., DAVIS, F., WILSBACHER, L., KING, D., TAKAHASHI, J. & WEITZ, C. 1998. Role of the CLOCK protein in the mammalian circadian mechanism. Science.

GHOSH, K. K., BUJAN, S., HAVERKAMP, S., FEIGENSPAN, A. & WÄSSLE, H. 2004. Types of bipolar cells in the mouse retina. *J Comp Neurol,* 469**,** 70-82.

GILLETTE, M. U. & REPPERT, S. M. 1987. The hypothalamic suprachiasmatic nuclei: circadian patterns of vasopressin secretion and neuronal activity in vitro. *Brain Res Bull,* 19**,** 135-9.

GLASS, J. D., DINARDO, L. A. & EHLEN, J. C. 2000. Dorsal raphe nuclear stimulation of SCN serotonin release and circadian phase-resetting. *Brain Res,* 859**,** 224-32.

GLASS, J. D., GROSSMAN, G. H., FARNBAUCH, L. & DINARDO, L. 2003. Midbrain raphe modulation of nonphotic circadian clock resetting and 5-HT release in the mammalian suprachiasmatic nucleus. *J Neurosci,* 23**,** 7451-60.

GLOSMANN, M. & AHNELT, P. K. 1998. Coexpression of M- and S- opsin extends over the entire inferior mouse retina. Investigative Ophthalmology and Visual Science.

GOLDSTEIN, E. 2013. *Sensation and Perception,* California, USA, Wadsworth, Cengage Learning.

GOLOMBEK, D. A. & RALPH, M. R. 1995. Circadian responses to light: the calmodulin connection. *Neurosci Lett,* 192**,** 101-4.

GOLOMBEK, D. A. & ROSENSTEIN, R. E. 2010. Physiology of circadian entrainment. *Physiol Rev,* 90**,** 1063-102.

GOOLEY, J. J., RAJARATNAM, S. M., BRAINARD, G. C., KRONAUER, R. E., CZEISLER, C. A. & LOCKLEY, S. W. 2010. Spectral responses of the human circadian system depend on the irradiance and duration of exposure to light. *Sci Transl Med,* 2**,** 31ra33.

GREEN, D. J. & GILLETTE, R. 1982. Circadian rhythm of firing rate recorded from single cells in the rat suprachiasmatic brain slice. *Brain Res,* 245**,** 198-200.

GRIBKOFF, V., PIESCHL, R., WISIALOWSKI, T., VAN DEN POL, A. & YOCCA, F. 1998. Phase shifting of circadian rhythms and depression of neuronal activity in the rat suprachiasmatic nucleus byneuropeptide Y: mediation by different receptor subtypes. *The Journal of Neuroscience,* 18**,** 3014-3022.

GRIBKOFF, V. K., PIESCHL, R. L. & DUDEK, F. E. 2003. GABA receptor-mediated inhibition of neuronal activity in rat SCN in vitro: pharmacology and influence of circadian phase. *J Neurophysiol,* 90**,** 1438-48.

GRIBKOFF, V. K., PIESCHL, R. L., WISIALOWSKI, T. A., PARK, W. K., STRECKER, G. J., DE JEU, M. T., PENNARTZ, C. M. & DUDEK, F. E. 1999. A reexamination of the role of GABA in the mammalian suprachiasmatic nucleus. *J Biol Rhythms,* 14**,** 126-30.

GROOS, G. & HENDRIKS, J. 1982. Circadian rhythms in electrical discharge of rat suprachiasmatic neurones recorded in vitro. *Neurosci Lett,* 34**,** 283-8.

GROOS, G. & MASON, R. 1978. Maintained discharge of rat suprachiasmatic neurons at different adaptation levels. *Neurosci Lett,* 8**,** 59-64.
GROOS, G. A. & HENDRIKS, J. 1979. Regularly firing neurones in the rat suprachiasmatic nucleus. *Experientia,* 35**,** 1597-8.
GROSSMAN, G. H., MISTLBERGER, R. E., ANTLE, M. C., EHLEN, J. C. & GLASS, J. D. 2000. Sleep deprivation stimulates serotonin release in the suprachiasmatic nucleus. *Neuroreport,* 11**,** 1929-32.
GRUNWALD, M. E. & YAU, K. W. 2000. Modulation of rod cGMP-gated cation channel by calmodulin. *Methods Enzymol,* 315**,** 817-28.
GRUNWALD, M. E., YU, W. P., YU, H. H. & YAU, K. W. 1998. Identification of a domain on the beta-subunit of the rod cGMP-gated cation channel that mediates inhibition by calcium-calmodulin. *J Biol Chem,* 273**,** 9148-57.
GUILLAUMOND, F., DARDENTE, H., GIGUÈRE, V. & CERMAKIAN, N. 2005. Differential control of Bmal1 circadian transcription by REV-ERB and ROR nuclear receptors. *J Biol Rhythms,* 20**,** 391-403.
GULER, A. D., ECKER, J. L., LALL, G. S., HAQ, S., ALTIMUS, C. M., LIAO, H. W., BARNARD, A. R., CAHILL, H., BADEA, T. C., ZHAO, H., HANKINS, M. W., BERSON, D. M., LUCAS, R. J., YAU, K. W. & HATTAR, S. 2008. Melanopsin cells are the principal conduits for rod-cone input to non-image-forming vision. *Nature,* 453**,** 102-5.
GÖZ, D., STUDHOLME, K., LAPPI, D. A., ROLLAG, M. D., PROVENCIO, I. & MORIN, L. P. 2008. Targeted destruction of photosensitive retinal ganglion cells with a saporin conjugate alters the effects of light on mouse circadian rhythms. *PLoS One,* 3**,** e3153.
HACK, I., FRECH, M., DICK, O., PEICHL, L. & BRANDSTÄTTER, J. H. 2001. Heterogeneous distribution of AMPA glutamate receptor subunits at the photoreceptor synapses of rodent retina. *Eur J Neurosci,* 13**,** 15-24.
HAESELEER, F., HUANG, J., LEBIODA, L., SAARI, J. C. & PALCZEWSKI, K. 1998. Molecular characterization of a novel short-chain dehydrogenase/reductase that reduces all-trans-retinal. *J Biol Chem,* 273**,** 21790-9.
HAMADA, T., ANTLE, M. C. & SILVER, R. 2004. Temporal and spatial expression patterns of canonical clock genes and clock-controlled genes in the suprachiasmatic nucleus. *Eur J Neurosci,* 19**,** 1741-8.
HAMADA, T., LIOU, S. Y., FUKUSHIMA, T., MARUYAMA, T., WATANABE, S., MIKOSHIBA, K. & ISHIDA, N. 1999a. The role of inositol trisphosphate-induced Ca2+ release from IP3-receptor in the rat suprachiasmatic nucleus on circadian entrainment mechanism. *Neurosci Lett,* 263**,** 125-8.
HAMADA, T., NIKI, T., ZIGING, P., SUGIYAMA, T., WATANABE, S., MIKOSHIBA, K. & ISHIDA, N. 1999b. Differential expression patterns of inositol trisphosphate receptor types 1 and 3 in the rat suprachiasmatic nucleus. *Brain Res,* 838**,** 131-5.
HANNIBAL, J. 2006. Roles of PACAP-containing retinal ganglion cells in circadian timing. *Int Rev Cytol,* 251**,** 1-39.
HANNIBAL, J., BRABET, P. & FAHRENKRUG, J. 2008. Mice lacking the PACAP type I receptor have impaired photic entrainment and negative masking. *Am J Physiol Regul Integr Comp Physiol,* 295**,** R2050-8.
HANNIBAL, J., DING, J., CHEN, D., FAHRENKRUG, J., LARSEN, P., GILLETTE, M. & MIKKELSEN, J. 1997. Pituitary adenylate cyclase activating peptide (PACAP) in the retinohypothalamic tract: a potential daytime regulator of the biological clock. *The Journal of Neuroscience,* 17**,** 2637–2644.
HANNIBAL, J., JAMEN, F., NIELSEN, H. S., JOURNOT, L., BRABET, P. & FAHRENKRUG, J. 2001. Dissociation between light-induced phase shift of the circadian rhythm and clock

gene expression in mice lacking the pituitary adenylate cyclase activating polypeptide type 1 receptor. *J Neurosci,* 21**,** 4883-90.
HANNIBAL, J., MØLLER, M., OTTERSEN, O. P. & FAHRENKRUG, J. 2000. PACAP and glutamate are co-stored in the retinohypothalamic tract. *J Comp Neurol,* 418**,** 147-55.
HARMAR, A. J., ARIMURA, A., GOZES, I., JOURNOT, L., LABURTHE, M., PISEGNA, J. R., RAWLINGS, S. R., ROBBERECHT, P., SAID, S. I., SREEDHARAN, S. P., WANK, S. A. & WASCHEK, J. A. 1998. International Union of Pharmacology. XVIII. Nomenclature of receptors for vasoactive intestinal peptide and pituitary adenylate cyclase-activating polypeptide. *Pharmacol Rev,* 50**,** 265-70.
HARRINGTON, M. & RUSAK, B. 1989. Photic responses of geniculo-hypothalamic tract neurons in the Syrian hamster. *Visual Neuroscience,* 2.
HARRINGTON, M. E. 1997. The ventral lateral geniculate nucleus and the intergeniculate leaflet: interrelated structures in the visual and circadian systems. *Neurosci Biobehav Rev,* 21**,** 705-27.
HARRINGTON, M. E. & HOQUE, S. 1997. NPY opposes PACAP phase shifts via receptors different from those involved in NPY phase shifts. *Neuroreport,* 8**,** 2677-80.
HARRINGTON, M. E., HOQUE, S., HALL, A., GOLOMBEK, D. & BIELLO, S. 1999. Pituitary adenylate cyclase activating peptide phase shifts circadian rhythms in a manner similar to light. *J Neurosci,* 19**,** 6637-42.
HARRINGTON, M. E., NANCE, D. M. & RUSAK, B. 1985. Neuropeptide Y immunoreactivity in the hamster geniculo-suprachiasmatic tract. *Brain Res Bull,* 15**,** 465-72.
HARRINGTON, M. E. & RUSAK, B. 1986. Lesions of the thalamic intergeniculate leaflet alter hamster circadian rhythms. *J Biol Rhythms,* 1**,** 309-25.
HASTINGS, M. H. 1991. Neuroendocrine rhythms. *Pharmacol Ther,* 50**,** 35-71.
HATORI, M., LE, H., VOLLMERS, C., KEDING, S. R., TANAKA, N., BUCH, T., WAISMAN, A., SCHMEDT, C., JEGLA, T. & PANDA, S. 2008. Inducible ablation of melanopsin-expressing retinal ganglion cells reveals their central role in non-image forming visual responses. *PLoS One,* 3**,** e2451.
HATTAR, S., KUMAR, M., PARK, A., TONG, P., TUNG, J., YAU, K. W. & BERSON, D. M. 2006. Central projections of melanopsin-expressing retinal ganglion cells in the mouse. *J Comp Neurol,* 497**,** 326-49.
HATTAR, S., LIAO, H. W., TAKAO, M., BERSON, D. M. & YAU, K. W. 2002. Melanopsin-containing retinal ganglion cells: architecture, projections, and intrinsic photosensitivity. *Science,* 295**,** 1065-70.
HATTAR, S., LUCAS, R. J., MROSOVSKY, N., THOMPSON, S., DOUGLAS, R. H., HANKINS, M. W., LEM, J., BIEL, M., HOFMANN, F., FOSTER, R. G. & YAU, K. W. 2003. Melanopsin and rod-cone photoreceptive systems account for all major accessory visual functions in mice. *Nature,* 424**,** 76-81.
HAVERKAMP, S., GRÜNERT, U. & WÄSSLE, H. 2001. Localization of kainate receptors at the cone pedicles of the primate retina. *J Comp Neurol,* 436**,** 471-86.
HAVERKAMP, S. & WÄSSLE, H. 2000. Immunocytochemical analysis of the mouse retina. *J Comp Neurol,* 424**,** 1-23.
HAVERKAMP, S., WÄSSLE, H., DUEBEL, J., KUNER, T., AUGUSTINE, G. J., FENG, G. & EULER, T. 2005. The primordial, blue-cone color system of the mouse retina. *J Neurosci,* 25**,** 5438-45.
HAY-SCHMIDT, A., VRANG, N., LARSEN, P. J. & MIKKELSEN, J. D. 2003. Projections from the raphe nuclei to the suprachiasmatic nucleus of the rat. *J Chem Neuroanat,* 25**,** 293-310.
HAYNES, L. & YAU, K. W. 1985. Cyclic GMP-sensitive conductance in outer segment membrane of catfish cones. *Nature,* 317**,** 61-4.

HERZOG, E. D., TAKAHASHI, J. S. & BLOCK, G. D. 1998. Clock controls circadian period in isolated suprachiasmatic nucleus neurons. *Nat Neurosci,* 1**,** 708-13.
HILLMAN, P., HOCHSTEIN, S. & MINKE, B. 1983. Transduction in invertebrate photoreceptors: role of pigment bistability. *Physiol Rev,* 63**,** 668-772.
HOFMAN, M. A. & SWAAB, D. F. 1994. Alterations in circadian rhythmicity of the vasopressin-producing neurons of the human suprachiasmatic nucleus (SCN) with aging. *Brain Res,* 651**,** 134-42.
HONMA, S., SHIRAKAWA, T., KATSUNO, Y., NAMIHIRA, M. & HONMA, K. 1998. Circadian periods of single suprachiasmatic neurons in rats. *Neurosci Lett,* 250**,** 157-60.
HOWARTH, M., WALMSLEY, L. & BROWN, T. M. 2014. Binocular integration in the mouse lateral geniculate nuclei. *Curr Biol,* 24**,** 1241-7.
HSU, Y. T. & MOLDAY, R. S. 1993. Modulation of the cGMP-gated channel of rod photoreceptor cells by calmodulin. *Nature,* 361**,** 76-9.
HUANG, S. K. & PAN, J. T. 1993. Potentiating effects of serotonin and vasoactive intestinal peptide on the action of glutamate on suprachiasmatic neurons in brain slices. *Neurosci Lett,* 159**,** 1-4.
HUBERMAN, A. D. & NIELL, C. M. 2011. What can mice tell us about how vision works? *Trends Neurosci,* 34**,** 464-73.
HUGHES, A. T., FAHEY, B., CUTLER, D. J., COOGAN, A. N. & PIGGINS, H. D. 2004. Aberrant gating of photic input to the suprachiasmatic circadian pacemaker of mice lacking the VPAC2 receptor. *J Neurosci,* 24**,** 3522-6.
HUGHES, A. T., GUILDING, C., LENNOX, L., SAMUELS, R. E., MCMAHON, D. G. & PIGGINS, H. D. 2008. Live imaging of altered period1 expression in the suprachiasmatic nuclei of Vipr2-/- mice. *J Neurochem,* 106**,** 1646-57.
HUGHES, A. T. & PIGGINS, H. D. 2008. Behavioral responses of Vipr2-/- mice to light. *J Biol Rhythms,* 23**,** 211-9.
HUGHES, S., WATSON, T. S., FOSTER, R. G., PEIRSON, S. N. & HANKINS, M. W. 2013. Nonuniform distribution and spectral tuning of photosensitive retinal ganglion cells of the mouse retina. *Curr Biol,* 23**,** 1696-701.
HUGHES, S., WELSH, L., KATTI, C., GONZÁLEZ-MENÉNDEZ, I., TURTON, M., HALFORD, S., SEKARAN, S., PEIRSON, S. N., HANKINS, M. W. & FOSTER, R. G. 2012. Differential expression of melanopsin isoforms Opn4L and Opn4S during postnatal development of the mouse retina. *PLoS One,* 7**,** e34531.
HUHMAN, K. L. & ALBERS, H. E. 1994. Neuropeptide Y microinjected into the suprachiasmatic region phase shifts circadian rhythms in constant darkness. *Peptides,* 15**,** 1475-8.
HULBERT, E. 1953. Explanation of the Brightness and Color of the Sky, Particularly the Twilight Sky.: The Journal of the Optical Society of America.
HURVICH, L. M. & JAMESON, D. 1957. An opponent-process theory of color vision. *Psychol Rev,* 64, Part 1**,** 384-404.
IBATA, Y., TAKAHASHI, Y., OKAMURA, H., KAWAKAMI, F., TERUBAYASHI, H., KUBO, T. & YANAIHARA, N. 1989. Vasoactive intestinal peptide (VIP)-like immunoreactive neurons located in the rat suprachiasmatic nucleus receive a direct retinal projection. *Neurosci Lett,* 97**,** 1-5.
INOUYE, S. & KAWAMURA, H. 1982. Characteristics of a circadian pacemaker in the suprachiasmatic nucleus. *Journal of comparative physiology,* 146**,** 153-160.
INOUYE, S. T. & KAWAMURA, H. 1979. Persistence of circadian rhythmicity in a mammalian hypothalamic "island" containing the suprachiasmatic nucleus. *Proc Natl Acad Sci U S A,* 76**,** 5962-6.

ISOLDI, M. C., ROLLAG, M. D., CASTRUCCI, A. M. & PROVENCIO, I. 2005. Rhabdomeric phototransduction initiated by the vertebrate photopigment melanopsin. *Proc Natl Acad Sci U S A,* 102**,** 1217-21.

ITRI, J. N., MICHEL, S., VANSTEENSEL, M. J., MEIJER, J. H. & COLWELL, C. S. 2005. Fast delayed rectifier potassium current is required for circadian neural activity. *Nat Neurosci,* 8**,** 650-6.

ITRI, J. N., VOSKO, A. M., SCHROEDER, A., DRAGICH, J. M., MICHEL, S. & COLWELL, C. S. 2010. Circadian regulation of a-type potassium currents in the suprachiasmatic nucleus. *J Neurophysiol,* 103**,** 632-40.

JACKSON, A. C., YAO, G. L. & BEAN, B. P. 2004. Mechanism of spontaneous firing in dorsomedial suprachiasmatic nucleus neurons. *J Neurosci,* 24**,** 7985-98.

JEON, C. J., STRETTOI, E. & MASLAND, R. H. 1998. The major cell populations of the mouse retina. *J Neurosci,* 18**,** 8936-46.

JIANG, Z. G., TESHIMA, K., YANG, Y., YOSHIOKA, T. & ALLEN, C. N. 2000. Pre- and postsynaptic actions of serotonin on rat suprachiasmatic nucleus neurons. *Brain Res,* 866**,** 247-56.

JOHNSON, C. H. 1999. Forty years of PRCs--what have we learned? *Chronobiol Int,* 16**,** 711-43.

JOHNSON, J., SHERRY, D. M., LIU, X., FREMEAU, R. T., SEAL, R. P., EDWARDS, R. H. & COPENHAGEN, D. R. 2004. Vesicular glutamate transporter 3 expression identifies glutamatergic amacrine cells in the rodent retina. *J Comp Neurol,* 477**,** 386-98.

JOHNSON, R. F., MOORE, R. Y. & MORIN, L. P. 1988a. Loss of entrainment and anatomical plasticity after lesions of the hamster retinohypothalamic tract. *Brain Res,* 460**,** 297-313.

JOHNSON, R. F., MORIN, L. P. & MOORE, R. Y. 1988b. Retinohypothalamic projections in the hamster and rat demonstrated using cholera toxin. *Brain Res,* 462**,** 301-12.

JUHL, F., HANNIBAL, J. & FAHRENKRUG, J. 2007. Photic induction of c-Fos in enkephalin neurons of the rat intergeniculate leaflet innervated by retinal PACAP fibres. *Cell Tissue Res,* 329**,** 491-502.

KALLINGAL, G. J. & MINTZ, E. M. 2006. Glutamatergic activity modulates the phase-shifting effects of gastrin-releasing peptide and light. *Eur J Neurosci,* 24**,** 2853-8.

KALSBEEK, A., PALM, I. F., LA FLEUR, S. E., SCHEER, F. A., PERREAU-LENZ, S., RUITER, M., KREIER, F., CAILOTTO, C. & BUIJS, R. M. 2006. SCN outputs and the hypothalamic balance of life. *J Biol Rhythms,* 21**,** 458-69.

KARATSOREOS, I. N., ROMEO, R. D., MCEWEN, B. S. & SILVER, R. 2006. Diurnal regulation of the gastrin-releasing peptide receptor in the mouse circadian clock. *Eur J Neurosci,* 23**,** 1047-53.

KAWAGUCHI, C., TANAKA, K., ISOJIMA, Y., SHINTANI, N., HASHIMOTO, H., BABA, A. & NAGAI, K. 2003. Changes in light-induced phase shift of circadian rhythm in mice lacking PACAP. *Biochem Biophys Res Commun,* 310**,** 169-75.

KAWAMURA, S. 1993. Rhodopsin phosphorylation as a mechanism of cyclic GMP phosphodiesterase regulation by S-modulin. *Nature,* 362**,** 855-7.

KAWAMURA, S., HISATOMI, O., KAYADA, S., TOKUNAGA, F. & KUO, C. H. 1993. Recoverin has S-modulin activity in frog rods. *J Biol Chem,* 268**,** 14579-82.

KENNAWAY, D. J. 2004. Resetting the suprachiasmatic nucleus clock. *Front Biosci,* 9**,** 56-62.

KENT, J. & MEREDITH, A. L. 2008. BK channels regulate spontaneous action potential rhythmicity in the suprachiasmatic nucleus. *PLoS One,* 3**,** e3884.

KIM, D. Y., CHOI, H. J., KIM, J. S., KIM, Y. S., JEONG, D. U., SHIN, H. C., KIM, M. J., HAN, H. C., HONG, S. K. & KIM, Y. I. 2005. Voltage-gated calcium channels play crucial roles in the glutamate-induced phase shifts of the rat suprachiasmatic circadian clock. *Eur J Neurosci,* 21**,** 1215-22.

KIM, Y. I. & DUDEK, F. E. 1991. Intracellular electrophysiological study of suprachiasmatic nucleus neurons in rodents: excitatory synaptic mechanisms. *J Physiol,* 444**,** 269-87.
KISELEV, A. & SUBRAMANIAM, S. 1994. Activation and regeneration of rhodopsin in the insect visual cycle. *Science,* 266**,** 1369-73.
KO, C. H. & TAKAHASHI, J. S. 2006. Molecular components of the mammalian circadian clock. *Hum Mol Genet,* 15 Spec No 2**,** R271-7.
KOCH, K. W. & STRYER, L. 1988. Highly cooperative feedback control of retinal rod guanylate cyclase by calcium ions. *Nature,* 334**,** 64-6.
KOLB, H. 1982. The morphology of the bipolar cells, amacrine cells and ganglion cells in the retina of the turtle Pseudemys scripta elegans. *Philos Trans R Soc Lond B Biol Sci,* 298**,** 355-93.
KOLB, H., CUENCA, N., WANG, H. H. & DEKORVER, L. 1990. The synaptic organization of the dopaminergic amacrine cell in the cat retina. *J Neurocytol,* 19**,** 343-66.
KOLB, H., FERNÁNDEZ, E., AMMERMÜLLER, J. & CUENCA, N. 1995. Substance P: a neurotransmitter of amacrine and ganglion cells in the vertebrate retina. *Histol Histopathol,* 10**,** 947-68.
KOLB, H., NELSON, R. & MARIANI, A. 1981. Amacrine cells, bipolar cells and ganglion cells of the cat retina: a Golgi study. *Vision Res,* 21**,** 1081-1114.
KONONENKO, N. I., HONMA, S., DUDEK, F. E. & HONMA, K. 2008. On the role of calcium and potassium currents in circadian modulation of firing rate in rat suprachiasmatic nucleus neurons: multielectrode dish analysis. *Neurosci Res,* 62**,** 51-7.
KONONENKO, N. I., SHAO, L. R. & DUDEK, F. E. 2004. Riluzole-sensitive slowly inactivating sodium current in rat suprachiasmatic nucleus neurons. *J Neurophysiol,* 91**,** 710-8.
KOPP, M. D., MEISSL, H., DEHGHANI, F. & KORF, H. W. 2001. The pituitary adenylate cyclase-activating polypeptide modulates glutamatergic calcium signalling: investigations on rat suprachiasmatic nucleus neurons. *J Neurochem,* 79**,** 161-71.
KOUTALOS, Y. & YAU, K. W. 1996. Regulation of sensitivity in vertebrate rod photoreceptors by calcium. *Trends Neurosci,* 19**,** 73-81.
KRAFT, T. W., SCHNEEWEIS, D. M. & SCHNAPF, J. L. 1993. Visual transduction in human rod photoreceptors. *J Physiol,* 464**,** 747-65.
KUDO, T., LOH, D. H., KULJIS, D., CONSTANCE, C. & COLWELL, C. S. 2011. Fast delayed rectifier potassium current: critical for input and output of the circadian system. *J Neurosci,* 31**,** 2746-55.
KUHLMAN, S. J. & MCMAHON, D. G. 2004. Rhythmic regulation of membrane potential and potassium current persists in SCN neurons in the absence of environmental input. *Eur J Neurosci,* 20**,** 1113-7.
KUME, K., ZYLKA, M. J., SRIRAM, S., SHEARMAN, L. P., WEAVER, D. R., JIN, X., MAYWOOD, E. S., HASTINGS, M. H. & REPPERT, S. M. 1999. mCRY1 and mCRY2 are essential components of the negative limb of the circadian clock feedback loop. *Cell,* 98**,** 193-205.
KÜHN, H. 1978. Light-regulated binding of rhodopsin kinase and other proteins to cattle photoreceptor membranes. *Biochemistry,* 17**,** 4389-95.
KÜHN, H., BENNETT, N., MICHEL-VILLAZ, M. & CHABRE, M. 1981. Interactions between photoexcited rhodopsin and GTP-binding protein: kinetic and stoichiometric analyses from light-scattering changes. *Proc Natl Acad Sci U S A,* 78**,** 6873-7.
LALL, G. S., REVELL, V. L., MOMIJI, H., AL ENEZI, J., ALTIMUS, C. M., GULER, A. D., AGUILAR, C., CAMERON, M. A., ALLENDER, S., HANKINS, M. W. & LUCAS, R. J. 2010. Distinct contributions of rod, cone, and melanopsin photoreceptors to encoding irradiance. *Neuron,* 66**,** 417-28.
LEANDER, P., VRANG, N. & MØLLER, M. 1998. Neuronal projections from the mesencephalic raphe nuclear complex to the suprachiasmatic nucleus and the

deep pineal gland of the golden hamster (Mesocricetus auratus). *J Comp Neurol,* 399**,** 73-93.

LEE, C., ETCHEGARAY, J. P., CAGAMPANG, F. R., LOUDON, A. S. & REPPERT, S. M. 2001. Posttranslational mechanisms regulate the mammalian circadian clock. *Cell,* 107**,** 855-67.

LEWANDOWSKI, M. H. & USAREK, A. 2002. Effects of intergeniculate leaflet lesions on circadian rhythms in the mouse. *Behav Brain Res,* 128**,** 13-7.

LI, J. D., BURTON, K. J., ZHANG, C., HU, S. B. & ZHOU, Q. Y. 2009. Vasopressin receptor V1a regulates circadian rhythms of locomotor activity and expression of clock-controlled genes in the suprachiasmatic nuclei. *Am J Physiol Regul Integr Comp Physiol,* 296**,** R824-30.

LI, X., REN, C., HUANG, L., LIN, B., PU, M., PICKARD, G. E. & SO, K. F. 2015. The Dorsal Raphe Nucleus Receives Afferents From Alpha-Like Retinal Ganglion Cells and Intrinsically Photosensitive Retinal Ganglion Cells in the Rat. *Invest Ophthalmol Vis Sci,* 56**,** 8373-81.

LIOU, S. Y. & ALBERS, H. E. 1989. Single unit response of suprachiasmatic neurons to arginine vasopressin (AVP) is mediated by a V1-like receptor in the hamster. *Brain Res,* 477**,** 336-43.

LIOU, S. Y. & ALBERS, H. E. 1991. Single unit response of neurons within the hamster suprachiasmatic nucleus to neuropeptide Y. *Brain Res Bull,* 27**,** 825-8.

LIOU, S. Y., SHIBATA, S., IWASAKI, K. & UEKI, S. 1986. Optic nerve stimulation-induced increase of release of 3H-glutamate and 3H-aspartate but not 3H-GABA from the suprachiasmatic nucleus in slices of rat hypothalamus. *Brain Res Bull,* 16**,** 527-31.

LIU, C. & REPPERT, S. M. 2000. GABA synchronizes clock cells within the suprachiasmatic circadian clock. *Neuron,* 25**,** 123-8.

LIU, C., WEAVER, D. R., STROGATZ, S. H. & REPPERT, S. M. 1997. Cellular construction of a circadian clock: period determination in the suprachiasmatic nuclei. *Cell,* 91**,** 855-60.

LOKSHIN, M., LESAUTER, J. & SILVER, R. 2015. Selective Distribution of Retinal Input to Mouse SCN Revealed in Analysis of Sagittal Sections. *J Biol Rhythms,* 30**,** 251-7.

LOLLEY, R. N., FARBER, D. B., RAYBORN, M. E. & HOLLYFIELD, J. G. 1977. Cyclic GMP accumulation causes degeneration of photoreceptor cells: simulation of an inherited disease. *Science,* 196**,** 664-6.

LOLLEY, R. N. & RACZ, E. 1982. Calcium modulation of cyclic GMP synthesis in rat visual cells. *Vision Res,* 22**,** 1481-6.

LUCAS, R. J., DOUGLAS, R. H. & FOSTER, R. G. 2001. Characterization of an ocular photopigment capable of driving pupillary constriction in mice. *Nat Neurosci,* 4**,** 621-6.

LUCAS, R. J., FREEDMAN, M. S., MUÑOZ, M., GARCIA-FERNÁNDEZ, J. M. & FOSTER, R. G. 1999. Regulation of the mammalian pineal by non-rod, non-cone, ocular photoreceptors. *Science,* 284**,** 505-7.

LUCAS, R. J., HATTAR, S., TAKAO, M., BERSON, D. M., FOSTER, R. G. & YAU, K. W. 2003. Diminished pupillary light reflex at high irradiances in melanopsin-knockout mice. *Science,* 299**,** 245-7.

LUCAS, R. J., LALL, G. S., ALLEN, A. E. & BROWN, T. M. 2012. How rod, cone, and melanopsin photoreceptors come together to enlighten the mammalian circadian clock. *Prog Brain Res,* 199**,** 1-18.

LUPI, D., COOPER, H. M., FROEHLICH, A., STANDFORD, L., MCCALL, M. A. & FOSTER, R. G. 1999. Transgenic ablation of rod photoreceptors alters the circadian phenotype of mice. *Neuroscience,* 89**,** 363-74.

MACNEIL, M. A. & MASLAND, R. H. 1998. Extreme diversity among amacrine cells: implications for function. *Neuron,* 20**,** 971-82.
MANOOKIN, M. B., BEAUDOIN, D. L., ERNST, Z. R., FLAGEL, L. J. & DEMB, J. B. 2008. Disinhibition combines with excitation to extend the operating range of the OFF visual pathway in daylight. *J Neurosci,* 28**,** 4136-50.
MARCHANT, E. G. & MORIN, L. P. 1999. The hamster circadian rhythm system includes nuclei of the subcortical visual shell. *J Neurosci,* 19**,** 10482-93.
MARSHAK, D. W. & MILLS, S. L. 2014. Short-wavelength cone-opponent retinal ganglion cells in mammals. *Vis Neurosci,* 31**,** 165-75.
MASLAND, R. H. 2001. The fundamental plan of the retina. *Nat Neurosci,* 4**,** 877-86.
MASON, R. 1986. Circadian variation in sensitivity of suprachiasmatic and lateral geniculate neurones to 5-hydroxytryptamine in the rat. *J Physiol,* 377**,** 1-13.
MASON, R., HARRINGTON, M. E. & RUSAK, B. 1987. Electrophysiological responses of hamster suprachiasmatic neurones to neuropeptide Y in the hypothalamic slice preparation. *Neurosci Lett,* 80**,** 173-9.
MASU, M., IWAKABE, H., TAGAWA, Y., MIYOSHI, T., YAMASHITA, M., FUKUDA, Y., SASAKI, H., HIROI, K., NAKAMURA, Y. & SHIGEMOTO, R. 1995. Specific deficit of the ON response in visual transmission by targeted disruption of the mGluR6 gene. *Cell,* 80**,** 757-65.
MATHIE, A. 2007. Neuronal two-pore-domain potassium channels and their regulation by G protein-coupled receptors. *J Physiol,* 578**,** 377-85.
MATHUR, A., GOLOMBEK, D. A. & RALPH, M. R. 1996. cGMP-dependent protein kinase inhibitors block light-induced phase advances of circadian rhythms in vivo. *Am J Physiol,* 270**,** R1031-6.
MATSUYAMA, T., YAMASHITA, T., IMAMOTO, Y. & SHICHIDA, Y. 2012. Photochemical properties of mammalian melanopsin. *Biochemistry,* 51**,** 5454-62.
MATURANA, H. R. & VARELA, F. J. 1982. Color-opponent responses in the avian lateral geniculate: a study in the quail (Coturnix coturnix japonica). *Brain Res,* 247**,** 227-41.
MAYWOOD, E. S., CHESHAM, J. E., O'BRIEN, J. A. & HASTINGS, M. H. 2011. A diversity of paracrine signals sustains molecular circadian cycling in suprachiasmatic nucleus circuits. *Proc Natl Acad Sci U S A,* 108**,** 14306-11.
MAYWOOD, E. S., REDDY, A. B., WONG, G. K., O'NEILL, J. S., O'BRIEN, J. A., MCMAHON, D. G., HARMAR, A. J., OKAMURA, H. & HASTINGS, M. H. 2006. Synchronization and maintenance of timekeeping in suprachiasmatic circadian clock cells by neuropeptidergic signaling. *Curr Biol,* 16**,** 599-605.
MCMAHON, D. G., KNAPP, A. G. & DOWLING, J. E. 1989. Horizontal cell gap junctions: single-channel conductance and modulation by dopamine. *Proc Natl Acad Sci U S A,* 86**,** 7639-43.
MCPHERSON, P. S., KIM, Y. K., VALDIVIA, H., KNUDSON, C. M., TAKEKURA, H., FRANZINI-ARMSTRONG, C., CORONADO, R. & CAMPBELL, K. P. 1991. The brain ryanodine receptor: a caffeine-sensitive calcium release channel. *Neuron,* 7**,** 17-25.
MEDANIC, M. & GILLETTE, M. U. 1992. Serotonin regulates the phase of the rat suprachiasmatic circadian pacemaker in vitro only during the subjective day. *J Physiol,* 450**,** 629-42.
MEEKER, R. B., GREENWOOD, R. S. & HAYWARD, J. N. 1994. Glutamate receptors in the rat hypothalamus and pituitary. *Endocrinology,* 134**,** 621-9.
MEIJER, J. H., GROOS, G. A. & RUSAK, B. 1986. Luminance coding in a circadian pacemaker: the suprachiasmatic nucleus of the rat and the hamster. *Brain Res,* 382**,** 109-18.
MEIJER, J. H., WATANABE, K., SCHAAP, J., ALBUS, H. & DÉTÁRI, L. 1998. Light responsiveness of the suprachiasmatic nucleus: long-term multiunit and single-unit recordings in freely moving rats. *J Neurosci,* 18**,** 9078-87.

MELYAN, Z., TARTTELIN, E. E., BELLINGHAM, J., LUCAS, R. J. & HANKINS, M. W. 2005. Addition of human melanopsin renders mammalian cells photoresponsive. *Nature,* 433**,** 741-5.

MENDOZA, J., CLESSE, D., PÉVET, P. & CHALLET, E. 2008. Serotonergic potentiation of dark pulse-induced phase-shifting effects at midday in hamsters. *J Neurochem,* 106**,** 1404-14.

MENGER, N., POW, D. V. & WÄSSLE, H. 1998. Glycinergic amacrine cells of the rat retina. *J Comp Neurol,* 401**,** 34-46.

MEREDITH, A. L., WILER, S. W., MILLER, B. H., TAKAHASHI, J. S., FODOR, A. A., RUBY, N. F. & ALDRICH, R. W. 2006. BK calcium-activated potassium channels regulate circadian behavioral rhythms and pacemaker output. *Nat Neurosci,* 9**,** 1041-9.

MEYER-BERNSTEIN, E. & MORIN, L. 1996. Differential serotonergic innervation of the suprachiasmatic nucleus and the intergeniculate leaflet and its role in circadian rhythm modulation. The Journal of Neuroscience.

MEYER-BERNSTEIN, E. & MORIN, L. 1999. Electrical stimulation of the median or dorsal raphe nuclei reduces light-induced FOS protein in thesuprachiasmatic nucleus and causes circadian activity rhythm phase shifts. *Brain Research,* 92**,** 267-279.

MEYER-BERNSTEIN, E. L., BLANCHARD, J. H. & MORIN, L. P. 1997. The serotonergic projection from the median raphe nucleus to the suprachiasmatic nucleus modulates activity phase onset, but not other circadian rhythm parameters. *Brain Res,* 755**,** 112-20.

MIEDA, M., ONO, D., HASEGAWA, E., OKAMOTO, H., HONMA, K., HONMA, S. & SAKURAI, T. 2015. Cellular clocks in AVP neurons of the SCN are critical for interneuronal coupling regulating circadian behavior rhythm. *Neuron,* 85**,** 1103-16.

MIHAI, R., JUSS, T. S. & INGRAM, C. D. 1994. Suppression of suprachiasmatic nucleus neurone activity with a vasopressin receptor antagonist: possible role for endogenous vasopressin in circadian activity cycles in vitro. *Neurosci Lett,* 179**,** 95-9.

MIKKELSEN, J. D. 1992. The organization of the crossed geniculogeniculate pathway of the rat: a Phaseolus vulgaris-leucoagglutinin study. *Neuroscience,* 48**,** 953-62.

MILLER, J. D. & FULLER, C. A. 1990. The response of suprachiasmatic neurons of the rat hypothalamus to photic and serotonergic stimulation. *Brain Res,* 515**,** 155-62.

MOGA, M. M. & MOORE, R. Y. 1997. Organization of neural inputs to the suprachiasmatic nucleus in the rat. *J Comp Neurol,* 389**,** 508-34.

MOLDAY, R. S. & MOLDAY, L. L. 1998. Molecular properties of the cGMP-gated channel of rod photoreceptors. *Vision Res,* 38**,** 1315-23.

MOLNAR, A., HSUEH, H. A., ROSKA, B. & WERBLIN, F. S. 2009. Crossover inhibition in the retina: circuitry that compensates for nonlinear rectifying synaptic transmission. *J Comput Neurosci,* 27**,** 569-90.

MOORE, R. 1982. The suprachiasmatic nucleus and the organization of a circadian system. *Trends in Neurosciences,* 5**,** 404-407.

MOORE, R. & SILVER, R. 1998. Suprachiastmatic Nucleus Organization. Chronobiology International.

MOORE, R. Y. 1983. Organization and function of a central nervous system circadian oscillator: the suprachiasmatic hypothalamic nucleus. *Fed Proc,* 42**,** 2783-9.

MOORE, R. Y. 1995. Organization of the mammalian circadian system. *Ciba Found Symp,* 183**,** 88-99; discussion 100-6.

MOORE, R. Y. & CARD, J. P. 1994. Intergeniculate leaflet: an anatomically and functionally distinct subdivision of the lateral geniculate complex. *J Comp Neurol,* 344**,** 403-30.

MOORE, R. Y. & EICHLER, V. B. 1972. Loss of a circadian adrenal corticosterone rhythm following suprachiasmatic lesions in the rat. *Brain Res,* 42**,** 201-6.
MOORE, R. Y. & SPEH, J. C. 1993. GABA is the principal neurotransmitter of the circadian system. *Neurosci Lett,* 150**,** 112-6.
MOORE, R. Y., SPEH, J. C. & LEAK, R. K. 2002. Suprachiasmatic nucleus organization. *Cell Tissue Res,* 309**,** 89-98.
MOORE, R. Y., WEIS, R. & MOGA, M. M. 2000. Efferent projections of the intergeniculate leaflet and the ventral lateral geniculate nucleus in the rat. *J Comp Neurol,* 420**,** 398-418.
MORIN, L. & BLANCHARD, J. 2001. Organization of the hamster intergeniculate leaflet: NPY and ENK projections to the suprachiasmatic nucleus,intergeniculate leaflet and posterior limitans nucleus. *Visual Neuroscience,* 12.
MORIN, L. P. 2007. SCN organization reconsidered. *J Biol Rhythms,* 22**,** 3-13.
MORIN, L. P. 2013. Neuroanatomy of the extended circadian rhythm system. *Exp Neurol,* 243**,** 4-20.
MORIN, L. P., SHIVERS, K. Y., BLANCHARD, J. H. & MUSCAT, L. 2006. Complex organization of mouse and rat suprachiasmatic nucleus. *Neuroscience,* 137**,** 1285-97.
MORIN, L. P. & STUDHOLME, K. M. 2011. Separation of function for classical and ganglion cell photoreceptors with respect to circadian rhythm entrainment and induction of photosomnolence. *Neuroscience,* 199**,** 213-24.
MOTZKUS, D., LOUMI, S., CADENAS, C., VINSON, C., FORSSMANN, W. G. & MARONDE, E. 2007. Activation of human period-1 by PKA or CLOCK/BMAL1 is conferred by separate signal transduction pathways. *Chronobiol Int,* 24**,** 783-92.
MROSOVSKY, N. 2003. Contribution of classic photoreceptors to entrainment. *J Comp Physiol A Neuroethol Sens Neural Behav Physiol,* 189**,** 69-73.
MROSOVSKY, N. & HATTAR, S. 2005. Diurnal mice (Mus musculus) and other examples of temporal niche switching. *J Comp Physiol A Neuroethol Sens Neural Behav Physiol,* 191**,** 1011-24.
MURE, L., CORNUT, P., RIEUX, C., DROUYER, E., DENIS, P., GRONFIER, C. & COOPER, H. 2009. Melanopsin bistability: a fly's eye technology in the human retina. *PLos One,* 4**,** e5991.
MURE, L. S., RIEUX, C., HATTAR, S. & COOPER, H. M. 2007. Melanopsin-dependent nonvisual responses: evidence for photopigment bistability in vivo. *J Biol Rhythms,* 22**,** 411-24.
MUSCAT, L., HUBERMAN, A. D., JORDAN, C. L. & MORIN, L. P. 2003. Crossed and uncrossed retinal projections to the hamster circadian system. *J Comp Neurol,* 466**,** 513-24.
NAJJAR, R. P. & ZEITZER, J. M. 2016. Temporal integration of light flashes by the human circadian system. *J Clin Invest*.
NAKATANI, K., TAMURA, T. & YAU, K. W. 1991. Light adaptation in retinal rods of the rabbit and two other nonprimate mammals. *J Gen Physiol,* 97**,** 413-35.
NELSON, D. E. & TAKAHASHI, J. S. 1991. Sensitivity and integration in a visual pathway for circadian entrainment in the hamster (Mesocricetus auratus). *J Physiol,* 439**,** 115-45.
NELSON, D. E. & TAKAHASHI, J. S. 1999. Integration and saturation within the circadian photic entrainment pathway of hamsters. *Am J Physiol,* 277**,** R1351-61.
NEWMAN, L. A., WALKER, M. T., BROWN, R. L., CRONIN, T. W. & ROBINSON, P. R. 2003. Melanopsin forms a functional short-wavelength photopigment. *Biochemistry,* 42**,** 12734-8.
NIELSEN, H. S., HANNIBAL, J., KNUDSEN, S. M. & FAHRENKRUG, J. 2001. Pituitary adenylate cyclase-activating polypeptide induces period1 and period2 gene expression in the rat suprachiasmatic nucleus during late night. *Neuroscience,* 103**,** 433-41.

NIKONOV, S., LAMB, T. D. & PUGH, E. N. 2000. The role of steady phosphodiesterase activity in the kinetics and sensitivity of the light-adapted salamander rod photoresponse. *J Gen Physiol,* 116**,** 795-824.

NIKONOV, S., LL ZHU, X CRAFT, CMSWAROOP, APUGH, EN JR. 2005. Photoreceptors of Nrl -/- mice coexpress functional S- and M-cone opsins having distinct inactivation mechanisms. *The Journal of General Physiology,* 125**,** 287-304.

NIKONOV, S. S., KHOLODENKO, R., LEM, J. & PUGH, E. N. 2006. Physiological features of the S- and M-cone photoreceptors of wild-type mice from single-cell recordings. *J Gen Physiol,* 127**,** 359-74.

NISHINO, H. & KOIZUMI, K. 1977. Responses of neurons in the suprachiasmatic nuclei of the hypothalamus to putative transmitters. *Brain Res,* 120**,** 167-72.

NOMURA, A., SHIGEMOTO, R., NAKAMURA, Y., OKAMOTO, N., MIZUNO, N. & NAKANISHI, S. 1994. Developmentally regulated postsynaptic localization of a metabotropic glutamate receptor in rat rod bipolar cells. *Cell,* 77**,** 361-9.

NOMURA, K., TAKEUCHI, Y. & FUKUNAGA, K. 2006. MAP kinase additively activates the mouse Per1 gene promoter with CaM kinase II. *Brain Res,* 1118**,** 25-33.

O'MALLEY, D. M., SANDELL, J. H. & MASLAND, R. H. 1992. Co-release of acetylcholine and GABA by the starburst amacrine cells. *J Neurosci,* 12**,** 1394-408.

OKADA, T., ERNST, O. P., PALCZEWSKI, K. & HOFMANN, K. P. 2001. Activation of rhodopsin: new insights from structural and biochemical studies. *Trends Biochem Sci,* 26**,** 318-24.

OKAMURA, H., BÉROD, A., JULIEN, J. F., GEFFARD, M., KITAHAMA, K., MALLET, J. & BOBILLIER, P. 1989. Demonstration of GABAergic cell bodies in the suprachiasmatic nucleus: in situ hybridization of glutamic acid decarboxylase (GAD) mRNA and immunocytochemistry of GAD and GABA. *Neurosci Lett,* 102**,** 131-6.

PALCZEWSKI, K. & SAARI, J. C. 1997. Activation and inactivation steps in the visual transduction pathway. *Curr Opin Neurobiol,* 7**,** 500-4.

PANDA, S., ANTOCH, M. P., MILLER, B. H., SU, A. I., SCHOOK, A. B., STRAUME, M., SCHULTZ, P. G., KAY, S. A., TAKAHASHI, J. S. & HOGENESCH, J. B. 2002. Coordinated transcription of key pathways in the mouse by the circadian clock. *Cell,* 109**,** 307-20.

PANDA, S., NAYAK, S. K., CAMPO, B., WALKER, J. R., HOGENESCH, J. B. & JEGLA, T. 2005. Illumination of the melanopsin signaling pathway. *Science,* 307**,** 600-4.

PANDA, S., PROVENCIO, I., TU, D. C., PIRES, S. S., ROLLAG, M. D., CASTRUCCI, A. M., PLETCHER, M. T., SATO, T. K., WILTSHIRE, T., ANDAHAZY, M., KAY, S. A., VAN GELDER, R. N. & HOGENESCH, J. B. 2003. Melanopsin is required for non-image-forming photic responses in blind mice. *Science,* 301**,** 525-7.

PAUERS, M. J., KUCHENBECKER, J. A., NEITZ, M. & NEITZ, J. 2012. Changes in the colour of light cue circadian activity. *Anim Behav,* 83**,** 1143-1151.

PEICHL, L. 2005. Diversity of mammalian photoreceptor properties: adaptations to habitat and lifestyle? *Anat Rec A Discov Mol Cell Evol Biol,* 287**,** 1001-12.

PEICHL, L. & GONZÁLEZ-SORIANO, J. 1994. Morphological types of horizontal cell in rodent retinae: a comparison of rat, mouse, gerbil, and guinea pig. *Vis Neurosci,* 11**,** 501-17.

PENNARTZ, C. M., BIERLAAGH, M. A. & GEURTSEN, A. M. 1997. Cellular mechanisms underlying spontaneous firing in rat suprachiasmatic nucleus: involvement of a slowly inactivating component of sodium current. *J Neurophysiol,* 78**,** 1811-25.

PENNARTZ, C. M., DE JEU, M. T., BOS, N. P., SCHAAP, J. & GEURTSEN, A. M. 2002. Diurnal modulation of pacemaker potentials and calcium current in the mammalian circadian clock. *Nature,* 416**,** 286-90.

PENNARTZ, C. M., HAMSTRA, R. & GEURTSEN, A. M. 2001. Enhanced NMDA receptor activity in retinal inputs to the rat suprachiasmatic nucleus during the subjective night. *J Physiol,* 532**,** 181-94.
PEPE, I. M. & CUGNOLI, C. 1992. Retinal photoisomerase: role in invertebrate visual cells. *J Photochem Photobiol B,* 13**,** 5-17.
PEPPERBERG, D. R., CORNWALL, M. C., KAHLERT, M., HOFMANN, K. P., JIN, J., JONES, G. J. & RIPPS, H. 1992. Light-dependent delay in the falling phase of the retinal rod photoresponse. *Vis Neurosci,* 8**,** 9-18.
PERLMAN, I. & NORMANN, R. A. 1998. Light adaptation and sensitivity controlling mechanisms in vertebrate photoreceptors. *Prog Retin Eye Res,* 17**,** 523-63.
PERRY, V. H. & COWEY, A. 1985. The ganglion cell and cone distributions in the monkey's retina: implications for central magnification factors. *Vision Res,* 25**,** 1795-810.
PICKARD, G. E. 1994. Intergeniculate leaflet ablation alters circadian rhythms in the mouse. *Neuroreport,* 5**,** 2186-8.
PICKARD, G. E., RALPH, M. R. & MENAKER, M. 1987. The intergeniculate leaflet partially mediates effects of light on circadian rhythms. *J Biol Rhythms,* 2**,** 35-56.
PICKARD, G. E., SMITH, B. N., BELENKY, M., REA, M. A., DUDEK, F. E. & SOLLARS, P. J. 1999. 5-HT1B receptor-mediated presynaptic inhibition of retinal input to the suprachiasmatic nucleus. *J Neurosci,* 19**,** 4034-45.
PICKARD, G. E. & TUREK, F. W. 1983. The suprachiasmatic nuclei: two circadian clocks? *Brain Res,* 268**,** 201-10.
PIGGINS, H. D., ANTLE, M. C. & RUSAK, B. 1995. Neuropeptides phase shift the mammalian circadian pacemaker. *J Neurosci,* 15**,** 5612-22.
PIGGINS, H. D. & RUSAK, B. 1993. Electrophysiological effects of pressure-ejected bombesin-like peptides on hamster suprachiasmatic nucleus neurons in vitro. *J Neuroendocrinol,* 5**,** 575-81.
PIRES, S. S., HUGHES, S., TURTON, M., MELYAN, Z., PEIRSON, S. N., ZHENG, L., KOSMAOGLOU, M., BELLINGHAM, J., CHEETHAM, M. E., LUCAS, R. J., FOSTER, R. G., HANKINS, M. W. & HALFORD, S. 2009. Differential expression of two distinct functional isoforms of melanopsin (Opn4) in the mammalian retina. *J Neurosci,* 29**,** 12332-42.
PITTENDRIGH, C. S. & DAAN, S. 1976. A Functional Analysis of Circadian Pacemakers in Nocturnal Rodents. Journal of Comparative Physiology.
PITTS, G. R., OHTA, H. & MCMAHON, D. G. 2006. Daily rhythmicity of large-conductance Ca2+ -activated K+ currents in suprachiasmatic nucleus neurons. *Brain Res,* 1071**,** 54-62.
POHL, H. 1999. Spectral composition of light as a Zeitgeber for birds living in the high arctic summer. *Physiol Behav,* 67**,** 327-37.
POURCHO, R. G. & GOEBEL, D. J. 1983. Neuronal subpopulations in cat retina which accumulate the GABA agonist, (3H)muscimol: a combined Golgi and autoradiographic study. *J Comp Neurol,* 219**,** 25-35.
POURCHO, R. G. & GOEBEL, D. J. 1985. A combined Golgi and autoradiographic study of (3H)glycine-accumulating amacrine cells in the cat retina. *J Comp Neurol,* 233**,** 473-80.
PREITNER, N., DAMIOLA, F., LOPEZ-MOLINA, L., ZAKANY, J., DUBOULE, D., ALBRECHT, U. & SCHIBLER, U. 2002. The orphan nuclear receptor REV-ERBalpha controls circadian transcription within the positive limb of the mammalian circadian oscillator. Cell.
PROCYK, C. A., ELEFTHERIOU, C. G., STORCHI, R., ALLEN, A. E., MILOSAVLJEVIC, N., BROWN, T. M. & LUCAS, R. J. 2015. Spatial receptive fields in the retina and dorsal lateral geniculate nucleus of mice lacking rods and cones. *J Neurophysiol,* 114**,** 1321-30.

PROSSER, R. A., DEAN, R. R., EDGAR, D. M., HELLER, H. C. & MILLER, J. D. 1993. Serotonin and the mammalian circadian system: I. In vitro phase shifts by serotonergic agonists and antagonists. *J Biol Rhythms,* 8**,** 1-16.

PROSSER, R. A., MILLER, J. D. & HELLER, H. C. 1990. A serotonin agonist phase-shifts the circadian clock in the suprachiasmatic nuclei in vitro. *Brain Res,* 534**,** 336-9.

PROVENCIO, I., JIANG, G., DE GRIP, W. J., HAYES, W. P. & ROLLAG, M. D. 1998. Melanopsin: An opsin in melanophores, brain, and eye. *Proc Natl Acad Sci U S A,* 95**,** 340-5.

PROVENCIO, I., RODRIGUEZ, I. R., JIANG, G., HAYES, W. P., MOREIRA, E. F. & ROLLAG, M. D. 2000. A novel human opsin in the inner retina. *J Neurosci,* 20**,** 600-5.

PROVENCIO, I., ROLLAG, M. D. & CASTRUCCI, A. M. 2002. Photoreceptive net in the mammalian retina. This mesh of cells may explain how some blind mice can still tell day from night. *Nature,* 415**,** 493.

PROVENCIO, I., WONG, S., LEDERMAN, A. B., ARGAMASO, S. M. & FOSTER, R. G. 1994. Visual and circadian responses to light in aged retinally degenerate mice. *Vision Res,* 34**,** 1799-806.

PULVERMÜLLER, A., PALCZEWSKI, K. & HOFMANN, K. P. 1993. Interaction between photoactivated rhodopsin and its kinase: stability and kinetics of complex formation. *Biochemistry,* 32**,** 14082-8.

PURVES, D., AUGUSTINE, G. J., FITZPATRICK, D., KATZ, L. C., LAMANTIA, A.-S., MCNAMARA, J. O. & WILLIAMS, S. M. 2001. *Neuroscience,* Massachusetts, Sinauer Associates.

QIN, P. & POURCHO, R. G. 1999. Localization of AMPA-selective glutamate receptor subunits in the cat retina: a light- and electron-microscopic study. *Vis Neurosci,* 16**,** 169-77.

QUINTERO, J. E., KUHLMAN, S. J. & MCMAHON, D. G. 2003. The biological clock nucleus: a multiphasic oscillator network regulated by light. *J Neurosci,* 23**,** 8070-6.

RALPH, M. R., FOSTER, R. G., DAVIS, F. C. & MENAKER, M. 1990. Transplanted suprachiasmatic nucleus determines circadian period. *Science,* 247**,** 975-8.

RALPH, M. R. & MENAKER, M. 1989. GABA regulation of circadian responses to light. I. Involvement of GABAA-benzodiazepine and GABAB receptors. *J Neurosci,* 9**,** 2858-65.

RAVEN, M. A., STAGG, S. B. & REESE, B. E. 2005. Regularity and packing of the horizontal cell mosaic in different strains of mice. *Vis Neurosci,* 22**,** 461-8.

REA, M. A., BUCKLEY, B. & LUTTON, L. M. 1993. Local administration of EAA antagonists blocks light-induced phase shifts and c-fos expression in hamster SCN. *Am J Physiol,* 265**,** R1191-8.

REA, M. A., GLASS, J. D. & COLWELL, C. S. 1994. Serotonin modulates photic responses in the hamster suprachiasmatic nuclei. *J Neurosci,* 14**,** 3635-42.

REED, H. E., CUTLER, D. J., BROWN, T. M., BROWN, J., COEN, C. W. & PIGGINS, H. D. 2002. Effects of vasoactive intestinal polypeptide on neurones of the rat suprachiasmatic nuclei in vitro. *J Neuroendocrinol,* 14**,** 639-46.

REED, H. E., MEYER-SPASCHE, A., CUTLER, D. J., COEN, C. W. & PIGGINS, H. D. 2001. Vasoactive intestinal polypeptide (VIP) phase-shifts the rat suprachiasmatic nucleus clock in vitro. *Eur J Neurosci,* 13**,** 839-43.

REESE, B. E., RAVEN, M. A. & STAGG, S. B. 2005. Afferents and homotypic neighbors regulate horizontal cell morphology, connectivity, and retinal coverage. *J Neurosci,* 25**,** 2167-75.

REFINETTI, R. 2010. Entrainment of circadian rhythm by ambient temperature cycles in mice. *J Biol Rhythms,* 25**,** 247-56.

REFINETTI, R. 2015. Comparison of light, food, and temperature as environmental synchronizers of the circadian rhythm of activity in mice. *J Physiol Sci,* 65**,** 359-66.

RELÓGIO, A., WESTERMARK, P. O., WALLACH, T., SCHELLENBERG, K., KRAMER, A. & HERZEL, H. 2011. Tuning the mammalian circadian clock: robust synergy of two loops. *PLoS Comput Biol,* 7**,** e1002309.

RIEKE, F. & BAYLOR, D. A. 1998. Origin of reproducibility in the responses of retinal rods to single photons. *Biophys J,* 75**,** 1836-57.

ROENNEBERG, T. 1996. The complex circadian system of *Gonyaulax polyedra*. *Physiologica Plantarum,* 96**,** 733-737.

ROENNEBERG, T. & FOSTER, R. G. 1997. Twilight times: light and the circadian system. *Photochem Photobiol,* 66**,** 549-61.

ROENNEBERG, T. & MERROW, M. 2005. Circadian clocks - the fall and rise of physiology. *Nat Rev Mol Cell Biol,* 6**,** 965-71.

ROSEKIND, M. R., GREGORY, K. B., MALLIS, M. M., BRANDT, S. L., SEAL, B. & LERNER, D. 2010. The cost of poor sleep: workplace productivity loss and associated costs. *J Occup Environ Med,* 52**,** 91-8.

ROSKA, B., MOLNAR, A. & WERBLIN, F. S. 2006. Parallel processing in retinal ganglion cells: how integration of space-time patterns of excitation and inhibition form the spiking output. *J Neurophysiol,* 95**,** 3810-22.

RUBY, N. F., BRENNAN, T. J., XIE, X., CAO, V., FRANKEN, P., HELLER, H. C. & O'HARA, B. F. 2002. Role of melanopsin in circadian responses to light. *Science,* 298**,** 2211-3.

RUSAK, B., MEIJER, J. H. & HARRINGTON, M. E. 1989. Hamster circadian rhythms are phase-shifted by electrical stimulation of the geniculo-hypothalamic tract. *Brain Res,* 493**,** 283-91.

RÖHLICH, P., VAN VEEN, T. & SZÉL, A. 1994. Two different visual pigments in one retinal cone cell. *Neuron,* 13**,** 1159-66.

SAMPATH, A. P., STRISSEL, K. J., ELIAS, R., ARSHAVSKY, V. Y., MCGINNIS, J. F., CHEN, J., KAWAMURA, S., RIEKE, F. & HURLEY, J. B. 2005. Recoverin improves rod-mediated vision by enhancing signal transmission in the mouse retina. *Neuron,* 46**,** 413-20.

SATO, T. K., YAMADA, R. G., UKAI, H., BAGGS, J. E., MIRAGLIA, L. J., KOBAYASHI, T. J., WELSH, D. K., KAY, S. A., UEDA, H. R. & HOGENESCH, J. B. 2006. Feedback repression is required for mammalian circadian clock function. *Nat Genet,* 38**,** 312-9.

SCHERNHAMMER, E. S., LADEN, F., SPEIZER, F. E., WILLETT, W. C., HUNTER, D. J., KAWACHI, I. & COLDITZ, G. A. 2001. Rotating night shifts and risk of breast cancer in women participating in the nurses' health study. *J Natl Cancer Inst,* 93**,** 1563-8.

SCHERNHAMMER, E. S., LADEN, F., SPEIZER, F. E., WILLETT, W. C., HUNTER, D. J., KAWACHI, I., FUCHS, C. S. & COLDITZ, G. A. 2003. Night-shift work and risk of colorectal cancer in the nurses' health study. *J Natl Cancer Inst,* 95**,** 825-8.

SCHERNHAMMER, E. S., RAZAVI, P., LI, T. Y., QURESHI, A. A. & HAN, J. 2011. Rotating night shifts and risk of skin cancer in the nurses' health study. *J Natl Cancer Inst,* 103**,** 602-6.

SCHMAHL, C. & BÖHMER, G. 1997. Effects of excitatory amino acids and neuropeptide Y on the discharge activity of suprachiasmatic neurons in rat brain slices. *Brain Res,* 746**,** 151-63.

SCHMIDT, S. Y. & LOLLEY, R. N. 1973. Cyclic-nucleotide phosphodiesterase: an early defect in inherited retinal degeneration of C3H mice. *J Cell Biol,* 57**,** 117-23.

SCHMIDT, T. M. & KOFUJI, P. 2009. Functional and morphological differences among intrinsically photosensitive retinal ganglion cells. *J Neurosci,* 29**,** 476-82.

SCHMIDT, T. M. & KOFUJI, P. 2010. Differential cone pathway influence on intrinsically photosensitive retinal ganglion cell subtypes. *J Neurosci,* 30**,** 16262-71.

SCHMIDT, T. M. & KOFUJI, P. 2011. Structure and function of bistratified intrinsically photosensitive retinal ganglion cells in the mouse. *J Comp Neurol,* 519**,** 1492-504.

SCHMITZ, Y. & WITKOVSKY, P. 1997. Dependence of photoreceptor glutamate release on a dihydropyridine-sensitive calcium channel. *Neuroscience,* 78**,** 1209-16.
SCHNEEWEIS, D. & SCHNAPF, J. 1999. The photovoltage of macaque cone photoreceptors: adaptation, noise, and kinetics. *The Journal of Neuroscience,* 19**,** 1203-1216.
SCHNETKAMP, P. P. 2004. The SLC24 Na+/Ca2+-K+ exchanger family: vision and beyond. *Pflugers Arch,* 447**,** 683-8.
SCHWARTZ, W. J., COLEMAN, R. J. & REPPERT, S. M. 1983. A daily vasopressin rhythm in rat cerebrospinal fluid. *Brain Res,* 263**,** 105-12.
SCHWARTZ, W. J. & REPPERT, S. M. 1985. Neural regulation of the circadian vasopressin rhythm in cerebrospinal fluid: a pre-eminent role for the suprachiasmatic nuclei. *J Neurosci,* 5**,** 2771-8.
SHARMA, S., BALL, S. L. & PEACHEY, N. S. 2005. Pharmacological studies of the mouse cone electroretinogram. *Vis Neurosci,* 22**,** 631-6.
SHARPE, L. T. & STOCKMAN, A. 1999. Rod pathways: the importance of seeing nothing. *Trends Neurosci,* 22**,** 497-504.
SHIBATA, S. & MOORE, R. Y. 1993. Neuropeptide Y and optic chiasm stimulation affect suprachiasmatic nucleus circadian function in vitro. *Brain Res,* 615**,** 95-100.
SHIBATA, S., OOMURA, Y., KITA, H. & HATTORI, K. 1982. Circadian rhythmic changes of neuronal activity in the suprachiasmatic nucleus of the rat hypothalamic slice. *Brain Res,* 247**,** 154-8.
SHIBATA, S., WATANABE, A., HAMADA, T., ONO, M. & WATANABE, S. 1994. N-methyl-D-aspartate induces phase shifts in circadian rhythm of neuronal activity of rat SCN in vitro. *Am J Physiol,* 267**,** R360-4.
SHIRAKAWA, T. & MOORE, R. Y. 1994. Glutamate shifts the phase of the circadian neuronal firing rhythm in the rat suprachiasmatic nucleus in vitro. *Neurosci Lett,* 178**,** 47-50.
SLAUGHTER, M. M. & AWATRAMANI, G. B. 2002. On bipolar cells: following in the footsteps of phototransduction. *Adv Exp Med Biol,* 514**,** 477-92.
SMALE, L., MICHELS, K. M., MOORE, R. Y. & MORIN, L. P. 1990. Destruction of the hamster serotonergic system by 5,7-DHT: effects on circadian rhythm phase, entrainment and response to triazolam. *Brain Res,* 515**,** 9-19.
SMITH, B. N., SOLLARS, P. J., DUDEK, F. E. & PICKARD, G. E. 2001. Serotonergic modulation of retinal input to the mouse suprachiasmatic nucleus mediated by 5-HT1B and 5-HT7 receptors. *J Biol Rhythms,* 16**,** 25-38.
SMITH, R. D., TUREK, F. W. & SLATER, N. T. 1990. Bicuculline and picrotoxin block phase advances induced by GABA agonists in the circadian rhythm of locomotor activity in the golden hamster by a phaclofen-insensitive mechanism. *Brain Res,* 530**,** 275-82.
SOSCIA, S. J. & HARRINGTON, M. E. 2004. Neuropeptide Y attenuates NMDA-induced phase shifts in the SCN of NPY Y1 receptor knockout mice in vitro. *Brain Res,* 1023**,** 148-53.
SOSCIA, S. J. & HARRINGTON, M. E. 2005. Neuropeptide Y does not reset the circadian clock in NPY Y2-/- mice. *Neurosci Lett,* 373**,** 175-8.
SPITSCHAN, M., JAIN, S., BRAINARD, D. H. & AGUIRRE, G. K. 2014. Opponent melanopsin and S-cone signals in the human pupillary light response. *Proc Natl Acad Sci U S A,* 111**,** 15568-72.
SPROUSE, J., REYNOLDS, L., BRASELTON, J. & SCHMIDT, A. 2004. Serotonin-induced phase advances of SCN neuronal firing in vitro: a possible role for 5-HT5A receptors? *Synapse,* 54**,** 111-8.
STEPHAN, F. K. & ZUCKER, I. 1972. Circadian rhythms in drinking behavior and locomotor activity of rats are eliminated by hypothalamic lesions. *Proc Natl Acad Sci U S A,* 69**,** 1583-6.

SZÉL, A., RÖHLICH, P., CAFFÉ, A. R., JULIUSSON, B., AGUIRRE, G. & VAN VEEN, T. 1992. Unique topographic separation of two spectral classes of cones in the mouse retina. *J Comp Neurol,* 325**,** 327-42.

TAKAHASHI, J. S., DECOURSEY, P. J., BAUMAN, L. & MENAKER, M. 1984. Spectral sensitivity of a novel photoreceptive system mediating entrainment of mammalian circadian rhythms. *Nature,* 308**,** 186-8.

TAKATSUJI, K., MIGUEL-HIDALGO, J. J. & TOHYAMA, M. 1991. Retinal fibers make synaptic contact with neuropeptide Y and enkephalin immunoreactive neurons in the intergeniculate leaflet of the rat. *Neurosci Lett,* 125**,** 73-6.

TANAKA, K., SHIBUYA, I., HARAYAMA, N., NOMURA, M., KABASHIMA, N., UETA, Y. & YAMASHITA, H. 1997. Pituitary adenylate cyclase-activating polypeptide potentiation of Ca2+ entry via protein kinase C and A pathways in melanotrophs of the pituitary pars intermedia of rats. *Endocrinology,* 138**,** 4086-95.

TANAKA, K., SHIBUYA, I., NAGAMOTO, T., YAMASHITA, H. & KANNO, T. 1996. Pituitary adenylate cyclase-activating polypeptide causes rapid Ca2+ release from intracellular stores and long lasting Ca2+ influx mediated by Na+ influx-dependent membrane depolarization in bovine adrenal chromaffin cells. *Endocrinology,* 137**,** 956-66.

TANG, K. C. & PAN, J. T. 1993. Stimulatory effects of bombesin-like peptides on suprachiasmatic neurons in brain slices. *Brain Res,* 614**,** 125-30.

THANKACHAN, S. & RUSAK, B. 2005. Juxtacellular recording/labeling analysis of physiological and anatomical characteristics of rat intergeniculate leaflet neurons. *J Neurosci,* 25**,** 9195-204.

THOMSON, A. M. 1984. Slow, regular discharge in suprachiasmatic neurones is calcium dependent, in slices of rat brain. *Neuroscience,* 13**,** 761-7.

THOMSON, A. M. & WEST, D. C. 1990. Factors affecting slow regular firing in the suprachiasmatic nucleus in vitro. *J Biol Rhythms,* 5**,** 59-75.

THOMSON, A. M., WEST, D. C. & VLACHONIKOLIS, I. G. 1984. Regular firing patterns of suprachiasmatic neurons maintained in vitro. *Neurosci Lett,* 52**,** 329-34.

THORESON, W. B., BABAI, N. & BARTOLETTI, T. M. 2008. Feedback from horizontal cells to rod photoreceptors in vertebrate retina. *J Neurosci,* 28**,** 5691-5.

TISCHKAU, S. A., GALLMAN, E. A., BUCHANAN, G. F. & GILLETTE, M. U. 2000. Differential cAMP gating of glutamatergic signaling regulates long-term state changes in the suprachiasmatic circadian clock. *J Neurosci,* 20**,** 7830-7.

TREJO, L. J. & CICERONE, C. M. 1984. Cells in the pretectal olivary nucleus are in the pathway for the direct light reflex of the pupil in the rat. *Brain Res,* 300**,** 49-62.

TUCKER, P., MARQUIÉ, J. C., FOLKARD, S., ANSIAU, D. & ESQUIROL, Y. 2012. Shiftwork and metabolic dysfunction. *Chronobiol Int,* 29**,** 549-55.

VAN DEN POL, A. N. 1980. The hypothalamic suprachiasmatic nucleus of rat: intrinsic anatomy. *J Comp Neurol,* 191**,** 661-702.

VAN DEN POL, A. N., CAO, V. & HELLER, H. C. 1998. Circadian system of mice integrates brief light stimuli. *Am J Physiol,* 275**,** R654-7.

VAN DEN POL, A. N. & TSUJIMOTO, K. L. 1985. Neurotransmitters of the hypothalamic suprachiasmatic nucleus: immunocytochemical analysis of 25 neuronal antigens. *Neuroscience,* 15**,** 1049-86.

VAN ESSEVELDT, K. E., LEHMAN, M. N. & BOER, G. J. 2000. The suprachiasmatic nucleus and the circadian time-keeping system revisited. *Brain Res Brain Res Rev,* 33**,** 34-77.

VAN OOSTERHOUT, F., FISHER, S. P., VAN DIEPEN, H. C., WATSON, T. S., HOUBEN, T., VANDERLEEST, H. T., THOMPSON, S., PEIRSON, S. N., FOSTER, R. G. & MEIJER, J. H. 2012. Ultraviolet light provides a major input to non-image-forming light detection in mice. *Curr Biol,* 22**,** 1397-402.

VANEY, D. 1990. The mosaic of amacrine cells in the mammalian retina. *Progress in Retinal Research,* 9**,** 49-100.
VANEY, D. I. 1986. Morphological identification of serotonin-accumulating neurons in the living retina. *Science,* 233**,** 444-6.
VANSELOW, K. & KRAMER, A. 2007. Role of phosphorylation in the mammalian circadian clock. *Cold Spring Harb Symp Quant Biol,* 72**,** 167-76.
VARDI, N., DUVOISIN, R., WU, G. & STERLING, P. 2000. Localization of mGluR6 to dendrites of ON bipolar cells in primate retina. *J Comp Neurol,* 423**,** 402-12.
VAUDRY, D., GONZALEZ, B., BASILLE, M., YON, L., FOURNIER, A. & VAUDRY, H. 2000. Pituitary adenylate cyclase-activating polypeptide and its receptors: from structure to functions. *Pharmacological Reviews,* 52**,** 269–324.

VERWEIJ, J., KAMERMANS, M. & SPEKREIJSE, H. 1996. Horizontal cells feed back to cones by shifting the cone calcium-current activation range. *Vision Res,* 36**,** 3943-53.
VIDAL, L. & MORIN, L. P. 2007. Absence of normal photic integration in the circadian visual system: response to millisecond light flashes. *J Neurosci,* 27**,** 3375-82.
VINCENT, S. R. & HOPE, B. T. 1992. Neurons that say NO. *Trends Neurosci,* 15**,** 108-13.
VINDLACHERUVU, R. R., EBLING, F. J., MAYWOOD, E. S. & HASTINGS, M. H. 1992. Blockade of Glutamatergic Neurotransmission in the Suprachiasmatic Nucleus Prevents Cellular and Behavioural Responses of the Circadian System to Light. *Eur J Neurosci,* 4**,** 673-679.
VINEY, T. J., BALINT, K., HILLIER, D., SIEGERT, S., BOLDOGKOI, Z., ENQUIST, L. W., MEISTER, M., CEPKO, C. L. & ROSKA, B. 2007. Local retinal circuits of melanopsin-containing ganglion cells identified by transsynaptic viral tracing. *Curr Biol,* 17**,** 981-8.
VOSKO, A., VAN DIEPEN, H. C., KULJIS, D., CHIU, A. M., HEYER, D., TERRA, H., CARPENTER, E., MICHEL, S., MEIJER, J. H. & COLWELL, C. S. 2015. Role of vasoactive intestinal peptide in the light input to the circadian system. *Eur J Neurosci,* 42**,** 1839-48.
VRANG, N., MROSOVSKY, N. & MIKKELSEN, J. D. 2003. Afferent projections to the hamster intergeniculate leaflet demonstrated by retrograde and anterograde tracing. *Brain Res Bull,* 59**,** 267-88.
VUONG, T. M., CHABRE, M. & STRYER, L. 1984. Millisecond activation of transducin in the cyclic nucleotide cascade of vision. *Nature,* 311**,** 659-61.
WAGNER, S., CASTEL, M., GAINER, H. & YAROM, Y. 1997. GABA in the mammalian suprachiasmatic nucleus and its role in diurnal rhythmicity. *Nature,* 387**,** 598-603.
WANG, H. Y. & HUANG, R. C. 2004. Diurnal modulation of the Na+/K+-ATPase and spontaneous firing in the rat retinorecipient clock neurons. *J Neurophysiol,* 92**,** 2295-301.
WANG, Y. C. & HUANG, R. C. 2006. Effects of sodium pump activity on spontaneous firing in neurons of the rat suprachiasmatic nucleus. *J Neurophysiol,* 96**,** 109-18.
WANG, Y. V., WEICK, M. & DEMB, J. B. 2011. Spectral and temporal sensitivity of cone-mediated responses in mouse retinal ganglion cells. *J Neurosci,* 31**,** 7670-81.
WEBER, E. T., GANNON, R. L. & REA, M. A. 1995. cGMP-dependent protein kinase inhibitor blocks light-induced phase advances of circadian rhythms in vivo. *Neurosci Lett,* 197**,** 227-30.
WELSH, D. K., LOGOTHETIS, D. E., MEISTER, M. & REPPERT, S. M. 1995. Individual neurons dissociated from rat suprachiasmatic nucleus express independently phased circadian firing rhythms. *Neuron,* 14**,** 697-706.
WENG, S., ESTEVEZ, M. E. & BERSON, D. M. 2013. Mouse ganglion-cell photoreceptors are driven by the most sensitive rod pathway and by both types of cones. *PLoS One,* 8**,** e66480.
WERBLIN, F. S. & DOWLING, J. E. 1969. Organization of the retina of the mudpuppy, Necturus maculosus. II. Intracellular recording. *J Neurophysiol,* 32**,** 339-55.

WONG, K. 2012. A Retinal Ganglion Cell That Can Signal Irradiance Continuously for 10 Hours. *The Journal of Neuroscience,* 32**,** 11478 –11485.
WONG, K. Y., DUNN, F. A. & BERSON, D. M. 2005. Photoreceptor adaptation in intrinsically photosensitive retinal ganglion cells. *Neuron,* 48**,** 1001-10.
WONG, K. Y., GRAHAM, D. M. & BERSON, D. M. 2007. The retina-attached SCN slice preparation: an in vitro mammalian circadian visual system. *J Biol Rhythms,* 22**,** 400-10.
XU, J., DODD, R. L., MAKINO, C. L., SIMON, M. I., BAYLOR, D. A. & CHEN, J. 1997. Prolonged photoresponses in transgenic mouse rods lacking arrestin. *Nature,* 389**,** 505-9.
YAMAGUCHI, S., ISEJIMA, H., MATSUO, T., OKURA, R., YAGITA, K., KOBAYASHI, M. & OKAMURA, H. 2003. Synchronization of cellular clocks in the suprachiasmatic nucleus. *Science,* 302**,** 1408-12.
YAMAGUCHI, Y., SUZUKI, T., MIZORO, Y., KORI, H., OKADA, K., CHEN, Y., FUSTIN, J. M., YAMAZAKI, F., MIZUGUCHI, N., ZHANG, J., DONG, X., TSUJIMOTO, G., OKUNO, Y., DOI, M. & OKAMURA, H. 2013. Mice genetically deficient in vasopressin V1a and V1b receptors are resistant to jet lag. *Science,* 342**,** 85-90.
YAMAKAWA, G. R. & ANTLE, M. C. 2010. Phenotype and function of raphe projections to the suprachiasmatic nucleus. *Eur J Neurosci,* 31**,** 1974-83.
YAN, L. & OKAMURA, H. 2002. Gradients in the circadian expression of Per1 and Per2 genes in the rat suprachiasmatic nucleus. *Eur J Neurosci,* 15**,** 1153-62.
YAN, L. & SILVER, R. 2002. Differential induction and localization of mPer1 and mPer2 during advancing and delaying phase shifts. *Eur J Neurosci,* 16**,** 1531-40.
YANNIELLI, P. C. & HARRINGTON, M. E. 2001. The neuropeptide Y Y5 receptor mediates the blockade of "photic-like" NMDA-induced phase shifts in the golden hamster. *J Neurosci,* 21**,** 5367-73.
YING, S. W. & RUSAK, B. 1994. Effects of serotonergic agonists on firing rates of photically responsive cells in the hamster suprachiasmatic nucleus. *Brain Res,* 651**,** 37-46.
YING, S. W. & RUSAK, B. 1997. 5-HT7 receptors mediate serotonergic effects on light-sensitive suprachiasmatic nucleus neurons. *Brain Res,* 755**,** 246-54.
ZHANG, D. & RUSAK, B. 1989. Photic sensitivity of geniculate neurons that project to the suprachiasmatic nuclei or the contralateral geniculate. *Brain Research,* 504**,** 161-164
ZHAO, X., STAFFORD, B. K., GODIN, A. L., KING, W. M. & WONG, K. Y. 2014. Photoresponse diversity among the five types of intrinsically photosensitive retinal ganglion cells. *J Physiol,* 592**,** 1619-36.
ØSTERGAARD, J., HANNIBAL, J. & FAHRENKRUG, J. 2007. Synaptic contact between melanopsin-containing retinal ganglion cells and rod bipolar cells. *Invest Ophthalmol Vis Sci,* 48**,** 3812-20.

7.2 General Discussion

ANIKEEVA, P., ANDALMAN, A. S., WITTEN, I., WARDEN, M., GOSHEN, I., GROSENICK, L., GUNAYDIN, L. A., FRANK, L. M. & DEISSEROTH, K. 2012. Optetrode: a multichannel readout for optogenetic control in freely moving mice. *Nat Neurosci,* 15**,** 163-70.
BAVER, S. B., PICKARD, G. E. & SOLLARS, P. J. 2008. Two types of melanopsin retinal ganglion cell differentially innervate the hypothalamic suprachiasmatic nucleus and the olivary pretectal nucleus. *Eur J Neurosci,* 27**,** 1763-70.

BERSON, D. M., DUNN, F. A. & TAKAO, M. 2002. Phototransduction by retinal ganglion cells that set the circadian clock. *Science,* 295**,** 1070-3.
BROWN, T. M. & PIGGINS, H. D. 2009. Spatiotemporal heterogeneity in the electrical activity of suprachiasmatic nuclei neurons and their response to photoperiod. *J Biol Rhythms,* 24**,** 44-54.
BROWN, T. M., WYNNE, J., PIGGINS, H. D. & LUCAS, R. J. 2011. Multiple hypothalamic cell populations encoding distinct visual information. *J Physiol,* 589**,** 1173-94.
BUZSÁKI, G. 2002. Theta oscillations in the hippocampus. *Neuron,* 33**,** 325-40.
CHEN, S. K., BADEA, T. C. & HATTAR, S. 2011. Photoentrainment and pupillary light reflex are mediated by distinct populations of ipRGCs. *Nature,* 476**,** 92-5.
CHIAPPE, M. E., SEELIG, J. D., REISER, M. B. & JAYARAMAN, V. 2010. Walking modulates speed sensitivity in Drosophila motion vision. *Curr Biol,* 20**,** 1470-5.
DACEY, D. M., LIAO, H. W., PETERSON, B. B., ROBINSON, F. R., SMITH, V. C., POKORNY, J., YAU, K. W. & GAMLIN, P. D. 2005. Melanopsin-expressing ganglion cells in primate retina signal colour and irradiance and project to the LGN. *Nature,* 433**,** 749-54.
DIBNER, C., SCHIBLER, U. & ALBRECHT, U. 2010. The mammalian circadian timing system: organization and coordination of central and peripheral clocks. *Annu Rev Physiol,* 72**,** 517-49.
GOOLEY, J. J., RAJARATNAM, S. M., BRAINARD, G. C., KRONAUER, R. E., CZEISLER, C. A. & LOCKLEY, S. W. 2010. Spectral responses of the human circadian system depend on the irradiance and duration of exposure to light. *Sci Transl Med,* 2**,** 31ra33.
HAN, X. 2012. In vivo application of optogenetics for neural circuit analysis. *ACS Chem Neurosci,* 3**,** 577-84.
HARA, K. & HARRIS, R. A. 2002. The anesthetic mechanism of urethane: the effects on neurotransmitter-gated ion channels. *Anesth Analg,* 94**,** 313-8, table of contents.
HOWARTH, M., WALMSLEY, L. & BROWN, T. M. 2014. Binocular integration in the mouse lateral geniculate nuclei. *Curr Biol,* 24**,** 1241-7.
JONES, J. R., TACKENBERG, M. C. & MCMAHON, D. G. 2015. Manipulating circadian clock neuron firing rate resets molecular circadian rhythms and behavior. *Nat Neurosci,* 18**,** 373-5.
KALSBEEK, A., PALM, I. F., LA FLEUR, S. E., SCHEER, F. A., PERREAU-LENZ, S., RUITER, M., KREIER, F., CAILOTTO, C. & BUIJS, R. M. 2006. SCN outputs and the hypothalamic balance of life. *J Biol Rhythms,* 21**,** 458-69.
LEIN, E. S., HAWRYLYCZ, M. J., AO, N., AYRES, M., BENSINGER, A., BERNARD, A., BOE, A. F., BOGUSKI, M. S., BROCKWAY, K. S., BYRNES, E. J., CHEN, L., CHEN, T. M., CHIN, M. C., CHONG, J., CROOK, B. E., CZAPLINSKA, A., DANG, C. N., DATTA, S., DEE, N. R., DESAKI, A. L., DESTA, T., DIEP, E., DOLBEARE, T. A., DONELAN, M. J., DONG, H. W., DOUGHERTY, J. G., DUNCAN, B. J., EBBERT, A. J., EICHELE, G., ESTIN, L. K., FABER, C., FACER, B. A., FIELDS, R., FISCHER, S. R., FLISS, T. P., FRENSLEY, C., GATES, S. N., GLATTFELDER, K. J., HALVERSON, K. R., HART, M. R., HOHMANN, J. G., HOWELL, M. P., JEUNG, D. P., JOHNSON, R. A., KARR, P. T., KAWAL, R., KIDNEY, J. M., KNAPIK, R. H., KUAN, C. L., LAKE, J. H., LARAMEE, A. R., LARSEN, K. D., LAU, C., LEMON, T. A., LIANG, A. J., LIU, Y., LUONG, L. T., MICHAELS, J., MORGAN, J. J., MORGAN, R. J., MORTRUD, M. T., MOSQUEDA, N. F., NG, L. L., NG, R., ORTA, G. J., OVERLY, C. C., PAK, T. H., PARRY, S. E., PATHAK, S. D., PEARSON, O. C., PUCHALSKI, R. B., RILEY, Z. L., ROCKETT, H. R., ROWLAND, S. A., ROYALL, J. J., RUIZ, M. J., SARNO, N. R., SCHAFFNIT, K., SHAPOVALOVA, N. V., SIVISAY, T., SLAUGHTERBECK, C. R., SMITH, S. C., SMITH, K. A., SMITH, B. I., SODT, A. J., STEWART, N. N., STUMPF, K. R., SUNKIN, S. M., SUTRAM, M., TAM, A., TEEMER, C. D., THALLER, C., THOMPSON, C. L., VARNAM, L. R., VISEL, A., WHITLOCK, R. M., WOHNOUTKA, P. E., WOLKEY, C. K.,

WONG, V. Y., WOOD, M., et al. 2007. Genome-wide atlas of gene expression in the adult mouse brain. *Nature,* 445**,** 168-76.

LOCKLEY, S. W., BRAINARD, G. C. & CZEISLER, C. A. 2003. High sensitivity of the human circadian melatonin rhythm to resetting by short wavelength light. *J Clin Endocrinol Metab,* 88**,** 4502-5.

MADISEN, L., MAO, T., KOCH, H., ZHUO, J. M., BERENYI, A., FUJISAWA, S., HSU, Y. W., GARCIA, A. J., GU, X., ZANELLA, S., KIDNEY, J., GU, H., MAO, Y., HOOKS, B. M., BOYDEN, E. S., BUZSÁKI, G., RAMIREZ, J. M., JONES, A. R., SVOBODA, K., HAN, X., TURNER, E. E. & ZENG, H. 2012. A toolbox of Cre-dependent optogenetic transgenic mice for light-induced activation and silencing. *Nat Neurosci,* 15**,** 793-802.

MAGGI, C. A. & MELI, A. 1986a. Suitability of urethane anesthesia for physiopharmacological investigations in various systems. Part 1: General considerations. *Experientia,* 42**,** 109-14.

MAGGI, C. A. & MELI, A. 1986b. Suitability of urethane anesthesia for physiopharmacological investigations in various systems. Part 2: Cardiovascular system. *Experientia,* 42**,** 292-7.

MAIMON, G., STRAW, A. D. & DICKINSON, M. H. 2010. Active flight increases the gain of visual motion processing in Drosophila. *Nat Neurosci,* 13**,** 393-9.

MOORE, R. Y. & SPEH, J. C. 1993. GABA is the principal neurotransmitter of the circadian system. *Neurosci Lett,* 150**,** 112-6.

MOULAND, J., BROWN, T. & LUCAS, R. 2015. The SCN response to spatial patterns in the visual scene. *EBRS.* The University of Manchester.

NIELL, C. & STRYKER, M. 2010. Modulation of visual responses by behavioural state in mouse visual cortex. *Neuron,* 65**,** 472-479.

SCHWARZ, C., HENTSCHKE, H., BUTOVAS, S., HAISS, F., STÜTTGEN, M. C., GERDJIKOV, T. V., BERGNER, C. G. & WAIBLINGER, C. 2010. The head-fixed behaving rat--procedures and pitfalls. *Somatosens Mot Res,* 27**,** 131-48.

SMALLWOOD, P. M., OLVECZKY, B. P., WILLIAMS, G. L., JACOBS, G. H., REESE, B. E., MEISTER, M. & NATHANS, J. 2003. Genetically engineered mice with an additional class of cone photoreceptors: implications for the evolution of color vision. *Proc Natl Acad Sci U S A,* 100**,** 11706-11.

SPITSCHAN, M., JAIN, S., BRAINARD, D. H. & AGUIRRE, G. K. 2014. Opponent melanopsin and S-cone signals in the human pupillary light response. *Proc Natl Acad Sci U S A,* 111**,** 15568-72.

TANIGUCHI, H., HE, M., WU, P., KIM, S., PAIK, R., SUGINO, K., KVITSIANI, D., KVITSANI, D., FU, Y., LU, J., LIN, Y., MIYOSHI, G., SHIMA, Y., FISHELL, G., NELSON, S. B. & HUANG, Z. J. 2011. A resource of Cre driver lines for genetic targeting of GABAergic neurons in cerebral cortex. *Neuron,* 71**,** 995-1013.

VAN DIEPEN, H., RAMKISOENSING, A., PEIRSON, S. N., FOSTER, R. G. & MEIJER, J. H. 2013. Irradiance encoding in the suprachiasmatic nuclei by rod and cone photoreceptors. *The FASEB Journal,* Epub ahead of print.

VAN OOSTERHOUT, F., FISHER, S. P., VAN DIEPEN, H. C., WATSON, T. S., HOUBEN, T., VANDERLEEST, H. T., THOMPSON, S., PEIRSON, S. N., FOSTER, R. G. & MEIJER, J. H. 2012. Ultraviolet light provides a major input to non-image-forming light detection in mice. *Curr Biol,* 22**,** 1397-402.

WALMSLEY, L., HANNA, L., MOULAND, J., MARTIAL, F., WEST, A., SMEDLEY, A. R., BECHTOLD, D. A., WEBB, A. R., LUCAS, R. J. & BROWN, T. M. 2015. Colour as a signal for entraining the mammalian circadian clock. *PLoS Biol,* 13**,** e1002127.

WENG, S., ESTEVEZ, M. E. & BERSON, D. M. 2013. Mouse ganglion-cell photoreceptors are driven by the most sensitive rod pathway and by both types of cones. *PLoS One,* 8**,** e66480.

ZHANG, F., WANG, L. P., BRAUNER, M., LIEWALD, J. F., KAY, K., WATZKE, N., WOOD, P. G., BAMBERG, E., NAGEL, G., GOTTSCHALK, A. & DEISSEROTH, K. 2007. Multimodal fast optical interrogation of neural circuitry. *Nature,* 446**,** 633-9.

ZHAO, C., EISINGER, B. & GAMMIE, S. C. 2013. Characterization of GABAergic neurons in the mouse lateral septum: a double fluorescence in situ hybridization and immunohistochemical study using tyramide signal amplification. *PLoS One,* 8**,** e73750.

Appendix 1: Chapter 2 as published in the Journal of Physiology

Walmsley, L & Brown, T.M. (2015). *Eye-specific visual processing in the mouse suprachiasmatic nuclei*. The Journal of Physiology. 593, 1731-43

JPn Neuroscience

The Journal of Physiology

J Physiol 593.7 (2015) pp 1731–1743

Eye-specific visual processing in the mouse suprachiasmatic nuclei

Lauren Walmsley and Timothy M. Brown

Faculty of Life Sciences, University of Manchester, Manchester, UK

Key points

- Daily changes in global levels of illumination synchronise daily physiological rhythms via bilateral retinal projections to the suprachiasmatic nuclei.
- We aimed to determine how retinal signals are integrated within the suprachiasmatic nuclei.
- By monitoring electrophysiological responses to visual stimuli we show that most suprachiasmatic neurons receive input from just one eye.
- Our results establish that suprachiasmatic neurons measure local light intensity and that any assessment of global light levels occurs at the network level.

Abstract Internal circadian clocks are important regulators of mammalian biology, acting to coordinate physiology and behaviour in line with daily changes in the environment. At present, synchronisation of the circadian system to the solar cycle is believed to rely on a quantitative assessment of total ambient illumination, provided by a bilateral projection from the retina to the suprachiasmatic nuclei (SCN). It is currently unclear, however, whether this photic integration occurs at the level of individual cells or within the SCN network. Here we use extracellular multielectrode recordings from the SCN of anaesthetised mice to show that most SCN neurons receive visual input from just one eye. While we find that binocular inputs to a subset of cells are important for rapid responses to changes in illumination, we find no evidence indicating that individual SCN cells are capable of reporting the average light intensity across the whole visual field. As a result of these local irradiance coding properties, our data establish that photic integration is primarily mediated at the level of the SCN network and suggest that accurate assessments of global light levels would be impaired by non-uniform illumination of either eye.

(Received 1 December 2014; accepted after revision 27 January 2015; first published online 27 February 2015)
Corresponding author T. M. Brown: AV Hill Building, University of Manchester, Oxford Road, Manchester M13 9PT, UK. Email: timothy.brown@manchester.ac.uk

Abbreviations RGC, retinal ganglion cell; SCN, suprachiasmatic nuclei.

Introduction

The ability to anticipate recurring changes in the environment is crucial to the survival of all organisms. One especially pervasive mechanism by which this is achieved is via internal circadian clocks which can be synchronised to daily variations in the environment, most notably the solar cycle (Roenneberg & Foster, 1997). In mammals this process thus relies on direct retinal projections to the hypothalamic suprachiasmatic nuclei (SCN), site of the master circadian pacemaker (Golombek & Rosenstein, 2010; Lucas *et al.* 2012).

It has long been recognised that the quality of visual information that would be useful to the SCN is quite distinct from that which is important for more conventional visual pathways. Thus, retinal pathways supplying the thalamocortical visual system are organised to allow for a relatively stable representation of form and motion across the ~9 decimal orders of light intensity that separate the darkest night and the brightest day (Rieke

DOI: 10.1113/jphysiol.2014.288225

& Rudd, 2009). By contrast, detailed information about spatiotemporal patterns of illumination is presumably unimportant to the circadian system, which instead requires an accurate readout of global light intensity to infer time-of-day.

Consistent with this view, numerous behavioural studies have demonstrated that the response of the circadian system to light can be accurately predicted based on the total number of photons to which the animal is exposed (Nelson & Takahashi, 1991, 1999; Dkhissi-Benyahya *et al.* 2000; Lall *et al.* 2010; Lucas *et al.* 2012). Thus, for example, short bright light pulses evoke an adjustment in clock phase similar to longer dimmer stimuli. Although there are known to be specific situations where this relationship breaks down (Vidal & Morin, 2007; Lall *et al.* 2010), the accepted model of clock resetting is one whereby the retinorecipient SCN act as a photon counter and control circadian responses accordingly.

The intuitive separation between the desired properties of conventional and circadian visual processing is also supported by extensive anatomical data. Hence, retinal projections to conventional visual targets in the thalamus/tectum arise primary via the contralateral hemisphere, with ipsilateral projections coming exclusively from regions of the retina corresponding to the zone of binocular overlap (Coleman *et al.* 2009; Sterratt *et al.* 2013; Morin & Studholme, 2014). By contrast, the SCN receives dense bilateral retinal innervation (Morin & Studholme, 2014). Moreover, it is now clear that this retinal input to the SCN derives primarily from a subclass of intrinsically photosensitive retinal ganglion cell, termed M1 (Hattar *et al.* 2006). These cells appear specialised to encode irradiance and, unusually, projected bilaterally to the brain (Hattar *et al.* 2006; Brown *et al.* 2010, 2011), even when their retinal location places their field of view far outside the region of binocular overlap (Muscat *et al.* 2003).

This anatomical arrangement seems ideally placed to allow individual SCN neurons to measure the average light intensity from across the full visual field although, to date, this hypothesis remains untested. Existing data suggest that removing signals from one eye produces larger than expected deficits in circadian phase shifting and/or SCN Fos induction (Tang *et al.* 2002; Muscat & Morin, 2005). However, none of the many studies investigating visual response properties within the SCN (Meijer *et al.* 1986, 1992; Aggelopoulos & Meissl, 2000; Nakamura *et al.* 2004; Drouyer *et al.* 2007; Mure *et al.* 2007; Brown *et al.* 2011; van Diepen *et al.* 2013; Sakai, 2014) have extensively characterised binocular processing at the level of individual neurons. Here we set out to address this issue via multielectrode recordings from mouse SCN neurons using visual stimuli designed to determine the nature and extent of ipsi-/contralateral visual signals, both across the population and on individual cells.

Methods

Animals

All animal use was in accordance with the Animals (Scientific Procedures) Act 1986 (UK). Experiments were performed on adult male (50–80 days) Opn4$^{+/tau\text{-}lacZ}$ reporter mice and wild-type (Opn4$^{+/+}$) littermates ($n = 19$ and 14, respectively). Consistent with previous reports (Hattar *et al.* 2003; Lucas *et al.* 2003; Howarth *et al.* 2014), there were no observable abnormalities in the visual responses of reporter animals, hence the two datasets were combined for the analysis presented in this study. Prior to experiments, animals were housed under a strict 12 h dark/light cycle environment at a temperature of 22°C with food and water *ad libitum*.

In vivo neurophysiology

In preparation for stereotaxic surgery, mice were removed from their housing environment ∼2–3 h before lights off and anaesthetised with urethane (1.55 g kg^{-1} I.P. in 0.9% sterile saline). Mice were then prepared for stereotaxic surgery as previously described (Brown *et al.* 2011). Recording probes (Buzsaki 32L; NeuroNexus, Ann Abor, MI, USA) consisting of four shanks (spaced 200 μm), each with eight closely spaced recordings sites in diamond formation (intersite distance 20–34 μm) were coated with fluorescent dye (CM-DiI; Invitrogen, Paisley, UK) and then inserted into the brain parallel to the midline, 1 mm lateral and 0.3 mm caudal to bregma (centre of probe) at an angle of 9 deg relative to the dorsal–ventral axis. Electrodes were then lowered to the level of the SCN using a fluid-filled micromanipulator (MO-10, Narishige International Ltd, London, UK).

After allowing 30 min for neural activity to stabilise following probe insertion, wideband neural signals were acquired using a Recorder64 system (Plexon Inc., Dallas, TX, USA), amplified (×3000) and digitized at 40 kHz. Action potentials were discriminated from these signals offline as 'virtual'-tetrode waveforms using custom MATLAB (The Mathworks Inc., Natick, MA, USA) scripts and sorted manually using commercial principal components-based software (Offline sorter, Plexon) as described previously (Howarth *et al.* 2014). All surgical procedures were completed before the end of the home cage light phase, such that electrophysiological recordings spanned the late projected day–mid projected night, an epoch when the SCN light response is most sensitive (Brown *et al.* 2011).

Visual stimuli

Light measurements were performed using a calibrated spectroradiometer (Bentham Instruments, Reading, UK).

Full field visual stimuli were generated via two light-emitting diodes (LEDs) (λ_{max} 410 nm; half-width, ± 7 nm; Thorlabs, Newton, NJ, USA) independently controlled via LabVIEW (National Instruments, Austin, TX, USA) and neutral density filter wheels (Thorlabs). Light was supplied to the subject via 7 mm diameter flexible fibre optic light guides (Edmund Optics, York, UK), positioned 5 mm from each eye and enclosed within internally reflective plastic cones that fitted snugly over each eye to prevent off-target effects due to scattered light. Responses to these stimuli were then assessed as follows.

To determine the relative magnitude and sensitivity of eye-specific responses in SCN neurons, mice were maintained in darkness and 5 s light steps were applied in an interleaved fashion to contra- and/or ipsilateral eyes for a total of 10 repeats at logarithmically increasing intensities spanning 9.8–15.8 log photons cm^{-2} s^{-1} (inter-stimulus interval 20–50 s depending on intensity). Because all mouse photoreceptors display similar sensitivity to the wavelengths contained in our stimuli (Brown *et al.* 2012, 2013), after correction for pre-receptoral filtering (Govardovskii *et al.* 2000; Jacobs & Williams, 2007), effective photon fluxes for each mouse opsin were between 0.5 (M- and S-cone opsins) and 0.3 log units (melanopsin) dimmer than this value. Intensities reported in this article reflect effective irradiance for rod opsin, which is intermediate between these extremes (9.4–15.4 log photons cm^{-2} s^{-1}).

To determine the components of the SCN response that were dependent on stimulus brightness *vs.* stimulus contrast, a second protocol was also employed. Here we stepped light intensity independently at each eye every 5 s in a pseudorandom sequence spanning effective irradiances between 10.4 and 15.4 log photons cm^{-2} s^{-1} (total number of steps = 840). The sequence was generated such that, at any one time, the difference in intensity between the two eyes was no more than 2 decimal units and the instantaneous step in light intensity at each eye was one of five possible values (±2, 1 or 0 log units). To determine contrast-dependent components we then averaged cellular responses (0–500 ms post change in light intensity) as a function of step magnitude at either eye. Since we found that contrast–response relationships varied very little as a function of absolute irradiance, data reported in this article were averaged across all irradiances tested. For clarity, we only present data for steps providing contrast at one eye or equal contrast at both eyes.

To assess SCN response components that tracked stimulus brightness, we re-analysed the above to extract steady state firing (1 s epochs occurring at least 4 s after step in light intensity) as a function of absolute irradiance at either eye (independently or in combination).

Histology

At the end of each experiment, mice were perfused transcardially with 0.1 M phosphate-buffered saline (PBS) followed by 4% paraformaldehyde. The brain was removed, post-fixed in 4% paraformaldehyde for 30 min and subsequently cryoprotected in 30% sucrose. The following day, brains were sectioned (100–150 μm) on a freezing sledge microtome and either mounted directly onto slides (wild-type mice) using Vectashield (Vectorlaboratories Ltd, Peterborough, UK) or first processed for X-gal staining ($Opn4^{+/tau\text{-}lacZ}$) as described below.

X-gal staining was performed as previously described (Hattar *et al.* 2006). Brain sections were washed twice for 10 min each in buffer B (0.1 M PBS at pH 7.4, 2 mM $MgCl_2$, 0.01% sodium desoxycholate and 0.02% octylphenoxypolyethoxyethanol; Sigma, Poole, UK). Sections were then incubated for 4 h in staining solution (buffer B with potassium ferricyanide (5 mM), potassium ferrocyanide (5 mM) and X-gal (Bioline Reagents Ltd, London, UK; 1 mg ml^{-1})) at 37°C in darkness. Following staining, sections were washed twice for 5 min in 0.1 M PBS and mounted to slides using Vectashield as above.

After mounting DiI-labelled probe placements were visualised under a fluorescence microscope (Olympus BX51) with appropriate filter sets and, where appropriate, X-gal staining was visualised by standard light microscopy (Fig. 1*A*). Resulting images were then compared with appropriate stereotaxic atlas figures (Paxinos & Franklin, 2001) using the optic chiasm, SCN and 3rd ventricle as landmarks, to confirm appropriate probe placement. Consistent with previous anatomical and neurophysiological studies (Nakamura *et al.* 2004; Hattar *et al.* 2006; Brown *et al.* 2011; Morin & Studholme, 2014), visually evoked activity was exclusively observed at electrode sites located within the SCN or its immediate borders (Fig. 1).

Data analysis

In most cases, single cell responses are presented as the mean ± SEM change in firing across all trials (at least 10 per stimulus) relative to baseline (average firing rate 3 or 5 s before step in light intensity for light- and dark-adapted responses, respectively). Measures of monocular preference were calculated as $(Response_{CONTRA} - Response_{IPSI})/(Response_{CONTRA} + Response_{IPSI})$, such that contralateral biased responses tended towards 1 and ipsilateral biased responses towards −1. Where a cell did not show a significant response to stimulation of one of the two eyes (paired *t* test between firing during first 500 ms of light step and baseline, $P > 0.05$),

that response component was assigned a value of zero. The eye that evoked the largest response when analysed in this way was designated the 'dominant' eye. Binocular facilitation was analysed in a similar way: $(\text{Response}_{\text{BOTH}} - \text{Response}_{\text{DOMINANT}})/(\text{Response}_{\text{BOTH}} + \text{Response}_{\text{DOMINANT}})$. We classified as binocular any cell exhibiting significant responses to stimulation of both eyes individually or where the response to binocular stimulation was significantly different to that evoked by stimulating the dominant eye alone (unpaired *t* test based on response to 10 trials of each stimulus).

Where average population data are presented, in most cases responses were baseline subtracted (as above) and normalised on a within cell basis according to the largest response within a specific protocol. The exception to this rule was our analysis of brightness coding, where the absolute firing rates of each cell were normalised to range between 0 and 1 before averaging across the population.

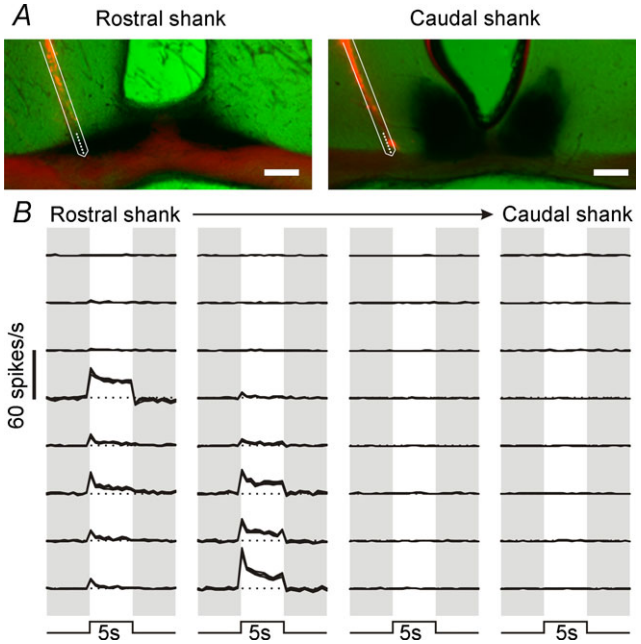

Figure 1. Light-evoked activity in the retinorecipient SCN region
A, X-gal-stained histological images showing multielectrode placement in the SCN region of an Opn4$^{+/tau\text{-}lacZ}$ reporter mouse. DiI-labelled probe tracks are in red, light microscopy for X-gal staining is pseudocoloured green (with melanopsin ganglion cell projections evident as darkly stained areas). Overlay (in white) shows projected locations of the 8 recording sites on each shank. Only the most rostral and caudal shanks for the 4-shank electrode are shown. Scale bars, 100 μm. *B*, multiunit activity detected across the 4 × 8 channel electrode placement shown in *A*, in response to 5 s light pulses presented to both eyes (405 nm; 15.4 log photons cm^{-2} s^{-1}). Traces represent the mean ± SEM change in firing (from 10 trials) over baseline (represented by dotted lines). Note that visual responses are absent from electrode sites located outside of the retinorecipient SCN region such as upper sites on the rostral shank and all sites on the caudal shank.

Statistical analyses were performed using GraphPad Prism v.6 (Graphpad Software Inc., San Diego, CA, USA). Data were, in most cases, fitted by 4-parameter sigmoid curves with the minimum constrained to zero as appropriate. Comparisons of sensitivity under various conditions were assessed by *F* test for differences in EC_{50}, Hill slope and/or maxima. Influences of eye-specific brightness/contrast on responses of various cell types were analysed by 2-way repeated measures ANOVA with dominant and non-dominant eye stimuli as factors.

Results

Binocular influences on SCN population activity

We first set out to determine how binocular signals were integrated to influence population firing activity within the SCN. To this end we performed multielectrode (32 channel) extracellular recordings of multiunit activity from the SCN and surrounding hypothalamus ($n = 33$ mice) and monitored responses to full field stimuli (410 nm LED; 5 s from darkness) applied at varying intensity to one or both eyes. Since all mouse photoreceptor classes are equally sensitive in this part of the spectrum (see Methods), any heterogeneity in the photoreceptor populations driving specific responses (Brown *et al.* 2011; van Oosterhout *et al.* 2012) should not influence sensitivity as assessed under these conditions.

Surprisingly, given the reported dense bilateral retinal innervation of the mouse SCN (Hattar *et al.* 2006; Brown *et al.* 2010; Morin & Studholme, 2014), we found that responses driven by the contralateral retina were reliably larger than those resulting from stimulation of the ipsilateral eye (Fig. 2*A* and *B*; $n = 252$ electrodes exhibiting visually evoked activity). Thus although the sensitivity of ipsi-/contralateral responses were similar (*F* test for difference in EC_{50} and/or Hill slope; $P = 0.64$) the maximum amplitudes of these were ~2-fold greater following stimulation of the contralateral eye (*F* test for difference in saturation point, $P = 0.003$). Interestingly, responses evoked by stimulating both eyes together were especially large. In line with the above, this significant difference in maximal response (*F* test *vs.* contralateral only; $P < 0.001$) was not associated with any appreciable difference in the sensitivity of binocular *vs.* monocular responses ($P = 0.77$).

Importantly, we found that SCN population activity driven by stimulation of both eyes was statistically indistinguishable from a simple linear sum of the observed responses to stimulating either eye alone (Fig. 2*B*; *F* test, $P = 0.69$). This surprising result indicates that SCN population activity does not accurately follow the total number of photons detected across both retinae. If this were the case, then, correcting for the 2-fold difference in total light intensity, the average response across the

paired SCN to monocular stimuli should be identical to that of an equivalent irradiance stimulus applied to both eyes. In fact, we found that the monocular responses were markedly smaller than expected given the binocular photon–response relationship (Fig. 2*C*; *F* test, $P < 0.001$). Indeed, to evoke a 50% maximal change in SCN population activity, monocular stimuli would need to be ~100-fold brighter than would be sufficient for light detected at both eyes.

Binocular integration in individual SCN neurons

Our data above reveal that population activity within the SCN does not (at least in all cases) exhibit the strict photon counting properties one might predict based on previous behavioural experiments (Nelson & Takahashi, 1991, 1999; Dkhissi-Benyahya *et al.* 2000; Lall *et al.* 2010; Lucas *et al.* 2012). Given this unexpected result, we next aimed to determine how these tissue level visual response properties arise through the sensory characteristics of individual SCN neurons.

From our multiunit recordings we were able to isolate the activity of 61 individual cells within or bordering the SCN, of which 51 were light sensitive. Across this population, we observed heterogeneity in eye-specific responses to light steps from darkness (Fig. 3*A*–*E*). This included many cells that responded solely to stimulation of either the contralateral (Fig. 3*A* and *E*; $n = 15$) or ipsilateral eye (Fig. 3*B* and *E*; $n = 19$) and other cells that exhibited clear responses to stimulation of either eye and/or substantially larger responses to binocular *vs.* monocular stimulation (Fig. 3*C*–*E*; $n = 17$).

Thus, we found that the majority (~67%) of visually responsive SCN neurons did not integrate binocular signals and, instead, faithfully reported monocular irradiance (Fig. 3*F*). In all cases, responses of these cells to stimulation of the dominant eye *vs.* both eyes were statistically identical (Fig. 3*E*; *t* tests based on responses to 10 trials, $P > 0.05$).

By contrast, for the smaller proportion of SCN cells that did have access to visual signals from either eye, responses were in most cases biased towards one retina, with the binocular influence most evident as an enhanced response to stimulation of both eyes (Fig. 3*E* and *G*). Surprisingly, here we found that average binocular responses were in fact significantly larger than even a linear sum of the two monocular inputs (*F* test for difference in saturation point, $P = 0.007$; not shown). This synergistic effect appeared to diminish over time, however (Fig. 3*C* and *D*), such that towards the end of the light steps (last 1 s) responses were not significantly different from the linear prediction (*F* test, $P = 0.69$).

Together, these SCN cellular properties explain the unexpectedly small SCN multiunit responses to monocular *vs.* binocular stimuli (Fig. 2): most SCN neurons are strongly biased towards one eye such that at any given intensity many more cells are activated by stimulating both

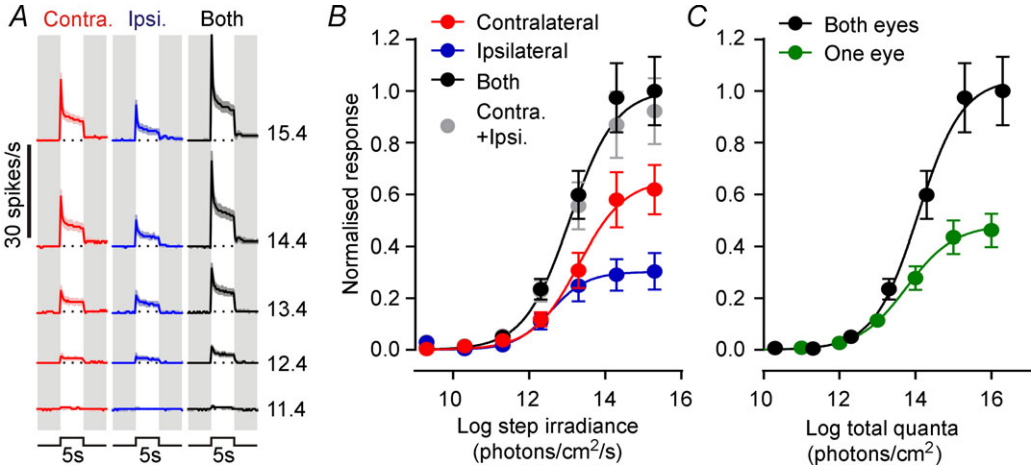

Figure 2. SCN population firing activity does not faithfully report global irradiance
A, mean ± SEM multiunit firing response profile across the retinorecipient SCN region ($n = 252$ electrodes from 33 mice) in response to 5 s light steps (410 nm LED, effective intensities 11.4–15.4 log photons cm^{-2} s^{-1}, from darkness) targeting the contralateral and/or ipsilateral eye. Data were normalised by subtracting pre-stimulus (5 s before light on) firing rates (represented by dotted lines). *B*, normalised multiunit firing response (change in spike rate averaged across 5 s light on, mean ± SEM) as a function of step irradiance. Responses to stimulating both eyes together were statistically indistinguishable from a linear sum of the measured response evoked by stimulation of contralateral and ipsilateral eyes alone (grey symbols, *F* test, $P = 0.69$). *C*, normalised multiunit firing response (conventions as in *B*), plotted as a function of total number of photons delivered. The predicted average across left and right SCN (green symbols; average of ipsilateral and contralateral responses from *B*) is significantly lower than the response to stimulating both eyes even when corrected for total number of photons (*F* test, $P < 0.0001$).

eyes. Surprisingly, however, the observed multiunit bias towards contralateral-driven visual responses (Fig. 2*B*) did not translate into an increased number of contralateral biased SCN neurons. In fact, we observed statistically equivalent proportions of ipsi-/contralateral biased SCN neurons ($n = 27$ and 24, respectively, Fisher's exact test, $P = 0.77$). These data imply that, across the population, contralateral inputs tend to drive larger responses in individual SCN neurons than do ipsilateral inputs (although among the sample of cells we collected this difference did not attain significance: 3.8 ± 0.7 *vs.* 2.7 ± 0.7 spikes s^{-1}, respectively, at 15.4 log photons cm^{-2} s^{-1}; paired *t* test, $P = 0.28$).

Together, our data above suggest that while a subset of SCN neurons receives inputs from both eyes, none of these cells alone can effectively integrate photons from across the visual scene to report the total amount of light in the environment. It is worth noting, however, that such light steps applied from darkness represent rather unnatural visual stimuli. Moreover, these do not allow one to distinguish response components that are dependent on the absolute irradiance of the signal *vs.* the relative change in irradiance (brightness *vs.* contrast). To better understand, then, how SCN neurons track spatio-temporal variations in light intensity under more natural conditions we next assessed responses to smaller modulations in light intensity, using a protocol that allowed us to dissociate response components dependent on stimulus brightness *vs.* contrast.

Response properties of SCN binocular cells

Since our data indicated that binocular influences were especially pronounced for the initial components of SCN

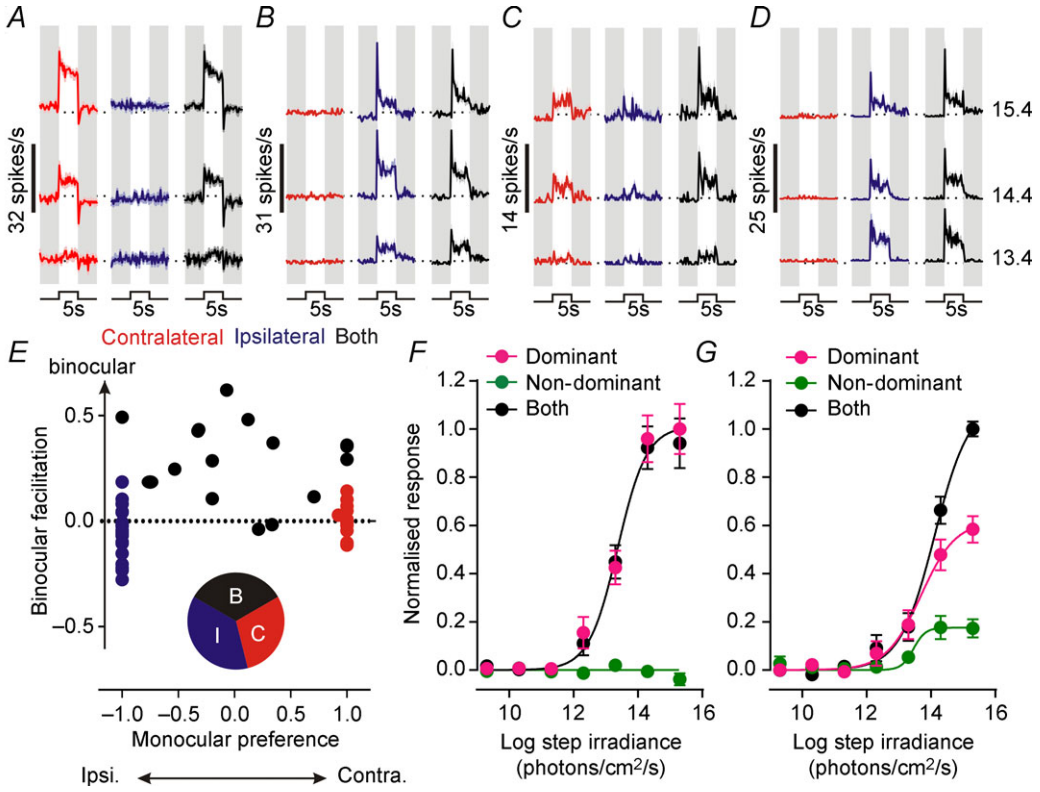

Figure 3. Eye-specific response properties of SCN neurons
A–D, example firing response profiles (mean ± SEM of 10 trials) for 4 SCN single units in response to 5 s light steps (410 nm LED, effective intensities 13.4–15.4 log photons cm^{-2} s^{-1}, from darkness) targeting the contralateral and/or ipsilateral eye. Many cells only showed clear responses to stimulation of either contralateral (*A*) or ipsilateral (*B*) eye, while a subset showed binocular responses of varying strength (*C* and *D*). *E*, population data for 51 visually responsive SCN neurons showing monocular preference (0, equally matched binocular response) *vs.* binocular facilitation (positive values, larger response to stimulation of both eyes *vs.* one eye; see Methods for details). Inset pie chart shows proportion of cells exhibiting purely ipsilateral (I), contralateral (C) or binocular responses (B). *F*, normalised acute response of monocular cells (change in spike rate across first 500 ms of light on, mean ± SEM, $n = 34$) as a function of step irradiance. Responses to stimulation of the dominant eye or both eyes together were statistically indistinguishable (*F* test; $P = 0.91$). *G*, normalised acute response of binocular cells (conventions as in *F*, $n = 17$). Binocular responses were significantly greater than those driven by the dominant eye alone (*F* test; $P = 0.004$).

neuronal responses under dark-adapted conditions, we first examined how binocular cells responded to acute changes in light intensity in the range up to ± 2 log units, applied under light-adapted conditions (11.4–14.4 log photons cm^{-2} s^{-1}).

Interestingly, we found that when changes in light intensity occurred simultaneously across both eyes, binocular cells exhibited very sharp and robust increases or decreases in firing (Fig. 4*A*) that were near-linear with respect to the log change in irradiance (Fig. 4*B*). By contrast, responses were smaller and much more sluggish when light steps occurred solely at the dominant eye and were virtually undetectable when applied to the non-dominant eye (Fig. 4*A* and *B*). Together, these data indicate that binocular integration functions in this population of cells to facilitate rapid responses to global changes in light levels.

We next determined the extent to which eye-specific signals influenced the ability of binocular cells to track brightness (Fig. 5*A*) by quantifying steady state firing (4–5 s after a change in light intensity) as a function of absolute irradiance. Given the data described above, one might expect the steady state firing of binocular cells to be strongly influenced by the overall irradiance across either eye. In fact, we found very little influence of binocular integration on the steady state firing of such cells. Thus, rather than following the mean irradiance across both eyes (Fig. 5*B*, *F* test, $P < 0.001$) binocular cell firing activity was, instead, entirely accounted for by the irradiance at the dominant eye, regardless of the interocular difference in brightness (Fig. 5*C*, *F* test, $P = 0.62$). Intriguingly, then, despite clear binocular influences on responses to rapid changes in light levels, basal firing of binocular cells was entirely driven by just one of the two eyes.

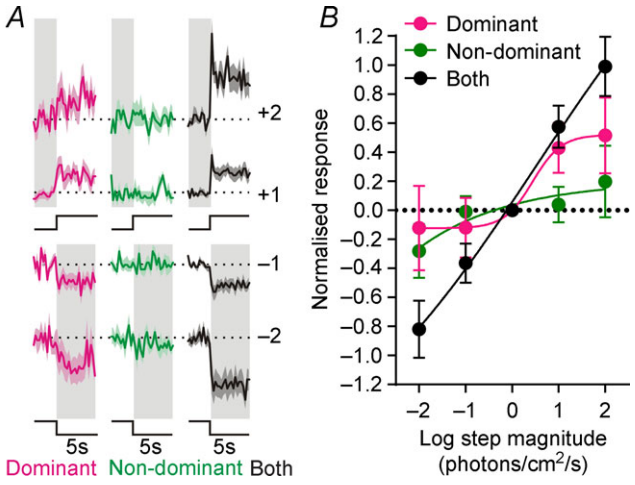

Figure 4. Binocular integration is required for robust contrast responses in a subset of SCN neurons
A, mean ± SEM normalised response of binocular cells ($n = 17$) to irradiance steps (−2 to +2 log units; 405 nm LED) applied to one or both eyes under light-adapted conditions (11.4–14.4 log photons cm^{-2} s^{-1}). *B*, quantification of data in *A* showing change in firing over first 500 ms of light step. Contrast responses were significantly larger upon stimulation of both eyes *vs.* the dominant eye only (*F* test, $P = 0.02$).

Response properties of SCN monocular cells

To better understand how the properties of binocular cells, outlined above, distinguished them from other visually responsive (monocular) SCN neurons, we also examined the brightness and contrast components of the monocular cell responses.

Surprisingly, we found that whereas binocular cells reliably exhibited 'ON' responses to visual contrast (i.e. a positive relationship between the step in light intensity and change in firing), only a subset of monocular cells exhibited this property (Fig. 6*A*; $n = 24/34$). Other cells exhibited decreases in firing in response to increased light intensity (OFF, $n = 5$) or displayed transient increases in firing in response to both light increments and decrements (ON/OFF, $n = 5$).

Unlike binocular cells (Fig. 4*B*), all these monocular populations exhibited robust, near-log linear changes in firing as a function of step magnitude at the dominant eye alone (Fig. 6*B*). Moreover, none of these monocular populations displayed any clear influence of non-dominant eye contrast (2-way repeated measures ANOVA, non-dominant eye and interaction terms all $P > 0.05$).

We have previously reported 'transient' cells in the mouse SCN (Brown *et al.* 2011), whose visual response properties appear consistent with those of the ON/OFF cells described above. By contrast, the presence of monocular cells exhibiting OFF responses under these conditions was surprising, not least because all of these cells exhibited excitatory responses to light steps applied from darkness (not shown). Interestingly, these OFF responses also appeared to exclusively originate with the ipsilateral eye (Fig. 6*B*). Based on our sample size there is a low probability that we could have failed to detect an equivalent population of contralateral-driven OFF cells (Fisher's exact text, $P = 0.053$). In sum then it appears that ipsilateral retinal influences on the SCN may be more diverse than the primarily ON responses originating with the contralateral eye (Fig. 6*B*).

In line with their responses to visual contrast described above, we found that, whereas the steady state firing of ON cells reliably increased as a function of monocular brightness, that of OFF cells decreased (Fig. 7*A* and *B*). Importantly, we were also able to identify both ON and OFF cells within the same recording (Fig. 7*A*), indicating that this unusual OFF behaviour could not simply reflect some state or circadian phase-dependent switch in general SCN responsiveness.

By contrast with the other SCN cell types, the steady state activity of ON/OFF cells did not vary as a function of irradiance (Fig. 8, repeated measures ANOVA, $P = 0.36$), indicating that this population specifically responds only to rapid changes in light intensity.

Discussion

Here we show that, despite the dense bilateral input that the SCN receive from the retina (Miura *et al.* 1997; Hattar *et al.* 2006; Brown *et al.* 2010; Morin & Studholme, 2014), few individual SCN neurons have access to visual signals from both eyes. Moreover, even where cells do receive input from both eyes, binocular influences are limited to just the initial components of any response to changing irradiance. As a result, no single SCN neuron is capable of providing direct information about global levels of irradiance across the full visual field.

These results are surprising for two reasons. Firstly, we have previously observed extensive binocular integration in the mouse visual thalamus, a region where eye-specific inputs were, until recently, believed to remain entirely segregated (Howarth *et al.* 2014). Indeed, using similar approaches to those employed here, we observed many single cells in the visual thalamus whose basal firing did encode mean binocular irradiance. Secondly, and more importantly, however, our present results are unexpected because the existing model posits that circadian photoentrainment is reliant on a quantitative assessment of the total amount of light in the environment (Nelson & Takahashi, 1991, 1999; Dkhissi-Benyahya *et al.* 2000; Lall *et al.* 2010; Lucas *et al.* 2012). Assuming this model to be correct, any such assessment of global irradiance could occur neither at the level of individual cells, nor by simply taking the average light-evoked activity across the population of such cells.

In fact, since the degree of visually evoked SCN activity is well correlated with the magnitude of circadian phase shifts (Meijer *et al.* 1992; Brown *et al.* 2011), our present data suggest that the current model of circadian photic integration may not be entirely accurate. Based on the light-evoked firing we observe in the SCN, we would predict that light falling on one, rather than both, eyes would result in a 50% reduction in phase shift magnitude, rather

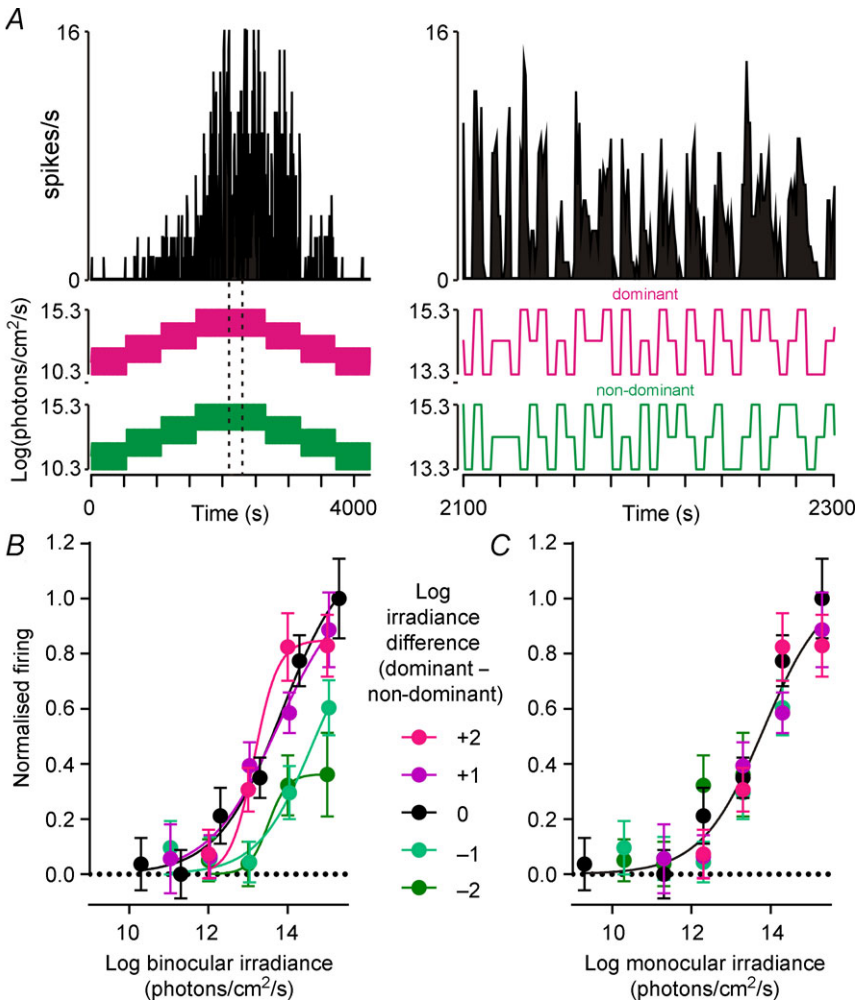

Figure 5. SCN binocular cells encode monocular irradiance
A, firing activity of a binocular SCN neuron presented with a pseudorandom irradiance sequence (see Methods). Right panels show a portion of the responses at higher temporal resolution (indicated by the dotted region bottom left). *B*, normalised steady state firing activity of binocular cells (spikes occurring 4–5 s after a step in irradiance; mean ± SEM, $n = 17$) plotted as a function of the average irradiance across the two eyes and split according to the interocular difference in irradiance. When expressed in this manner, irradiance–response relationships could not be described by a single sigmoid curve (F test, $P < 0.001$). *C*, data from *B* plotted according to irradiance at the dominant eye. Under these conditions, all data could be described by a single curve (F test, $P = 0.62$).

than a 50% reduction in apparent light intensity (0.3 log units). As far as we are aware, only one study has explicitly tested this possibility by performing a reversible monocular occlusion before applying phase shifting light stimuli (Muscat & Morin, 2005). Unfortunately, inter-individual variability in phase shift magnitude makes a robust assessment of the above difficult, although for long/bright stimuli, monocular phase shifts certainly appear better explained by a 50% reduction in amplitude rather than in total photon flux.

Accordingly, we propose that retinorecipient SCN neurons do accurately measure photon flux, but only within a portion of the visual field. Based on an established view of SCN organisation, suggesting the presence of weak oscillators that are readily reset by light and robust oscillators which integrate circadian inputs from the former (Albus *et al.* 2005; Brown & Piggins, 2009; Rohling *et al.* 2011), we propose a model whereby the retinorecipient cells are reset according to 'local' light intensity (Fig. 9). It is then the average phase information supplied by these retinorecipient oscillators that dictates the integrated circadian response. Such a mechanism would account for the behavioural response to monocular visual stimuli and the associated 50% reduction in the number of Fos-positive SCN neurons previously observed (Muscat & Morin, 2005).

We should also note that another study, employing unilateral optic nerve transection, found a much larger (~90%) reduction in light-induced Fos across the hamster SCN (Tang *et al.* 2002). The reason for this discrepancy is unclear but again this observation appears hard to incorporate into a model whereby the SCN response is proportional to the total level of ambient illumination.

Aside from the above, there have been very few investigations of cellular level integration of binocular signals in the SCN. Thus, most previous investigations of neurophysiological effects of light in the SCN have used exclusively monocular (Meijer *et al.* 1986; Nakamura *et al.* 2004; Brown *et al.* 2011) or binocular stimuli (Meijer *et al.* 1992; Aggelopoulos & Meissl, 2000; Drouyer *et al.* 2007; Mure *et al.* 2007; van Diepen *et al.* 2013). A few studies have investigated occularity of rat, degus and diurnal ground squirrel SCN cells (Meijer *et al.* 1989; Jiao *et al.* 1999), but in each case the number of cells ($n = 3$) and irradiance range tested was too low to draw any solid inferences on binocular processing in the clock of these species.

At present, there is also little information about the specific location(s) or number of retinal ganglion cells (RGCs) from which each retinorecipient SCN cell receives input. Whereas RGC projections to more conventional visual centres adopt a specific organisation to facilitate image forming vision (Sterratt *et al.* 2013), it feels unlikely that something similar should also be true for the SCN. Indeed, the SCN is known to deviate from this scheme by virtue of the fact it receives input from the nasal and superior regions of the ipsilateral retina (Morin *et al.* 2003). Moreover, while eye-specific inputs to the hamster SCN appear partially anatomically segregated (Muscat *et al.* 2003) this does not seem to hold true for the mouse (Brown *et al.* 2010; Morin & Studholme, 2014). If instead, then, retinal input to SCN neurons is essentially random, our data suggest that the number of RGC inputs to any one

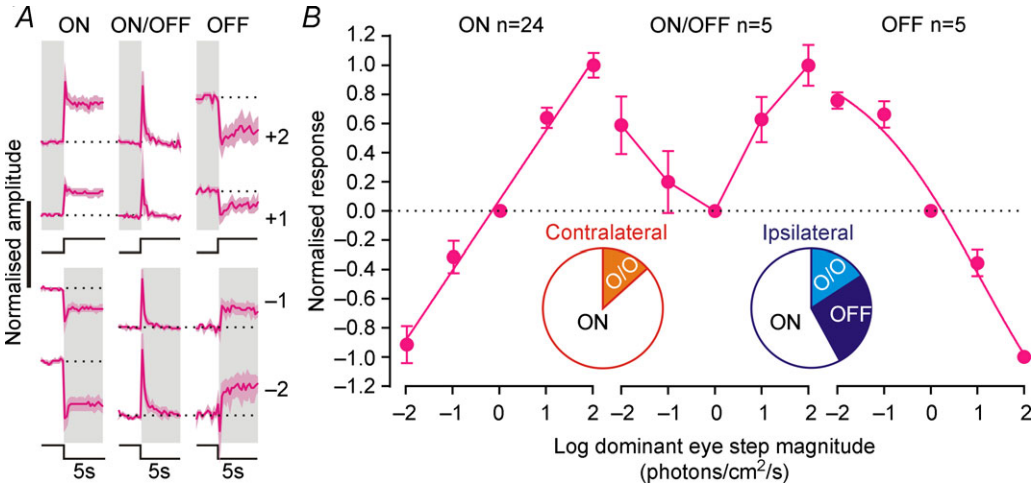

Figure 6. Monocular SCN neurons exhibit varying responses to visual contrast
A, mean ± SEM normalised response of monocular cell subpopulations to irradiance steps (−2 to +2 log units; 410 nm LED) applied to the dominant eye under light-adapted conditions (11.4–14.4 log photons cm^{-2} s^{-1}). For most cells, changes in firing rate were positively related to step magnitude (ON, $n = 24$), while other cells showed the inverse relationship (OFF, $n = 5$) or increased firing in response to both steps up and down in irradiance (ON/OFF, $n = 5$). *B*, quantification of data in *A* showing change in firing over first 500 ms of light step for the three populations. Inset pie charts indicate the proportion of each cell type driven by either eye ($n = 15$ and 19 total for contralateral and ipsilateral, respectively). Note, OFF cells were all driven by the ipsilateral eye.

cell must be small. In fact, the near equal numbers of contralateral, ipsilateral and binocularly responsive SCN neurons we observe suggests that, on average, each of these cells samples from two RGCs.

If correct, our suggestion above would imply that most SCN neurons could only measure light intensity within very restricted patches of the visual field (<30 deg given the known dendritic field sizes of the melanopsin RGCs that provide most of the input; Berson *et al.* 2010). Accordingly, individual SCN cells could detect quite different daily patterns of illumination (e.g. if they monitored light intensity exclusively from the lower rather than upper visual field). We tentatively suggest that such a mechanism could contribute to the pronounced,

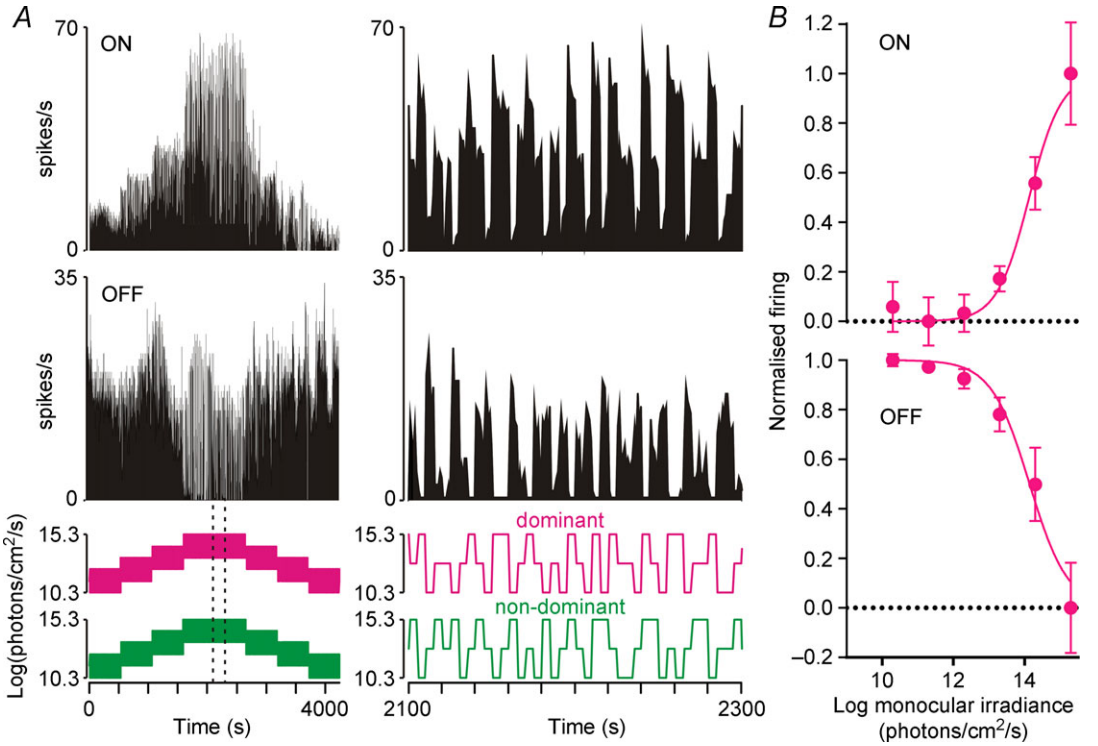

Figure 7. Brightness and darkness coding in SCN monocular cells
A, firing activity of simultaneously recorded ON (top) and OFF (bottom) SCN neurons presented with a pseudo-random irradiance sequence (see Methods). Right panels show a portion of the responses at higher temporal resolution (indicated by the dotted region bottom left). *B*, normalised steady state firing activity of monocular ON and OFF cells (spikes occurring 4–5 s after a step in irradiance; mean ± SEM, $n = 24$ and 5, respectively) plotted as a function of irradiance at the dominant eye.

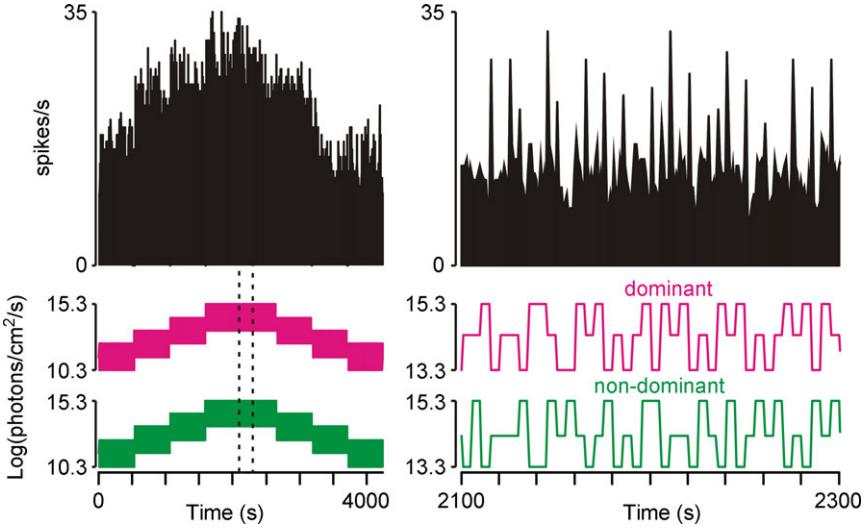

Figure 8. SCN ON/OFF cells do not track irradiance
Firing activity of an ON/OFF SCN neuron presented with a pseudorandom irradiance sequence (see Methods). Right panels show a portion of the responses at higher temporal resolution (indicated by the dotted region bottom left). Note that steady state firing does not vary as a function of irradiance.

photoperiod-dependent, phase differences in the electrical activity exhibited by SCN neurons (VanderLeest *et al.* 2007; Brown & Piggins, 2009).

It is also interesting to speculate as to the functional significance of the binocular input to a subset of SCN cells. It is clear from our data that this input makes little contribution to irradiance coding and instead acts to promote rapid and robust responses to sudden changes in light intensity. It is currently unclear why such a property would be useful to the clock; however, existing data indicate that high frequency retinal input and subsequent SCN cell firing are important for triggering internal calcium mobilisation (Irwin & Allen, 2007). It may then be the case that the initial transient response of SCN cells (which often overshoot the steady state level attained for a given irradiance) are especially significant for initiating the intracellular signalling cascade required for phase shifting.

As a final note here, since our SCN recordings were performed in anaesthetised mice, it is important to consider the possibility that responses recorded under our experimental conditions do not fully recapitulate those observed in freely behaving animals. On the basis of the available data, we think it unlikely that the anaesthetic we employed here would result in any qualitative change in the visual responses of SCN neurons. Hence, multiunit recordings in freely moving mice (van Oosterhout *et al.* 2012; van Diepen *et al.* 2013) reveal visual responses with essentially identical sensitivity and temporal profile to those we report here and have observed previously (Brown *et al.* 2011).

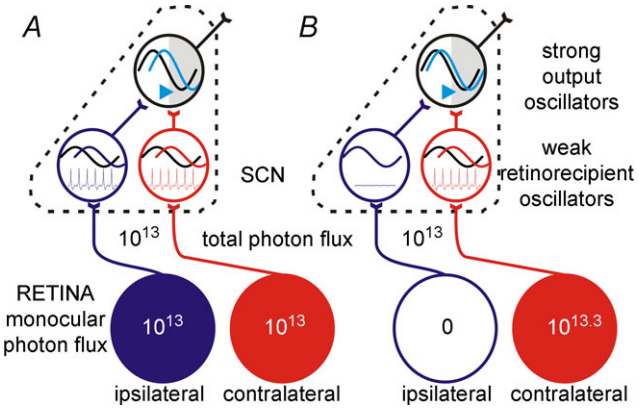

Figure 9. Model of binocular integration in the SCN
Retinorecipient clock cells, with easily perturbed oscillators, are reset according to 'local' irradiance (at most brightness across one visual hemisphere). Strong output oscillators integrate circadian signals from the retinorecipient cells and adjust their phase according to the average of this input. As a consequence, illumination of both eyes drives a substantially larger adjustment in clock output (*A*) than a 2-fold increase in irradiance applied to just one (*B*).

Aside from the above, our data also add to existing literature indicating a surprising amount of diversity in the visual responses of hypothalamic neurons (Aggelopoulos & Meissl, 2000; Drouyer *et al.* 2007; Brown *et al.* 2011). In line with earlier anatomical data (Sollars *et al.* 2003; Guler *et al.* 2008), we previously reported that a subset of cells within or bordering the SCN lacked functional melanopsin input and sustained responses to light (Brown *et al.* 2011). Another study performed in awake (head-fixed) mice also reports a small subset of SCN cells with apparently similar properties (Sakai, 2014). Here we confirm that these non-irradiance-coding SCN cells in fact specifically encode rapid light increments or decrements. None of these cells exhibited binocular responses, suggesting that this population primarily (if not exclusively) signals visual contrast within a restricted portion of the visual field, as described above for irradiance-coding SCN cells. Given these properties, we think it unlikely that such cells play a major role in circadian entrainment, although it is possible that they contribute to more direct SCN-dependent modulations in physiology such as effects on corticosterone secretion (Kiessling *et al.* 2014).

We also identify an especially unusual population of cells that exhibit OFF responses to visual contrast and whose steady state firing activity is thus inversely related to irradiance. While light-suppressed SCN cells have been reported previously (Meijer *et al.* 1986, 1992; Aggelopoulos & Meissl, 2000; Drouyer *et al.* 2007; Brown *et al.* 2011), the population of mouse neurons we report here are distinct in that under dark-adapted conditions they display robust excitatory responses. Moreover the inhibitory responses of these OFF cells under light adaptation are much more rapid than those of the very rare light-suppressed SCN cells we previously reported in the mouse (Brown *et al.* 2011).

As far as we are aware, then, the ON to OFF switching behaviour we describe above has never previously been reported. Although possible that these observations reflect a circadian phase-dependent effect (light-adapted recordings always followed dark-adapted in our experiments) we think this is unlikely to reflect a global change across the SCN. Hence we routinely observed the more conventional ON responses among simultaneously recorded neurons. It is noteworthy here that all of the OFF cells we recorded were exclusively driven by the ipsilateral retina, suggesting that there may be some differential processing of eye-specific signals within the SCN. For example, the switch from excitatory to inhibitory responses might reflect a changing balance between direct and indirect ipsilateral visual input following light adaption. Such indirect visual input could arise locally via the opposing SCN or indeed via other brain regions such as the intergeniculate leaflet (Tang *et al.* 2002; Blasiak & Lewandowski, 2013; Howarth *et al.* 2014). At present we

can only speculate as to the functional significance of the 'darkness-coding' behaviour that these OFF cells exhibit. Presumably the presence of such cells increase the variety of output signals that the SCN is able to transmit, allowing for differential regulation of various aspects of physiology (Kalsbeek *et al.* 2006).

In summary, our data provide new insight into the mechanisms through which the circadian clock processes visual signals. Most notably, we show that the ability of individual SCN neurons to detect irradiance is restricted to only a portion of the full visual field. The implication of this arrangement is that asymmetries in the amount of illumination between left and right eyes could lead the circadian system to substantially underestimate the total amount of ambient illumination. Our data thus predict that, in the absence of any compensatory reorganisation, loss of one eye should result in an unexpectedly large deficit in photic integration within the SCN.

References

Aggelopoulos NC & Meissl H (2000). Responses of neurones of the rat suprachiasmatic nucleus to retinal illumination under photopic and scotopic conditions. *J Physiol* **523**, 211–222.

Albus H, Vansteensel MJ, Michel S, Block GD & Meijer JH (2005). A GABAergic mechanism is necessary for coupling dissociable ventral and dorsal regional oscillators within the circadian clock. *Curr Biol* **15**, 886–893.

Berson DM, Castrucci AM & Provencio I (2010). Morphology and mosaics of melanopsin-expressing retinal ganglion cell types in mice. *J Comp Neurol* **518**, 2405–2422.

Blasiak T & Lewandowski MH (2013). Differential firing pattern and response to lighting conditions of rat intergeniculate leaflet neurons projecting to suprachiasmatic nucleus or contralateral intergeniculate leaflet. *Neuroscience* **228**, 315–324.

Brown TM, Allen AE, al-Enezi J, Wynne J, Schlangen L, Hommes V & Lucas RJ (2013). The melanopic sensitivity function accounts for melanopsin-driven responses in mice under diverse lighting conditions. *PLoS One* **8**, e53583.

Brown TM, Gias C, Hatori M, Keding SR, Semo M, Coffey PJ, Gigg J, Piggins HD, Panda S & Lucas RJ (2010). Melanopsin contributions to irradiance coding in the thalamo-cortical visual system. *PLoS Biol* **8**, e1000558.

Brown TM & Piggins HD (2009). Spatiotemporal heterogeneity in the electrical activity of suprachiasmatic nuclei neurons and their response to photoperiod. *J Biol Rhythms* **24**, 44–54.

Brown TM, Tsujimura S, Allen AE, Wynne J, Bedford R, Vickery G, Vugler A & Lucas RJ (2012). Melanopsin-based brightness discrimination in mice and humans. *Curr Biol* **22**, 1134–1141.

Brown TM, Wynne J, Piggins HD & Lucas RJ (2011). Multiple hypothalamic cell populations encoding distinct visual information. *J Physiol* **589**, 1173–1194.

Coleman JE, Law K & Bear MF (2009). Anatomical origins of ocular dominance in mouse primary visual cortex. *Neuroscience* **161**, 561–571.

Dkhissi-Benyahya O, Sicard B & Cooper HM (2000). Effects of irradiance and stimulus duration on early gene expression (Fos) in the suprachiasmatic nucleus: temporal summation and reciprocity. *J Neurosci* **20**, 7790–7797.

Drouyer E, Rieux C, Hut RA & Cooper HM (2007). Responses of suprachiasmatic nucleus neurons to light and dark adaptation: relative contributions of melanopsin and rod-cone inputs. *J Neurosci* **27**, 9623–9631.

Golombek DA & Rosenstein RE (2010). Physiology of circadian entrainment. *Physiol Rev* **90**, 1063–1102.

Govardovskii VI, Fyhrquist N, Reuter T, Kuzmin DG & Donner K (2000). In search of the visual pigment template. *Vis Neurosci* **17**, 509–528.

Guler AD, Ecker JL, Lall GS, Haq S, Altimus CM, Liao HW, Barnard AR, Cahill H, Badea TC, Zhao H, Hankins MW, Berson DM, Lucas RJ, Yau KW & Hattar S (2008). Melanopsin cells are the principal conduits for rod-cone input to non-image-forming vision. *Nature* **453**, 102–105.

Hattar S, Kumar M, Park A, Tong P, Tung J, Yau KW & Berson DM (2006). Central projections of melanopsin-expressing retinal ganglion cells in the mouse. *J Comp Neurol* **497**, 326–349.

Hattar S, Lucas RJ, Mrosovsky N, Thompson S, Douglas RH, Hankins MW, Lem J, Biel M, Hofmann F, Foster RG & Yau KW (2003). Melanopsin and rod-cone photoreceptive systems account for all major accessory visual functions in mice. *Nature* **424**, 76–81.

Howarth M, Walmsley L & Brown TM (2014). Binocular integration in the mouse lateral geniculate nuclei. *Curr Biol* **24**, 1241–1247.

Irwin RP & Allen CN (2007). Calcium response to retinohypothalamic tract synaptic transmission in suprachiasmatic nucleus neurons. *J Neurosci* **27**, 11748–11757.

Jacobs GH & Williams GA (2007). Contributions of the mouse UV photopigment to the ERG and to vision. *Doc Ophthalmol* **115**, 137–144.

Jiao YY, Lee TM & Rusak B (1999). Photic responses of suprachiasmatic area neurons in diurnal degus (*Octodon degus*) and nocturnal rats (*Rattus norvegicus*). *Brain Res* **817**, 93–103.

Kalsbeek A, Perreau-Lenz S & Buijs RM (2006). A network of (autonomic) clock outputs. *Chronobiol Int* **23**, 521–535.

Kiessling S, Sollars PJ & Pickard GE (2014). Light stimulates the mouse adrenal through a retinohypothalamic pathway independent of an effect on the clock in the suprachiasmatic nucleus. *PLoS One* **9**, e92959.

Lall GS, Revell VL, Momiji H, Al Enezi J, Altimus CM, Guler AD, Aguilar C, Cameron MA, Allender S, Hankins MW & Lucas RJ (2010). Distinct contributions of rod, cone, and melanopsin photoreceptors to encoding irradiance. *Neuron* **66**, 417–428.

Lucas RJ, Hattar S, Takao M, Berson DM, Foster RG & Yau KW (2003). Diminished pupillary light reflex at high irradiances in melanopsin-knockout mice. *Science* **299**, 245–247.

Lucas RJ, Lall GS, Allen AE & Brown TM (2012). How rod, cone, and melanopsin photoreceptors come together to enlighten the mammalian circadian clock. *Prog Brain Res* **199**, 1–18.

Meijer JH, Groos GA & Rusak B (1986). Luminance coding in a circadian pacemaker: the suprachiasmatic nucleus of the rat and the hamster. *Brain Res* **382**, 109–118.
Meijer JH, Rusak B & Ganshirt G (1992). The relation between light-induced discharge in the suprachiasmatic nucleus and phase shifts of hamster circadian rhythms. *Brain Res* **598**, 257–263.
Meijer JH, Rusak B & Harrington ME (1989). Photically responsive neurons in the hypothalamus of a diurnal ground squirrel. *Brain Res* **501**, 315–323.
Miura M, Dong K, Ahmed FA, Okamura H & Yamadori T (1997). The termination of optic nerve fibers in the albino mouse. *Kobe J Med Sci* **43**, 99–108.
Morin LP, Blanchard JH & Provencio I (2003). Retinal ganglion cell projections to the hamster suprachiasmatic nucleus, intergeniculate leaflet, and visual midbrain: bifurcation and melanopsin immunoreactivity. *J Comp Neurol* **465**, 401–416.
Morin LP & Studholme KM (2014). Retinofugal projections in the mouse. *J Comp Neurol* **522**, 3733–3753.
Mure LS, Rieux C, Hattar S & Cooper HM (2007). Melanopsin-dependent nonvisual responses: evidence for photopigment bistability in vivo. *J Biol Rhythms* **22**, 411–424.
Muscat L, Huberman AD, Jordan CL & Morin LP (2003). Crossed and uncrossed retinal projections to the hamster circadian system. *J Comp Neurol* **466**, 513–524.
Muscat L & Morin LP (2005). Binocular contributions to the responsiveness and integrative capacity of the circadian rhythm system to light. *J Biol Rhythms* **20**, 513–525.
Nakamura TJ, Fujimura K, Ebihara S & Shinohara K (2004). Light response of the neuronal firing activity in the suprachiasmatic nucleus of mice. *Neurosci Lett* **371**, 244–248.
Nelson DE & Takahashi JS (1991). Sensitivity and integration in a visual pathway for circadian entrainment in the hamster (*Mesocricetus auratus*). *J Physiol* **439**, 115–145.
Nelson DE & Takahashi JS (1999). Integration and saturation within the circadian photic entrainment pathway of hamsters. *Am J Physiol Regul Integr Comp Physiol* **277**, R1351–R1361.
Paxinos GF & Franklin KBJ (2001). *The Mouse Brain in Stereotaxic Coordinates, Second Edition.* Academic Press, San Diego.
Rieke F & Rudd ME (2009). The challenges natural images pose for visual adaptation. *Neuron* **64**, 605–616.
Roenneberg T & Foster RG (1997). Twilight times: light and the circadian system. *Photochem Photobiol* **66**, 549–561.
Rohling JH, vanderLeest HT, Michel S, Vansteensel MJ & Meijer JH (2011). Phase resetting of the mammalian circadian clock relies on a rapid shift of a small population of pacemaker neurons. *PLoS One* **6**, e25437.
Sakai K (2014). Single unit activity of the suprachiasmatic nucleus and surrounding neurons during the wake-sleep cycle in mice. *Neuroscience* **260**, 249–264.
Sollars PJ, Smeraski CA, Kaufman JD, Ogilvie MD, Provencio I & Pickard GE (2003). Melanopsin and non-melanopsin expressing retinal ganglion cells innervate the hypothalamic suprachiasmatic nucleus. *Vis Neurosci* **20**, 601–610.
Sterratt DC, Lyngholm D, Willshaw DJ & Thompson ID (2013). Standard anatomical and visual space for the mouse retina: computational reconstruction and transformation of flattened retinae with the Retistruct package. *PLoS Comput Biol* **9**, e1002921.
Tang IH, Murakami DM & Fuller CA (2002). Unilateral optic nerve transection alters light response of suprachiasmatic nucleus and intergeniculate leaflet. *Am J Physiol Regul Integr Comp Physiol* **282**, R569–R577.
VanderLeest HT, Houben T, Michel S, Deboer T, Albus H, Vansteensel MJ, Block GD & Meijer JH (2007). Seasonal encoding by the circadian pacemaker of the SCN. *Curr Biol* **17**, 468–473.
van Diepen HC, Ramkisoensing A, Peirson SN, Foster RG & Meijer JH (2013). Irradiance encoding in the suprachiasmatic nuclei by rod and cone photoreceptors. *FASEB J* **27**, 4204–4212.
van Oosterhout F, Fisher SP, van Diepen HC, Watson TS, Houben T, VanderLeest HT, Thompson S, Peirson SN, Foster RG & Meijer JH (2012). Ultraviolet light provides a major input to non-image-forming light detection in mice. *Curr Biol* **22**, 1397–1402.
Vidal L & Morin LP (2007). Absence of normal photic integration in the circadian visual system: response to millisecond light flashes. *J Neurosci* **27**, 3375–3382.

Additional information

Competing interests

None declared.

Author contributions

T.M.B. designed the research; L.W. performed the experiments; L.W. and T.M.B. analysed the data; L.W. and T.M.B. wrote the manuscript. All experiments were performed at the University of Manchester.

Funding

This research was supported by a Biotechnology and Biological Sciences Research Council (BBSRC, UK) David Philips fellowship to T.M.B. (BB/I017836/1).

Appendix 2: Chapter 3 as published in PloS Biology

Walmsley, L., Hanna, L., Mouland, J., Martial, F., West, A., Smedley A. R., Bechtold, D. A., Webb, A. R., Lucas, R. J. & Brown, T. M. (2015). *Colour as a signal for entraining the mammalian circadian clock*. PLoS Biology, 13(4):e1002127

PLOS | BIOLOGY

RESEARCH ARTICLE

Colour As a Signal for Entraining the Mammalian Circadian Clock

Lauren Walmsley[1], Lydia Hanna[1], Josh Mouland[1], Franck Martial[1], Alexander West[1], Andrew R. Smedley[2], David A. Bechtold[1], Ann R. Webb[2], Robert J. Lucas[1]*, Timothy M. Brown[1]*

1 Faculty of Life Sciences, University of Manchester, Manchester, United Kingdom, **2** School of Earth, Atmospheric and Environmental Sciences, University of Manchester, Manchester, United Kingdom

* robert.lucas@manchester.ac.uk (RJL); timothy.brown@manchester.ac.uk (TMB)

OPEN ACCESS

Citation: Walmsley L, Hanna L, Mouland J, Martial F, West A, Smedley AR, et al. (2015) Colour As a Signal for Entraining the Mammalian Circadian Clock. PLoS Biol 13(4): e1002127. doi:10.1371/journal.pbio.1002127

Academic Editor: Achim Kramer, Charité - Universitätsmedizin Berlin, GERMANY

Received: November 7, 2014

Accepted: March 11, 2015

Published: April 17, 2015

Data Availability Statement: All relevant data are within the paper and its Supporting Information files.

Funding: Funded by Biotechnology and Biological Sciences Research Council (www.bbsrc.ac.uk) grants BB/I017836/1 (TMB), BB/I018654 /1 (DAB) and European Research Council (www.erc.europa.eu) Melovision (RJL). The funders had no role in study design, data collection and analysis, decision to publish, or preparation of the manuscript.

Competing Interests: The authors have declared that no competing interests exist.

Abstract

Twilight is characterised by changes in both quantity ("irradiance") and quality ("colour") of light. Animals use the variation in irradiance to adjust their internal circadian clocks, aligning their behaviour and physiology with the solar cycle. However, it is currently unknown whether changes in colour also contribute to this entrainment process. Using environmental measurements, we show here that mammalian blue–yellow colour discrimination provides a more reliable method of tracking twilight progression than simply measuring irradiance. We next use electrophysiological recordings to demonstrate that neurons in the mouse suprachiasmatic circadian clock display the cone-dependent spectral opponency required to make use of this information. Thus, our data show that some clock neurons are highly sensitive to changes in spectral composition occurring over twilight and that this input dictates their response to changes in irradiance. Finally, using mice housed under photoperiods with simulated dawn/dusk transitions, we confirm that spectral changes occurring during twilight are required for appropriate circadian alignment under natural conditions. Together, these data reveal a new sensory mechanism for telling time of day that would be available to any mammalian species capable of chromatic vision.

Author Summary

Animals use an internal brain clock to keep track of time and adjust their behaviour in anticipation of the coming day or night. To be useful, however, this clock must be synchronised to external time. Assessing external time is typically thought to rely on measuring large changes in ambient light intensity that occur over dawn/dusk. The colour of light also changes over these twilight transitions, but it is currently unknown whether such changes in colour are important for synchronising biological clocks to the solar cycle. Here we show that the mammalian blue–yellow colour discrimination axis provides a more reliable indication of twilight progression than a system solely measuring changes in light intensity. We go on to use electrical recordings from the brain clock to reveal the presence of many neurons that can track changes in blue–yellow colour occurring during

Abbreviations: ipRGCs, intrinsically photosensitive retinal ganglion cells; LD, light–dark; LWS, long-wavelength sensitive; MWS, medium wavelength sensitive; SCN, suprachiasmatic nuclei; UVS, ultraviolet sensitive.

natural twilight. Finally, using mice housed under lighting regimes with simulated dawn/dusk transitions, we show that changes in colour are required for appropriate biological timing with respect to the solar cycle. In sum, our data reveal a new sensory mechanism for estimating time of day that should be available to all mammals capable of chromatic vision, including humans.

Introduction

The ability to predict and adapt to recurring events in the environment is fundamental to survival. Organisms across the living world achieve this using endogenous circadian clocks [1–3]. However, if such clocks are to fulfil their ethological function they need to be regularly reset to local time. This is achieved by sensory inputs that report changes in the physical environment providing a useful proxy for time of day. By far the best characterised of these input pathways is that recording the diurnal change in the overall quantity of light reaching the earth's surface (irradiance). In the case of mammals, a dedicated retino-hypothalamic projection brings this visual information to the brain's "master" clock in the suprachiasmatic nuclei (SCN) [4–7].

The retino-hypothalamic projection is formed by a unique class of retinal ganglion cells (RGCs), which are intrinsically photosensitive thanks to their expression of melanopsin [4]. Although these so-called ipRGCs can therefore entrain the clock even in the absence of the conventional rod and cone photoreceptors, all photoreceptor classes are capable of influencing the clock in intact animals [8–13]. This arrangement has previously been considered only insofar as it allows the clock to respond to changes in irradiance. However, the inclusion of cones in this pathway allows for the possibility that the clock could also receive information about changes in the spectral composition of light (colour) [14]. There has previously been speculation that such colour signals could provide a reliable method of telling time of day [3,15] but, to date, there has been no direct test of that possibility in mammals.

The ability to discriminate colour relies on comparing the relative activation of photopigments with divergent spectral sensitivities. In mammals, this task is achieved via differential processing of cone photoreceptor signals in the retina [16]. At least 90% of mammalian species are believed capable of this form of colour discrimination [17] which, with the exception of Old World primates, allows for dichromatic vision. Thus, most mammals express just two distinct classes of cone opsin, one maximally sensitive to short wavelengths (ultraviolet–blue) and a second with peak sensitivity to longer wavelengths (green–red) [18]. Here we show that, in mice, this primordial colour discrimination axis (equivalent to human blue–yellow colour vision) is an influential regulator of SCN activity, essential for appropriate circadian timing relative to the natural solar cycle.

Results

Changes in Colour across Twilight

We first set out to determine whether changes in spectral composition associated with the earth's rotation could provide reliable information about solar angle that the circadian clock could use to estimate time of day. To this end, we obtained high resolution measurements of natural variations in spectral irradiance across multiple days (Manchester, August–October 2005, $n = 36$ d).

As expected, these measurements revealed highly predictable changes in both irradiance and spectral composition as a function of solar angle (Fig 1A and 1B). In particular, we

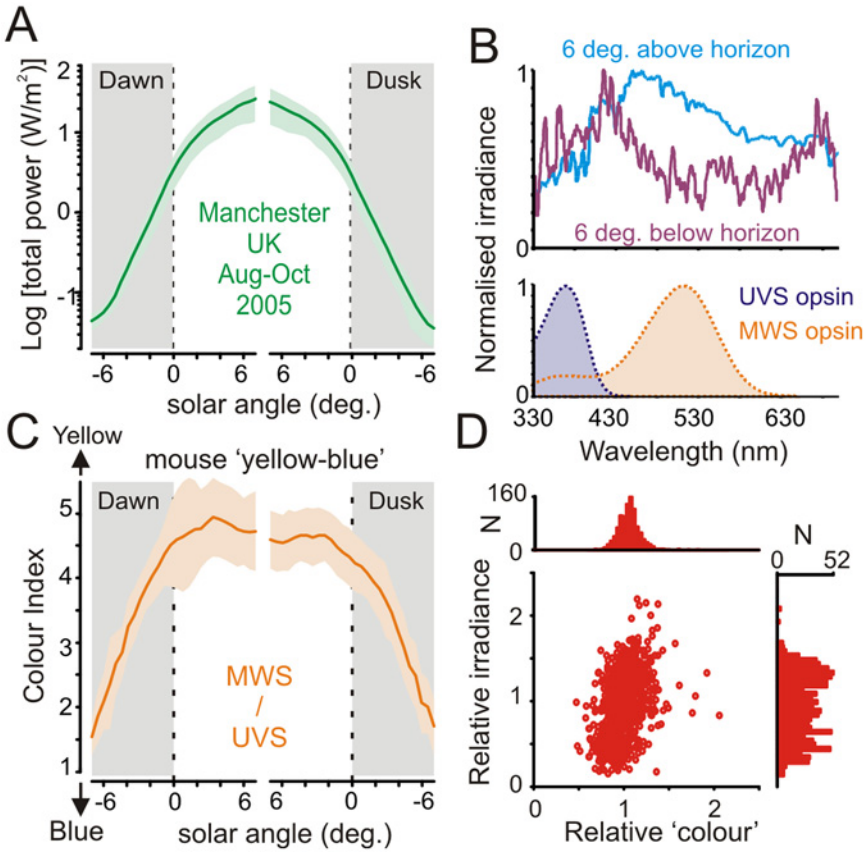

Fig 1. Spectral composition of ambient illumination is predictive of solar angle. (**A**) Mean (±SD) total optical power of ambient illumination around dawn/dusk as a function of solar angle relative to horizon (n = 36 d, Aug–Sep 2005; Lat.: 53.47, Long.: -2.23, Elevation 76 m). (**B**, top) Normalised mean spectral power distribution observed at solar angles ±6° relative to horizon. Note relative enrichment of short-wavelength light at negative solar angles. Bottom panel shows mouse ultraviolet and medium wavelength sensitive (UVS and MWS) cone opsin sensitivity profiles after correction for prereceptoral filtering. (**C**) Mean (±SD) "yellow–blue" colour index (effective activation of MWS/UVS opsin) as a function of solar angle around dawn/dusk. (**D**) Relationship between colour and irradiance (see Methods for definition), corrected according to mean for each solar angle (n = 994; -7 to 0° in 0.5° bins × 71 dawn/dusk observations; for clarity, six observations with especially high relative brightness (2.6–4.5) but normal colour (1.3–1.5) are not shown in the scatter plot). Note tighter distribution for relative "colour" versus irradiance. The data used to make this figure can be found in S1 Data.

doi:10.1371/journal.pbio.1002127.g001

observed a progressive enrichment of short-wavelength light across negative solar angles: a result of the increasing amount of ozone absorption and consequent Chappuis band filtering of green–yellow light when the sun was below the horizon [14].

We next calculated the extent to which this change in spectral composition was detectable to the mammalian visual system. Taking the mouse as a representative species, we employed previously validated approaches to quantify the relative excitation of its ultraviolet and medium wavelength sensitive (UVS/MWS) cone opsins [12,19,20]. This analysis revealed a robust change in the ratio of excitation between the two pigments (Fig 1C) that would constitute substantial changes in apparent colour along the blue–yellow axis. These changes were restricted to the twilight transition, with the UVS:MWS ratio fairly invariant throughout the day, indicating that measuring the change in colour could provide a useful method of tracking the progression of dawn and dusk.

To ascertain how reliably this blue–yellow colour signal alone could be used to estimate phase of twilight, relative to simple measures of irradiance, we next compared the day-to-day variability of colour and irradiance measurements across our dataset (Fig 1D). Surprisingly, we found that colour was in fact more predictive of sun position across twilight (-7 to 0° below horizon) than was irradiance (78.5 ± 0.1% versus 75.8 ± 0.1% of variance explained by solar angle; mean ± SD). Accordingly, for any fixed solar angle, the range of observed colour values was considerably more tightly clustered than those for irradiance. These observations most likely reflect the fact that cloud cover can change overall brightness quite dramatically, but exerts only relatively minor effects on spectral composition.

Colour Coding in the SCN

Importantly, then, measuring colour could provide a more reliable estimate of the approach of night or day than measuring irradiance. However, while the mammalian circadian clock is certainly known to respond to diurnal variations in irradiance [8–13], there has been no investigation of whether the SCN also receives colour signals. Accordingly, we next asked whether the central clock showed electrophysiological responses to changes in colour by recording extracellular activity in the mouse SCN.

In order to identify colour-sensitive cells, we set out to generate test stimuli which differentially modulated the UVS and MWS mouse cone opsins. While, in principle, producing such stimuli is straightforward, the close spectral sensitivity of mouse opsins makes it difficult to achieve this aim without concomitant changes in the activation of rods and/or melanopsin. To circumvent this problem, we employed a well-validated transgenic model in which the native mouse MWS opsin is replaced by the human long-wavelength sensitive (LWS) opsin (*Opn1mw*^{R}; [8,12,19]). Cones in these animals develop and function normally, with LWS opsin expression entirely recapitulating that of the native MWS opsin [21]. Importantly, however, the resultant shift in cone spectral sensitivity in *Opn1mw*^{R} mice facilitates the generation of stimuli that provide selective modulation of individual opsin classes [22].

Using this *Opn1mw*^{R} model, we first established a background lighting condition (using a three-primary LED system), whose spectral composition recreated a wild-type mouse's experience of natural daylight (S1A Fig). We next designed a set of manipulations of this background spectrum that allowed us to modulate excitation of one or both cone opsins without any concomitant change in rod or melanopsin activation. Under these conditions, we were then able to unambiguously distinguish colour-sensitive neurons based on the following criteria: (1) the presence of larger responses to chromatic versus achromatic changes in cone excitation and (2) responses of opposite sign to selective activation of UVS and LWS opsin in isolation (i.e., excitatory/ON versus inhibitory/OFF).

To achieve the largest possible change in colour, we started by selectively modulating UVS and LWS cone opsin excitation in antiphase ("colour"; S1B Fig). We then compared responses to this stimulus with those elicited by one in which the change in UVS and LWS opsin activation occurred in unison ("brightness"; S1B Fig). Any spectrally opponent cells should be more responsive to the "colour" as opposed to "brightness" condition. We found that 17/43 SCN units (from 15 mice) that responded to these stimuli showed a significant preference for the pair in which UVS and LWS activation was modulated in antiphase (Fig 2A and 2B; paired *t* test, $p<0.05$, $n = 17$). As there were an additional 26 visually responsive units that did not respond to either of these analytical stimuli (paired *t* tests, $p>0.05$), these data indicate that at least one quarter of light-responsive SCN neurones show chromatic opponency.

Interestingly, we found that cone inputs exerted a much more powerful influence over the firing activity of cells exhibiting a preference for chromatic stimuli relative to than achromatic

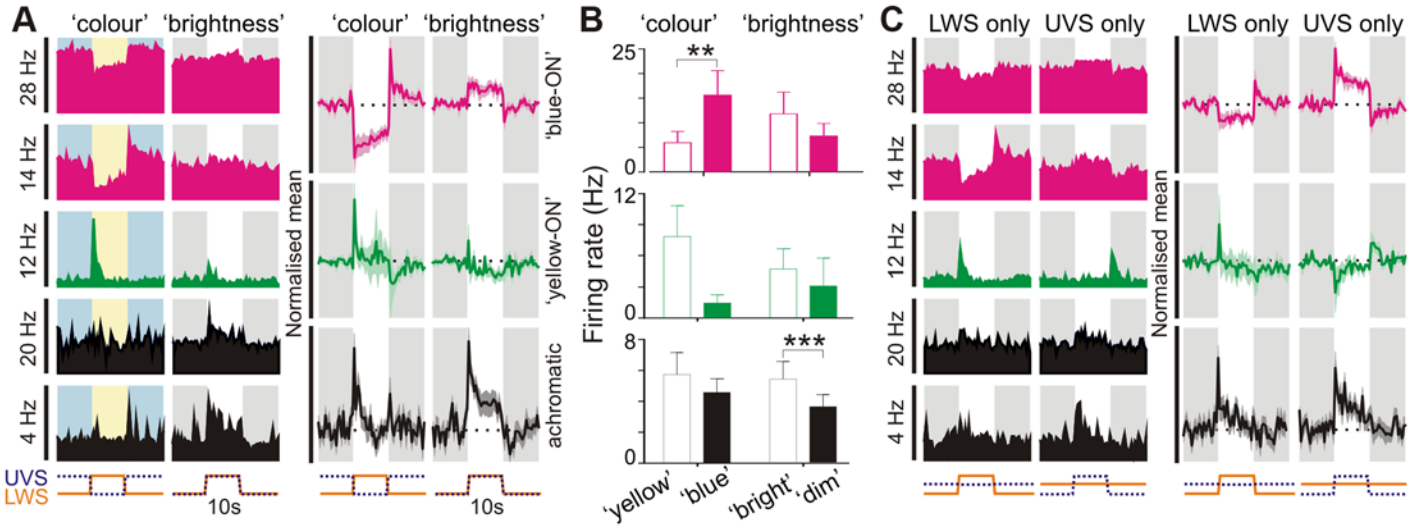

Fig 2. Colour opponent responses in suprachiasmatic neurons. (**A**: left) Example responses of 5 SCN neurons to stimuli modulating UVS and LWS opsin excitation in antiphase ("colour") or in unison ("brightness"; both 70% Michelson contrast). Individual cells were preferentially excited by blue–yellow transitions ("blue ON"; pink traces), yellow-blue transitions ("yellow ON"; green traces) or dim-bright transitions ("achromatic"; black traces). Shaded areas represent blue/yellow or dim/bright stimulus phase; *y*-axis scale bars reflects peak firing rate in spikes/s; *x*-axis scale bars indicate temporal profile of UVS/LWS opsin excitation. (**A**: right) Normalised mean (±SEM) change in firing for cells classified as "blue-ON", "yellow-ON" or achromatic (n = 13, 4 and 26 respectively). Conventions as above. (**B**) Mean (±SEM) firing rates of SCN cell populations tested with colour and brightness stimuli immediately following transitions (0–500 ms) from "blue"–"yellow"/"dim"–"bright" or vice versa. Data were analysed by paired *t* test; *** $p<0.001$, ** $p<0.01$. (**C**: left) Responses of cells from **A** to selective modulation of LWS or UVS opsin excitation, indicating "blue"-ON/"yellow-OFF", "yellow-ON"/"blue-OFF" or non-opponent responses (conventions as in **A**). (**C**: right) Normalised mean (±SEM) change in firing for SCN cell populations evoked by LWS and UVS opsin isolating stimuli. Note, normalisation and scaling for data in **A** and **C** is identical. The data used to make this figure can be found in S2 Data.

doi:10.1371/journal.pbio.1002127.g002

cells (Fig 2B; absolute change for responses of chromatic cells = 8.1 ± 2.3 spikes/s versus 1.9 ± 0.5 spikes/s for achromatic cells, n = 17 and 26 respectively; *t* test: $p<0.01$). Moreover, we found that the spiking activity for the majority (13/17) of colour-sensitive SCN neurons was highest during the stimulus phase biased towards UVS opsin activation (Fig 2A), and that these cells exhibited especially robust and sustained changes in firing (Fig 2A and 2B).

Our data above therefore indicate that cone inputs constitute a dominant influence on the firing activity of colour-sensitive SCN neurons and that most of these cells exhibit blue-ON/yellow-OFF colour opponency. We confirmed this by selectively modulating brightness for each of these cone opsins independently (stimulus shown in S2A Fig); as expected, these cells reliably increased firing in response to selective increases in UVS opsin activation and decreased firing following increases in LWS opsin activation (Fig 2C). Conversely, the remaining colour-sensitive cells exhibited the opposite preference (yellow-ON/blue-OFF; Fig 2C).

An aspect of mouse retinal organisation that poses a challenge to colour vision is that most cones in this species co-express UVS and MWS opsin [23]. The exceptions are rare "primordial S-cones" that only express UVS opsin [24] and peripheral cones that may express either pigment alone [25]. One might expect that chromatic opponency would rely on comparisons between these rare single pigment cones. If this were the case, then responses to LWS- and UVS-specific stimuli of defined contrast should be insensitive to changes in the spectral composition of the background light. In fact, we found that this was not the case (S2A–S2C Fig), indicating involvement of the more common opsin co-expressing cones in the chromatic responses of SCN neurons.

By contrast with chromatic SCN neurons, none of the cells identified as achromatic exhibited any overt OFF response to selective activation of either UVS or LWS cone opsin. Instead,

these achromatic cells exhibited pure ON responses to stimuli targeting one or both opsin classes, such that on average the population showed little bias towards UVS/LWS opsin-driven responses under background spectra resembling natural daylight (Fig 2C). Adjusting the background spectra to equalise basal activation of the two cone opsins skewed responses in favour of UVS opsin, however (S2D Fig), consistent with previous suggestions that ipRGCs are relatively enriched in the UVS opsin-biased dorsal retina [26].

We next asked whether colour opponent cells also received irradiance information from the melanopsin-expressing ipRGCs that dominate retinal input to the SCN [4,6,7]. To this end, we used changes in spectral composition to selectively modulate melanopsin excitation (see Methods; 14/15 mice above tested with these stimuli). When presented with large steps in melanopsin excitation (92% Michelson contrast) generated in this way, "blue"-ON cells showed slow and sustained increases in firing (Fig 3A; peak response = 3.2 ± 0.8 spikes/s above baseline; paired *t* test, $p<0.01$, $n = 13$), as previously described for melanopsin-driven responses [8,27,28]. The behaviour of the rare "yellow" ON cells to this stimulus was variable (Fig 3B; $n = 4$), while colour-insensitive cells showed the expected excitatory response (Fig 3A; peak response = 1.8 ± 0.2 spikes/s above baseline; paired *t* test, $p<0.01$, $n = 23$). These data therefore reveal that both chromatic and achromatic cells have access to melanopsin-dependent information about irradiance.

Of note, for the smaller changes in opsin excitation applied above (70% Michelson; ~0.75 log units), we found that the inclusion of melanopsin contrast had little impact on the integrated cellular response. Thus for both chromatic and achromatic populations, responses evoked by spectrally neutral increases in irradiance ("energy") were very similar in magnitude to those observed where changes in irradiance were restricted to just cone opsins (Fig 3A; subtraction: energy – "brightness"). This was true even for steady-state components of the SCN response (last 1 s of step)—we found no significant difference in responses to two conditions (paired *t* test; $p>0.05$ for both blue-ON and achromatic populations). Thus SCN responses to relatively modest changes in light intensity and/or spectral composition are, in fact, dominated by those originating with cones.

How then do chromatic and irradiance responses interact to encode time of day under more natural conditions? To address this question, we produced stimuli that recreated, for *Opn1mw*^{R} mice, the change in irradiance and colour experienced by wild-type (green cone) mice across the twilight to daylight transition (Fig 4A). We presented these as discrete light steps from darkness, to simulate the challenge in telling time of day faced by a rodent emerging from a subterranean burrow to sample the light environment. Due to their scarcity, we were unable to determine the behaviour of yellow-ON cells under these conditions. However, blue ON cells reliably exhibited a near linear increase in firing rate as a function of simulated solar angle (Fig 4B and 4C; $n = 9$ from 7 mice), indicating that their sensitivity is well suited to track changes in colour/irradiance occurring across the twilight to daylight transition. Interestingly, the range of solar angles to which these neurons responded was substantially greater than that for achromatic cells recorded in the same set of mice (Fig 4D and 4E; see also S3 Fig; $n = 8$) indicating that they may be an especially important source of temporal information for the clock around twilight.

To determine the extent to which this ability of blue-ON cells to encode solar angle relied upon their chromatic opponency, we next presented stimuli that recreated the natural change in irradiance over twilight but in which colour was invariant. Two versions of these stimuli were produced, in which colour was fixed either to that at the lowest solar angle for which data was available ("night") or to that recorded in daylight ("day"; Fig 4A). Whereas achromatic cells were unable to distinguish between these two stimulus sets (Fig 4D and 4E; F-test, $p = 0.72$), the relationship between solar angle and blue-ON cell firing rate was consistently

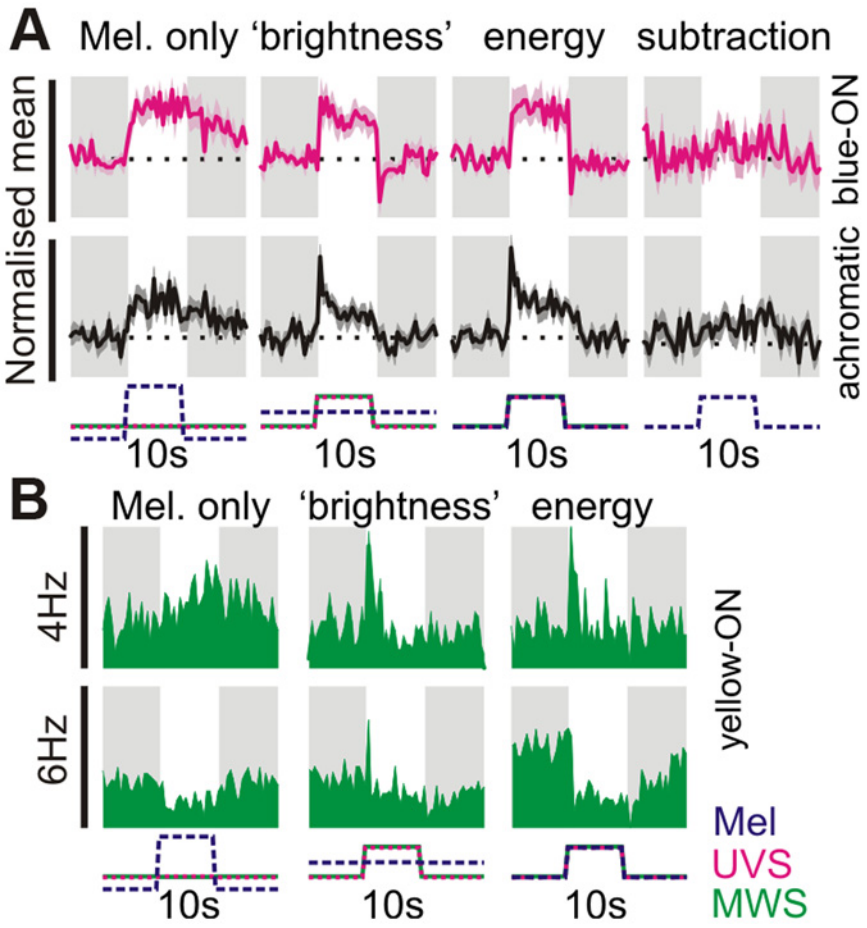

Fig 3. Melanopsin signals influence both colour- and brightness-sensitive cells. (**A**) Normalised mean (±SEM) response of blue-ON colour-sensitive (n = 13) and achromatic cells (n = 23 tested) to stimuli targeting melanopsin and/or cones. Melanopsin-isolating stimuli presented a 92% Michelson contrast change (~1.4 log units), all other stimuli were 70% Michelson contrast (see S1A Fig for details of "colour" and "brightness" stimuli). The energy condition reflects a spectrally neutral modulation in light intensity, providing 70% Michelson contrast for all retinal opsins. Far right panels reflect the predicted melanopsin contribution to the 70% energy condition (obtained by subtracting the responses to UVS + LWS only –"brightness"). Responses were normalised on a within-cell basis across all three stimulus conditions and are plotted on the same scale to highlight relative response amplitude. *X*-axis scale bars indicate temporal profile of UVS/LWS opsin and melanopsin excitation. (**B**) Example responses of yellow-ON colour-sensitive cells (bottom panels) to stimuli targeting melanopsin and/or cones or melanopsin. Melanopsin-isolating contrast had more heterogeneous effects in yellow-ON cells, with 1/4 cells exhibiting a reduction in firing and 2 cells displaying no obvious response (not shown). Conventions as above except that data are presented as raw firing rates. *Y*-axis scale bars represent peak firing in spikes/s. The data used to make this figure can be found in S3 Data.

doi:10.1371/journal.pbio.1002127.g003

disrupted under these conditions (Fig 4B and 4C; F-test, p = 0.009; see also S3A Fig). Thus, firing was reliably higher for "night" and lower for "day" conditions than appropriate for that time of day. These effects are consistent with the blue-ON nature of the chromatic units and confirm that these cells employ a combination of colour and irradiance signals in order to encode time of day.

Colour Sets Circadian Phase

These electrophysiological recordings indicate a significant fraction of neurons in the SCN convey information about changes in spectral composition occurring during natural twilight. We

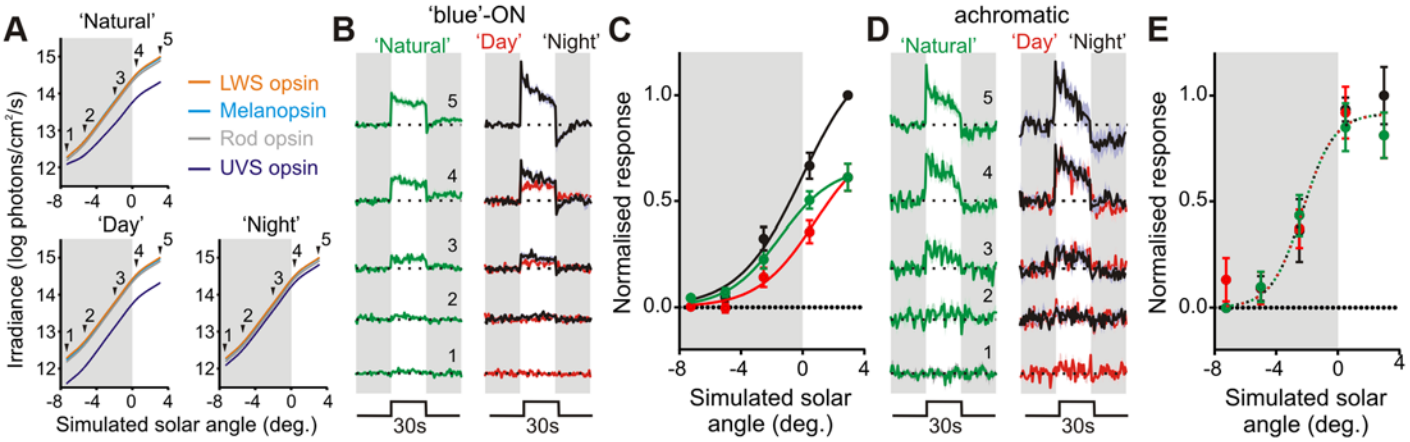

Fig 4. Colour-signals control irradiance coding in suprachiasmatic neurons. (**A**) Stimuli used to examine twilight coding: top panel indicates natural change in effective photon flux for each mouse opsin as a function of solar angle (0° represents sunrise/sunset), indicated points were recreated using a three-primary LED system. Note: values for LWS opsin stimulation were chosen to replicate those calculated for the wild-type MWS opsin under natural conditions. Bottom panels indicate control stimuli, which replicated the "natural" change in irradiance but lacked changes in colour (UVS opsin excitation held at a constant ratio relative to LWS, to mimic "day" or "night" spectra). (**B**) Mean (±SEM) normalised responses of blue-ON cells ($n = 9$) to 30-s light steps recreating the indicated stages of twilight. Responses were normalised on a within-cell basis according to the largest response observed across all three stimulus sets. (**C**) Initial (0–10 s) responses of cells from **B** as a function of simulated solar angle, fit with four-parameter sigmoid curves. Note influence of twilight spectral composition on the solar angle response curve (F-test for difference in curve parameters; $p = 0.009$; direct comparisons between each pair of curves also revealed significant differences $p<0.05$). (**D and E**) Responses of achromatic cells ($n = 8$), conventions as in **B** and **C**. Achromatic cell responses to the three stimulus sets were statistically indistinguishable (F-test; $p = 0.72$). The data used to make this figure can be found in S4 Data.

doi:10.1371/journal.pbio.1002127.g004

hypothesised, therefore, that by improving the SCN's ability to estimate solar angle, activation of the colour mechanism would influence the phasing of circadian rhythms under natural conditions. To determine whether this was indeed the case, we scaled up our twilight stimuli to produce an artificial sky that could be presented to freely moving mice over many days in their home cage. We aimed then to compare the phase of circadian rhythms (assayed using body temperature telemetry) under exposure to lighting conditions that recreated natural changes in irradiance across dawn/dusk transitions, with or without the associated alterations in colour (S4 Fig; "irradiance only" twilight replicated "night" spectral composition). To maximise our ability to detect changes in phasing under these conditions, we modelled the temporal profile of these photoperiods on the extended twilight of a northern-latitude summer (S4C Fig). To allow us to readily separate irradiance and colour elements, we undertook these experiments in *Opn1mw*^{R} mice. Importantly, however, we designed the stimuli to recreate the change in colour across twilight that is experienced by normal, wild-type mice.

We found that the inclusion of colour significantly altered the phase of circadian entrainment. Peak body temperature occurred consistently later when irradiance and colour elements of twilight were included compared to the irradiance signal alone (Fig 5A; 31 ± 8 min; paired *t* test, $p = 0.003$; $n = 10$). This distinction was absent in mice lacking cone phototransduction (*Cnga3*$^{-/-}$, [29,30]; Fig 5B; 6 ± 9 min; paired *t* test, $p = 0.51$; $n = 9$), confirming that it originated with cone-dependent colour coding, rather than any differences in the pattern of rod/melanopsin activation between the two photoperiods.

As further confirmation that these differences in body temperature cycles reflected an action on the timing of central clock output, we also monitored SCN firing rate rhythms in a subset of mice via ex vivo multielectrode array recordings. We and others have previously shown that the distribution of daily electrical activity patterns among individual SCN neurons encodes photoperiod duration, resulting in broad phase distributions under summer days [31,32]. Consistent with this work, peak multiunit firing (sampled across small groups of neurons) in the ex

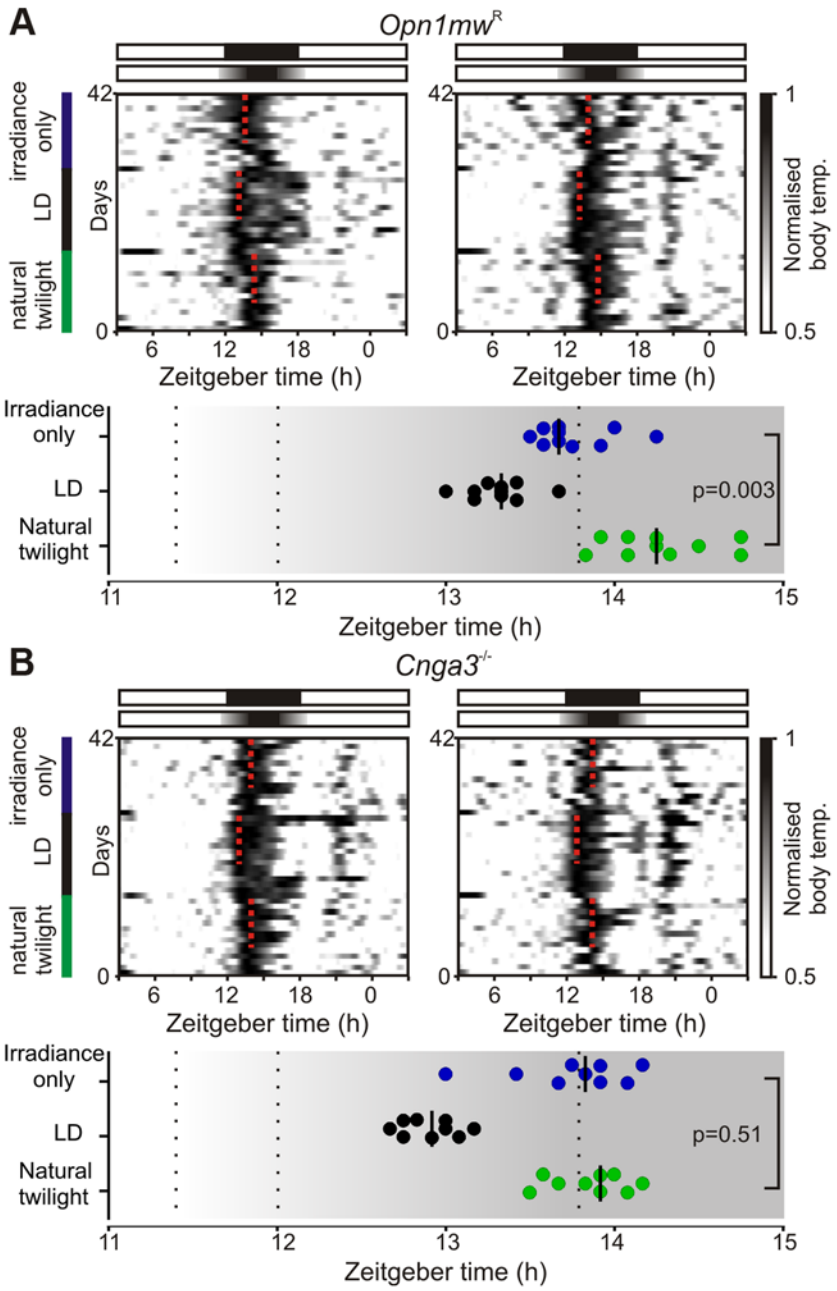

Fig 5. Colour changes associated with natural twilight influence circadian entrainment. (A) Top: Example body temperature traces from two *Opn1mw*^{R} mice. Mice were exposed to sequential 14 d epochs of (i) simulated "natural" twilight (replicating natural changes in irradiance and colour during a northern-latitude summer), (ii) 18:6 square wave LD cycle, and (iii) a twilight photoperiod which lacked changes in colour (irradiance profile identical to "natural" but relative cone opsin excitation fixed to mimic night spectra). Dotted red lines indicate timing of peak body temperature from last 9 d in each photoperiod. Bottom plot indicates timing of peak body temperature for each individual ($n = 10$); bars represent median. Temperature cycles were significantly phase-advanced under the irradiance-only versus natural twilight (paired t test; $p = 0.003$). (**B**) Mice lacking functional cone phototransduction (*Cnga3*$^{-/-}$) exhibit identical phase of entrainment under both photoperiods (conventions as in **A**; paired t test; $p = 0.51$, $n = 9$) with peak body temperature occurring significantly earlier versus wild-type mice under natural but not irradiance-only twilight (unpaired t tests, $p = 0.005$ and 0.91 respectively). The data used to make this figure can be found in S5 Data.

doi:10.1371/journal.pbio.1002127.g005

vivo SCN of twilight-housed mice was widely distributed across recording epochs corresponding to projected day. Importantly, in line with our body temperature data, this distribution was centred around the middle of the projected day for *Opn1mw*^{R} mice exposed to "natural" twilight (Fig 6A; n = 124 SCN electrodes from seven slices) but shifted substantially earlier when mice were housed under twilight that lacked changes in colour (Fig 6B; $p<0.001$, bootstrap percentiles; n = 170 SCN electrodes from six slices). A similarly early phase of peak SCN electrical activity was also observed in slices prepared from *Cnga3*$^{-/-}$ individuals housed under natural twilight (S5 Fig; $p<0.001$ versus *Opn1mw*^{R}, bootstrap percentiles), confirming that the cone-dependent colour signal is indeed required for appropriate biological alignment with twilight. We also found that, across the three groups, *Opn1mw*^{R} mice exposed to "irradiance-only" twilight exhibited a significantly broader distribution of SCN phasing (Brown-Forsythe test, $p = 0.01$), suggesting that the inappropriate cone signals under this photoperiod partially impair SCN synchrony.

Discussion

Here we demonstrate that the mammalian clock has access to information about not just the amount but also the spectral composition of ambient illumination, in the form of a cone-dependent colour opponent input that reports blue–yellow colour. The idea that chromatic signals associated with twilight might provide important cues for circadian photoentrainment has been proposed previously [3,15]. However, the significant technical challenges inherent in distinguishing the influence of changes in colour versus brightness have left the specific role of colour untested, until now.

Our work thus represents the first demonstration that colour-opponent signals influence the circadian clock in any mammalian species. It is clear, from the long history of housing animals under artificial lighting, that colour signals are not necessary for circadian entrainment per se. However, our data indicates that most mammals could use colour [18,33–35] to provide additional information about sun position, above that available from simply measuring irradiance. Our entrainment experiments likely underestimate the importance of that colour signal

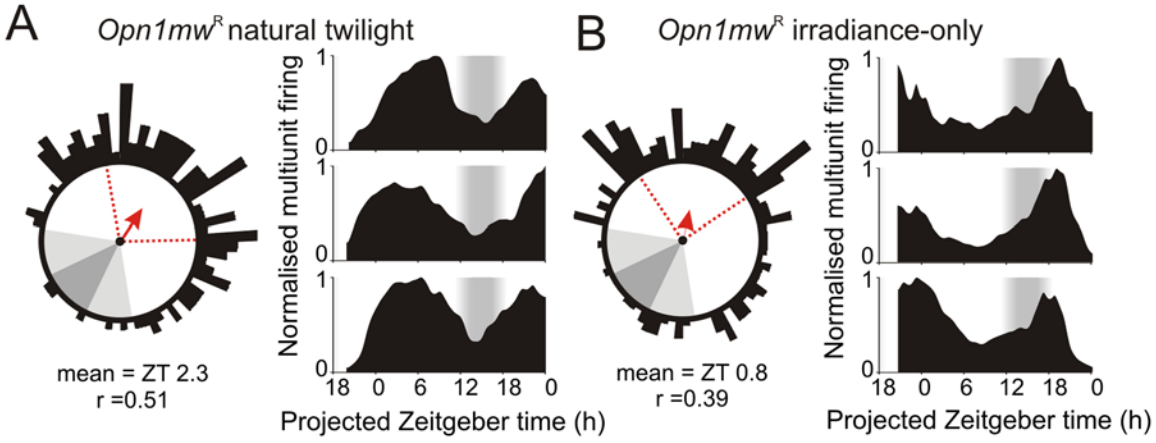

Fig 6. Twilight spectral composition regulates photoperiodic encoding in the suprachiasmatic nuclei. (**A**–**B**) Phasing of SCN firing rhythms from ex vivo multielectrode array recordings of *Opn1mw*^{R} mice housed under natural (**A**) or irradiance-only (**B**) twilight photoperiods. Left panels show Rayleigh vector plots for peak firing activity (n = 124 and 170 SCN electrodes from seven and six slices in **A** and **B** respectively). Grey-shaded areas correspond to timing of night/twilight transitions, red dotted lines indicate central 50% of the data distribution, arrows indicate mean vector direction. Right panels show representative multiunit traces. Consistent with body temperature data (Fig 5), SCN activity peaks later in mice housed under "natural" relative to irradiance-only twilight ($p<0.001$ based on bootstrap percentiles). The data used to make this figure can be found in S6 Data.

doi:10.1371/journal.pbio.1002127.g006

under field conditions as they lack the daily variation in cloud cover that makes irradiance-alone a less reliable indicator of time of day. Nevertheless, even under these conditions, we find a significant impact of the twilight spectral change on the phasing of entrained rhythms. This reveals that spectral opponency contributes to the most fundamental function of the entrainment mechanism, ensuring correct timing of physiological and behavioural rhythms.

Given the nature of the change in spectral composition, we might expect that it would be available to any species capable of comparing the activity of short with middle/longer wavelengths. Our own subjective experience is that the event is detectable to humans, and a chromatic opponency equivalent to that described here could account for previous reports of subadditivity for polychromatic illumination in human melatonin suppression [36,37]. It is also noteworthy that the majority of mammalian species have retained the short and mid-/long-wavelength cone opsins required to detect changes in spectral composition associated with twilight (for a detailed discussion of the exceptions to this rule see [17,18]). Similarly, earlier studies have identified the capacity for blue–yellow colour discrimination in the pineal/parietal organs of a number of non-mammalian vertebrates, including reptiles, amphibians, and fish (for review see [38]). By directly influencing melatonin secretion, chromatic signals are thus presumably also a key component of the neural mechanisms responsible for appropriate alignment of non-mammalian physiology relative to dawn and dusk. Alongside our present data, it appears then that the use of colour as an indicator of time of day is an evolutionarily conserved strategy, perhaps even representing the original purpose of colour vision.

The specific sensory properties of the circadian photoentrainment mechanism in mammals have long remained a subject of debate [2]. SCN neurons are known to receive input from all major classes of retinal photoreceptor [8–13]. However, since "cone-only" mice do not reliably entrain to conventional light–dark cycles, current models posit that photoentrainment is primary driven by a combination of rod and melanopsin inputs [11,12]. By contrast, the proposed role of cones has been to allow the clock to track relatively high frequency changes in light—a signal that does not appear to play much role in circadian entrainment under conditions most commonly employed in the laboratory (but see [12]). Our data thus establish an important new role for cones in photoentrainment, one which would not be apparent under standard laboratory conditions but will act as an essential regulator of biological timing in more natural settings.

Insofar as most retinal input to the clock is provided by ipRGCs [4,6,7] the appearance of colour opponency in this subset of retinal ganglion cells would provide a simple explanation for the chromatic responses of SCN neurons observed here. Colour opponency has not yet been documented in mouse ipRGCs [39], but has been reported in primates [40] (although it is unknown whether any of these cells project to the SCN). Interestingly, the dominant form of spectral opponency we observe here in the mouse SCN (blue-ON/yellow-OFF) is opposite to that reported for primate ipRGCs and, most recently, for chromatic response of the pupil in humans [41]. While this would, by no means, rule out a role for chromatic influences on the human circadian system, it is also currently unclear whether such yellow-ON/blue-OFF responses are a characteristic feature of all primate ipRGCs. Indeed, such behaviour certainly appears inconsistent with the sensory properties of human melatonin regulation, which seems to exhibit a short- rather than long-wavelength bias [42].

Of course, alternative possibilities to that outlined above are that colour information reaches SCN neurons via the small number of non-melanopsin-expressing RGC inputs or is generated by a mechanism distinct from the conventional retinal colour processing circuitry. Previous work indicates that asymmetries in the gradient of cone opsin expression in the mouse retina could impose an indirect form of chromatic bias for stimuli larger than the cells' receptive field [43]. Alternatively, opponent responses in the SCN may be generated centrally, e.g., via local

processing or indirect visual input from the intergeniculate leaflet. Indeed, based on our identification of a rare yellow-ON cell exhibiting inhibitory responses to melanopsin contrast, we speculate that central processing could contribute to at least some of the responses reported here.

Regardless of their biological origin, chromatic signals provide the SCN with additional information about solar angle, above that available from measuring brightness alone, allowing the clock to appropriately time its output under natural photoperiods. Based on the widespread capacity for colour vision among mammals (and the previous identification of colour opponent ipRGCs in primates), we suggest related mechanisms are likely to be broadly applicable across many mammalian species.

Methods

Animals

All animal use was in accordance with the Animals (Scientific Procedures) Act of 1986 (United Kingdom). Electrophysiological experiments were performed under urethane anaesthesia; other procedures were conducted under isfluorane anaesthesia. Unless otherwise stated, animals used in this study (homozygous *Opn1mw*^{R} and *Cnga3*$^{-/-}$ mice) were housed under a 12-h dark/light cycle at a temperature of 22°C with food and water available ad libitum.

Environmental Measurements

Spectral irradiance measurements (280–700 nm, 0.5 nm bins) were collected in Manchester, UK (Lat.: 53.47, Long.: -2.23, Elevation 76 m) every minute across the solar cycle using a MET-CON diode array spectroradiometer contained within a temperature stabilised weatherproof housing. The global entrance optics was levelled and mounted at a rooftop monitoring site, providing a horizon relatively clear of obstructions, the entrance optics being connected to the spectrometer by way of a 600 μm diameter 5 m long optical fibre. Instrument calibrations were carried out with reference to spectral irradiance standards, traceable to NIST (National Institute of Standards and Technology, United States). Instrument dark counts were observed to be spectrally flat and were removed by subtracting the mean value for wavelengths $<$290 nm (where no ground-level solar signal is present).

Environmental Data Modelling

Data analysed were spectral irradiance measurements collected between 31 August and 14 October 2005 (41 d). Due to gaps in the data collection record, we were able to extract from these 71 complete dawn/dusk transitions (from 36 d). No attempt was made to select data on the basis of weather condition although the period was broadly representative in comparison to relevant climatological averages.

For each twilight transition, we first calculated the average spectral irradiance profile as a function of solar angle relative to the Horizon (0.5° bins, 2–5 measurements/bin). We restricted this analysis to solar angles greater than 7° below the horizon, since our detector was specifically optimised to obtain measurements across light intensities encountered through civil twilight to daytime (making night-time measurements less reliable). We next converted these spectral irradiance profiles into effective photon fluxes as experienced by mouse opsin proteins, using established and validated procedures [19,20,22] based on Govardovski visual pigment templates [44] and published values for mouse lens transmission [45]. Calculations presented in the manuscript were based on the following peak sensitivity (λmax): UVS cone opsin-365 nm, Melanopsin-480 nm, Rhodopsin-498 nm, MWS cone opsin 511 nm.

The resulting series" of photon flux versus solar angle values for each opsin were then analysed individually or in combination (additive or as ratios). Specifically, we calculated the percentage of variance for the dataset in question that was explained by sun position, using the following calculation (with N representing the total number of data points, K the number of dawn/dusk observations and P the number of solar angle bins):

$$\mathrm{Var}|\theta = 100K\frac{\sum_{h=1}^{P}(\bar{X}_h - \bar{X})^2}{\sum_{i=1}^{N}(X_i - \bar{X})^2}$$

Since there was no apparent difference in photon flux versus solar angle profiles obtained during dawn or dusk transitions, we pooled these data for the above analysis, treating each as an independent observation.

For comparisons of colour versus irradiance based estimates of solar angle (Fig 1D and associated text), irradiance was defined as effective photon flux at UVS+MWS cone opsins. Values obtained using other mouse opsins (singly or in combination) produced essentially identical results. For the aforementioned comparisons, estimates of mean and standard deviation for Var|θ were obtained based on bootstrap replicates (every possible combination of 69 out of the total 71 dawn/dusk observations). Similar analysis to those described above, but performed using only observations taken at either dawn or dusk also produced essentially identical results. Calculations of ""blue–yellow""colour index (Fig 1C and 1D) were based on the ratio of MWS: SWS cone opsin activation ([MWS+LWS]/SWS for human visual system).

In Vivo Electrophysiological Recordings

Urethane (1.55 g/kg) anaesthetised adult (60–120 d) male *Opn1mw*^{R} mice were prepared for stereotaxic surgery as previously described [8]. Recording probes (Buszaki 32L; Neuronexus, MI, US) consisting of four shanks (spaced 200 μm), each with eight closely spaced recordings sites in diamond formation (intersite distance 20–34 μm) were coated with fluorescent dye (CM-DiI; Invitrogen, Paisley, UK) and then inserted into the brain 1 mm lateral and 0.4 mm caudal to bregma at an angle of 9° relative to the dorsal-ventral axis. Electrodes were then lowered to the level of the SCN using a fluid-filled micromanipulator (MO-10, Narishige International Ltd., London, UK).

After allowing 30 min for neural activity to stabilise following probe insertion, wideband neural signals were acquired using a Recorder64 system (Plexon, TX, US), amplified (x3000) and digitized at 40 kHz. Action potentials were discriminated from these signals offline as "virtual"-tetrode waveforms using custom MATLAB (The Mathworks Inc., MA, US) scripts and sorted manually using commercial principle components based software (Offline sorter, Plexon, TX, US) as described previously [46].

Surgical procedures were completed 1–2 h before the end of the home cage light phase, such that electrophysiological recordings spanned the late projected day-early projected night, an epoch when the SCN light response is most sensitive. Cells were initially characterised as light responsive on the basis of responses to bright mono and polychromatic light steps (10–30 s dur.; intensity $>10^{14}$ photons/cm^2/s). Once visual responsiveness was confirmed, experimental stimuli were applied as described below. Following the experiment, accurate electrode placement was confirmed histologically as described previously [8]. Projected anatomical locations of light response units reported in this study are presented in S6 Fig.

Visual Stimuli

All visual stimuli were delivered in a darkened chamber from a custom built source (Cairn Research Ltd, Kent, UK) consisting of independently controlled UV, blue and amber LEDs (λmax: 365, 460, and 600 nm respectively). Light was combined by a series of dichroic mirrors and focused onto a 5 mm diameter piece of opal diffusing glass (Edmund Optics Inc., York, UK) positioned <1 mm from the eye (contralateral to the recording probe for SCN recordings). LED intensity was controlled by a PC running LabView 8.6 (National instruments).

Light measurements were performed using a calibrated spectroradiometer (Bentham instruments, Reading, UK). LED intensity was initially calibrated (using the principles described above) to recreate for *Opn1mw*^{R} individuals the effective rod, cone and melanopsin excitation experienced by a wild-type (green cone) mouse visual system under typical natural daylight (average values from our environmental data above at a solar angle 3° above the horizon; S1A Fig). We also carefully calibrated differential modulations in the intensity of each LED to produce stimuli that independently varied in apparent brightness for one or both cone opsin classes (either in unison or antiphase) with no apparent change in rod or melanopsin excitation (S1B Fig). In each case, brightness for the stimulated opsin was varied by ±70%, to produce an overall 4.7-fold increase in intensity of between "bright" and "dim" phases of the stimulus. Transitions between the two stimulus phases occurred smoothly over 50ms (half sinusoid profile). We also applied stimuli that selectively modulated melanopsin excitation (±92%), without changing effective cone excitation. These later also, in principle, modulated apparent brightness for rod photoreceptors (±84%), however we think a rod contribution to the resulting responses unlikely owing to the high background light levels (14.9 rod effective photons/cm^2/s) and our previous work suggesting that rods have little influence on acute electrophysiological light responses in the SCN [8]. Indeed, similar stimuli evoke very little response in the lateral geniculate nuclei of melanopsin knockout animals [22].

In a subset of experiments (7/15) we also applied a second set of stimuli designed to recreate various stages of twilight, using our calculations of the effective photon fluxes experienced by mouse opsins at solar angles between -7 and 3° relative to the horizon. These were applied as light steps (30 s) from darkness in random sequence with an interstimulus interval of 2 min. To confirm whether elements of the resulting responses were dependent on spectral composition, these stimuli were interspersed with two additional stimulus sets which were identical except that irradiance for the UVS opsin was fixed at a constant ratio relative to LWS (mimicking either day or night spectral composition).

For behavioural experiments, we used similar principles to generate photoperiods that smoothly recreated our measured changes in twilight illumination, with ("natural") or without the associated change in spectral composition (irradiance-only: spectra fixed to mimic "night"). Stimuli were generated by an array of three violet (400 nm) and three amber (590 nm) high-power LEDs (LED Engin Inc., San Jose CA, US) placed behind a polypropylene diffusing screen covering the top of the cage. The combination of multiple LEDs allowed a larger range of brightness (from dark up to approximately 25 W/m2 for the violet and 10 W/m2 for the amber). Intensity of each LED was independently controlled by a voltage controlled driver (Thorlabs Inc., Newton NJ, US). The light intensity modulation signals were provided by a PC running Labview through a voltage output module (National Instruments), and followed a temporal profile that recreated the sun's progression during a northern latitude summer (calculations based on Stockholm, Sweden; Lat: 59, Long: 18, Elevation 76 m, 20 June 2013; total twilight duration = 2.3 h).

Twilight Entrainment Study

To determine the impact of twilight spectral changes on mouse entrainment, female *Opn1mw^R and Cnga3$^{-/-}$* mice (housed under an 18:6 light–dark [LD] cycle) were first implanted with iButton temperature loggers (Maxim, DS1922L-F5#). To reduce weight and size, these were dehoused and encapsulated in a 20% Poly(ethylene-co-vinyl acetate) and 80% paraffin mixture as described by Lovegrove [47]. For implantation, mice were anaesthetised with isoflurane (1%–5% in O_2) and the temperature logger implanted into the peritoneal cavity. Following surgery, animals were given a 0.03 mg/kg subcutaneous dose of buprenorphine and allowed to recover for at least 9 d in 18:6 LD before the start of the experiment. The timing of lights off under this cycle was designated as *Zeitgeber* time (ZT) 12 and the timing of experimental photoperiods were set to align their midnight (ZT15) with this square wave LD cycle.

Following recovery, group housed mice (five per cage) were transferred to the natural twilight photoperiod. The cage environment contained an opaque plastic hide, allowing the animals to choose their own light sampling regime. After 14 d, mice were then returned to 18:6 LD for a further 14 d and finally transferred to the "irradiance-only" twilight photoperiod.

At the end of the experiment, mice were culled by cervical dislocation and temperature loggers recovered. Temperature data (recorded in 30 min time bins) was processed by upsampling to 5 min resolution (cubic spline interpolation), Gaussian smoothing (SD = 45 min), and normalisation as a fraction of daily temperature range. Phase of entrainment was estimated as the timing of peak body temperature from that individual's daily average profile (calculated from the last 9 d in each photoperiod).

Ex Vivo SCN Recordings

Opn1mw^R and Cnga3$^{-/-}$ mice were housed under twilight stimuli of either "natural" or "night" composition (as described above) for at least 14 d prior to experiments. Mice were removed from the home cage 30–60 min after the end of the dawn transition (~ZT19) and culled by cervical dislocation followed by decapitation. The brain was then rapidly removed, mounted onto a metal stage and cut using a 7000 smz vibrating microtome (Campden Instrument, UK) in ice-cold (~4°C) sucrose-based slicing solution composed of (in mM): sucrose (189); D-glucose (10); $NaHCO_3$ (26); KCl (3); $MgSO_4$ (5); $CaCl_2$ (0.1); NaH_2PO_4 (1.25); oxygenated with 95% O_2/5% CO_2 mixture. Coronal brain slices containing the SCN (350 μm) were then immediately transferred into a petri dish containing oxygenated artificial cerebrospinal fluid (aCSF) composed of (in mM): NaCl (124); KCl (3); $NaHCO_3$ (24); NaH_2PO_4 (1.25); $MgSO_4$ (1); glucose (10); $CaCl_2$ (2); slices were then left to rest at room temperature (22 ± 1°C).

Approximately 30 min after slice preparation, slices were placed, recording side down, onto 6x10 perforated multielectrode arrays (pMEAs; Multichannel Systems, MCS, Germany). Slices were visualised under the microscope and photos were taken with a GXCAM-1.3 camera (GX Optical, UK) in order to confirm appropriate slice placement over pMEA electrode sites. Slices were held in place by both the suction via the MEA perforations and a harp slice grid (ALA Scientific Instruments Inc., US). The pMEA recording chamber was continuously perfused with pre-warmed oxygenated aCSF (34 ± 1°C) to both slice surfaces at a rate of 2.5–3 ml/min. Neural signals were acquired as time-stamped action potential waveforms using a USB-ME64 system and a MEA1060UP-BC amplifier (MCS, Germany). Signals were sampled at 12.5 kHz, High pass filtered at 200 Hz (second order Butterworth) with a threshold of usually at -16.5 μV. Recordings were maintained for a total duration of 30 h.

At the end of each recording, slices were treated with bath applications of 20μM NMDA to confirm maintained cell responsiveness, followed by 1 μM TTX to confirm acquired signals exclusively reflected Na^+-dependent action potentials. All drugs were purchased from Tocris

(UK), kept as stock solutions at -20°C (dissolved in dH_2O), and were diluted to their respective final concentrations directly in pre-warmed, oxygenated aCSF; all drugs were bath applied for 5 min.

Multiunit action potential firing rates detected at electrodes located within the SCN region were then selected for further analysis. Data were subsequently binned (60 s) and smoothed via boxcar averaging (width: 2 h) to determine the timing of peak activity. Channels where peak firing did not decay by >50% within ±12 h, or where peak firing was less than 0.2 spikes/s were excluded from this analysis, such that on average 22 ± 2 SCN electrodes were analysed for each experiment. Based on peak firing rates observed (mean ± SEM: 6.9 ± 0.5 spikes/s) we estimate these typically represent recordings from less than four neurons.

To assess for significant differences in the timing of population activity under our different experimental conditions, we drew 1,000 samples of 100 randomly selected neurons from each condition (*Opn1mw*^{R} "natural", *Opn1mw*^{R} "night", *Cnga3*$^{-/-}$ "natural"). By calculating the circular mean phase for each sample, we thus obtained estimates of the probability that the observed population means differed by chance.

Supporting Information

S1 Data. Excel spreadsheet containing, in separate sheets, the numerical data and statistical analysis for Fig 1A–1D and underlying raw values used to generate those averages (total optical power, colour index, MWS and UVS opsin flux versus solar angle for each observation).
(XLSX)

S2 Data. Excel spreadsheet containing, in separate sheets, the numerical data and statistical analysis for Figs 2A–2C and S2C and S2D and underlying raw values used to generate averages (peristimulus time histograms for all blue ON, yellow ON, and achromatic cells responses to each stimulus condition).
(XLSX)

S3 Data. Excel spreadsheet containing, in separate sheets, the numerical data and statistical analysis for Fig 3A and 3B and underlying raw data values (peristimulus time histograms for all blue ON, yellow ON, and achromatic cells responses to each stimulus condition).
(XLSX)

S4 Data. Excel spreadsheet containing, in separate sheets, the numerical data and statistical analysis for Figs 4A–4E and S3A–S3C and underlying raw values used to generate averages (peristimulus time histograms for all blue ON and achromatic cells responses to each stimulus condition and "unclassified" cell responses to natural twilight).
(XLSX)

S5 Data. Excel spreadsheet containing the numerical data and statistical analysis for Fig 5A and 5B and underlying raw values used to generate averages (daily body temperature profiles for *Opn1mw*^{R} and *cnga3*$^{-/-}$ mice under both photoperiods).
(XLSX)

S6 Data. Excel spreadsheet containing, in separate sheets, the numerical data and statistical analysis for Figs 6A and 6B and S5A and sampled distributions used to assess significant differences in phase.
(XLSX)

S1 Fig. Selective modulation of colour and brightness in red cone knock-in mice. (**A**) Top panel shows normalised spectral profile of daytime ambient illumination (blue line; +3°) alongside sensitivity profiles for native mouse opsins. Numbers above traces indicate the calculated photon flux for each photoreceptor class (Log photons/cm^2/s). Bottom panel shows spectral profile of three-primary LED system used to recreate natural daylight from red cone knock-in mice (*Opn1mw*^{R}). Note the shift in cone sensitivity from MWS (top panel) to LWS (bottom panel): the photon flux experienced by wild-type mouse MWS cones (15 log photons/cm2/s) is translated here into an equivalent photon flux for the LWS cone knock-in. (**B**) Illustration of spectral modulations used to selectively evoke changes in relative ("colour"; top) or absolute ("brightness"; bottom) activation of UV and long-wavelength sensitive (UVS/LWS) cone opsins. Numbers on traces reflect Log photon flux at blue versus yellow (top panel) or dim versus bright (bottom panel) stimulus phases. These equate to 4.7-fold changes (70% Michelson contrast) in cone opsin activation with essentially no effective change in melanopsin excitation (<1% Michelson). Effective changes in rod excitation are omitted for clarity but are also very small (6.5% and 4.5% Michelson for "brightness" and "colour" respectively), however, owing to the overall intensity of the stimuli, it is highly unlikely that rods could contribute to any response even with much larger contrasts.
(TIF)

S2 Fig. Effect of background spectra on SCN spectral sensitivity. (**A**) Spectral modulations used to selectively evoke changes in LWS (top) or UVS opsin excitation (bottom) under "natural" daylight and a "white" background where basal activation of UVS and LWS opsin were equivalent. In each case, effective change for the modulated opsin is 70% Michelson contrast (non-modulated ("silent") opsins <1% Michelson). Note that, since most mouse cones co-express both opsins (and must sum over all photons detected), the net change in cone photon flux presented by these stimuli is influenced both by the relative background photon flux at each of the two opsin classes and by the degree of co-expression in each cone. (**B**) Model of the effective change in irradiance presented by cone opsin-isolating stimuli, as a function of relative opsin co-expression, under "natural" and "white" backgrounds. (**C**: top) Normalised mean (±SEM) responses to UVS/LWS contrast under natural and white background spectra for all blue-ON and yellow-ON cells (n = 13 and 4 respectively). Shading indicates "dim" to "bright" transition, x-axis scale bars indicate temporal profile of UVS/LWS opsin excitation. Note, LWS and UVS opsin specific responses are modulated by changes in background spectra consistent with the involvement of cone that co-express both opsins. (**C**: bottom) Example responses of two colour-sensitive cells whose opponency was highly dependent on background spectra (one other blue-ON cell exhibited similar behaviour, not shown). Y-axis scale bar indicates firing frequency in spikes/s. (**D**) Example achromatic cell response (top) and normalised population mean (±SEM; bottom) for UVS and LWS contrast under the two backgrounds. The data used to make this figure can be found in S2 Data.
(TIF)

S3 Fig. Responses of SCN neurons to simulated twilight. (**A**: top) Mean (±SEM) normalised responses (5s bins) of blue-ON (left; n = 9) and achromatic units (right; n = 8) to stimuli with "natural" or "day" spectra at intensities corresponding to dawn (solar angle 0.5° above horizon; spectra 4 from Fig 4A). Data analysed by one-way RM-ANOVA with Sidak post-hoc test; ** $p<0.01$, * $p<0.05$. Bottom plots show mean response time course. Note the significantly larger responses of blue-ON cells to "natural" versus "day" stimuli despite only very small differences in the effective UVS opsin excitation produced by these two stimuli (~5%, 0.02 log units). (**B**) Steady state firing rates in darkness and under "day-time" illumination (equivalent to solar angle of 3° above horizon; last 10 s of 30 s light step) for various light-responsive SCN

cell classes. Data analysed by paired *t* test between light and dark, *** $p<0.001$. (**C**) Mean (±SEM) normalised responses of SCN cells that could not be classified as brightness/colour sensitive ($n = 25$) to 30 s light steps recreating various stages of twilight. These were qualitatively similar to those of brightness sensitive cells (Fig 4D and 4E). The data used to make this figure can be found in S3 Data.
(TIF)

S4 Fig. Assessing influences of twilight spectra on circadian entrainment. (**A**) Schematic of housing conditions for experiments assessing the influence of twilight spectra. Mice (with temperature sensors implanted i.p.) were group housed (5/cage) and uniform illumination applied across the entire top surface of the cage via an artificial sky (comprising multiple amber and violet LEDs controlled by pulse width modulation). Mice could freely move between the open cage and an opaque plastic hide, allowing individuals to choose their own light sampling regimen. (**B**) Artificial sky was calibrated to replicate, for *Opn1mw*^{R} individuals, a wild-type mouse's experience of twilight (left: "natural"). A second, analytical twilight stimulus was calibrated to match the natural change in irradiance but with relative activation of cone opsins fixed to match the night spectra (right: "night"). (**C**) To maximise our ability to distinguish differences in phase of entrainment under the above conditions, twilight stimuli were set to a cycle that simulated the sun's progression during a northern latitude summer (calculations based on Stockholm, Sweden; Lat.: 59, Long.: 18, Elevation 76 m, 20 June 2013) for a total ""twilight""duration of 2.3 h.
(TIF)

S5 Fig. Photoperiodic encoding in the suprachiasmatic nuclei of coneless mice. Phasing of SCN firing rhythms from ex vivo multielectrode array recordings of *Cnga3*$^{-/-}$ mice housed under a simulated natural twilight photoperiod. Left panel shows Rayleigh vector plots for peak firing activity ($n = 103$ SCN electrodes from five slices). Grey shaded area corresponds to timing of night/twilight transitions, red dotted lines indicate central 50% of the data distribution, arrow indicates mean vector direction. Right panels show representative multiunit traces. Consistent with body temperature data (Fig 5), SCN activity peaks earlier in *Cnga3*$^{-/-}$ mice relative to Opn1mwR animals housed under "natural" twilight (Fig 6A; $p<0.001$ based on bootstrap percentiles). The data used to make this figure can be found in S6 Data.
(TIF)

S6 Fig. Anatomical locations of visually responsive cell types in the suprachiasmatic nuclei. Projected anatomical locations of the visually responsive SCN cells reported in this study, split according to response type. The Unclassified population corresponds to cells that responded to light steps from darkness but not to cone-isolating stimuli.
(TIF)

Author Contributions

Conceived and designed the experiments: TMB RJL. Performed the experiments: LW LH TMB JM ARS AW DAB. Analyzed the data: TMB LW LH ARS. Contributed reagents/materials/analysis tools: FM ARS ARW DAB. Wrote the paper: TMB RJL.

References

1. Golombek DA, Rosenstein RE (2010) Physiology of circadian entrainment. Physiol Rev 90: 1063–1102. doi: 10.1152/physrev.00009.2009 PMID: 20664079
2. Lucas RJ, Lall GS, Allen AE, Brown TM (2012) How rod, cone, and melanopsin photoreceptors come together to enlighten the mammalian circadian clock. Prog Brain Res 199: 1–18. doi: 10.1016/B978-0-444-59427-3.00001-0 PMID: 22877656

3. Roenneberg T, Foster RG (1997) Twilight times: light and the circadian system. Photochem Photobiol 66: 549–561. PMID: 9383985
4. Guler AD, Ecker JL, Lall GS, Haq S, Altimus CM, et al. (2008) Melanopsin cells are the principal conduits for rod-cone input to non-image-forming vision. Nature 453: 102–105. doi: 10.1038/nature06829 PMID: 18432195
5. Freedman MS, Lucas RJ, Soni B, von Schantz M, Munoz M, et al. (1999) Regulation of mammalian circadian behavior by non-rod, non-cone, ocular photoreceptors. Science 284: 502–504. PMID: 10205061
6. Hatori M, Le H, Vollmers C, Keding SR, Tanaka N, et al. (2008) Inducible ablation of melanopsin-expressing retinal ganglion cells reveals their central role in non-image forming visual responses. PLoS ONE 3: e2451. doi: 10.1371/journal.pone.0002451 PMID: 18545654
7. Ingham ES, Gunhan E, Fuller PM, Fuller CA (2009) Immunotoxin-induced ablation of melanopsin retinal ganglion cells in a non-murine mammalian model. J Comp Neurol 516: 125–140. doi: 10.1002/cne.22103 PMID: 19575450
8. Brown TM, Wynne J, Piggins HD, Lucas RJ (2011) Multiple hypothalamic cell populations encoding distinct visual information. J Physiol 589: 1173–1194. doi: 10.1113/jphysiol.2010.199877 PMID: 21224225
9. van Oosterhout F, Fisher SP, van Diepen HC, Watson TS, Houben T, et al. (2012) Ultraviolet light provides a major input to non-image-forming light detection in mice. Curr Biol 22: 1397–1402. doi: 10.1016/j.cub.2012.05.032 PMID: 22771039
10. Dkhissi-Benyahya O, Gronfier C, De Vanssay W, Flamant F, Cooper HM (2007) Modeling the role of mid-wavelength cones in circadian responses to light. Neuron 53: 677–687. PMID: 17329208
11. Altimus CM, Guler AD, Alam NM, Arman AC, Prusky GT, et al. (2010) Rod photoreceptors drive circadian photoentrainment across a wide range of light intensities. Nat Neurosci 13: 1107–1112. doi: 10.1038/nn.2617 PMID: 20711184
12. Lall GS, Revell VL, Momiji H, Al Enezi J, Altimus CM, et al. (2010) Distinct contributions of rod, cone, and melanopsin photoreceptors to encoding irradiance. Neuron 66: 417–428. doi: 10.1016/j.neuron.2010.04.037 PMID: 20471354
13. van Diepen HC, Ramkisoensing A, Peirson SN, Foster RG, Meijer JH (2013) Irradiance encoding in the suprachiasmatic nuclei by rod and cone photoreceptors. FASEB J 27: 4204–4212. doi: 10.1096/fj.13-233098 PMID: 23796782
14. Hulbert E (1953) Explanation of the Brightness and Color of the Sky, Particularly the Twilight Sky. Journal of the Optical Society of America 43: 113–118.
15. Pauers MJ, Kuchenbecker JA, Neitz M, Neitz J (2012) Changes in the colour of light cue circadian activity. Anim Behav 83: 1143–1151. PMID: 22639465
16. Puller C, Haverkamp S (2011) Bipolar cell pathways for color vision in non-primate dichromats. Vis Neurosci 28: 51–60. doi: 10.1017/S0952523810000271 PMID: 21070688
17. Jacobs GH (2013) Losses of functional opsin genes, short-wavelength cone photopigments, and color vision—a significant trend in the evolution of mammalian vision. Vis Neurosci 30: 39–53. doi: 10.1017/S0952523812000429 PMID: 23286388
18. Peichl L (2005) Diversity of mammalian photoreceptor properties: adaptations to habitat and lifestyle? Anat Rec A Discov Mol Cell Evol Biol 287: 1001–1012. PMID: 16200646
19. Brown TM, Allen AE, al-Enezi J, Wynne J, Schlangen L, et al. (2013) The melanopic sensitivity function accounts for melanopsin-driven responses in mice under diverse lighting conditions. PLoS ONE 8: e53583. doi: 10.1371/journal.pone.0053583 PMID: 23301090
20. Enezi J, Revell V, Brown T, Wynne J, Schlangen L, et al. (2011) A "melanopic" spectral efficiency function predicts the sensitivity of melanopsin photoreceptors to polychromatic lights. J Biol Rhythms 26: 314–323. doi: 10.1177/0748730411409719 PMID: 21775290
21. Smallwood PM, Olveczky BP, Williams GL, Jacobs GH, Reese BE, et al. (2003) Genetically engineered mice with an additional class of cone photoreceptors: implications for the evolution of color vision. Proc Natl Acad Sci U S A 100: 11706–11711. PMID: 14500905
22. Brown TM, Tsujimura S, Allen AE, Wynne J, Bedford R, et al. (2012) Melanopsin-based brightness discrimination in mice and humans. Curr Biol 22: 1134–1141. doi: 10.1016/j.cub.2012.04.039 PMID: 22633808
23. Applebury ML, Antoch MP, Baxter LC, Chun LL, Falk JD, et al. (2000) The murine cone photoreceptor: a single cone type expresses both S and M opsins with retinal spatial patterning. Neuron 27: 513–523. PMID: 11055434
24. Haverkamp S, Wassle H, Duebel J, Kuner T, Augustine GJ, et al. (2005) The primordial, blue-cone color system of the mouse retina. J Neurosci 25: 5438–5445. PMID: 15930394

25. Nikonov SS, Kholodenko R, Lem J, Pugh EN Jr. (2006) Physiological features of the S- and M-cone photoreceptors of wild-type mice from single-cell recordings. J Gen Physiol 127: 359–374. PMID: 16567464

26. Hughes S, Watson TS, Foster RG, Peirson SN, Hankins MW (2013) Nonuniform distribution and spectral tuning of photosensitive retinal ganglion cells of the mouse retina. Curr Biol 23: 1696–1701. doi: 10.1016/j.cub.2013.07.010 PMID: 23954426

27. Berson DM, Dunn FA, Takao M (2002) Phototransduction by retinal ganglion cells that set the circadian clock. Science 295: 1070–1073. PMID: 11834835

28. Brown TM, Gias C, Hatori M, Keding SR, Semo M, et al. (2010) Melanopsin contributions to irradiance coding in the thalamo-cortical visual system. PLoS Biol 8: e1000558. doi: 10.1371/journal.pbio.1000558 PMID: 21151887

29. Barnard AR, Appleford JM, Sekaran S, Chinthapalli K, Jenkins A, et al. (2004) Residual photosensitivity in mice lacking both rod opsin and cone photoreceptor cyclic nucleotide gated channel 3 alpha subunit. Vis Neurosci 21: 675–683. PMID: 15683556

30. Biel M, Seeliger M, Pfeifer A, Kohler K, Gerstner A, et al. (1999) Selective loss of cone function in mice lacking the cyclic nucleotide-gated channel CNG3. Proc Natl Acad Sci U S A 96: 7553–7557. PMID: 10377453

31. Brown TM, Piggins HD (2009) Spatiotemporal heterogeneity in the electrical activity of suprachiasmatic nuclei neurons and their response to photoperiod. J Biol Rhythms 24: 44–54. PMID: 19227579

32. VanderLeest HT, Houben T, Michel S, Deboer T, Albus H, et al. (2007) Seasonal encoding by the circadian pacemaker of the SCN. Curr Biol 17: 468–473. PMID: 17320387

33. Amann B, Hirmer S, Hauck SM, Kremmer E, Ueffing M, et al. (2014) True blue: S-opsin is widely expressed in different animal species. J Anim Physiol Anim Nutr (Berl) 98: 32–42. doi: 10.1111/jpn.12016 PMID: 23173557

34. Hut RA, Kronfeld-Schor N, van der Vinne V, De la Iglesia H (2012) In search of a temporal niche: environmental factors. Prog Brain Res 199: 281–304. doi: 10.1016/B978-0-444-59427-3.00017-4 PMID: 22877672

35. Jacobs GH (1993) The distribution and nature of colour vison among the mammals. Biol Rev 68: 413–471. PMID: 8347768

36. Revell VL, Barrett DC, Schlangen LJ, Skene DJ (2010) Predicting human nocturnal nonvisual responses to monochromatic and polychromatic light with a melanopsin photosensitivity function. Chronobiol Int 27: 1762–1777. doi: 10.3109/07420528.2010.516048 PMID: 20969522

37. Figueiro MG, Bullough JD, Parsons RH, Rea MS (2004) Preliminary evidence for spectral opponency in the suppression of melatonin by light in humans. Neuroreport 15: 313–316. PMID: 15076759

38. Dodt E, Meissl H (1982) The pineal and parietal organs of lower vertebrates. Experientia 38: 996–1000. PMID: 6751863

39. Weng S, Estevez ME, Berson DM (2013) Mouse ganglion-cell photoreceptors are driven by the most sensitive rod pathway and by both types of cones. PLoS ONE 8: e66480. doi: 10.1371/journal.pone.0066480 PMID: 23762490

40. Dacey DM, Liao HW, Peterson BB, Robinson FR, Smith VC, et al. (2005) Melanopsin-expressing ganglion cells in primate retina signal colour and irradiance and project to the LGN. Nature 433: 749–754. PMID: 15716953

41. Spitschan M, Jain S, Brainard DH, Aguirre GK (2014) Opponent melanopsin and S-cone signals in the human pupillary light response. Proc Natl Acad Sci U S A 111: 15568–15572. doi: 10.1073/pnas.1400942111 PMID: 25313040

42. Thapan K, Arendt J, Skene DJ (2001) An action spectrum for melatonin suppression: evidence for a novel non-rod, non-cone photoreceptor system in humans. J Physiol 535: 261–267. PMID: 11507175

43. Chang L, Breuninger T, Euler T (2013) Chromatic coding from cone-type unselective circuits in the mouse retina. Neuron 77: 559–571. doi: 10.1016/j.neuron.2012.12.012 PMID: 23395380

44. Govardovskii VI, Fyhrquist N, Reuter T, Kuzmin DG, Donner K (2000) In search of the visual pigment template. Vis Neurosci 17: 509–528. PMID: 11016572

45. Jacobs GH, Williams GA (2007) Contributions of the mouse UV photopigment to the ERG and to vision. Doc Ophthalmol 115: 137–144. PMID: 17479214

46. Howarth M, Walmsley L, Brown TM (2014) Binocular integration in the mouse lateral geniculate nuclei. Curr Biol 24: 1241–1247. doi: 10.1016/j.cub.2014.04.014 PMID: 24856206

47. Lovegrove BG (2009) Modification and miniaturization of Thermochron iButtons for surgical implantation into small animals. J Comp Physiol B 179: 451–458. doi: 10.1007/s00360-008-0329-x PMID: 19115060